Factor XIIIA Genotypes to Outcome in Epithelial Ovarian Cancer

Kathryn Tierney Hutchinson

Submitted in accordance with the requirements for the degree of
Doctor of Philosophy

The University of Leeds
School of Medicine

September, 2019

The candidate confirms that the work submitted is her own and that appropriate credit has been given where reference has been made to the work of others.

Acknowledgements

I would like to extend grateful thanks to my supervisors Dr Rashida Anwar, Prof Tim Perren and Prof Sir Alex Markham for all their guidance and support throughout this PhD project. I am especially grateful to Dr Rashida Anwar for her help and advice during my periods of data collection and writing, and for the exciting scientific discussions which helped to direct me in this PhD. Thank you Rashida for encouraging me when I had lost faith and patience. Thank you to Prof Perren for his support, discussions, perspective and advice regarding the clinical data acquisition and interpretation and thanks to Prof Sir Markham for his advice and all his support throughout my PhD.

Thank you to all the colleagues who have assisted me, this includes but is not limited to Dr Sandra Bell (ovarian cancer sample cohort), Dr Adam Davison (microscopy and Incucyte) Dr James Poulter (sequencing), Dr Milène Volpatu (immunofluorescence and mentorship), Dr Mark Handley (advice and loan of reagents), Prof Tom Hughes (advice and mentorship) and Ms Sarah Perry (training, advice, guidance and endless patience).
It has been a pleasure to work with the Anwar Lab, but special thanks are extended to Dr Elmena Elfaki with whom I shared many a late night acquiring data.

Thank you to my family and incredibly talented friends I have made throughout this PhD: Michael Hutchinson, Alice Webb, Luke Souter, Laura Rice, Chris Partington, Catriona Marshall, Michelle Umpierrez, Dr Eleanor Gibson-Forty and many others. We have shared laughs, tears, cake, gin, wine and ideas for alternative career plans! I couldn't have done this without you.

To the light of my stars, Gareth York, thank you for unwavering love and faith in me, for your patience, and for your cwtches. I cannot wait to marry you.

I could not have completed this work without the hundreds of women who consented for their blood and tissue samples to be used in translation clinical research – thank you for your generosity.

I dedicate this thesis to my wonderful parents, Ian and Anita Hutchinson, who have been the greatest cheerleaders in my life. They raised me to know I could achieve anything I set my mind and heart to, and that I am not a quitter. The words on this page will never be enough to express my love and gratitude, but thank you and I love you. I hope I continue to make you proud.

"Constant grinding can turn an iron rod into a needle." – Chinese Proverb

Abstract

Epithelial ovarian cancer (EOC) is often diagnosed at the more aggressive stages of disease and its heterogeneity makes treatment challenging. Factor XIIIA (FXIIIA) is a transglutaminase which crosslinks fibrin to form stable blood clots, as well as having other roles in inflammation and angiogenesis. FXIIIA plasma levels, activity and protein expression have been linked to cancer, including a brief study in ovarian cancer (OC). The gene for FXIIIA, *F13A1*, is highly polymorphic with several single nucleotide polymorphisms (SNPs) linked to thrombotic disease and cancers.

In this PhD project, *F13A1* SNPs 1951G>A and 1954G>C were associated with OC overall survival detriment and benefit, respectively. This was maintained in long-term survival (>20 year, n=252). *F13A1* SNPs were further investigated for associations with range of survival intervals in a cohort of newly diagnosed patients (ICON7 translational cohort, n=448). The SNP 103G>T (Val34Leu), which has been linked to faster activation of the transglutaminase, and has been linked to cancer risk and thrombotic disease, was associated with survival in EOC. Heterozygotes for this SNP in particular benefited for survival post-progression and overall survival.

Expression of FXIIIA protein was explored for the first time in OC tissues and was present in OC stroma, with evidence of poor prognosis with positive stroma staining. However, 34Leu carriers survived longer than wildtype patients when stroma staining was present. As FXIIIA is involved in angiogenesis, when 34Leu protein variants were used in angiogenesis assays, the presence of active Leu variants produced smaller angiogenic networks at a slower rate than wildtype protein, and evidence of a reduction in migratory signalling was seen. The benefit to survival for 34Leu carrying patients is hypothesised to be due to less successful blood vessel recruitment which results in smaller tumours which are easier to treat, posing a potentially exciting future for this protein in EOC.

List of Tables

List of Figures

List of Abbreviations

aa	amino acid
Ab	antibody
Akt	protein Kinase B
AURELIA	Avastin Use in Platinum-Resistant Epithelial Ovarian Cancer
bp	basepairs
BRAF	proto-oncogene B-raf; v-Raf murine sarcoma viral oncogene homolog B
BSA	bovine serum albumin
Ca^{2+}	calcium ions
CA-125	Cancer antigen 125
cFXIII	cellular Factor XIII
CP	carboplatin plus paclitaxel chemotherapy
CP+B	carboplatin plus paclitaxel plus bevacizumab chemotherapy
CT	computerised tomography
DAB	3,3'-dimanobenzidine
dH_2O	Milli-Q water: filtered and deionised
DMSO	dimethylsulphoxide
DNA	deoxyribose nucleic acid
dNTP	deoxynucleotide-triphosphate
ECM	extracellular matrix
ECOG	European Cooperative Oncology Group
EDTA	ethylenediaminetetra-acetic acid disodium salt
Egr-1	Early growth response protein 1
EGF	epidermal growth factor
ELISA	enzyme-linked immunosorbent assay
EMT	epithelial mesenchymal transitioning
EOC	epithelial ovarian cancer
ERK	extracellular signal-related kinases; also known as mitogen-activated protein kinase (MAPK)
F13A1	the gene for Factor XIIIA
FCS	fetal calf serum
FIGO	International Federation of Gynaecology and Obstetrics
FXIII	Factor XIII
FXIIIA	Factor XIII protein, A homodimer
FXIIIB	Factor XIII protein, B homodimer
g	gram
GEO	gene expression omnibus
Gln	glutamine
Glu	glutamic acid
gnomAD	genome aggregation database
GSE	genomic spatial events
HCl	hydrochloric acid
HPA	Human Protein Atlas
HRP	horseradish peroxidase
HUVEC	human umbilical cord endothelial cell
HWE	Hardy Weinburg Equilibrium
ICON7	International Collaboration on Ovarian Neoplasms 7
Ig	immunoglobulin
IU	International Unit
KCl	potassium chloride
kDa	kilo-Daltons
L	litre
LB	Luria-Bertoni (agar/broth)
Leu	leucine
M	molar
mg	milligram
$MgCl_2$	magnesium chloride

min	minutes
mL	milliliter
mM	millimolar
MRI	magnetic resonance imaging
NaCl	sodium chloride
NaOH	sodium hydroxide
ng	nanogram
OC	ovarian cancer
OCEANS	Ovarian Cancer Study Comparing Efficacy and Safety of Chemotherapy and Anti-Angiogenic Therapy in Platinum-Sensitive Recurrent Disease
PBS	phosphate buffered saline
PBS-T	phosphate buffered saline plus 0.1% Tween-20
PCR	polymerase chain reaction
Phe	phenyl-alanine
PET	positron emission tomography
PrEST	recombinant protein epitope signature tag
Pro	proline
rcf	relative centrifugal force
RMA	robust multi-array average
RMI	Relative Malignancy Index
RT	room temperature
SDS	sodium dodecyl sulphate
SDS-PAGE	sodium dodecyl sulphate polyacrylamide gel electrophoresis
SNP	single nucleotide polymorphism
SSCP	single strand conformational polymorphism
TAE	Tris-acetate-ethylenediaminetetraacetic acid
TBS	Tris-buffered saline
TBS-T	Tris-buffered saline plus 0.1% Tween-20
TGM2	transglutaminase-2
TGF-ß	transforming growth factor-beta
TMA	tissue microarray
Tris	Tris(hydroxymethyl)-aminomethane
Tris-HCl	Tris(hydroxymethyl)-aminomethane-hydrochloric acid
TSP-1	thrombospondin-1
Tyr	tyrosine
U	units (of enzyme)
Val	valine
VEGF	vascular endothelial-like growth factor
VEGF-A	vascular endothelial-like growth factor A
VEGFR2	vascular endothelial-like growth factor receptor 2
v/v	volume per volume
WT	wildtype
WT-1	Wilms tumour protein 1
%	percentage
>	greater than
<	less than
°C	degrees Centigrade
αvß3	alpha 5 beta 3
µl	microliter
µM	micromolar
µm	micrometer, micron

Chapter 1: Introduction

1.1 Ovarian Cancer

Ovarian cancer (OC) is a gynaecological malignancy often diagnosed at the later, more aggressive stages of disease due to the asymptomatic clinical presentation of OC (1). In the presence of symptoms, a lack of recognition can lead to the late diagnosis of advanced disease. As a result, OC is considered one of the most lethal gynaecological malignancies, worldwide, with 295414 new cases of OC diagnosed worldwide in 2018 (2). In England alone, the average 5-year survival rate is 44% (3,4). Later stage of disease and later patient age of diagnosis all result in lower survival rates compared to earlier stage disease and younger women (age 15-39). Later stage disease is metastatic and later age also makes a patient more difficult to treat and there is an increase in the risk of comorbidities (3).

There are several types of OC, named after the suspected origin of the primary cancer. Epithelial ovarian cancer (EOC) is the most common type of ovarian cancer and can be further described based on the histology of the tumour (Section 1.1.1). Other OC types include, stromal, sex-cord and germ-cell but as EOC is the main focus of this thesis, the rarer OCs will not be expanded upon here. However, thorough reviews on these rarer OCs are available (5,6).

1.1.1 Morphology of Epithelial Ovarian Cancer

Serous histology is the most common type of EOC. Other histologies include endometrioid, clear cell, mucinous, mixed or undifferentiated disease. Rather than treating the histologies as separate entities, they have been grouped into a binary classification (7). Type I EOC comprises low grade serous, mucinous, clear cell and transitional tumours whereas Type II comprises high grade serous and undifferentiated disease. Type I and II tumours differ in their aggression, mutations and response to chemotherapy (Table 1-1, 1-2) and therefore are of great interest to developments in personalised medicine. The binary classification is based on the tumorigenesis pathways proposed by Shih and Kurman 2004, rather than as a change to histology definitions. The precursors

Table 1-1: Summary of Epithelial Ovarian Cancer Type Characteristics

A

Type of EOC	Histology	Common Genes which are mutated
Type I	Low-Grade Serous	*BRAF, KRAS*
	Borderline (MPSC)	tbd
	Mucinous	*KRAS*
	Endometriod	*PTEN, B-catenin, KRAS*
	Clear Cell	*KRAS, TGFB RII*, Microsatellite Instability
	Transitional (Brenner)	tbd
Type II	High-Grade Serous	*TP53, HER2/neu* and *AKT2* gene overexpression, *p16* gene inactivation
	Undifferentiated	tbd
	Carcinosarcoma - mixed mesodermal	*TP53*

B

Serous	Low Grade Serous (25%)	Slow, less aggressive, poor responder to chemotherapy	*KRAS* (35%) *BRAF* (30%) *TP53* (0%)	HLA-G Expression (0%)	Ki-67 Proliferation (10-15%)
	High Grade Serous (75%)	Rapid, aggressive, good responder but common to recur	*KRAS* (0%) *BRAF* (0%) *TP53* (50-80%)	HLA-G Expression (61%)	Ki-67 Proliferation (>50%)

Tables summarized from those produced by Shih and Kurman 2004 (7).

cells/tissues from which Type I and Type II EOCs originate differs greatly. Although clearly summarised by Shih and Kurman 2004, in short, Type I tumours arise from borderline tumours, likely themselves coming from cystadenomas or adenofibromas, endometriosis in the case of endometrioid EOC, and inclusion cysts or ovary surface epithelium (OSE) for mucinous and serous EOC (7). The exact precursor for the more aggressive Type II is far less clear, and it is hypothesised that these tumours develop from *de novo* events in the surface epithelium or inclusion cysts (8). However, as mentioned by the same authors in their joint publication six years later, reaching for a “de novo” explanation is likely due to ignorance on the complexity of the events surrounding the development of Type II tumours rather than as a result of an event arising from “nothing” (7,9).

Incessant ovulation was thought to be the cause of EOC due to animal studies suggesting that persistent ovulation may damage the OSE resulting in formation of cysts which then go on to form tumours (10). Decrease in ovulation by hormone-controlled means, such as the contraceptive pill, or pregnancy and decreases EOC risk (11–13) , but those with polycystic ovary syndrome which results in fewer ovulation cycles have an increased risk of EOC (14,15). Persistent ovulation is therefore a hypothesis which is not fully supported. A full review of other risks and protective factors in ovarian cancer has been recently published by Momenimovahed and colleagues in 2019 (16).

Another hypothesis suggested that serous EOC arises from the fallopian tubes (17–19). Patterns of gene expression from serous OC correlated with normal fallopian tube epithelium signatures (20). The surface ‘epithelium’ of the ovary is structurally unlike other epithelium, covered in a single layer of mesothelial cells, (17). Although not classical epithelium, the histology of EOC tumours resembles the cells of tubal epithelium. Tubal epithelium covers the fallopian tubes, peritoneal cavity and uterus (17). In a study of tissues resected during bilateral salpingo-oophrectomies in women with familial history of OC or breast cancer gene (*BRCA*) mutations, a large proportion of tissues had abnormal cells or hyperplasial lesions (an increase in cell number) in tubal epithelium, called “tubal intraepithelial carcinoma” (TIC or serous TIC (STIC)) (18,21,22). A high percentage of *TP53* mutations and p53 protein are present in the TICs, much like in high grade serous ovarian cancer (23,24). Advanced serous OC tissues were

found to have TIC regions, but these regions were not identified in mucinous or endometrioid OC histology (25,26). When the TIC regions were specifically extracted from the tissue, the *TP53* mutational status was identical to that of the metastatic OC, demonstrating shared clonality and supporting the hypothesis that TIC regions are precursors to serous OC (24,27). However, TIC is not present in all high grade serous OCs (17), so the exact precursor of the disease or that of low grade serous disease remains to be fully understood.

The oncogenes and tumour suppressor genes which are mutated in EOC differ between the two Types of EOC. Type I EOCs often have mutations in *BRAF* and *KRAS* (28–30), genes which are responsible for proteins for transductive signalling from cells into the nucleus. Mutations result in constitutively active signalling cascade, and this aberrant signalling leads to pro-survival and increased cell proliferation associated with cancer. *KRAS* and *BRAF* mutations are not seen in Type II EOCs, with *TP53* being mutated in 50-80% of Type II tumours (23,31–33). Type II tumours also often have mutations in *Her2/neu* (34,35) and *AKT2* (36–39) which result in increase of proliferation and differential response to chemotherapy. Increased expression of Ki-67 (40,41) and human leukocyte antigen-G (HLA-G) (42,43), the former associated with increase in proliferation and the latter hypothesised to have involvement in tumour immune evasion.

1.1.2 Molecular Subtypes of High Grade Serous Ovarian Cancer

Within the last ten years, the increase in the use of gene expression and functional genomics, has led to classification of ovarian cancer, particularly for serous EOC, beyond the definitions of high grade serous ovarian cancer (HGSOC) and low grade serous ovarian cancer (LGSOC). For HGSOC in particular, the aggressive nature of the disease means that understanding of the disease is vital for early and effective treatment (44). Gene expression profiling of 285 serous and endometrioid tumours by Tothill *et al.* 2008 was one of the first milestones in molecular subtyping of disease, identifying a total of 6 molecular subtypes, 2 for low-grade endometrioid and serous tumours with low metastatic potential and 4 for high grade serous EOCs (45). These 4 subtypes were validated by The Cancer Genome Atlas (TCGA) in a study of 489 tumours and named: “proliferative”, “mesenchymal”, “immunoreactive” and “differentiated” (46). This work by TCGA has been further developed to determine survival

outcome through a combination of subtype gene signatures and survival gene expression signatures (47). The gene signatures defined by the TCGA were applied to an independent cohort of 174 patients, with the immunoreactive subtype demonstrating the longest survival and the mesenchymal subtype demonstrating the shortest survival (48). The study by Konecny *et al.* determined other gene expression signatures which fit within the TCGA subtype definitions and that the definitions of subtypes would benefit from molecular subtypes lying on a spectrum which would provide a greater appreciation for tumours in which there is a small amount of overlap between gene signatures, rather than the implied "mutual exclusivity" of the TCGA defined molecular subtypes (48).

From these studies, there was still no clear consensus on the precise definitions of the subtypes, and one of the main gaps which remained was a lack of specific treatments for each subtype. The issue of the limited variety of the patient tumours studied i.e. detailed clinical data was not available for all patients and the variation in surgical resection was a confounding factor which affected survival outcome (49). Therefore Wang *et al.* sought to determine whether HGSOC molecular subtypes could also be associated with surgical outcomes in addition to survival by generating their own *de novo* subtypes and comparing them to those defined by the TCGA (49), using a pooled cohort of 2100 patients. Whilst confirming that the original 4 subtypes defined by the TCGA were applicable in their larger cohort, gene expression analysis resulted in further branches for the "differentiated" subtype (DIF), the "anti-mesenchymal (ANM)" subtype due to the downregulation of genes which are upregulated by the mesenchymal (MES) subtype.

These developments further the understanding of ovarian cancer as a heterogeneous collection of diseases that certainly do not fit in a singular OC "box". However, much remains to be developed with respect to treatment strategies. Molecular subtyping has been unable to identify a consistent subtype for platinum-refractory/resistance (49). The results from the gene expression profiles could certainly assist in the determination of which therapies

Table 1-2: Defined Molecular Subtypes of High Grade Serous EOC

Tothill *et al.* Molecular Subtypes	TCGA Molecular Subtypes	Wang *et al.* Molecular Subtypes	Wang *et al.* Gene Upregulation
C1	Mesenchymal (MES)	Mesenchymal (s1.MES)	cancer associated fibroblast signatures EMT/Stem-like drivers Fibronectin TGF-beta VEGF signalling ECM-receptor interactions
C2	Immunoreactive (IMM)	Immunoreactive (s2.IMM)	Antigen Presentation PD-L1 T-Cell receptor signalling
C5	Proliferative (PRO)	Proliferative (s3.PRO)	Lower BRCA mutation rate Cell Cycle-associated proteins Notch signalling DNA Repair pathways
C4	Differentiated (DIF)	Differentiated (s4.DIF)	Metabolic Ribsome Cytochrome P450
		Anti-Mesenchymal (s5.ANM)	Lower BRCA mutation rate Oxidative Phosphorylation Peroxisome

The subtypes given in the above table were explored in the key publications (45,49).

Figure 1-A: A schematic of the prognosis of the different molecular subtypes of high grade serous EOC. This figure presents a schematic as defined by Wang and colleagues, (Wang C *et al.* 2017; (49)). The order of subtypes from worst to best prognosis was: mesenchymal (MES), proliferative (PRO), differentiated (DIF), anti-mesenchymal (ANM) and immunoreactive (IMM).

may be most applicable, but further gene expression analyses in specified treatment groups i.e. responders vs non-responders would be required to determine whether molecular sub-types could be determined for chemotherapy.

1.1.3 Staging of Ovarian Cancer

Although the more binary classification is used to class OC, staging of the disease still takes place under the International Federation of Gynaecology and Obstetrics (FIGO) criteria. First published in 1973, the staging criteria have been updated several times, with the most recent updated in 2014 (50). A summary of staging is provided in Figure 1-B (51). Stage I and II are the least aggressive, and diagnosis at this early stage often leads to a better prognosis. Diagnosis at Stages III and IV, which demonstrate a metastatic component to lymph nodes, the peritoneal cavity or to other organs, often leads to far poorer prognosis, even with rapid treatment.

1.1.4 Diagnosis and Treatment of Ovarian Cancer

Diagnosis of OC is confirmed through a variety of tests and imaging methodologies. The Risk of Malignancy Index (RMI) is a combination of serum levels of cancer-antigen 125 (CA-125), ultrasound, and menopausal status, (Figure 1-C) (52). If RMI is over 200, the chance of malignancy is highly likely, and a range of imaging modalities are used to locate and determine tumour stage. Computerised tomorgraphy (CT) and magnetic resonance imaging (MRI) are used, often in combination with one another, due to the differing sensitivities of the respective modalities to detect lesions (51,53).

OC is treated with a combination of platinum-based chemotherapy and where possible, surgical resection (54,55). Radiotherapy is not commonly used in initial treatment due to the proximity of the ovaries to highly radio-sensitive organs such as the bowel and kidneys, and whole abdomen radiotherapy can be highly toxic (56). However, radiotherapy can provide symptomatic relief in metastatic disease. OC has demonstrated radiosensitivity (57) and the development of intensity modulated radiotherapy and an increased understanding of ovarian cancer subtypes may lead to the use of radiotherapy becoming more common for OC treatment (56). The standard chemotherapy regimen is paclitaxel and carboplatin, often supplemented with other chemotherapeutic agents such as

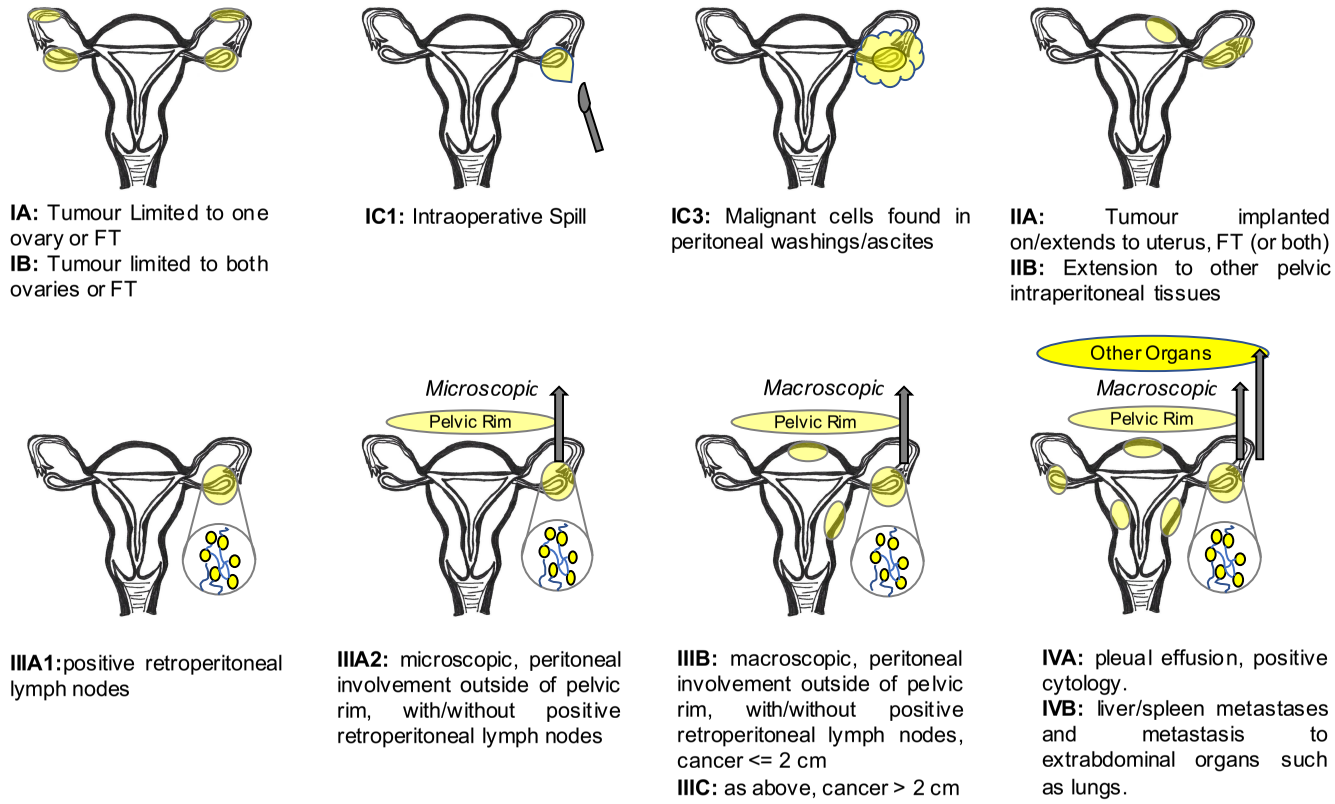

Figure 1-B: Staging of Ovarian Cancer defined by the International Federation for Gynaecology and Oncology (FIGO). Stage I disease is limited to the ovary or the fallopian tubes (FT), with an increase in the Stage I cascade increasing if there was evidence of intraoperative spill during ressective surgery. Peritoneal washings are part of ressective surgery to determine whether the cancer has spread outside of the suspected primary site. Stage II is rarer and is difficult to define but limits the spread of the cancer to the tissues within the intraperitoneal cavity. Stage III disease is disease which has spread to the lymph nodes and increase in aggression leads to microscopic and macroscopic disease outside of the pelvic rim. Stage IV is the most aggressive disease, with the poorest prognosis due to the presence of pleural effusion, also known as fluid in the thoracic cavity, multiple lesions and metastases present in the other organs such a spleen, liver and lungs. Adapted from Javadi et al. (2016) American Journal of Roentgenology 206(6).

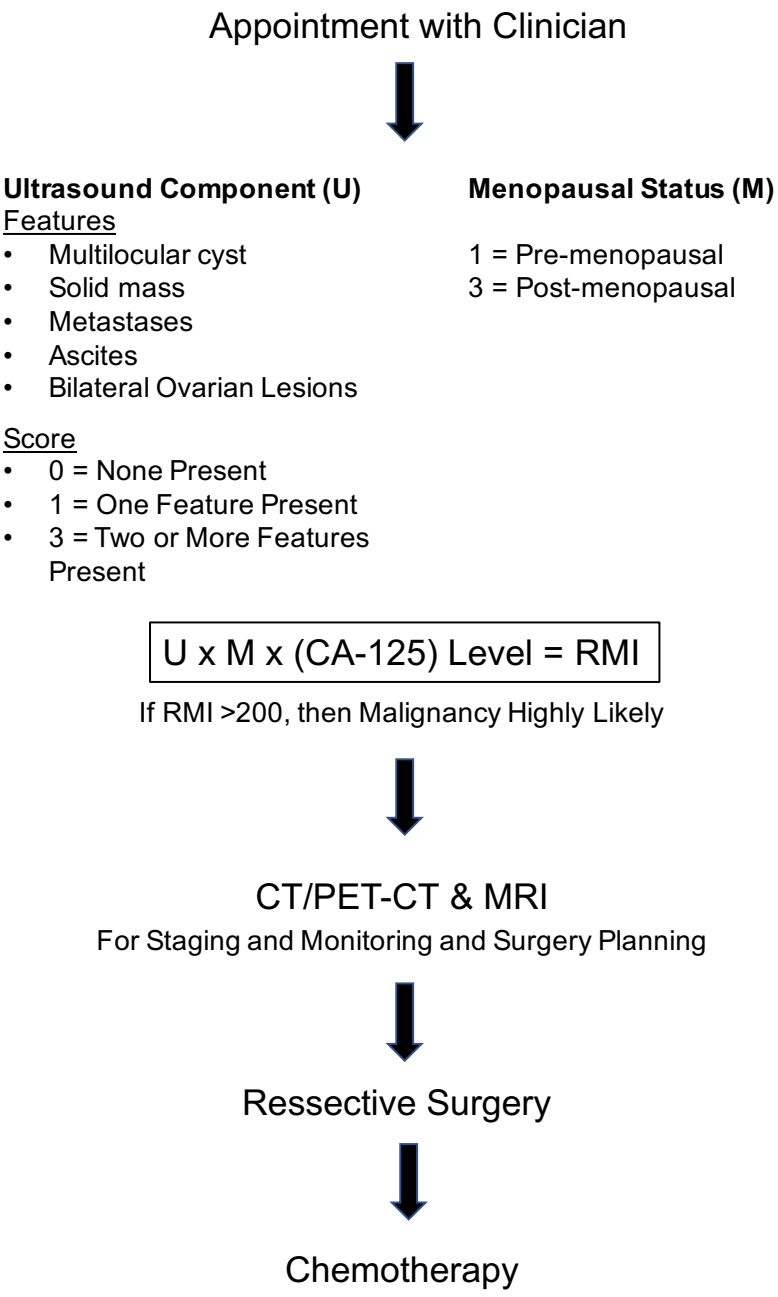

Figure 1-C: Flowchart of Diagnosis Steps for Ovarian Cancer. Blood serum levels of cancer antigen-125 (CA-125) are multiplied by a calculated ultrasound component, based on the features present in the imaging, and multiplied by the menopausal status of the patient to give a score for the Relative Malignancy Index (RMI). If no clinical features are present in the ultrasound are present, the RMI score will be 0 and other imaging may be required, or the CA-125 levels will continue to be monitored. If the RMI score is > 200, then the chance that malignancy is present is highly likely and imaging modalities such as computerised tomography (CT), positron emission tomography (PET)-CT, and magnetic resonance imaging (MRI), all of which are used to stage disease and design further treatment plans for surgery and chemotherapy. Surgical resection of the tumour takes place and then margin of disease remaining is determined and then chemotherapy, traditionally platinum-based is started. The disease and recurrence are monitored throughout follow-up.

other DNA-targeting drugs or anti-angiogenics.

1.1.4.1 Platinum Resistance in Ovarian Cancer

Platinum-based chemotherapy, such as carboplatin and cisplatin, disrupt DNA replication by causing crosslinking of the double helix at guanine bases, resulting in attempts by cells to correct errors through nucleotide excision repair (58,59). If cells are unable to repair the damage, then cells are pushed towards apoptosis. OC is known for its sensitivity to platinum-based chemotherapy, however platinum resistance in ovarian cancer is becoming a growing concern in the clinical setting. OC is either unresponsive to the platinum agents as first line therapy or the recurrent disease is resistant to re-treatment with the same agents. The heterogeneous populations present within tumours mean that not all cells within the tumour respond to platinum-based chemotherapy and even through the tumour mass shrinks, the recurrent disease may be made up from the remaining resistant population which proliferates into a far more resistant tumour. As platinum-based chemotherapy is one of the cornerstones of OC treatment, novel agents and treatment regimens are required in order to tackle these resistant cancers.

The progression-free survival period for women with advanced OC is approximately 18 months and 80% of women will experience tumour recurrence (60). In clinical trials, the platinum-free interval (PFI) is used to determine subsequent chemotherapies: “platinum-refractory” disease is that which progresses during therapy or within 4 weeks of the last dose of platinum chemotherapy, “platinum-resistant” disease is that which progresses within 6 months, “partially platinum sensitive” disease progress between 6 to 12 months and “platinum-sensitive” disease progresses after a PFI of over 12 months (61,62). Although the defined molecular subtypes of ovarian cancer do demonstrate differential platinum-sensitivity, the exact molecular biology underlying sensitivity or resistance remains to be fully understood.

Platinum-resistance does not necessarily negate the use of platinum-based agents for the recurrent disease, as different dosing schedules and combinations of supplementary agents have been used during and beyond first-line therapy (60). Paclitaxel, a tubulin-targeting agent which prevents the unwinding of the

DNA helix during DNA replication (63) is used alongside first-line chemotherapy in order to improve treatment efficacy, especially when resistance is not yet clear (64). Other treatment regimens have included gemcitabine (65,66), or PEGylated liposomal doxorubicin (67–69). Other supplementary agents will be expanded upon in Section 1.1.4.2.

1.1.4.2 Supplementary Chemotherapies & Agents

1.1.4.2.1 Anti-angiogenics

Anti-angiogenics are also common in OC treatment. As angiogenesis is one of the classic hallmarks of cancer (70), and it is well established that vascular endothelial-like growth factor A (VEGFA) expression is associated with EOC at an early stage. Blood vessel density is dependent on the OC molecular subtype (71). Anti-angiogenic drugs are used in OC treatment in the UK, but in a recent review of current treatment management, anti-angiogenics are not recommended to be used as standalone agents, but as a combinatory therapy to the already established surgery and chemotherapy treatment plans (72). Just like in platinum resistance, concerns over OC resistance to anti-angiogenic therapy are present. A number of anti-angiogenics have performed well in Phase I and II trials, although performance at Stage III has overall been disappointing, but improvements to progression-free survival (PFS) and overall survival (OS) have been seen.

Bevacizumab (Avastin ®, Roche) (73) is a monoclonal antibody against all the isoforms of VEGFA , and can be used in first-line chemotherapy in OC (74–77). Its efficacy as a supplementary chemotherapy has been tested in a number of clinical trials including the GOG-0218 (74) , ICON7 for primary OC (78,79) and OCEANS (80), AURELIA (81) and GOG-0213 (82) for recurrent cancer. There have been other trials which have been well summarised by Colombo and colleagues (77). VEGFR2-specific inhibitors include ramucirumab (IMC-112B) an IgG_1 specific against the receptor (83). Other tyrosine kinase inhibitors include sofafenib (84), sunitinib (85) and pazopanib (86). Anti-angiogenics do however, come with a host of side-effects that can negatively impact patient quality of life such as bowel perforation (87–89).

1.1.4.2.2 DNA-Repair Targeted Agents

Olaparib (a poly(ADP)-ribose polymerase (PARP) inhibitor) is a common DNA replication targeted agent used in OC. Hereditary OC commonly results from germline mutations in *BRCA* genes (90), and there is some evidence of somatic mutations BRCA1 in OC tumours, too (91). *BRCA1* and *BRCA2*, results in defective homologous repair of DNA, and following treatment with platinum which creates crosslinks between the DNA helices which homologous repair attempts to remove (92,93). Olaparib is therefore a strong candidate for use alongside platinum-agents, resulting in two-pronged approach: generate the damage, and then fail to repair said damage. Olaparib, and other PARP-inhibitors niraprib and rucaparib has proven useful for treatment of platinum-sensitive OC (93,94).

1.1.4.2.3 Other therapy types

There are many alternative chemotherapy agents in OC that have recently been thoroughly reviewed by Vetter and Hays 2018 (95). Touching upon a few others, inhibitors against the mitogen-associated protein kinase (MAPK)/mammalian target of rapamycin (mTOR) pathways, have proved to have quite toxic effects, mostly likely to the broad spectrum of the pathways in which these proteins are involved. However, as with tyrosine kinase receptors, compensatory signalling events can occur which inhabits therapy effectiveness (96–98). The folate alpha receptor has also proved to be a promising target due to its overexpression in OC making it target for cancer detection and for therapy (99,100). The receptor is specific for folates, which are involved in DNA synthesis, repair and methylation as they have a role in purine and thymidine biosynthesis (101). Farletuzumab is an antibody against folate alpha receptor which has been taken into Phase III clinical trials but results remain unclear (100).

1.1.5 The Role of the Extracellular Matrix in Ovarian Cancer

The extracellular matrix (ECM) plays an important role in OC as it not only influences the structure in which a tumour develops, but also influences metastatic progression, angiogenic signalling and therapeutic response. Fibronectin, fibrinogen and collagen, substrates of Factor XIIIA (FXIIIA) crosslinking, have been associated with poor OC prognosis. Fibronectin levels within ascites fluid is correlated with tumour stage and is present in OC tumour stroma (102,103). Fibronectin promotes metastases and cell migration (104–

106). The increased expression of fibronectin in OC has led to consideration of its use as therapeutic target (107) using the small peptide, pUR4B (108) to decrease vessel thickness (109), decrease deposition of fibronectin and other ECM components and limited vasculogenesis *in vitro* (110).

The most abundant component of ovarian ECM is collagen I (111). Collagen is involved in ECM remodelling and density of collagen and resulting increase in matrix stiffness increased aggression of cancer (112–115) and has even been linked to therapeutic resistance by regulation of tau protein leading to paclitaxel resistance (116,117). Matrix metalloproteinases (MMPs) are heavily involved in the tumour microenvironment (118) and can cleave matrix proteins and lead to adhesion in the peritoneal cavity (105). Differential expression of MMPs, in terms of the specific MMP and its location, contributes to OC stage (119), metastasis (120) and survival (121). MMPs are also able to modulate angiogenic network development e.g. MMP-9 promotes the release of VEGF from endothelial cells (122).

1.2 Factor XIII

Factor XIII (FXIII) is a member of the transglutaminase (TG) family of proteins (123) and is the final member of the coagulation cascade. FXIIIA is a zymogen, a protein which exists as an inactive precursor which requires a biochemical change for conversion to its active form (124). It is activated in the presence of calcium and thrombin to exert transglutaminase activity by which it cross-links monomers of fibrin and other components to form stable fibrin clots (125). Cross-linking occurs through the formation of gamma-glutamyl-epsilon-lysyl bonds, or isopeptide bonds (detailed in section 1.2.2). This protein has numerous roles outside of its crosslinking function, and details of which and details on its activation, structure and genetics will be provided below. FXIII is expressed in the plasma, platelets, fibroblasts, monocytes, and tissues such as skin, adipose and soft tissues, osteoblasts, placenta, and testis (126). Levels of the heterotetramer in normal human plasma 21.6 µg/mL (127).

1.2.1 Structure and Forms of FXIII

There are two forms of Factor XIII: a plasma form (pFXIII) which exists as a 320 kDa heterotetramer comprised of two A and two B subunits (FXIII-A_2B_2), and a cellular form (cFXIII) which exists as a homodimer of A subunits found in cells of bone marrow origin (128,129). The FXIIIB homodimer circulates in excess in the human plasma (130). The methods of activation of these forms differ and will be discussed in Section 1.2.2. Crystal structures of native FXIIIA are not available, only the crystal structures of recombinant FXIIIA (Protein Data Bank: 1F13), representative of cFXIII, have been generated, but have proved useful in determining the structure, activation and interactions of FXIIIA (131–133). More recently, the structure of the heterotetramer, which has eluded researchers for years due to its size and complexity, has been published using more recent techniques such as atomic force microscopy (134). The X-ray structure of recombinant FXIIIA is presented in Figure 1-D (132,135,136).

The catalytic FXIIIA homodimer is responsible for the transglutaminase activity. Each A subunit is 83 kDa and consists of a 37 amino acid activation peptide, a beta-sandwich, a core domain and two beta-barrels (137). The non-catalytic

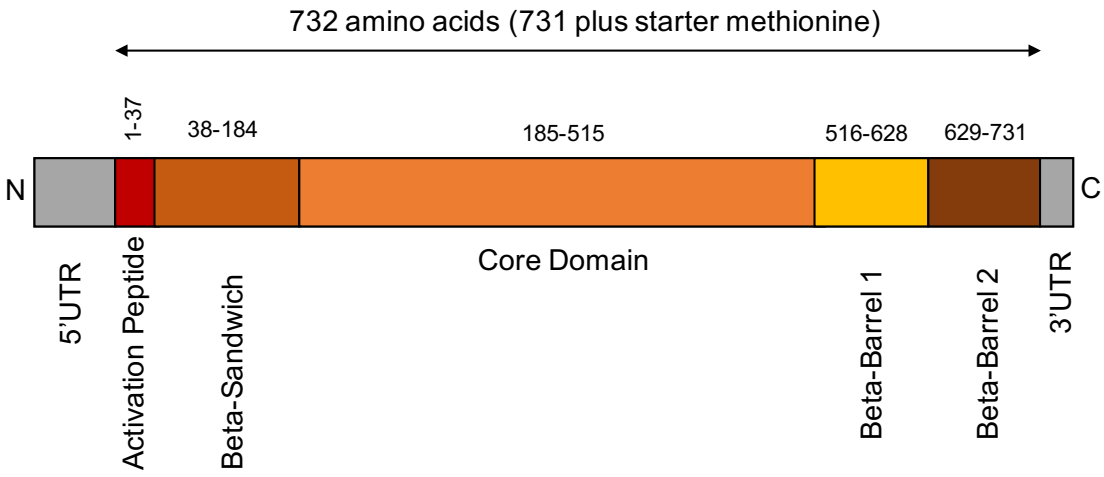

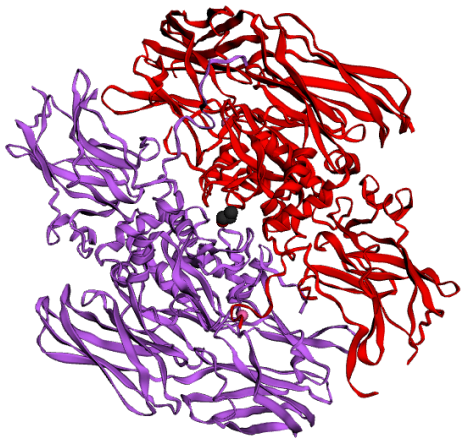

Figure 1-D: Domains and Structure of FXIIIA. Top: Schematic of the domains present with each FXIIIA subunit, with amino acid residues noted above each domain, not to scale. FXIIIA circulates as a homodimer of A-subunits. The N and C termini are flanked by untranslated regions (UTR). The activation peptide is cleaved between from the beta-sandwich between Arginine-37 and Glycine-38, by thrombin in the presence of calcium. Left: the X-ray crystallography structure of recombinant FXIIIA with two A subunits shown (Protein Database Number: P00488, ID: 1evu) , one in red and one in purple. In the centre is calcium bound in the ion site (black). This structure was visualised in the 3Dmol.js display (Nicholas Rego and David Koes 3Dmol.js: molecular visualization with WebGL Bioinformatics (2015) 31 (8): 1322-1324. doi:10.1093/bioinformatics/btu829) of the Protein Database Summary (PDBsum, EMBL-EBI, Fox *et al.* 1999 (132) Garzon *et al.* (unpublished work; 135). PDBSum ref: Laskowski RA, Jabłońska J, Pravda L, Vařeková RS, Thornton JM. PDBsum: Structural summaries of PDB entries. Protein science. 2018 Jan;27(1):129-34.

FXIIIB homodimer is made up of 10 sushi domains (138,139), synthesised in hepatocytes, was once thought to be purely protective of the FXIIIA homodimer against accidental activation within the plasma but is now considered to have a role in regulation (140) fibrinogen binding (141) and roles in other bleeding disorders (134,142). In the plasma, the heterotetramer is bound to fibrinogen (143).

1.2.2 Activation of FXIIIA

Activation of plasma Factor XIIIA requires the presence of thrombin and calcium ions (Ca^{2+}) in order to cleave the 37 amino acid activation peptide (FXIII-AP) from the N-terminus of the protein (144). The activation peptide is unique to FXIII, as none of the other transglutaminases possess one. Cleavage of the FXIII-AP and binding of calcium results in a conformational change of the FXIIIA homodimer subunit and dissociation of the FXIIIB homodimer (133,145). Change to the conformation results in the exposure of the catalytic triad: Cysteine-314, Histidine-373 and Asparagine-396 (131,146). Once the FXIII-AP is cleaved, although the X-ray crystallography structures of the inactive and activated proteins do not differ greatly, biochemical experiments have demonstrated a number of structural changes occur with various acetylation and alkylation steps resulting in FXIIIA activation, which has been nicely summarised by Komáromi and colleagues (130). The active site is located at cysteine-314. Due to the lack of crystal structure for the FXIII heterotetramer, a lot of the current knowledge heavily relies on computer modelling and biochemical assays.

Intracellular FXIII (cFXIII) does not require thrombin cleavage of the FXIII-AP for exertion of its transglutaminase activity (124,147–149). cFXIII is found in platelets (124,150), in the cytoplasm of cells of monocytes and macrophages (129), in osteoblasts where secretion leads to extracellular matrix formation within the bone (151,152) and in nuclei of macrophages culture *in vitro* (153). However, as the FXIII lacks the classical secretory signalling tags, it is still unclear how FXIII gets out of these cells. Recently, however, FXIIIA has been found to interact with endothelial cells and FXIIIA was found on the surface of platelets (150), and may be transported to the cell surface of nucleated haematopoietic cells but the exact nature of secretion still remains to be determined (154).

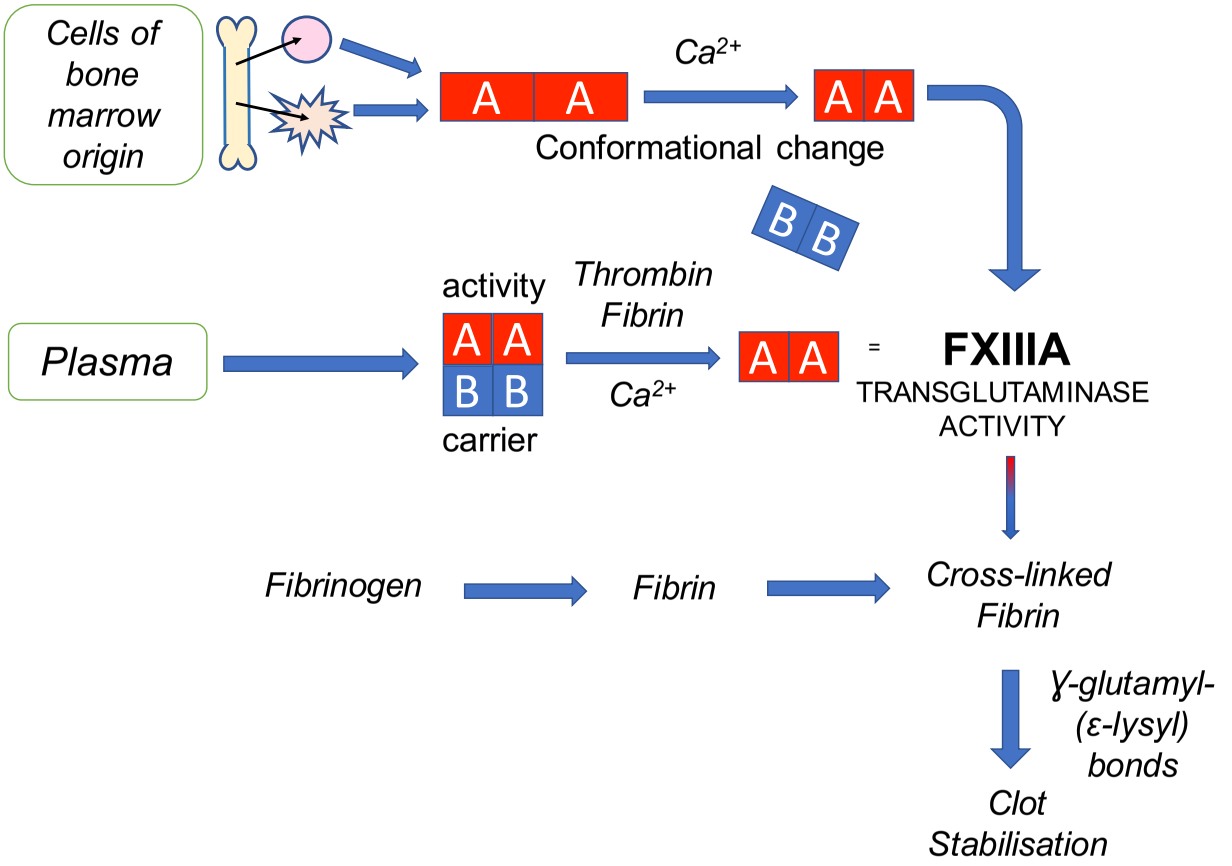

Figure 1E: Schematic of Factor XIII activation and course of action. Factor XIII (FXIII) is found in cells of bone marrow origin (cellular FXIII) and also circulates freely in the plasma (plasma FXIII). Plasma FXIII is found as a heterotetramer of two homodimers, A2 and B2. B2 acts as the carrier protein and is cleaved by thrombin in the presence of fibrin, and calcium ion presence results in activation of the FXIIIA to give rise to its transglutaminase activity. Cellular FXIII is activated by calcium ions (Ca2+) and this induces a conformational change which allows FXIIIA to exert its transglutaminase activity through crosslinking via the formaiton of isopeptide bonds (gamma-glutamyl-(epsilon-lysyl)) bonds. Adapated from Muszbek et al. 2011 (164).

Once FXIIIA is activated, it is able to crosslink a variety of substrates including fibrin, vitronectin, collagen, and fibronectin (155). Although fully summarized by Ariëns and colleagues in their review of fibrin clot formation, in short, the transglutaminase activity forms isopeptide bonds between substrate monomers to form complex molecular matrices (156,157). A complex is formed between protein-bound glutamine residue and the catalytic triad, resulting in the release of ammonia when a thioester bond is made between the glutamine and active site (158). This highly reactive thioester bond and will react with an acyl-acceptor amine such as a primary amine, polyamine or protein-bound lysine which forms the final isopeptide bond (156,159–161). A summary of the cross-linking of fibrin in shown in Figure 1-F (161). FXIIIA often becomes crosslinked within the matrices, and is also able to bind inhibitors of fibrinolysis such as a2-antiplasminogen (155,162). Over 100 potentially reactive glutamine residues have been identified with which FXIIIA may interact (155,163).

1.2.3 The Roles of FXIIIA

1.2.3.1 Pregnancy and Miscarriage

FXIIIA has numerous roles, well summarised in the 2011 review of Factor XIII by Muszbek and colleagues (164), in addition to the previously mentioned cross-linking and subsequent stabilisation of fibrin clots. FXIIIA is necessary for the maintenance of pregnancy due to its role in healthy placental development (13,165–168). Mutations within the gene for FXIIIA (Section 1.2.4) can result in FXIII deficiency and patients suffer recurrent miscarriage, and this symptom often leads to the initial diagnosis of FXIII deficiency (169). The 34Leu variant from the single nucleotide polymorphism (SNP) Val34Leu has been associated with recurrent miscarriage and reviewed several times in the recent literature (170–172). The polymorphism Tyr204Phe has also been associated with miscarriage (166).

1.2.3.2 Inflammation and Associated Disease

FXIII is also involved in inflammation and immune-response (173,174), as FXIIIA is highly expressed in monocytes and macrophages. An upregulation of FXIIIA mRNA was identified in macrophages stimulated with interleukin-4 (IL-4) (representing the alternative pathway for macrophages) with protein expression 11-fold higher than baseline on day 5 of cell culture (175). Stimulation of the ‘classical’ activation pathway for macrophages in this same study resulted in a

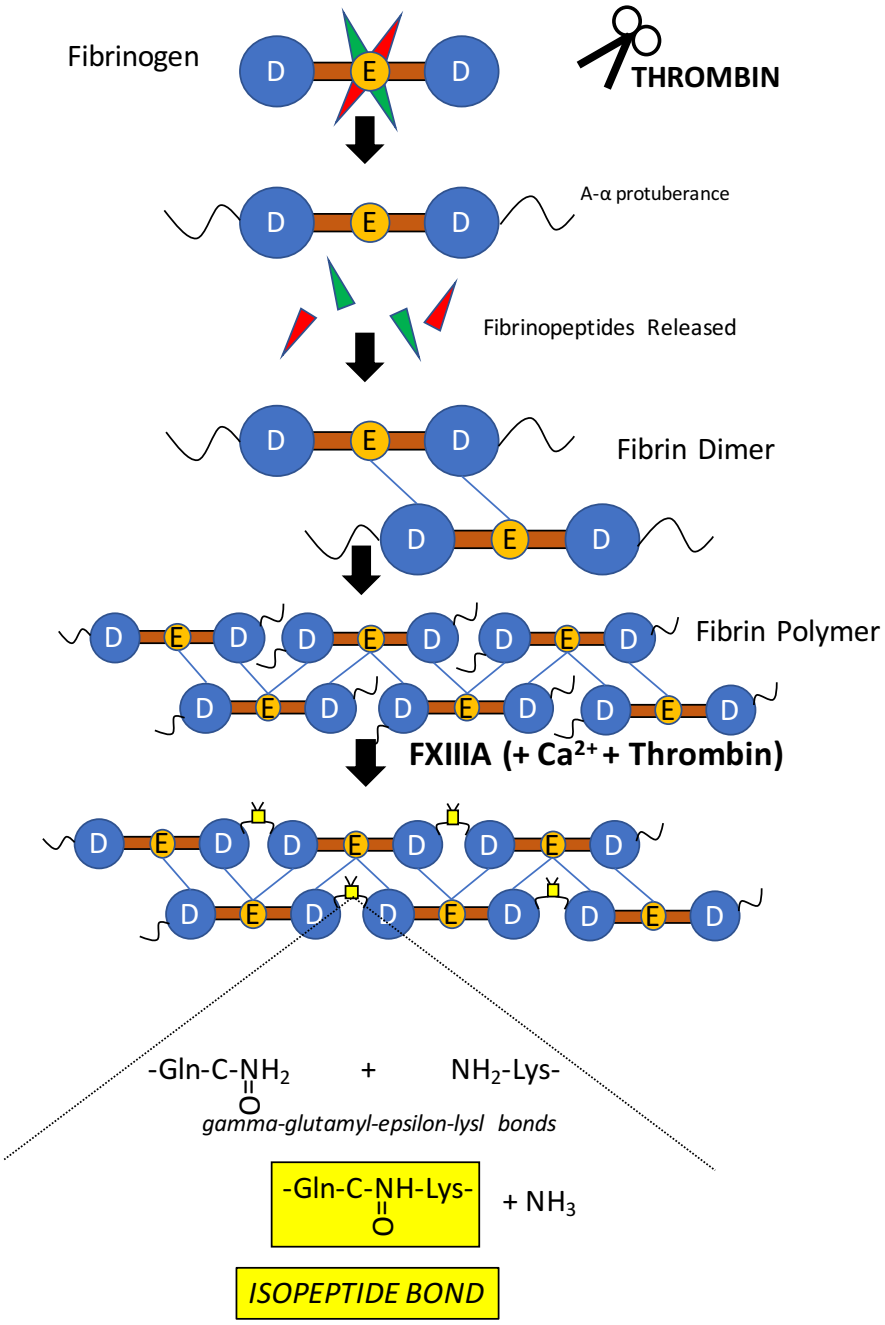

Figure 1-F: Cartoon of Fibrin Crosslinking by Factor XIIIA. As well as activating the transglutaminase, FXIIIA, thrombin cleaves fibrinogen into its fibrin monomers, resulting in the release of fibrinopeptides. Fibrin monomers rapidly form dimers through bonds between their E and D subunits. Fibrin polymers are formed though the crosslinking reaction catalysed by transglutaminases such as FXIIIA. Adapted from Shi and Wang (2017) (161).

downregulation of FXIIIA mRNA. FXIIIA has been associated with inflammatory disease such as arthritis (176), asthma (177), ulcerative colitis (174) and necrotizing enterocolitis (178).

Coagulation factors, including FXIIIA, have been linked to osteoclast deposition of bone matrices (151,152) and inflammation which can lead to progression in inflammatory arthritis. Collagen makes up a large percentage of the bone matrix and fibrinogen circulating in the plasma forms the majority of the fibrin-component (179,180) and is a substrate for both transglutaminase-2 (TGM2) and FXIIIA (181). Elimination of FXIIIA limited the development and progression of arthritis through a decrease in pro-inflammatory cytokines interleukin-6 (IL-6) and interleukin 1-beta (IL-1b) and a decrease in pro-osteoclast differentiation by nuclear factor-kB ligand (RANKL) (176). However, some have found that bone mineralisation and deposition is unaffected in FXIIIA -/- mice (182), and suggest that the role of FXIIIA may instead be involved in degradation of the matrix rather than bone mineralization. A lack of FXIIIA also increased bone marrow adipogenesis and in FXIIIA -/- mice plasma fibrinogen was retained in the serum and the bone marrow instead of bone deposition (181). The role of FXIIIA in inflammatory diseases such as arthritis requires further exploration as the precise signalling and effects on disease remain to be fully understood.

1.2.3.3 Angiogenesis

FXIIIA is involved in the promotion of angiogenic signalling, (Figure 1-G). Angiogenesis is not to be confused with neovasculogenesis, as angiogenesis is recruitment of an already established blood supply rather development of new vessels such as in embryogenesis (183). Dardik and colleagues have performed most of the experiments and developed the hypotheses surrounding the molecular mechanisms through which FXIIIA exerts its angiogenic effect (184). As FXIII was already demonstrated to be vital for pregnancy, tissue remodelling and wound-healing, Dardik *et al.* hypothesised that FXIII was having an effect on angiogenic signalling, as angiogenesis is an important component for these processes (185). Stimulation of human umbilical vein endothelial cells (HUVECs) with activated FXIIIA identified that FXIIIA increased HUVEC migration in Boyden chamber and wound-migration assays.

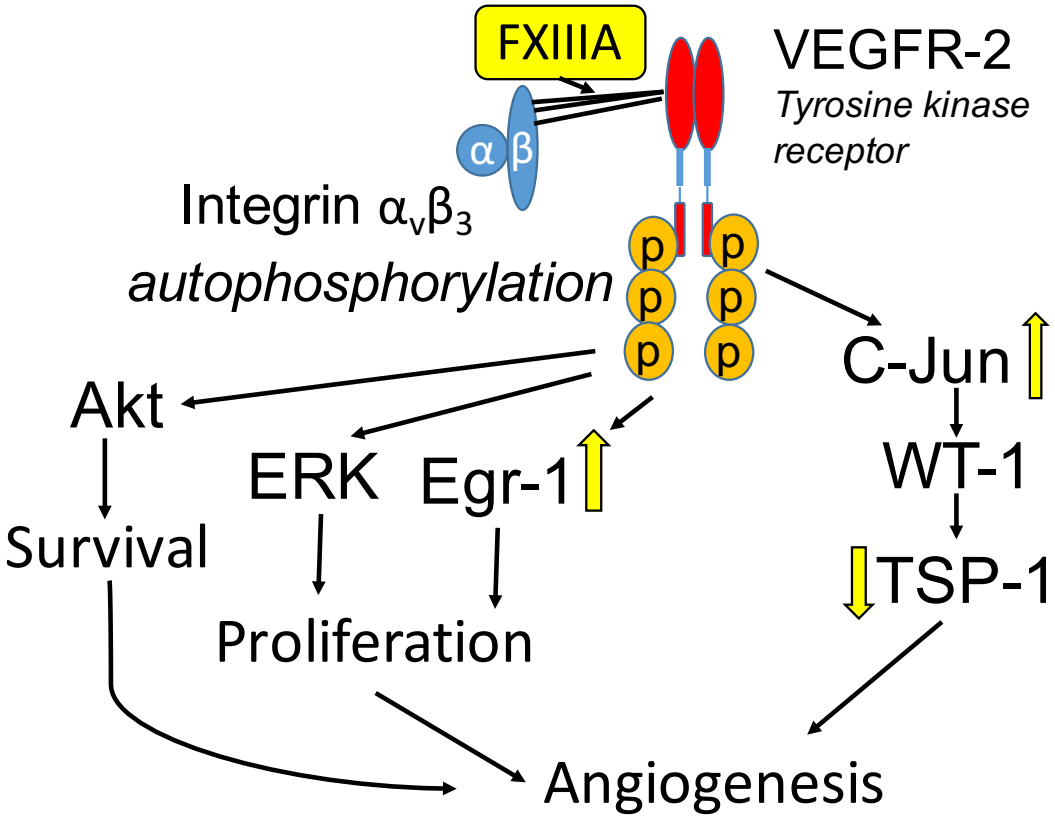

Figure 1-G: The role of Factor XIIIA in the promotion of angiogenic signalling. Active FXIIIA crosslinks the of the β3 portion of the integrin αvβ3 to the tyrosine kinase receptor, VEGFR2, to form a non-covalent complex which results in phosphorylation i.e. activation or the receptor. Phosphorylation of the tyrosine kinase receptor (RTK) leads to the phosphorylation of pro-proliferative and pro-survival signalling, with demonstrated upregulation of Egr-1 (yellow arrows). There is also upregulation of c-Jun, resulting in a cascade of signalling which inhibits TSP-1, an inhibitor of angiogenesis, which leads to the promotion of angiogenesis. Abbreviations: protein kinase B (Akt), extracellular signal-related kinases (ERK), early growth response protein-1 (Egr-1), Wilm's Tumour progein (WT-1), thrombospondin-1 (TSP-1), vascular endothelial-like growth factor-2 (VEGFR2). Adapted from Dardik *et al.* 2006 (186).

FXIIIA-treated HUVECs also exhibited a decrease in apoptosis and an increase in survival. Analysis of mRNA identified near complete absence of mRNA for thrombospondin-1 (TSP-1), an inhibitor of angiogenic signalling, suggesting that FXIIIA promotes angiogenesis through downregulation of a key system brake. Experiments performed *in vivo* on rabbit corneas by the same team also resulted a visible increase in blood vessel formation, and immunohistochemical staining demonstrated positive TSP-1 staining in stromal fibroblasts which were negative for staining in the FXIIIA-treated corneas. Subsequent co-immunoprecipitation experiments later on, revealed FXIIIA mediated the crosslinking of the β3 portion of the integrin αvβ3 to the vascular endothelial-like growth factor receptor-2 (VEGFR2) and led to phosphorylation of VEGFR2 (187). The formation of the complex was dependent on the transglutaminase activity of FXIIIA.

Classical activation of the VEGFR2 by vascular endothelial-like growth factor-A (VEGFA) is traditionally how angiogenic signalling is thought to be promoted, and indeed the kinetics of the VEGFA-induced VEGFR2 phosphorylation are faster than FXIIIA-induced VEGFR2 phosphorylation, but Dardik *et al.*'s work suggested that FXIIIA crosslinking of the integrin and receptor was important in maintenance of the angiogenic signalling. FXIIIA was unable to enhance the maximal VEGFA-induced proliferation and cell migration seen in HUVECS and FXIIIA did not increase the amounts of VEGFA or VEGFR2 protein (187). Further work, in the same 2005 study, through mRNA and protein expression analysis via Western Blot detailed the effects of FXIIIA-induced VEGFR2 phosphorylation on angiogenic signalling, (Figure 1-G).

1.2.4 Gene

The gene for Factor XIIIA, *F13A1*, is found on chromosome 6 (p24- 25) and is comprised of 15 exons and encode for the 83 kDa Factor XIIIA subunit. Two of these subunits make up the Factor XIIIA homodimer which is responsible for the catalytic activity of the protein. The *F13A1* gene is highly polymorphic, but only a handful of SNPs are present >1% in the normal population and have been investigated for their contribution to diseases and deficiency of FXIII.

1.2.4.1 SNP Numbering

Numbering of single nucleotide polymorphisms in this thesis will follow numbering with the starter methionine (ATG= 0) (164), (Figure 1-H).

1.2.4.2 Important SNPS in *F13A1*

There are several common non-synonymous SNPs within the *F13A1* gene, (Table 1-H,C). The 5 commonly researched are: 103G>T, Val34Leu:(rs5985); 614A>T, Tyr204Phe:(rs3024477); 1694C>T, Pro564Leu:(rs5982); 1951G>A, Val650Ile:(rs5987); and 1954G>C, Glu651Gln:(rs5988). The promoter region SNP -246G>A (-2331 bases from the translation start codon) with a rare allele frequency of 0.27 was not included in this thesis due to lack of lack of information on its associations with disease and its biochemical/molecular interactions/consequences. The SNP T1766A (L588Q) in exon 13 also has a rare allele frequency of 3%, and no work to date has associated it with disease (188).

These SNPs have been investigated for associations with numerous diseases, discussed further in Sections 1.2.5 and 1.2.6, and how they influence the levels and activity of FXIIIA (166,189). Leu34, Tyr204 and Leu564 variants were associated with high specific activity of FXIIIA (166). Leu564 was also associated with low plasma levels (189). Amino acid changes at the 650 and 651 codons appeared to have very little effect on the specific activity of FXIIIA. An earlier study by Kohler *et al*. also found 34Leu to be associated with higher crosslinking activity (190), likely due to an increase in the cleavage rate by thrombin for this variant (191). In a linkage study, the only main functional polymorphism which affected FXIIIA activity was 103G>T (Val34Leu) (192).

1.2.5 FXIII and Thrombotic Disease

Polymorphisms within *F13A1* have been linked to numerous thrombotic diseases, such as ischaemic stroke (IS) (193,194), deep vein thrombosis (DVT) (195,196) and myocardial infarction (MI) (197,198). The crosslinking of fibrin gamma and alpha monomers forms stable clots at sites of wound-healing (156,157,194). Crosslinks increase the stiffness of the clot and crosslinking of plasma proteins

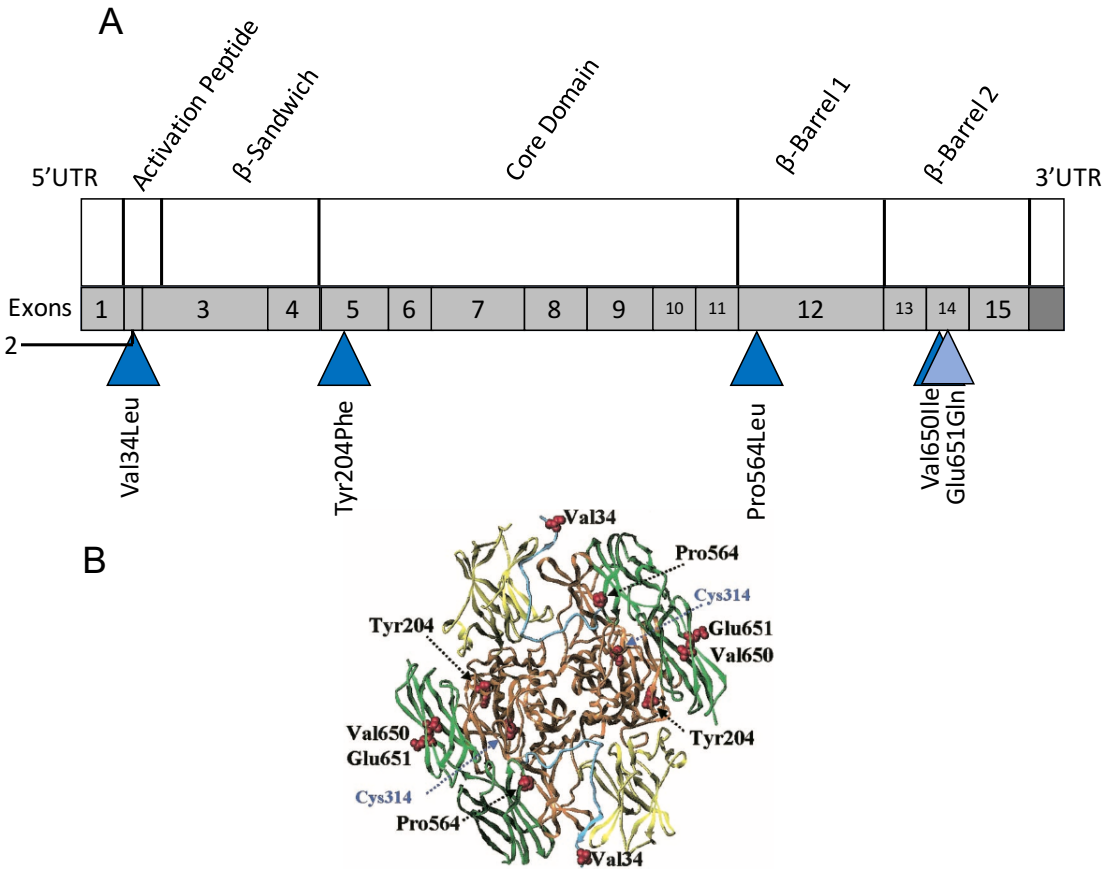

C

Frequent Single Nucleotide Polymorphisms (SNPs) in *F13A1*				
SNP	**rs Number**	**Amino Acid Change**	***F13A1* Exon**	**Allele Frequency**
103G>T	rs5985	Val34Leu	2	0.76/0.24
614A>T	rs3024477	Tyr204Phe	5	0.97/0.03
1694C>T	rs5982	Pro564Leu	12	0.79/0.21
1951G>A	rs5987	Val650Ile	14	0.95/0.05
1954C>T	rs5988	Glu651Gln	14	0.78/0.22

Figure 1-H: Location of Common Single Nucleotide Polymorphisms in the *F13A1* gene. (A) Schematic diagram of single nucleotide polymorphism locations with respect to the domains within the FXIIIA protein, adapted from Muszbek *et al.* 2011. (B) Location of SNPs with respect to the secondary structure of the FXIIIA protein. This diagram was republished with permission of American Society of Hematology from Ariëns *et al*. 100(3) 2002; permission conveyed through Copyright Clearance Centre, Inc. The image from Ariëns *et al* used the x-ray crystallography coordinates from Weiss *et al.* (1998). (C) A table of SNPs with an allele frequency > 1% in the normal population. Allele frequencies were acquired from the genome aggregation database (gnomAD, https://gnomad.broadinstitute.org) for a European population.

such as α2-antiplasmin and type-2 plasminogen-activator inhibitor to fibrin prevent it's degradation (162,199,200).

Contraction of FXIII-deficient clots appeared to have impaired clot retraction (201–203) but results have proved to be mixed in conclusion. Some concern lay in the experimental methodologies as cystamine, an inhibitor of transglutaminases, and used in clot contraction studies and may have decreased thrombin activity so differences seen may because of altered thrombin, which affected fibrinogen cleavage and FXIIIA activation, both heavily involved in clot formation (204). Composition of the clots may be affected by FXIIIA as deficiency led to an decrease in the red blood cell (RBC) content of thrombi due to changed clot elasticity and a loss of RBC trapping (205–207).

The SNPs 103G>T (Val34Leu) and 1694C>T (Pro564Leu) have been associated with ischemic stroke (208), The 34Leu variant produced tighter crosslinking (191) which alters clot stiffness as composition, as mentioned above, and this may lead to clots which are more difficult to break down (209). It is not just polymorphisms which may contribute to thrombotic disease, as levels and activity of FXIII in patients with early stage DVT or patients with pulmonary embolisms (PE) were significantly decreased (196,210). It was suggested that the decrease seen in D-dimer, a product of crosslinked fibrin, and plasma fibrinogen levels meant that in PE coagulation factor consumption was higher. However, the findings of the Val34Leu contribution to thrombotic risk has been debated. Some protective effects of Leu-carriers, limited to men, have been seen by Van Hylckama and colleagues (196). In a large meta-analysis of 3807 cases and 4993 controls found a very weak to no association between the Val34Leu polymorphism and ischemic stroke (193). Therefore, a greater breadth of studies is required to establish links between FXIIIA polymorphisms and ischemic stroke and thrombotic disease risks.

1.2.6 Factor XIII and Cancer

Transglutaminases, including FXIII, have been explored in cancer (211). Factor XIII has been explored in several cancer types in terms of its activity, plasma levels, protein expression and mutational status, with quite varying results with regard to its contribution to cancer prognosis. Lower levels of plasma FXIII were

seen in breast cancer and melanoma, compared to other tumours (212). Bone metastases have higher levels of FXIIIA compared to liver and lymph nodes metastases when studied in prostate cancer-associated metastases (213), and was hypothesised to be involved in angiogenic recruitment. FXIIIA activity levels were higher in patients with advanced non-small cell lung cancer (NSCLC) compared to early-stage and healthy control patients (214). However, a study of B-cell lymphoblastic leukaemia found that positive FXIIIA expression levels within B-cell lineage leukemic lymphoblasts (215), measured by flow-cytometry, was associated with long term survival indicating a benefit of FXIIIA to cancer prognosis (216). Earlier studies had established FXIIIA as marker of mono- and megakaryocytic acute myeloid leukaemia and chronic myelomonocytic leukaemia, but little is known about the influence of FXIIIA on survival for these types of leukaemia (217,218). With respect to FXIIIA polymorphisms, heterozygous patients for Val34Leu had a decreased risk of colorectal cancer (219) but heterozygotes and homozygous Leu-carriers for the SNP had an increased risk of oral cancer development (220).

1.2.6.1 Factor XIII and Ovarian Cancer

Investigations into FXIIIA with respect to OC have been limited in sample size, but did result in some interesting hypotheses. FXIIIA plasma levels were measured in a small study of 58 patients with malignant (n=32) or benign tumours (n=26) (221). Of these patients, 9 had evidence of metastases in lymph nodes or in peritoneal tissues. This set of 58 patients were compared to an age-matched healthy control group of women (n=31). Plasma FXIIIA levels were significantly higher in those with tumours, including benign and malignant tumours, compared to the healthy control group. It was hypothesised that FXIIIA may be released by cells within the tumour. However, malignant tumours that had metastasized had significantly lower levels compared to non-metastatic tumours. It was hypothesised that this may be due to the consumption of FXIIIA during the crosslinking to form the tumour matrices. Van Wersch noted that earlier work had established an increase in coagulation activation and reactive fibrinolysis in gynaecological tumours.

Van Wersch also suggested that the decrease in metastatic OC tumours maybe due to the degradation of FXIIIA by granulocyte proteases in the tumour microenvironment, although levels of granulocyte proteases were not measured

in this study. Interestingly, plasma fibrinogen levels measured in this same study, did not significantly differ between healthy controls, benign, non-metastatic and metastatic disease. This suggested that the decrease in FXIIIA plasma levels was more due to consumption during matrix crosslinking of other proteins or perhaps FXIIIA was exerting another role in metastatic OC.

1.3 Development of the PhD Project

The work, albeit limited, by van Wersch *et al.* established that Factor XIII may have a role in ovarian cancer (OC), particularly for metastatic disease. Decreased plasma levels in metastatic tumours compared to benign disease suggests that Factor XIII may be being used up whilst exerting an affect. Further work was required to elucidate the role Factor XIII may be having in OC. Up until this point however, very little work was undertaken to explore FXIII in OC. Fibrin has been identified in the lining of the peritoneum and ascites of tumour-bearing mice (222). Microvasculature in the tumours studied also allowed for deposition of fibrinogen, suggesting a link between fibrin deposition and the initiation of angiogenesis and tumour stroma (222). A crosslinked fibrin matrix is very important for the development of an angiogenic network and has been explored in matrices with different components and fibrin densities (223–225). Given the associations between polymorphisms in FXIIIA and other cancers, a gap opened up in the literature for a more in-depth study, exploring a different facet of FXIII contribution to OC.

1.3.1 The Edinburgh Leeds Oxford (ELO) Patient Cohort

The Anwar Lab at the University of Leeds proceeded to undertake a multicentre study of OC patients from Edinburgh, Leeds and Oxford (ELO) (n=612, Table 1-3). Patient genotypes were analysed for SNPs within *F13A1* and the cohort was examined for associations between prognostic factors in OC and overall survival (OS) which ultimately formed the foundation of this PhD Project. The key findings of this study identified associations between OS and two *F13A1* SNPs 1951G>A and 1954G>C. These SNPs had not been previously associated with disease

Table 1-3: Distribution of Prognostic Factors from the ELO Cohort of Ovarian Cancer Patients (n=629)

	Edinburgh (n = 269)	Leeds (n = 258)	Oxford (n = 102)	Total (n = 629)
Age at entry into study, Yrs				
Mean	61.5	62.1	60.5	61.5
Median	63.0	61.0	63.0	62.0
Range	31-88	29-89	22-84	22-89
Age at diagnosis, Yrs				
Mean	59.4	59.5	58.2	59.2
Median	60.0	59.0	60.0	60.0
Range	28-88	25-88	22-79	22-88
FIGO Stage at diagnosis (%)				
I	24.2	16.7	25.5	21.3
II	12.6	12.8	12.7	12.7
III	49.8	55.0	47.1	51.5
IV	11.9	14.0	14.7	13.2
Unknown	1.5	1.6	0.0	1.3
Tumour grade (%)				
I	7.1	7.0	39.2	12.2
II	25.7	20.5	33.3	24.8
III	63.2	45.3	26.5	49.9
Unclassified	4.1	27.1	1.0	13.0
Histology (%)				
Serous	52.4	40.7	55.9	48.2
Endometriod	25.7	20.2	27.5	23.7
Clear cell	9.3	8.9	4.9	8.4
Other	6.3	22.1	5.9	12.7
Unclassified	6.3	8.1	5.9	7.0

The median age at diagnosis was 60 years but the median age into the study was 62 years of age, therefore on average and prior entry to the study, patients had survived for two years. Other histologies comprised mucinous, mixed cell, undifferentiated, mullerian mixed and translational cell carcinomas and adenocarcinomas. FIGO (International Federation of Gynaecology and Obstetrics). Table from Anwar R *et al*. Coagulation factor XIIIA and cancer (unpublished manuscript).

phenotypes and demonstrated to not have any significant effect on levels or specific activity of FXIIIA (166). These two SNPs are found in complete linkage disequilibrium with one another: 1951A is not found without 1954C, however 1954C can be found on its own.

Carriage of 1951A was significantly associated with geographical location (p=0.001) and tumour histology (p=0.001). In univariate survival analysis, carriers of the alternative allele 1951A (G/A and A/A) demonstrated a poorer prognosis compared to wildtype individuals (p=0.004), whereas carriers of 1954C (where 1951G>A genotype was wildtype (G/G)) appeared to have a better prognosis, although not significantly so, compared to wildtype individuals (p=0.087), (Table 1-4). Upon exploration in multivariate modelling via a Cox Proportional Hazards Regression Model, (Figure 1-I and Table 1-5), both 1951G>A and 1954G>C were significant predictors of overall survival. Patients who carried the alternative allele for SNP 1951G>A (G/A or A/A) were twice as likely to die compared to wildtype patients (HR=2.10, p=0.002, 95% CI: 1.32-3.33). In contrast, 1954C carriers (G/C or C/C) had a significant benefit to their OS with a hazard ratio <1.00 (HR=0.6, p=0.003, 95% CI: 0.42-0.84).

1.3.1.1 Mature Survival Data: The Leeds Sub-cohort

Mature survival data was available for the Leeds sub-cohort of the ELO cohort of OC patients and presented an opportunity to demonstrate whether the associations seen in the initial analysis held for long term survival follow-up. Long term follow-up is very valuable to cancer studies as analyses can be repeated to see how associations may change over time i.e. is the benefit of a SNP only beneficial up until a certain time, and then its benefit is lost? By exploring the mature survival data, the respective detriment and benefit to overall survival of 1951G>A and 1954G>C can be tested to assess their contribution to long term survival, as OC is typically followed up for many years if first-line therapy and subsequent treatments are successful.

1.3.2 ICON7

It was clear that any associations between *F13A1* SNPs and ovarian cancer would have to be repeated in another cohort of patients, but ideally, a newly diagnosed cohort of women. This cohort would remove the inherent bias towards

Table 1-4: Summary of Univariate Survival Analysis in ELO Cohort

Factor	Total (n)	Dead [n (%)]	Censored [n (%)]	Median OS	*p*
1951G>A[‡§]					0.004
G/G	554	179 (32.3)	375 (67.7)	7.8 (6.0, 9.6)	
G/A or A/A	66	33 (50.0)	33 (50.0)	3.9 (3.1, 4.8)	
1954G>C					0.676
G/G	362	127 (35.1)	235 (64.9)	7.2 (5.6, 8.7)	
G/C or C/C	258	85 (33.0)	173 (67.0)	7.5 (4.7, 10.3)	
1954G>C[‖]					0.087
G/G	362	127 (35.1)	235 (64.9)	7.2 (5.6, 8.7)	
G/C or C/C	192	52 (27.1)	140 (72.9)	10.9 (5.0, 16.7)	

The table above demonstrates the total number of patients per genotype, the % dead, % censored/alive at the end of follow-up and the median overall survival (OS) with the lower and uppermost values for OS given in parentheses. The **bold 1954G>C** presents the cases that were all homozygous at 1951G>A (G/G) and therefore represent s the benefit of 1954C on its own with overall survival in univariate analysis. P-values considered significant if p<0.05. Taken from Anwar R *et al*. Coagulation factor XIIIA and cancer (unpublished manuscript).

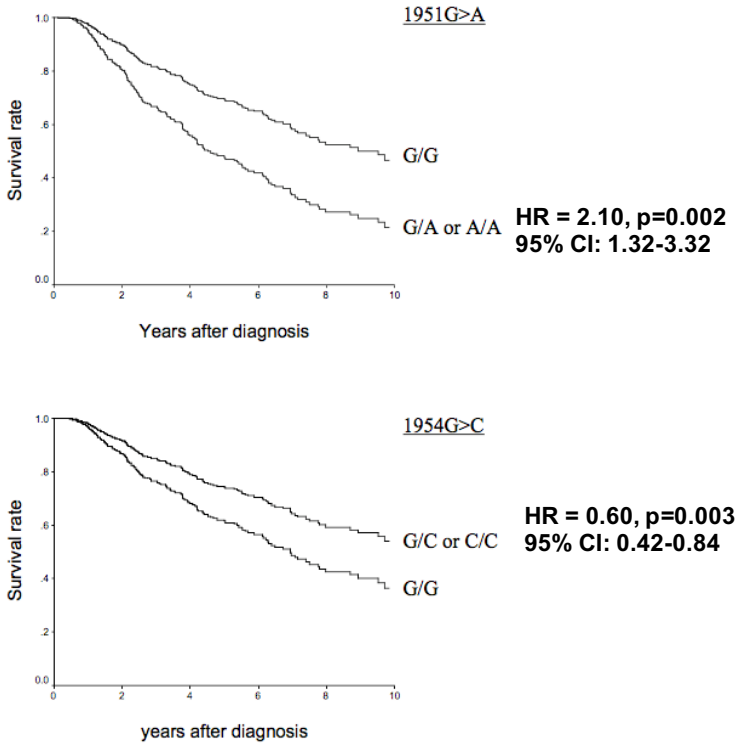

Figure 1-I: Survivor function plots from the Cox Model generated for the ELO Cohort to demonstrate overall survival for carriers of the *F13A1* SNPs 1951G>A and 1954G>C**.** Hazard Ratios (HR) and 95% Confidence Intervals (CI) are given for each plot. Carriage of the alternative A allele at 1951G>A resulted in a poorer overall survival compared to wildtype patients. Carriage of the alternative C allele at 1954G>C resulted in improved overall survival compared to wildtype patients. These two SNPs are in complete linkage disequilibrium with one another: 1951A is not found without 1954C, but 1954C can be found on its own, but SNPs were plotted separately to clearly demonstrate their respective effects. Figures taken from Anwar R *et al*. Coagulation factor XIIIA and cancer (unpublished manuscript)

Table 1-5: Cox Proportional Hazards Regression Model for ELO Cohort

Prognostic factors	Total (n)	HR[†]	95% CI[‡]	*P*
Age at Diagnosis, yrs				<0.000
44 or under	55	1.00		
45-54	153	1.41	0.73 to 2.70	0.305
55-64	195	1.40	0.74 to 2.61	0.300
65-74	153	2.18	1.15 to 4.14	0.017
75 or over	56	3.80	1.85 to 7.79	0.000
FIGO Stage[§]				<0.000
I	131	1.00		
II	80	2.01	0.89 to 4.55	0.092
III	320	5.99	3.11 to 11.52	<0.000
IV	81	11.78	5.91 to 23.51	<0.000
Histology				0.008
Serous	297	1.00		
Endometriod	147	0.49	0.33 to 0.74	<0.001
Clear Cell	51	1.13	0.55 to 2.32	0.746
Other	76	1.06	0.68 to 1.64	0.798
Unclassified	41	1.18	0.69 to 2.01	0.554
1951G>A				0.002
G/G	547	1.00		
G/A or A/A	65	2.10	1.32 to 3.33	0.002
1954G>C				0.003
G/G	356	1.00		
G/C or C/C	256	0.60	0.42 to 0.84	0.003

The Cox Proportional Hazards Regression Model was used to calculate hazard ratios (HR) and to test the significance of covariates as predictors of overall survival. Eight cases for which FIGO (international Federation of Gynaecology and Obstetrics) stage was unknown were excluded from the model. The analysis was stratified by 'centre'. Age at diagnosis was treated as a continuous variable. A stepwise regression methodology to systematically remove non-significant covariates from the model until only significant covariates as predictors of survival remained. A hazard ratio >1 indicates an increased risk of death compared to the baseline covariate (HR=1.00), and a hazard ratio <1 indicates a decreased risk of death compared to the baseline covariate. 95% confidence intervals (CI) are provided, and p-values were considered significant if $p<0.05$. Taken from Anwar R *et al*. Coagulation factor XIIIA and cancer (unpublished manuscript).

survivors of at least two years, which was present in the ELO Cohort, and noted in the long median survival of 7.2 years. A newly diagnosed cohort of patients was available through the ICON7 clinical trial, which compared treatment arms: 1) the addition of bevacizumab (7.5 mg/kg given for 12 months, every 3 weeks), a monoclonal antibody against all isoforms VEGFA, to the standard OC treatment regimen of carboplatin (AUC 5 or 6, AUC= area under curve, based on the Calvert Formula (226,227), every 3 weeks for 6 cycles) and paclitaxel (175 mg/m^2, every 3 weeks for 6 cycles); 2) carboplatin and paclitaxel only in the aforementioned dosing schedule (78). A sub-cohort of the full cohort (n=448) consented for their blood and tissues samples to be used in translational research, and these samples were available for study in this PhD project.

The ICON7 trial (n=1528) outcomes demonstrated a significant benefit of only 1.7 months in median progression free survival (17.3 month for chemotherapy alone vs. 19.0 months for bevacizumab and chemotherapy, HR=0.81, 95% CI: 0.70-.94, p=0.004). Women at high risk of disease progression (a novel variable defined as women with inoperable or with >1 cm of disease margin remaining post-surgery and/or FIGO Stage IIIC/IV disease) responded better in terms of median PFS with a benefit of 5.4 month for those treated with bevacizumab, compared to those treated with chemotherapy alone (HR=0.68, 95% CI: 0.55-0.85, p<0.001). After completion of follow-up for those in the clinical trial, Oza and colleagues presented the final findings of the ICON7 trial for the survival intervals measured: PFS and OS (79). Progression-free survival findings complemented the initial analysis (78), although there was a reduced effect with the extended follow up (log rank test, p=0.25) in the high risk group. No overall survival benefit was identified when the whole trial was analysed, but a benefit to OS was seen for women with high risk of disease progression (restricted mean survival time 34.5 months for standard chemotherapy and 39.3 months for additional bevacizumab (log rank test p=0.03)).

The reason why women with high risk of disease progression benefited with bevacizumab over those who were not at high risk, presents hypotheses regarding potential interactions between bevacizumab and advanced cancer or differences between the risk states of the patients that make them more responsive to the anti-angiogenic therapy.. Although there are many processes

and proteins involved in angiogenesis and therapeutic response, one protein which could be contributing is Factor XIIIA. It has already been established that plasma levels of FXIIIA are increased in patients with OC, and lower in metastatic compared to non-metastatic disease (221) and that FXIIIA has a role in pro-angiogenic signalling by crosslinking integrin avb3 to VEGFR2, the same tyrosine kinase receptor that VEGFA, the target of bevacizumab, activates. FXIIIA may be influencing the tumour microenvironment, either through crosslinking tumour matrices or through an effect of the angiogenic receptor cross-linking, in such a way that makes bevacizumab treatment more successful in those at high risk of disease progression.

The ELO cohort study by the Anwar Lab identified that carriage of the 1951G>A polymorphism results in poorer overall survival, meaning that these patients are more likely to progress in their disease. Therefore, is it possible that 1951G>A is associated with higher risk disease and do women with this SNP respond better to bevacizumab? 1954G>C which appears protective may be associated with lower risk of disease progression. FXIIIA variants do influence levels, activity and structure of the crosslinked products, and to date, no studies have been performed to investigate the effect that these variants may be having in OC. These variants may be influencing therapeutic response in some manner yet to be understood.

Therefore, it was important to explore the FXIIIA variants in the available sub-cohort of OC patients from the ICON7 clinical trial (n=448), and to test whether the variants of FXIIIA were associated with prognostic factors and survival intervals in OC. This work would confirm the findings seen in the ELO Cohort by Anwar *et al.* and could shed light on how, if at all, FXIIIA is affecting OC and whether variants are associated with therapeutic response to bevacizumab or to the standard chemotherapy regimen. Tissues, set into tissue microarrays were also available from the ICON7 sub-cohort and this would be the first study to stain for FXIIIA protein in OC to determine whether the protein is present, and if so, to what extent and in which locations. Associations between FXIIIA variants and levels of staining could also be tested for, which again, would make this one of the first studies to do so in OC. From these findings, there would be potential to explore FXIIIA in *in vitro* experiments to test whether variants could be influencing

vital cancer processes such as angiogenesis. Even if 1951G>A and 1954G>C FXIIIA variants are not associated directly with survival intervals or therapeutic response in the ICON7 cohort, the breadth of the available variables within the clinical data mean that novel associations may be identified.

1.3.3 Key Questions and Aims for this PhD

- **Aim:** Are *F13A1* SNPs of value for long-term survival?

  Hypothesis: SNPs 1951G>A and 1954>C will maintain their respective influences on survival in long term follow-up.

- **Aim:** Are *F13A1* SNPs associated with OC prognostic factors, survival intervals and therapeutic response in a newly diagnosed cohort of women?

  Hypotheses: FXIIIA variants are associated with OC prognostic factors, survival intervals and therapeutic response. As this is a newly diagnosed cohort of women, novel associations, particularly for early survival may be found. It would be expected that 1951G>A and 1954G>C would have their respective detrimental and beneficial effect on OS in the newly diagnosed cohort of women.

- **Aim:** Is FXIIIA expressed in OC tissues and if so, is expression associated with prognostic factors, survival or therapeutic response?

  Hypothesis: FXIIIA will be highly expressed in OC stroma, given it's role as a crosslinker of cancer associated extracellular matrix proteins and role in angiogenesis. It also may be expressed in tumour-associated immune cells given the expression of cFXIII in monocytes and macrophages

- **Aim:** Are the variants of FXIIIA influencing cancer associated molecular events such as angiogenesis?

Hypotheses: Based on the results from the clinical data cohorts (ELO and ICON7), and the tissue expression analysis, is it possible that if FXIIIA is affecting survival intervals either through its variants or very presence, could it be influencing angiogenesis? Even in the absence of direct influence on OC outcome, these experiments are still worth performing as the influence of FXIIIA variants on its role in angiogenesis is yet to be explored.

Chapter 2: Materials and Methods

2.1 Patient Samples

2.1.1 Peripheral Blood DNAs

Peripheral blood DNAs for patients from the Leeds Cohort were extracted from fully consenting patients by E. Valleley and L. Gallivan, University of Leeds. Ethics approval was granted by the Leeds Clinical Research Ethics Committee: Project No: 00/189 (Appendix 1). Peripheral blood DNA samples from the ICON7 translation cohort were kindly provided by the Medical Research Council (MRC) Council ICON7 Trial Biorepository (n=448) at University College London. Samples were provided at a DNA concentration of 1 µg in 20 µl (1 µl = 50 ng). Samples were diluted to 7.14 ng/µl in 10 mM Tris-HCL pH 7.5 (10 µl of stock DNA (500 ng) + 60 µl of 10 mM Tris-HCl pH 7.5) and stored at -20°C. Ethical approval was granted for ICON7 samples in translational research (MREC Approval Number: 06/MRE02/52, ISTCTN: 91273375, 21/09/2006 v1) and this project was reviewed and approved by the ICON7 Committee before sample release (Appendix 1). Separate ethical approval is not required for approved projects.

2.1.2 Tissue Microarrays

Tumour/stroma microarrays were also kindly provided by the Medical Research Council ICON7 Trial. Tumour/stroma microarrays were prepared and sectioned at the University of Cambridge and 4 µm sections were cut onto SuperFrost Plus glass slides (Thermo Scientific, Fisher Scientific). Tissues were arranged into the tissue microarrays by a histopathologist at The University of Cambridge and three types of microarray were made: Tumour, Tumour and Stroma, Stroma.

2.1.3 Frozen OC Tissues

Tumour and benign frozen tissue samples were kindly provided by the Leeds Research Tissue Bank (LRTB, http://mulitrtb.leeds.ac.uk/index.php) upon approval of our project by the LRTB Committee and separate ethical approval is not required for approved projects as all samples collected have approval for translational research. These tissues were mounted on autoclaved, de-ionised MilliQ water and cut on a cryostat for slides at 7 µm sections onto SuperFrost Plus glass slides.

2.1.4 Tissues for Antibody Workup

Fully anonymised formalin-fixed paraffin-embedded tissues were kindly provided by the Pathology department (University of Leeds) for work up of the antibodies used in immunohistochemistry. All tissues were completely anonymised and had ethics in place for translational research and for workup purpose.

2.2 Common Buffers and Solutions

- **Milli-Q water (dH_2O):** filtered and deionised water, henceforth stated as dH_2O, unless water source otherwise stated.
- **Tris Buffered Saline (TBS):** A 10X working stock of TBS was made by dissolving 24 g of Tris Base (MW: 121.14 g/mol, Cat #: BP151-1, Fisher Scientific, Fairlawn, NJ, USA) and 88 g of sodium chloride (NaCl, MW: 58.44 g, Cat #: 27810.364, VWR Chemicals, Lutterworth, UK) in 800 millilitres (mL) of dH_2O, with pH adjusted to 7.6 with concentrated HCl, and then made up to a total volume of 1 litre (L) with dH_2O. A 1X working stock was made by diluted 100 mL of 10X TBS with 900 mL of dH_2O.
- **Tris Buffered Saline plus Tween (TBS-T):** 10X TBS was diluted to a 1X working stock plus 0.0125% Tween-20 (Cat #: BP337-100, Fisher Scientific, Fairlow, NJ, USA). Final molar concentration of 1X solution were 20 mN Tris and 150 mM NaCl.
- **Phosphate Buffered Saline (PBS):** 5 solid PBS tablets (Cat #: P4417-1, Sigma Aldrich) were dissolved in 1 L of dH_2O to give working 1X PBS stock solution.
- **PBS plus Tween (PBS-T):** 1X PBS plus 0.0125% Tween-20.
- **Ethylenediaminetetraacetic acid (EDTA) Buffer:** 0.1 M stock of EDTA made and pH was adjusted to 8.0 with sodium hydroxide (NaOH).
- **Tris-Acetate-EDTA Buffer for Horizontal Agarose Gel Electrophoresis:** 50X stock solution made with pH adjusted to 8.0 with sodium hydroxide. The 1X working solution final concentration was 40 mM Tris-acetate and 1 mM EDTA.
- **Nuclease Free Water:** not-DEPC treated (Cat No: AM9937 (Ambion, Fisher Scientific)
- **5% Non-fat Dried Milk in PBS for Western Blotting:** 2.5 g of skimmed milk powder (Marvel) was dissolved in 50 mL of PBS.

- **Citrate Buffer for Antigen Retrieval:** A 10 mM citrate buffer was made and pH was adjusted to 6.0 with concentrated HCl.
- **RIPA Buffer for Protein Extraction:** 150 mM sodium chloride, 1% nonidet p-40 (NP-40), 0.5% sodium deoxycholate, 0.1% sodium dodecyl sulfate (SDS) and 50 mM of pH 8.0 Tris.

2.3 PCR Amplification of Exons

2.3.1 Primers

All primers were purchased from Sigma-Aldrich and a summary of primers used in PCR can be found in Table 2-1. Primers were made up to a concentration of 100 mM with the manufacturer recommended volume of nuclease free water and stored at -20°C. Primer mastermixes of forward and reverse primers were made at 5X working concentration (10 µl of 100 mM Forward primer, 10 µl of 100 mM Reverse primer, 180 µl of nuclease-free water) and were stored at -20°C.

Table 2-1: Primer Sequences for *F13A1* Amplification

F13A1 Exon	Direction	Primer Sequence (5' to 3')	Primer Length (bp)	Annealing Temperature (AT) (℃)	Product Size (bp)
Exon 2	Forward	TAT GCA AAC GGC AAA ATG TG	20	65	384
	Reverse	ACC CCA GTG GAG ACA GAG G	19		
Exon 12	Forward	CCC AAC AAG TGC AGT ACA CG	20	63	454
	Reverse	ACG GGC AAT AAC ACC TAG CA	20		
Exon 14	Forward	TGT ATC ATA AAA CTC TAG TAA AAG TG	26	58	328
	Reverse	TGG GGA GCA GAT CTA TG	17		

2.3.2 PCR Set-up and Protocol

Each PCR Reaction was performed in a total volume of 10-20 µl with corresponding volumes of reagents adjusted accordingly. For a 10 µl reaction volume: 5 µl of HotShot Diamond PCR Mastermix (Clent Life Science, Stourbridge, UK), 2 µl of 5X primer mastermix (see Section 2.2.2) and 3 µl of peripheral blood DNA with every reaction having at least 20 ng of DNA per reaction. PCR Reactions were run for 40 cycles on a PTC-200 Thermal Cycler (MJ Research, DNA Engine, Ramsey, USA): Step 1: 96°C for 6 mins, Step 2 92°C for 2 mins, Step 3 Annealing Temperature (AT) (see Table 2-1) for 1 min, Step 4: 72°C for 1 min, cycling back through Steps 2 through 4 for 39 more cycles, followed by a final cycle for 2 mins at 92°C, 1 min at the AT, and a final extension step at 72°C for 10 mins.

2.3.3 Horizontal Gel Electrophoresis

PCR products were visualised following amplification using agarose gels via horizontal gel electrophoresis. Agarose concentrations varied between 1.5% and

3% depending on size of PCR product amplified. Agarose (Cat #: 50004, SeaKem LG Agarose, Lonza, Basel, Switzerland) was weighed out, mixed with 50X TAE and made up to the appropriate volume of water to give a final percentage of TAE which matched the agarose concentration in w/v i.e. 1.5 g of agarose plus 3 mL of 50X TAE plus 97 mL dH_2O gives a 1.5X final TAE concentration. The solution was boiled in a microwave to melt the agarose. Ethidium bromide was added to the gel and poured into gel cassettes. Gels were run at 60-120V, the higher the percentage, the lower the voltage, for 45-80 minutes, the higher percentage the longer the time. Images were then taken on a UV transilluminator (Bio-Rad).

2.4 Sanger Sequencing

2.4.1 Clean-up of PCR Product

PCR products were purified using the ExoSAP-IT Cleanup Reagent (Affymetrix, Thermo Fisher Scientific, Waltham, MA, USA), for use in sequencing and further PCR reactions. Briefly, 1 µl of ExoSAP-IT was used for every 2.5 µl of PCR product. Products were incubated at 37°C for 30 mins followed by 80°C for 15 mins to inactivate the enzyme.

2.4.2 Sequencing Reaction

BigDye Terminator Cycle sequencing v3.1 (2.1.1) was used to sequence PCR products in order to analyse genotypes in of *F13A1* in patient samples. In a reaction, 1 µl of BigDye v3.1 Ready Reaction Mix, 2 µl of 5X BigDye sequencing buffer, 3 µl of PCR product cleaned up with ExoSAP-IT (2.3.1) and 4 µl of nuclease-free dH_2O was placed in a thermocycler and incubated at 96°C for 1 minute, followed by 25 cycles of 96°C for 10 seconds, 50°C for 5 seconds, 60°C for 5 seconds, with a final extension step at 60°C for 4 minutes.

2.4.3 DNA Precipitation

Sequencing reaction products (10 µl) were precipitated by EDTA/Ethanol precipitation (3.1 µl of 100 mM EDTA and 29.4 µl of 100% ethanol, for a final concentration of 9.5 mM EDTA and 90.5% ethanol) and the plate was centrifuged at 2960 relative centrifugal force (rcf) for 30 minutes at room temperature. Excess solution was tapped out of the plate onto tissue in one swift but gentle motion, and the plate was then placed upside down onto tissue in the centrifuge for a 3 second spin at 10 rcf removed the final remnants. Wells were washed with an

ethanol wash of 60 µl of 70% ethanol), and centrifuged for 15 minutes at 4°C at 780 rcf. Excess solution was removed from the plates as before onto tissue with a gentle spin onto tissue at 10 rcf for 7 seconds. Plates were dried on a hot block until all ethanol had evaporated.

2.4.4 Sequence Visualisation

Precipitates were resuspended in 10 µl of HiDi Formamide (Applied Biosystems) and resolved at 60°C using a 36 centimetre (cm) array on an ABI3130xl Genetic Analyser (Applied Biosystems) using POP7 polymer, 3730 sequencing buffer and FragmentAnalysis36_pop7_1 modules for all runs. Electropherograms were processed and base-called then visualised in 4Peaks (http://nucleobytes.com/4peaks), Figure 2-A.

2.5 Immunohistochemistry

2.5.1 Tissue Sectioning

Formalin-fixed paraffin-embedded tissues were sectioned at a thickness of 4 um onto SuperFrost Plus slides and left to dry at 37°C overnight. Slides were then recovered in a layer of paraffin-wax to prevent any antigen degradation.

2.5.2 Antibodies

Tissues were stained for FXIIIA protein using the Human Protein Atlas Antibody HPA001804 (Rabbit IgG_1) against the recombinant protein epitope signature tag (PREST Antigen) for *F13A1* at a dilution of 1:200 on paraffin-embedded tissue sections, (Table 2-2). Antibody specificity was confirmed via Western Blot with detection of the expected 83 kDa fragment in human peripheral blood monocytic cell lysate and recombinant yeast lysates for FXIIIA wildtype protein and control AH22 yeast lysate (kindly provided by E. Elfaki, University of Leeds), (Figure 2-A).

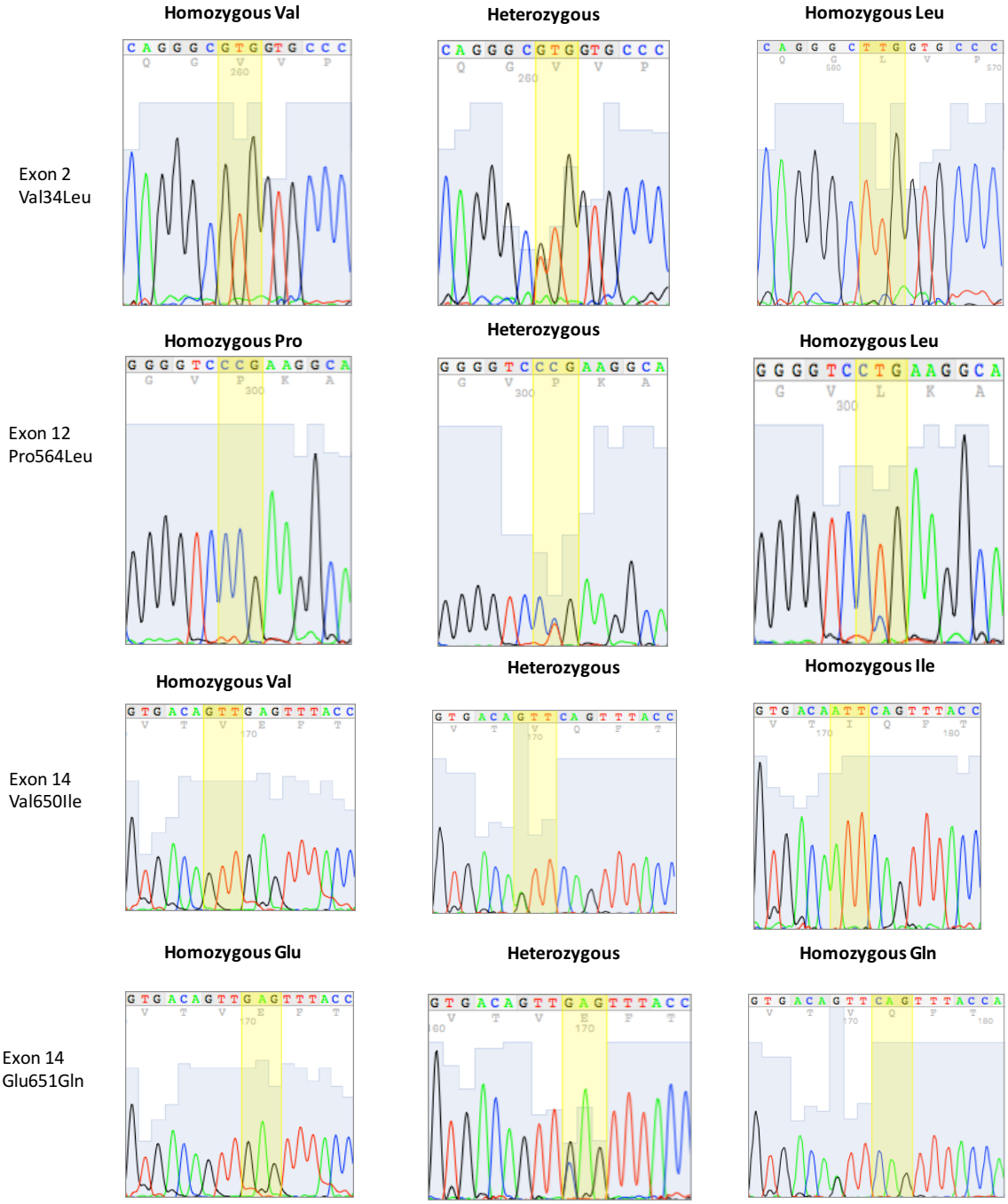

Figure 2-A: Representative Electropherograms in 4Peaks software, to analyse sequencing traces for the *F13A1* SNPs in amplified exons from patient peripheral blood DNA. The SNPs and the exon in which they are present are listed on the left. The codon of interest is highlighted in yellow. If homozygous, the electropherogram peak is clearly defined by the presence of a single peak. In the case of heterozygous carriage of alleles, two, near-overlapping peaks are present, representing detection of each possible allele.

Table 2-2: Details of Antibodies used in Immunohistochemistry and Immunofluorescence

A

Technique	Antibody	Antibody ID	Target	Company	Isotype	Species	Dilution
Immunohistochemsitry	HPA001804	AB_1078792	F13A1	Atlas Antibodies	IgG-1	Rabbit Polyclonal	1 in 200
Immunofluorescence	HPA001804	AB_1078792	F13A1	Atlas Antibodies	IgG-1	Rabbit Polyclonal	1 in 100
	HPA029518	AB_10603133	TGM2	Atlas Antibodies	IgG-1	Rabbit Polyclonal	1 in 100
	15841-1-AP	AB_2103801	Fibrinogen-Gamma	ProteinTech	IgG	Rabbit Polyclonal	1 in 100
	81D1c2	AB_304383	Isopeptide	Abcam	IgG-1	Mouse Monoclonal	1 in 100

B

PREST Antigen	Recombinant Protein Fragment Amino Acid Sequence	Length (aa)
F13A1	LNVTSVHLFKERWDTNKVDHHTDKYENNKLIVRRGQSFYVQIDFSRPYDP RRDLFRVEYVIGRYPQENKGTYIPVPIVSELQSGKWGAKIVMREDRSVRL SIQSSPKCIVGKFRMYVAVWTPYGVLRTSRNPETDT	136
TGM2	VEPVINSYLLAERDLYLENPEIKIRILGEPKQKRKLVAEVSLQNPLPVAL EGCTFTVEGAGLTEEQKTVEIPDPVEAGEEVKVRMDLLP	89

A: Details of antibodies used in immunohistochemistry and immunofluorescence. Antibody IDs are from The Antibody Registry (http://www.antibodyregistry.org). **B:** Details of the recombinant Protein Epitope Signature Tag (PrEST) antigen sequence used as the epitope for the antibodies. Length in amino acids (aa) is provided in the last column.

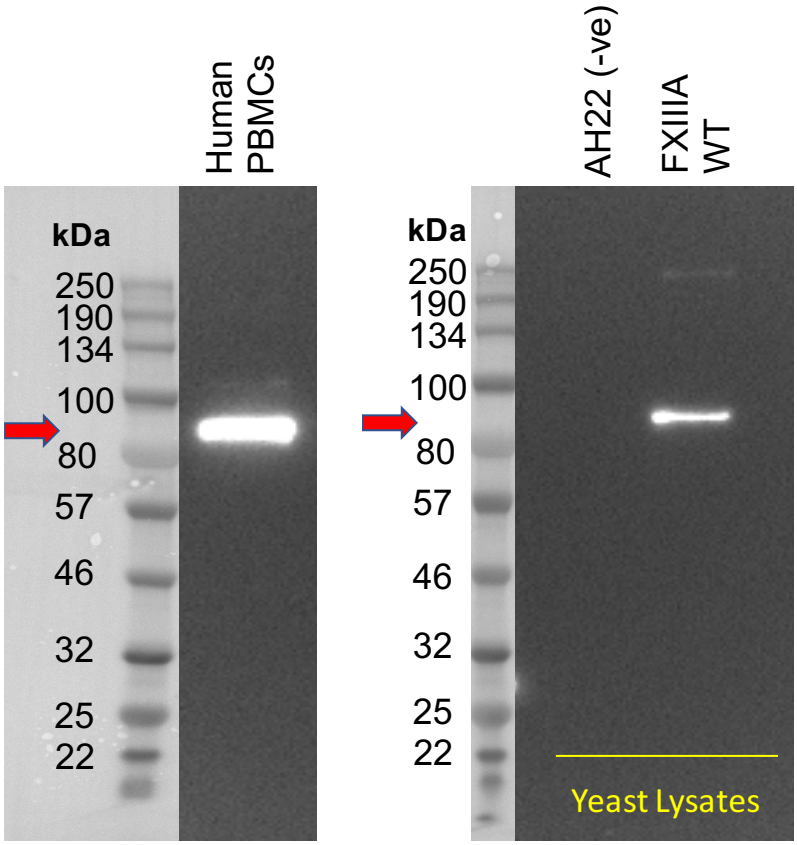

Figure 2-B: Western Blot to confirm detection of FXIIIA using antibody HPA001804. The expected size of the FXIIIA subunit is 83 kDa (with approximate location on the maker given by the red arrow. In each lane, 20 ng of protein was loaded and run on a 4-12% Bis-Trix Novex Gel (ThermoFisher Scientific, UK) Human peripheral blood monocytic cells (Human PBMCs) and recombinant AH22 *Saccromyces cerevisae* lysate (yeast lysates) from FXIIIA wildtype recombinant yeast and yeast without the plasmid (AH22 –ve (negative)) were used to test antibody specificity. Proteins were transferred to PVDF membrane. Membrane was blocked in 5% non-fat dried milk and incubated with the primary antibody (HPA001804, at 1:500) overnight at 4C. Following washes, membrane was incubated with the secondary goat-anti rabbit-HRP (1:2000) for 2 hours at room temperature, with subsequent washes and chemi-luminescent substrate detection (Section 2.10).

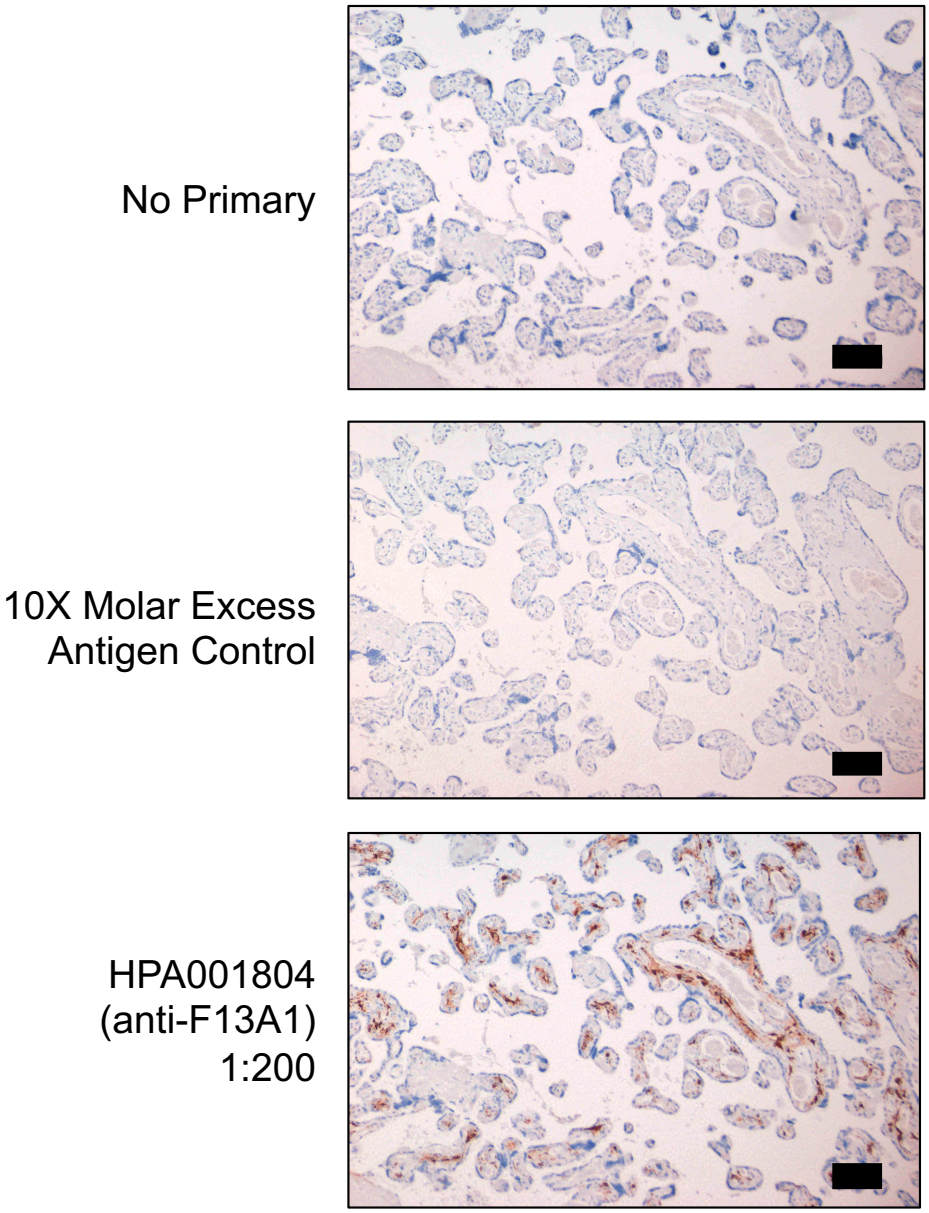

Figure 2-C: Staining of human placenta to test HPA001804 for the detection of FXIIIA. Human placenta is a positive control tissue, as FXIIIA protein is highly expressed. Top: no primary antibody incubated with the tissue, only antibody diluent was used. A 10X molar excess of the recombinant protein epitope signature tag (PrEST antigen) was incubated with HPA001804 according to the manufacturer's instructions for 30 mins at room temperature and then incubated with the tissue for 2 hours as per the standard immunohistochemistry protocol. The presence of the epitope in excess would ensure complete binding of the antibody so that it was unavailable to bind to FXIIIA in the tissue. This is a control to ensure the antibody is specific to the epitope it was raised against. Bottom: positive staining of FXIIIA protein detected in human placenta, as shown by the brown staining. The blue staining is from counterstaining of nuclei with haematoxylin. The black bar in the bottom right hand corner represents 100 µm. Images have been manually increased by 40% for brightness for clarity. Images taken on a Nikon Eclipse E1000 Microscope, using a 10X objective lens.

2.5.3 Staining Protocol

Slides were dewaxed in 3 washes of xylene (Cat #: X/0200/17, Fisher Scientific) and rehydrated in 3 washes in absolute ethanol (Cat #: 32221, Sigma Aldrich), and rinsed in running tap water for 5 mins. Slides underwent antigen retrieval by boiling in 10 mM citrate buffer, pH 6.0, for 10 minutes followed by a 20-minute cooling period at room temperature. Slides were rinsed in 1X TBS for 5 minutes.

An endogenous peroxidase block solution was made by adding 10 mL of 30% v/v hydrogen peroxide (Cat #: H/1800/15, Fisher Scientific) into 250 mL of methanol (Cat #: M/4056/17, Fisher Scientific). This solution was made fresh just prior to the endogenous peroxidase block step and slides placed into the solution for 20 minutes at room temperature and then rinsed in running tap water for 5 mins. Tissues were then blocked for background with undiluted antibody diluent (Cat #: 003128, Life Technologies, Frederick, MD, USA) for 15 mins at room temperature in a humidity chamber.

Primary antibody was diluted in undiluted antibody diluent and incubated with the tissue for 2 hours. Controls for staining included: a) no primary: undiluted antibody diluent in the absence of primary antibody b) Isotype control: to test whether the backbone of the primary antibody IgG_1 would interact with the tissue. Isotype control was the same species as the primary (rabbit IgG_1) and used at the same final concentration as the primary antibody. Slides were washed three times, twice with TBS-T and once with TBS. Tissues were incubated with horseradish peroxidase (HRP)-conjugated anti-rabbit/mouse secondary antibody (EnVision Dual Link System-HRP (DAB+), Cat #: K4065, Dako, Carpinteria, CA, USA) and slides were washed as before.

Positive staining was detected by diaminobenzene (DAB) interaction with HRP to produce brown staining. 100 µl of DAB solution made according to the manufacturer's instruction in the kit (EnVision, Dako) was added to each tissue and incubated in the fume hood for 10 minutes. Slides were rinsed in running tap water for 5 minutes. Counter-staining was performed with Mayer's Haemotoxylin (Cat #: MH832, Sigma Aldrich) and Scott's Tap water (20 g sodium bicarbonate plus 3.5 g magnesium sulphate dissolved in 1 L of dH_2O). After dehydration ethanol and xylene, coverslips were mounted onto each slide with xylene-based

DePex mounting reagent. (Cat #: 18243.02, Serva Electropheresis GmbH, Heidelberg, Germany).

2.5.4 Quantification in QuPath

Tissue microarray staining for FXIIIA was quantified using the QuPath software. Firstly, slides were scanned by the Pathology department. Raw images were loaded into QuPath. For each tissue microarray slide, the image was de-arrayed to identify each core and each core was manually checked for quality control purpose. Any folded cores or cores in which artefacts were clearly present were labelled as “missing”. Staining vectors were estimated for haematoxylin and DAB staining, and these vectors were used in the script for analysis of each tissue microarray. A simple tissue detection scan was performed and then positive cells were detected with measurements taken at defined weak, intermediate and strong staining. H-Score and Allred scores were generated for each core and data was exported as a text file for later collation with clinical data and subsequent statistical analysis.

A full copy of the QuPath script used is provided in the Appendix 2.

2.6 Immunofluorescence

2.6.1 Cryosectioning of Frozen Tissues

Tissues were sectioned on a cryostat at 7 µm sections onto SuperFrost Plus glass slides. Slides were left to air dry at room temperature for at least 30 minutes. Slides were tightly wrapped in tinfoil to prevent frost formation and stored at -80°C.

2.6.2 Antibodies

Antibodies dilutions were worked up on frozen control tissues. A full list of antibodies used for immunofluorescent staining can be found in Table 2-2. Antibodies were diluted in a freshly prepared antibody diluent comprised of 1X PBS and 1% bovine serum albumin (BSA).

2.6.3 Staining Protocol for Frozen Tissues

Slides were defrosted for 30 mins at room temperature, and then fixed in 4% paraformaldehyde in PBS (Cat #: SC-281692, Chem Cruz, Santa Cruz

Biotechnology, Dallas, TX, USA) for 20 mins, washed three times for 5 mins each in 1X PBS, then permeabilised with methanol at -20°C for 10 mins. No antigen-retrieval was performed for frozen section. Tissues were then blocked in a freshly prepared blocking buffer (1X PBS with 5% normal goat serum (G9023, Sigma Aldrich)) for 1 hour. Primary antibodies were diluted in freshly prepared antibody dilution buffer (1X PBS plus 1% bovine serum albumin) and incubated with the tissue for 2 hours. Slides were washed with 3, 5 minute washes in PBS and then incubated with an AlexaFluor-conjugated secondary antibody for 1 hour, (Table 2-3). Slides were washed and coverslips were mounted using ProLong Gold with DAPI (Cat #: P36935, Invitrogen, ThermoFisher Scientific).

Table 2-3: Secondary Antibodies used in Immunofluorescent Staining

Species	Isotype	AlexaFluor Conjugate	Company	Dilution	Catalog Number	Final Conc
Goat anti-Rabbit	IgG	AF488	Invitrogen	1 in 2000	A-11034	2 µg/mL
Goat anti-Mouse	IgG	AF594	Invitrogen	1 in 2000	A-11032	2 µg/mL

2.6.4 Microscopy

Immunofluorescent staining was visualised with a Zeiss Microscope (Zeiss Imager.Z1 Ax10) and images visualised in AxioVS40 V4.8.2.0. A FITC Emission filter (wavelength 530 nm) was used for the detection of the AF488-conjugated secondary antibody. A TexasRed Emission filter (wavelength 610 nm) was used for the detection of the AF594-conjugated secondary antibody. A DAPI emission filter (wavelength 440 nm) was used to detect DAPI-stained nuclei. Images were acquired with a 63X oil objective lens.

2.7 Cell Culture

Human umbilical vein endothelial cells (HUVEC) were purchased from Lonza (Cat #: C2519AS, pooled HUVEC in EGM-2, pre-screened for angiogenesis) and cultured in fully supplemented EGM-2 medium, according to the recommendations by Lonza (see 2.7.1 for details). Cell doubling time for HUVEC is approximately 27 hours (Figure 2-D), in line with expected doubling times provided by Lonza (228).

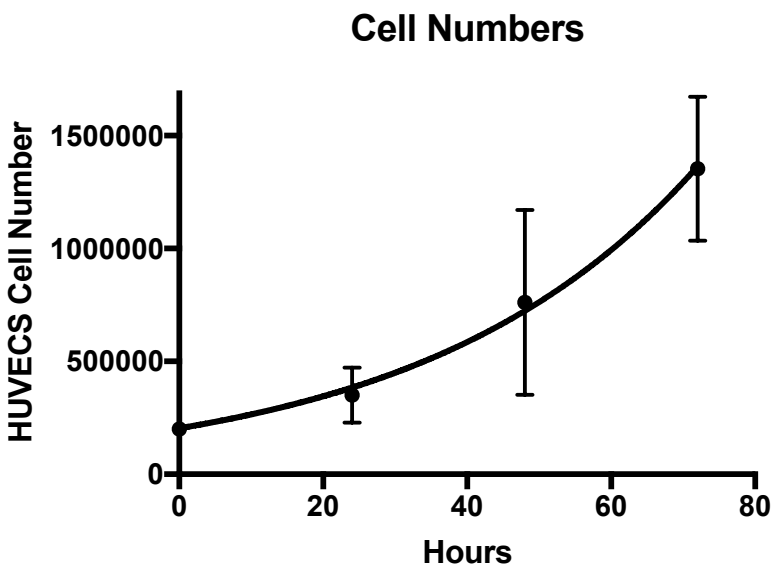

Figure 2-D: Cell Doubling Time for HUVEC. 200000 cells (HUVECs, passage 2) were seeded in triplicate T25 cell culture flasks, for 4 time points (12 flasks in total) in fully supplemented EGM-2 Medium at 37°C, 5% CO_2. Every 24 hours, cells from triplicate flasks for the respective time points were trypisinised and counted using Trypan Blue and the Countess Slides for use in the Countess II Automated Cell Counter System (ThermoFisher Scientific). Results above are from a single experiment with each time point representative of counts from triplicate T25 flasks (n=3). Data were plotted in Graphpad Prism and an exponential growth curve was fitted to the data (Y=Y0*exp(k*X)). Error bars represent standard deviation around the mean.

2.7.1 Cell Culture Reagents

- **Cell Culture Medium:** HUVEC were culture in fully supplemented endothelial cell growth medium, EGM-2, according to the culturing recommendations provided by Lonza. EGM-2 (Cat #: CC-3162, Endothelial Cell Growth Medium-2 BulletKit, Lonza) was comprised of EBM-2 Basal Medium (EBM) and supplemented with SingleQuots (Cat #: CC-4716, Lonza). Supplement concentrations were proprietary information, but the final volumes of growth factors were as follows: 2% fetal calf serum, 0.04% hydrocortisone, 0.4% human fibroblastic growth factor-B, 0.1% vascular endothelial-like growth factor, 0.1% R3-insulin-like growth factor, 0.1% human epidermal growth factor, 0.1% gentamicin sulfate-Amphotericin, 0.1% heparin. The final concentration of VEGF in the supplemented medium was between 1.4-2.3 ng/mL (personal communication, Lonza Scientific Support). Medium stored at 4°C.
- **Trypsin-EDTA:** A 10X stock (Cat #: 15400-054, Life Technologies, Carlsbad, USA) was diluted with sterile Dubecco's PBS (see below) before use. Components of 10X Stock: Tryspin 0.5% w/v, EDTA salt 0.9 mM, sodium chloride 146.5 mM. Stored at 4°C.
- **Fetal Calf Serum (FCS):** (Cat #: F7524-500ML, Sigma Aldrich, St Louis, USA). Stored at 4°C.
- **Phosphate Buffered Saline (PBS):** Dulbecco's Sterile 1X PBS (Cat #: 14190-094, Sigma Aldrich), lacking calcium chloride and magnesium chloride, stored at room temperature.
- **Freezing Medium:** 90% FCS plus 10% dimethyl sulfoxide (DMSO, Cat # D8418, Sigma Aldrich), stored at 4°C.

2.7.1 Generation of Frozen Cell Stocks

HUVEC were grown to 80% confluence in a T75 culture flask, trypsin added and detached cells spun at 200 G for 5 mins. Cells were resuspended in 1 mL of freezing medium and transferred to a cryovial. Cryovials were placed into a Mr Frosty filled with isopropanol (BP2618-212, Fisher Scientific) slow-cool box at -80°C for at least 24 hours. Cryovials were then transferred to liquid nitrogen for long-term storage.

2.8 Cell Viability and Proliferation Tests

Cell viability was measured using (3-(4,5-dimethylthiazol-2-yl)-2,5-diphenyltetrazolium bromide) (MTT) reagent (229) (Cat #: M2128, Sigma Aldrich) which is reduced by viable cells from a yellow, water soluble solution to purple formazan crystals, which are insoluble. Medium was removed from cells and then were incubated with MTT reagent at final concentration of 1 mg/mL in EGM-2 medium for 3 hours at 37°C, 5% CO_2. The MTT reagent was then removed of and disposed of via appropriate hazardous waste routes. Formazan crystals were resuspended in 100 µl of isopropanol (Cat #: BP2618-212, Fisher Scientific) and shaken on a flatbed rotary shaker for 15 mins at room temperature. The optical density of the now purple solution was on a plate reader at 620 nm. Background measurements were taken from medium only wells.

This test can be used as a measure of proliferation, and was initially developed by Mosmann and colleagues as an alternative to radioactive thymidine incorporation into DNA to measure proliferation(229,230). However, it is a measure of cell viability and therefore only assumptions regarding proliferation can be made i.e. it is assumed that the increase in proliferation compared to a control well (set at 100% viability) results from viability measures >100%.

2.8.1 Effect of VEGFA on HUVEC Viability

HUVECs were seeded in 96 well plates at 10000 cells/well using two independent populations of HUVECs. Cells were allowed to adhere overnight and the following morning were treated with VEGFA-165 (Cat #: H9166-10UG, Sigma Aldrich) at a range of concentrations from 0.5 ng/mL-50 ng/mL in EGM-2 medium, in triplicate wells. Bevacizumab (Avastin, Roche) was used in wells at a 2.6 : 1 molar ratio of bevacizumab to VEGFA concentrations of 25 ng/mL and 50 ng/mL. Bevacizumab was diluted to appropriate working concentrations from its 25 mg/mL stock with sterile 0.9% sodium chloride. Cells were incubated with the treatment for 48 hours, to allow one cell replication to occur, given the cell doubling time of approximately 32 hours). Treatment medium was removed and MTT reagent

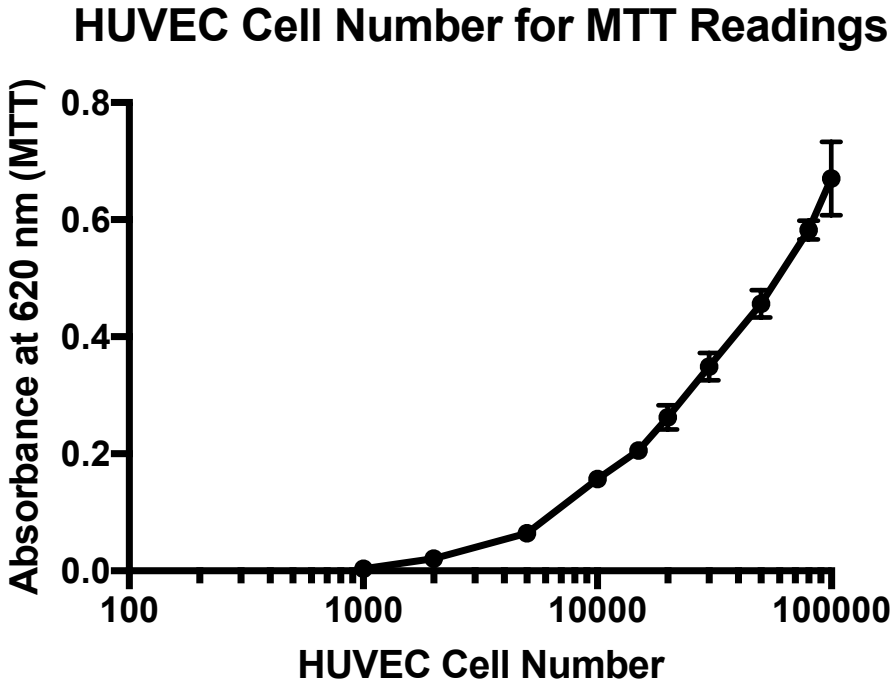

Figure 2-E: HUVEC Cell number required for absorbance measurement in an MTT Assay. HUVEC cells were plated from 1000-100000 cells per well and left to adhere overnight. The following morning cells were incubated with MTT reagent (1 mg/mL in EGM-2 medium) for 3 hours at 37°C, 5% CO_2. MTT agent was removed and formazan crystals resuspended in 100 µl of isopropanol and read at 620 nm. The purpose of this experiment was to assess on average, the absorbance measurement for different HUVEC seeding densities. As too few cells would result in inaccurate measurements due to issues in assay sensitivity.

added as described in Section 2.8, above. HUVEC viability was also measured over a 72-hour period to assess whether 10 ng/mL or 25 ng/mL VEGFA was most appropriate for long-term endothelial tube formation i.e. was there any toxicity from long term exposure.

2.9 Endothelial Tube Formation Assay (ETFA)

2.9.1 Thin-layer angiogenesis assay

An adapted protocol from Faulkner and colleagues was used to generate thin layer angiogenesis assays (231). A thin layer of GelTrex LDEV-free Low Growth Factor basement matrix (Cat #: A1413202, Gibco, ThermoFisher Scientific, Waltham, MA, USA) was pipetted using a multistep pipette to deposit 5 µl of matrix per well of a 96 well plate incubated on ice. Matrix was then spread gently using the insert of a 1 mL combi-tip. Matrix covered plates were incubated at 37°C for at least 30 minutes to solidify the matrix. HUVECs were serum-starved for 3.5 hours (232,233) in EBM medium without FCS or any supplements. HUVECs were seeded at test densities (2000-16000 cells per well) and then for later experiments, cells were seeded at the chosen density of 6000 cells per well of a 96 well plate. Cell counts were performed using the Countess II Automated Cell Counter (Cat #: AMQAX1000, ThermoFisher Scientific). A final volume of cell growth medium, containing cells and treatments, of 200 µl was added on top of the matrix and incubated at 37°C, 5% CO_2 in the Incucyte (Essen Bioscience, Welwyn Garden City, UK) (Section 2.9.3) or on the LIPSI (Nikon, Amsterdam, Netherlands) (Section 2.9.4) for 24 hours. Cells were stimulated to form tubes by the addition of VEGFA-165 (Cat #: H9166-10UG, a 10000 ng stock of lyophylised powder resuspended in filter sterilised 0.1% bovine serum albumin). Cells were stained with CytoPainter-488 (500X stock lyophilised powder resuspended in 500 µl of DMSO, Cat # ab176735, Abcam, Cambridge, UK) for 10 mins at room temperature prior to plating, to aid cell tracking on the imaging platforms.

2.9.2 Activation of FXIIIA variants for use in ETFA

Factor (FXIIIA) variants were added to the treatment medium in the ETFA in either active or inactive states. Purified recombinant protein was purified and activity measured by FXIIIA activity assay by E. Elfaki (University of Leeds). The circulating concentration of FXIIIA within the plasma is approximately 1 International Unit (IU)/mL, with 0.01-0.03 IU/mL being sufficient to prevent bleeding (234). Factor XIIIA was activated in the presence of bovine thrombin (0.1 U per 0.02 IU of FXIIIA), (185) and 10 mM calcium chloride for 30 minutes at

37°C, 5% CO_2. Bovine thrombin stock (2000 U/mL Stock, Cat #: T4648-1KU, Sigma Aldrich). Thrombin was then inhibited with D-phenylalanyl-N-[(1S)-4-[(aminoiminomethyl)amino]-1-(2-chloroacetyl)butyl]-L-prolinamide, trifluoroacetate salt (PPACK, 1 mg/mL stock from lyophilised powder resuspended in DMSO, Cat #15160, Cayman Chemical, Ann Arbor, USA): 140 ug/mL inhibits 0.5 U of thrombin, for 10 mins at 37°C, 5% CO_2. (235). Inactive FXIIIA variants were treated in the same way as the active variants but in the absence of thrombin and PPACK, with PBS used to replace volumes.

In the Incucyte & LIPSI Experiments, 0.05 IU/mL of FXIIIA was used. In the 12 well assay for protein harvest from HUVECs actively undergoing tube formation, 0.005 IU/mL was used. Cells were stimulated with ten times less FXIIIA (0.005 IU/mL rather than 0.05 IU/mL) as preliminary experiments identified that the new batch of FXIIIA recombinant protein which was generated and purified for these experiments, although had a lower activity in an activity assay and activated in the same manner as the protein for the LIPSI experiment, the density of the crosslinks meant that the cells were unable to migrate. A lower concentration of FXIIIA resulted in migration similar to that seen in the LIPSI experiment, and was used in the 12 well assay.

2.9.3 HUVEC Seeding Density for ETFA: Incucyte

Thin layer tube formation assays were generated as described in Section 2.9.1. Cells were stained with Cytopainter-488 (as described in Section 2.9.1) and were plated at test densities of 2000-16000 cells per well in triplicate wells and incubated in the Incucyte for 23 hours. Live cells images from each well were recorded every hour and average network length was quantified using the Angiogenesis Analyzer for ImageJ (236,237).

2.9.4 Effect of FXIIIA Variants on Endothelial Tube Formation: LIPSI

The purpose of these experiments was to assess the effect of FXIIIA Val34Leu variants on endothelial tube formation. A thin layer ETFA were set up as described in Section 2.9.1, but plated in black 96-well plates (Greiner Bio-One SCREENSTAR, Cat #655866, FisherScientific). HUVECs were seeded at 6000 cells/well. Cells were treated with VEGFA at 25 ng/mL alone or VEGFA plus 0.05 IU/mL of active or inactive FXIIIA variants: Val/Val (wildtype), Val/Leu (heterozygous) or Leu/Leu (homozygous alternative) for a total of 32 hours.

Appropriate buffer controls were FXIIIA variants were activated as described in Section 2.9.2. Tube networks were manually measured for triplicate wells over 23 hours using the Nikon Elements Advanced Research (AR) software.

2.9.5 Measure of Angiogenic Signalling Axis in Active HUVEC Tube Formation

Cells were harvested according to the protocol developed by Xie and colleagues (238). ETFA experiments were scaled up to 12 well plates, with 100 ul of GelTrex basement matrix spread on the base of the wells. FXIIIA variants (0.005 IU/mL) and VEGFA (25 ng/mL) were added to HUVECs seeded at density of 1.5 $x10^5$ cells per well in triplicate wells per condition. Medium only and VEGFA only controls were also performed. Briefly, plates were transferred to ice where cell medium was removed and cells were washed with 1 mL of 1X ice-cold Dulbecco's PBS. 1 mL of ice-cold PBS-2.5 mM EDTA buffer was added to the wells and incubated on ice for 10 mins. Cells were dislodged using a 1000 µl pipette tip with the end cut off to make a wide-bore pipette tip, and transferred to a cold 15 ml falcon tube kept on ice at all times. Wells were washed at least 4 times with ice-cold PBS-2.5 mM EDTA until all matrix and cells had been dislodged. Tubes were kept on ice for 4 hours and inverted every 30 minutes until the extracellular matrix had dissolved. Falcon tubes were then spun at 1620 rcf at 0°C, supernatant was removed and cell pellets resuspended in 1 mL of ice cold PBS and placed into a 1.5 mL centrifuge tube. Tubes were then spun for 5 minutes at 3000 rcf at 0°C. Supernatant was removed and cell pellets were lysed, as per Section 2.10.1.

2.10 Western Blotting

2.10.1 Protein Extraction

Proteins were extracted from HUVECs using RIPA buffer supplemented with cOmplete™ EDTA-free protease inhibitor (Roche, Cat#: 11873580001, working stock made according to the manufacturer's instructions) on ice for 30 minutes on ice and then spun at maximum rpm on a benchtop mini-centrifuge at 4°C. Protein concentration assays were undertaken using a Pierce BCA assay (Cat #: 23225, ThermoFisher Scientific), according to the manufacturer's instructions.

Proteins were extracted from HUVEC actively undergoing endothelial tube formation. Cells were harvested after 5.5 hours of incubation. Phosphatase inhibitors were not used in these experiments. In hindsight, this would have been used to ensure that there was no degradation of phospho-proteins during cell

lysis. However, all steps prior to cell lysis from the point of cell harvest were performed on ice or spun at 0°C. Prior to lysis the cells were on ice for 4 hours and it is highly unlikely that any cell enzymes would be active at these temperatures. The demonstration of successful phospho-proteins in the Western Blots presented in Chapter 6, Figure 6-G, indicates that phosphotases were unlikely to have been active as the cells were chilled for a significant period of time. If phosphatases were active, then little or very poor-quality staining would have been seen across the Western Blot membrane. However, for future experiments, the use of phosphatase inhibitors such as PhosSTOP™(Sigma, Cat #: 4906845001) would be an extra step to ensure no degradation by phosphatases occurs within cell lysate samples.

2.10.2 SDS-PAGE

Samples were prepared to desired protein concentrations in 10X Bolt LDS Sample Reducing Agent (Cat #: B0009, Invitrogen, ThermoFisher Scientific) and 4X Bolt LDS Sample Buffer (Cat #: B0007, Invitrogen, ThermoFisher Scientific) and heated to 70°C for ten minutes. Samples were loaded onto 10 well or 15 well 4-12% Bis-Tris NuPAGE Gels (Cat #: NP0321BOX, 10 well or NP0336BOX, 15 well, Invitrogen, ThermoFisher Scientific) and run at 80V for 2hr 30mins in NuPAGE MOPS SDS Running Buffer (made to 1X working stock from the 20X Stock, Cat #: NP0001, Invitrogen, ThermoFisher Scientific). Proteins were transferred onto PVDF 0.45 µm Transfer Membrane (Cat #: 88518, Invitrogen, ThermoFisher Scientific) using NuPAGE Transfer Buffer (made to 1X from the 20X Stock, Cat #: NP0006, Invitrogen, ThermoFisher Scientific) supplemented with Bolt Antioxidant (Cat #: BT0005, Invitrogen, ThermoFisher Scientific. Proteins were transferred for 2 hours. The membrane was then blocked with 5% non-fat dried milk in PBS for 1 hour.

2.10.3 Antibodies and Incubation Protocol

A full list of all primary antibodies used for Western Blots can be found in Table 2-3. The secondary antibodies were: Goat anti-Rabbit HRP-conjugated or Goat anti-Mouse HRP-conjugated for detection by chemiluminescent methods (Section 2.9.4). Antibodies were diluted at the appropriate concentrations in 5% non-fat dried milk or 5% BSA in PBS for phospho-primary antibodies. Membranes were incubated overnight at 4°C. Membranes were washed with 3, 10 minute

washes with PBS and then incubated with secondary appropriate to the species of the primary: Goat anti-Rabbit-HRP in 5% non-fat dried milk (1:2000).

2.9.3.1 Loading Control

GAPDH (Cat #: GTX10018, Genetex, 1:10000) was used a loading control and secondary used was Goat-anti Mouse-HRP (Cat #: M32407, Life Technologies) in 5% non-fat dried milk (1:2000).

2.9.4 Chemiluminescent Detection of HRP-linked Secondary Antibodies

Following 3, 10 minute washes with PBS, membranes were incubated in a 1:1 ratio of solutions A and B from the SuperSignal West Femto Maximum Sensitivity Substrate (Cat #: 34095, ThermoFisher Scientific) for a few minutes at room temperature before being imaged on a ChemiDoc (BioRad).

2.9.5 Quantification

Fiji is Just ImageJ (Fiji) was used to quantify the protein bands detected on the Western Blot, using the Gel Analysis Toolset (237,239). Bands were normalised to the normally growing HUVEC passage 4 protein levels and to a GAPDH loading control. Graphpad Prism 7 for MacOS (v7.0d) was used to generate figures and run statistical analysis, where appropriate.

2.10 Statistical Analysis

2.10.1 Software

Analysis of the clinical cohorts and survival data analysis was undertaken in Stata v13.11 and later, v15.1. Many thanks to the Epidemiology Team (Clinical Sciences Building, University of Leeds) for help and guidance during the transfer of the files to the new software. Analysis of other experiments was undertaken in Graphpad Prism 7 for MacOS. Power analysis was performed in ‘R’ (R 3.6.0 GUI 1.70 El Capitan build (7657) (240).

2.10.2 Power Analysis

Owzar *et al*.’s rare allele frequency survSNP package (241)was used to run the power analysis for multivariate modelling. The full manual for the survSNP package is available online through https://bitbucket.org/kowzar/survsnp (242). Variables used: Genotype Hazard Ratio (GHR): 0.5-2.0 (in increments of 0.1),

Table 2-4: Details of Antibodies used in Western Blotting Experiments

Technique	Antibody	Antibody ID	Target	Company	Isotype	Species	Dilution
Western Blot	HPA001804	AB_1078792	F13A1	Atlas Antibodies	IgG-1	Rabbit Polyclonal	1 in 500
	mAB 2478	AB_331377	Phospho-VEGF Receptor 2	Cell Signalling Technology	IgG	Rabbit Monoclonal	1 in 1000
	mAB 4060	AB_2315049	Phospho-Akt	Cell Signalling Technology	IgG	Rabbit Monoclonal	1 in 1000
	mAB 6943	AB_10013641	Phospho-Src	Cell Signalling Technology	IgG	Rabbit Monoclonal	1 in 1000
	mAB 8556	AB_10891442	Phospho-FAK	Cell Signalling Technology	IgG	Rabbit Monoclonal	1 in 1000
	mAB 4511	AB_2139682	Phospho-p38 MAPK	Cell Signalling Technology	IgG	Rabbit Monoclonal	1 in 1000
	mAB 8713	AB_10890863	Phospho-PLCY1	Cell Signalling Technology	IgG	Rabbit Monoclonal	1 in 1000
	mAB 4370	AB_2315112	Phospho-p44/42 MAPK (Erk1/2)	Cell Signalling Technology	IgG	Rabbit Monoclonal	1 in 1000

Details of antibodies used in western blotting. Antibody IDs are from The Antibody Registry (http://www.antibodyregistry.org).

Sample size (n): 256 (Leeds) and 488 (ICON7), Relative risk allele frequency (raf): dependent on *F13A1* SNP, Event Rate (erate): death rate 0.410 (Leeds) and 0.546 (ICON7), probability that the time to event in the population exceeds landmark lm (pilm): 0.5, Landmark (lm):1, model “additive”, test “additive”, alpha: 0.5. Power was calculated for each SNP and then plotted in Microsoft Excel for Mac.

2.10.3 Descriptive Statistics

Analysis of cell work took place in GraphPad Prism. For the network lengths from endothelial tube formation, average network length was calculated for each hour from triplicate wells. Overall average for all hours (0-23) was also calculated. D’Agostino & Pearson and Shapiro-Wilk normality tests were run to test for normal distribution of the data. Non-normality resulted in non-parametric tests between groups to be used i.e. Kruskal-Wallis Test with Dunn’s multiple comparison test was used to compare the differences between average group ranks.

2.10.4 Tests for Associations

Clinical data cohort analyses were undertaken in Stata. Chi-square tests of association were performed between categorical variables of prognostic factors and SNPs. Alpha was set at 0.05, and p-value were considered significant if $p<0.05$.

2.10.5 Survival Analysis

There was only one survival interval available for the Leeds Cohort (Chapter 3): overall survival. There were three survival intervals available for the ICON7 cohort: progression-free survival (PFS) which represents time from entry to a progression-event (as defined by the ICON7 protocol (243)), overall survival (OS) which represents the time from entry to death or censorship, and survival post-progression (SPP) which is the time between the progression event and death.

2.10.5.1 Univariate Survival Analysis: Kaplan-Meier & Log Rank Tests

For univariate survival analysis, which tested the contribution of a single categorical variable on survival intervals, Kaplan-Meier plots were generated to provide a visual representation of the relationships between the covariate of interest and survival. Log rank tests examined the significance of the covariate on survival, with $p<0.05$ indicating a significant association with the survival interval.

2.10.5.2 Multivariate Survival Analysis: Cox Proportional Hazards Regression Modelling

Cox Proportional Hazards Regression Modelling was used as a multivariate assessment of covariates on the survival intervals. An “all-in-one” approach rather than a step-wise regression approach was used in model generation with all covariate results reported, regardless of whether they were significant predictors of survival were reported. It was felt that this was more appropriate when studying the contribution of SNPs and prognostic factors in survival as the contribution of each covariate in a disease as heterogeneous and complex as cancer is unknown. Where the number within each category was small, categories were combined in order to prevent skew by small numbers. The Cox Proportional Hazards Model assumes proportional hazards and this assumption was tested for each model produced.

Chapter 3: *F13A1* SNPs in Ovarian Cancer: Mature Survival Data

3.1 Introduction

The ability of FXIIIA to crosslink extracellular matrices and it further roles within inflammation, wound-healing and angiogenesis and the differing plasma levels between benign and metastatic disease could be important in ovarian cancer (OC)development and/or maintenance. Studies have already assessed the role of FXIIIA protein in terms of levels and activity in the plasma in several cancers (212,214,221). Investigations have also been undertaken to assess the role polymorphisms within the gene for FXIIIA, *F13A1*, may have with regard to their contribution to disease development i.e. 103G>T (Val34Leu) and thrombotic disease. The work on OC and FXIIIA to date is limited, but has demonstrated a potential role for this protein and its respective gene in OC.

Previous work in 2003 undertaken by the Anwar Lab investigated a national, multi-centre, study (n=629) of a cross-section of patients at various stages of disease follow-up, and identified that two SNPs within *F13A1*, 1951G>A (rs5987) and 1954G>C (rs5988) were associated with overall survival prognosis in OC patients (Chapter 1, Project Development, unpublished work). Patients were recruited from centres in Edinburgh, Leeds and Oxford (ELO). In the ELO Cohort, there was a high median survival of 7.2 years which was likely due to the inherent bias in the cohort towards EOC patients who had survived at least two years prior to their recruitment into the study.

The mature, most recent follow-up, survival data collected in October 2016, was available for the Leeds sub-cohort, only. This provided a valuable opportunity to assess whether the previously seen associations with OS still held over the 13-year period, or whether any new associations could be identified for either benefit or detriment to OS. Analysis of long term survival has been undertaken in other cancer types to help identify those patients who survive and what makes them or their cancer different from others (244–246). Understanding of long-term survival assists disease management and ultimately leads to better outcomes for patients. For the purpose of this analysis, the Leeds sub-cohort (n=258/629) was extracted from the original ELO study and analysed independently by K Hutchinson to

ensure the ELO findings held within this smaller cohort of patients. Secondly, the mature survival data was then analysed and the findings are compared and discussed.

3.2 The Leeds Cohort (n=258)

3.2.1 Cohort Characteristics

A summary of the distribution of prognostic factors can be found in Table 3-1. A total of 258 women consented for their peripheral blood DNA to be collected and clinical data used in translational research. Maximum follow-up time was 21.9 years (Range: 0.11-21.86 years), and median survival was 7.07 years, Figure 3-A. At the end of follow-up in 2003, 105 patients had died (41%) and 151 were alive (59%), n=256 as survival data was missing for two patients.

3.2.2. Power Analysis

Power analysis tools are widely available for case-control studies and the study of SNP genotypes on disease risk. In case-control studies, SNP prevalence is measure in a “control/normal/healthy” population and is compared to a “test/disease-state population. However, the cohort under investigation in this chapter is not a case-control type of study, as all patients have ovarian cancer and the outcome of interest is time-to-event data i.e. death or survival. A tool found to assist with measuring the power for this cohort size was the ‘survSNP’ package, developed by Owzar and colleagues at Duke University, for the statistical software ‘R’ (241). Full details of the package can be found in Chapter 2 (Section 2.10 – Statistical Analysis).

Rare allele frequencies (RAF), also known as minor allele frequencies (MAF) were obtained from the genome association database (gnomAD) for each of the SNPs investigated. An analysis of power for hazard ratios between 0.5 and 2.0 is presented in Figure 3-A. It is harder to detect small changes in hazard ratio without a larger cohort, and the smaller the RAF, the greater the cohort size required for detecting changes in hazard ratios.

3.3 Leeds Cohort *F13A1* Genotypes

Peripheral blood DNA was extracted from each patient and genotyped for single nucleotide polymorphisms in *F13A1* by E. Valleley and L. Gallivan (University of

Table 3-1: Distribution of Prognostic Factors in Leeds Cohort (n=258)

Prognostic Factor	n	%
Age at Diagnosis		
Up to 54	88	34.4
55-64	80	31.3
65 and over	88	34.4
Grade		
1	18	7.0
2	53	20.5
3	117	45.3
unknown	70	27.1
Stage		
I	43	16.7
II	33	12.8
III	142	55.0
IV	36	14.0
Unknown	4	1.6
Histology		
Serous	105	40.7
Other	57	22.1
Clear Cell	23	8.9
Endometrioid	52	20.2
Unclassified	21	8.1

Age Categories were defined as above, as a diagnosis of ovarian cancer is most likely to occur in a woman's post-menopausal years. The higher the age at diagnosis, the poorer the prognosis, commonly due to age-related co-morbidities or complications. Stage is based on the classification by the International Federation of Gynaecology and Obstetrics.

Leeds). SNP genotype data was collected 'blind' i.e. before the clinical data was acquired, and then added for each patient's clinical data and statistical analysis was performed. The distribution of genotypes for *F13A1* SNPs can be found in Table 3-2. The SNPs analysed all had an allele frequency >1% in the normal population.

3.3.1 Allele Frequencies Compared to the Normal Population

Allele frequencies for the *F13A1* SNPs were calculated for the Leeds Cohort (n=258) and compared to the expected values for a normal European population from the genome aggregation database (gnomAD), (Table 3-3). All allele frequencies measured were found to be in Hardy-Weinberg Equilibrium (HWE) and did not significantly differ from the expected allele frequencies. The SNP genotypes frequencies observed also did not differ from the frequencies predicted by the Hardy-Weinberg equation for each observed SNP frequency.

3.3.2 Linkage Disequilibrium

Estimates of Lewontin's D', the measure of linkage disequilibrium between SNPs are summarised in Table 3-4A, with chi-square tests for association between the genotypes presented in Table 3-4B. The only SNPs found to be in complete linkage disequilibrium, and therefore are linked to one another, are 1951G>A and 1954G>C. The alternative 'A' at 1951, is always found with the alternative 'C' at site 1954, suggesting that both of these nucleotides are on the same allele.

3.4 Associations between OC Prognostic Factors and *F13A1* SNPs

Chi-square tests were performed to examine whether prognostic factors and *F13A1* SNPs were associated with one another. If SNPs are associated with prognostic factors, then this may give an insight of how the SNP may be contributing to the cancer phenotype. Stage and histology were significantly associated with one another ($p<0.001$), (Table 3-5). Clear cell and endometrioid histology had a greater proportion of early stage diagnosed and serous histology was diagnosed at later stages, (Table 3-5C). The SNP 614A>T was significantly associated with stage. However, when the distributions were analysed, the small number of heterozygotes were distributed at 60% for Stage I and 40% for Stage III, with 0% in Stages II and IV, (Table 3-5D).

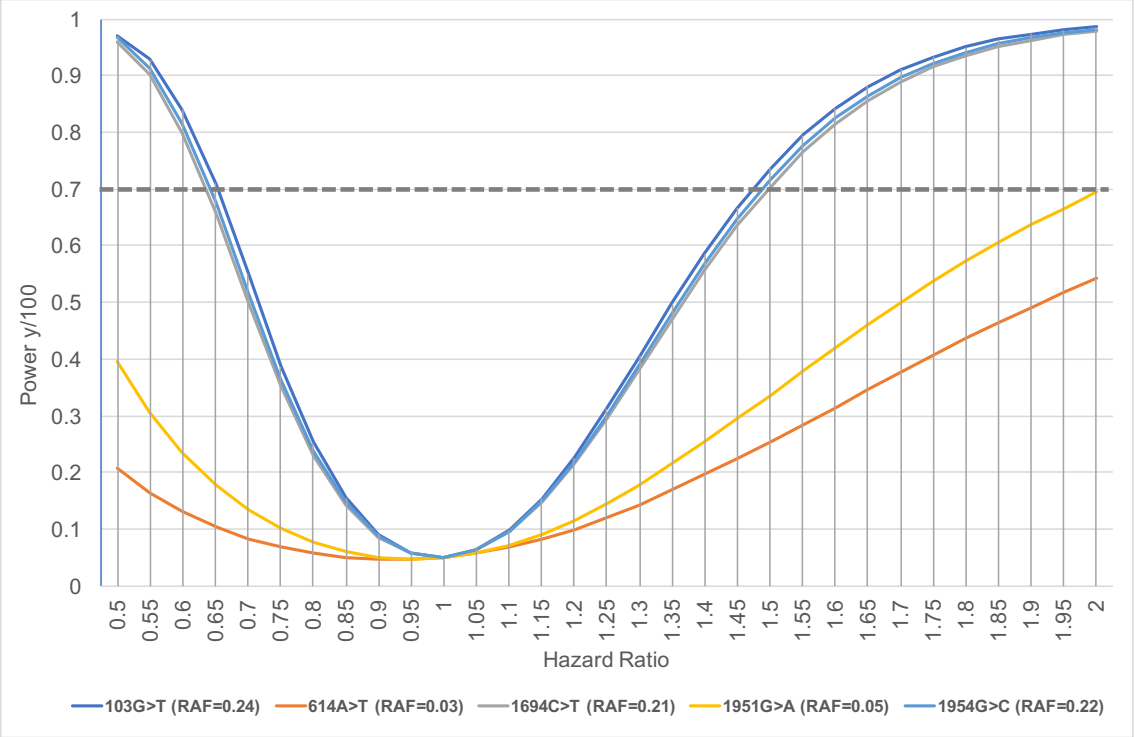

Figure 3-A: Graph to show power to detect hazard ratios for *F13A1* SNPs in a cohort of 258 patients. Power detected using the survSNP package by Owzar *et al*. 2012 (241). It is harder to detect smaller changes in hazard ratios (HR) without a larger cohort, and for very low rare allele frequencies (RAF). The grey horizontal reference line is at 70% power, and any hazard ratios from the point of intersection this line are sufficiently powered at 70% power. For the SNPs with RAF>0.20, hazard ratios are sufficiently powered from HR=0.5-0.65 and HR=1.5-2.0. The RAF for each SNP was obtained from the genome annotation database (gnomAD) for a Caucasian population (Table 3-3). The event rate was tested at 41%, as 105/256 patients had died (survival status data was missing for 2 patients in this cohort, n=256/258).

Table 3-2: Distribution of Alleles for *F13A1* SNPs

SNP (Amino Acid Change)	Observed	Observed (%)	Allele Frequenices	Expected	HWE p-value
103G>T (Val34Leu)					
GG	146	57	0.74/0.26	141	0.119
G/T	89	35		99	
TT	22	9		17	
614A>T (Tyr204Phe)					
AA	241	96	0.98/0.02	241	0.723
A/T	11	4		11	
TT	0	0		0	
1694C>T (Pro564Leu)					
CC	174	67	0.81/0.19	170	0.113
C/T	71	28		79	
TT	13	5		9	
1951G>A (Val650Ile)					
GG	222	86	0.93/0.07	221	0.583
G/A	34	13		35	
AA	2	1		2	
1954G>C (Glu651Gln)					
GG	146	57	0.76/0.24	148	0.468
G/C	99	38		95	
CC	13	5		15	
650 + 651 Haplotypes					
GG + GG	146	57			
GG + G/C or C/C	76	29			
G/A or A/A + G/C or C/C	36	14			

For each SNP, the top line presents the wildtype genotype, followed by the heterozygous genotype and finally the homozygous alternative genotype, for each SNP. The corresponding amino acid change for each SNP site is given in the parentheses. For analyses, 1951G>A (Val650Ile) heterozygotes and homozygous alternative patients were combined in order to prevent the effect of small numbers as n<5. Data was missing for six patients for 614A>T (Tyr204Phe) genotype (n=252), and one patient was missing data for 103G>T (Val34Leu) (n=257). For the allele frequencies, the number to the left of the '/' is the frequency of the wildtype allele, and the number to the right is the frequency of the alternative allele. The allele frequencies, expected values and test for whether the population was in Hardy Weinberg Equilibrium(HWE) for each SNP was run using the "genhwi" package in Stata (see Chapter 2 Materials and Methods for more details). SNPs were in HWE if p>0.05, as the null hypothesis, that population is in HWE for this SNP, could not be rejected.

Table 3-3: Observed and Expected Allele Frequencies for *F13A1* SNPs

F13A1 SNP (Amino Acid Change)	Allele Frequency		Significantly Different from Expected? (p-value)
	Leeds Cohort (n=258)	gnomAD	
103G>T (Val34Leu)	0.74/0.26	0.76/0.24	No (0.744)
614A>T (Tyr204Phe)	0.98/0.02	0.97/0.03	No (0.651)
1694C>T (Pro564Leu)	0.81/0.19	0.79/0.21	No (0.724)
1951G>A (Val650Ile)	0.93/0.07	0.95/0.05	No (0.552)
1954G>C (Glu651Gln)	0.76/0.24	0.78/0.22	No (0.737)

For the allele frequencies, the number to the left of the '/' is the frequency of the wildtype allele, and the number to the right is the frequency of the alternative allele. The expected allele frequency values were obtained from the genome aggregation database (gnomAD) for the European population. A Chi-squared test was performed to test whether there was significant difference between the observed allele frequencies in the Leeds Cohort and the expected values in the European population, as reported on gnomAD. If p>0.05, then no significant difference was detected.

Table 3-4: Lewontin's-D' Results for Linkage Disequilibrium

A

***F13A1* SNP**	**103G>T (Val34Leu)**	**614A>T (Tyr204Phe)**	**1694C>T (Pro564Leu)**	**1951G>A (Val650Ile)**	**1954G>C (Glu651Gln)**
103G>T (Val34Leu)					
614A>T (Tyr204Phe)	(-)0.18				
1694C>T (Pro564Leu)	0.02	0.32			
1951G>A (Val650Ile)	(-)0.29	0.15	(-)0.23		
1954G>C (Glu651Gln)	(-)0.07	0.35	(-)0.26	1	

B

***F13A1* SNP**	103G>T	614A>T	1694C>T	1951G>A	1954G>C
103G>T		0.569	0.677	0.099	0.561
614A>T			0.104	0.208	0.356
1694C>T				0.297	0.144
1951G>A					<0.001
1954G>C					

A: Estimated Lewontin's-D' results for linkage disequilibrium for *F13A1* SNPs, see Chapter 2 Materials and Methods for details of calculations (Chapter 2, Section 2.11.X). **B**: Results of Chi-squared tests for association between *F13A1* SNPs. Results considered significant if p-value was <0.05, with significant results highlighted in yellow. The only significant association between SNP genotypes was for the SNPs 1951G>A and 1954G>C, as these SNPs are in linkage disequilibrium with one another in the normal population, with 1951A always found with 1954C.

Table: 3-5: Tests for Association between Prognostic Factors and *F13A1* SNPs

A

Prognostic Factor	Prognostic Factor			
	Age	Grade	Stage	Histology
Age		0.143	0.056	0.623
Grade			0.072	0.193
Stage				<0.001
Histology				

B

Prognostic Factor	*F13A1* SNP				
	103G>T	614A>T	1694C>T	1951G>A	1954G>C
Age	0.323	0.744	0.339	0.157	0.057
Grade	0.871	0.354	0.242	0.410	0.468
Stage	0.431	0.001	0.392	0.930	0.158
Histology	0.377	0.345	0.733	0.422	0.927

C

Histology	Stage			
	I	II	III	IV
Serous	7 (7%)	7 (7%)	75 (72%)	15 (14%)
Other	4 (7%)	8 (14%)	37 (66%)	7 (13%)
Clear Cell	11 (50%)	2 (9%)	5 (23%)	4 (18%)
Endometrioid	17 (33%)	12 (23%)	18 (35%)	5 (10%)
Unclassified	4 (20%)	4 (20%)	7 (35%)	5 (25%)

D

Tyr204Phe	Stage			
	I	II	III	IV
TT	33 (14%)	31 (13%)	138 (58%)	36 (15%)
T/Y	6 (60%)	0	4 (40%)	0

A: Results of chi-square tests for association between the prognostic factors in the Leeds Initial Cohort (n=258). **B**: Results of the chi-Square tests for association between *F13A1* SNPs and prognostic factors in the cohort. Results of the chi-square tests were considered significant if $p<0.05$, and are highlighted in light yellow. **C:** Distribution of histologies and stage, with percentage calculated from the total of each histology. **D:** Distribution of 614A>T(Tyr204Phe) genotypes and stage of disease with percentage calculated from total histology.

3.5 Univariate Survival Analysis

3.5.1 Prognostic Factors

Prognostic factors are named as such, because they are often able to predict prognosis of a disease. Kaplan-Meier plots provide a visual representation of how the population of patients for a given factor or set of factors survive over the time period measured for the cohort. Every “death” results in a “step” in the graph, as the proportion of patients surviving decreases over time. The log rank test is used to measure the equality of the survivor function, asking the question, do patients with a given factor have an equal chance of surviving? Kaplan-Meier plots and results of log rank tests are given in Figure 3-B. Age at diagnosis, stage of disease and histology were all significantly associated with survival. Higher age and stage resulted in poorer prognosis. For patients with endometrioid histology, prognosis appeared better compared to all others.

3.5.2 *F13A1* SNPs

One of the main aims of this investigation was to assess whether those in the Leeds sub-cohort from the larger ELO study had the same associations between certain *F13A1* SNPs and survival, in particular, 1951G>A and 1954G>C. The first step was to perform a trend test for association between the number of alternative alleles (i.e. 0 if wildtype, 1 if heterozygous and 2 if homozygous alternative) and the event measured, i.e. death. A significant association was identified between event status and SNPs 103G>T, 1951G>A and then haplotypes of 1951G>A and 1954G>C, (Table 3-6). A negative trend was seen for 103G>T: the more alternative alleles carried, the greater the survival. And with 1951G>A, 1954G>C and the haplotypes of these two SNPs, a positive trend was identified, therefore the greater the number of alternative alleles, the poorer the prognosis.

Kaplan-Meier plots were generated and log rank tests were run to test for associations between *F13A1* SNPs and overall survival, to further establish how the carriage of alternative alleles affects prognosis. Just like in the ELO analysis (n=628), the SNP significantly associated with overall survival was 1951G>A (Figure 3-C, Plot D). None of the other SNPs were significantly associated with overall survival. As these two SNPs are in linkage disequilibrium, it was important to assess how the haplotypes were associated with survival, as this is how the

Table 3-6: Results of Trend Test for Association with Survival Status

F13A1 SNP (Amino Acid Change)	Number Alternative Alleles	Alive	Dead	z	Trend Test for Association (p-value)	Level of Significance
103G>T (Val34Leu)	0	79	67	-2.01	0.045	*
	1	54	33			
	2	17	5			
614A>T (Tyr204Phe)	0	138	101	-0.39	0.699	ns
	1	7	4			
1694C>T (Pro564Leu)	0	100	72	-0.31	0.756	ns
	1	44	27			
	2	7	6			
1951G>A (Val650Ile)	0	137	83	2.63	0.009	**
	1	13	21			
	2	1	1			
1954G>C (Glu651Gln)	0	92	53	1.73	0.084	ns
	1	53	45			
	2	6	7			
1951G>A and 1954G>C Haplotypes	0	92	53	2.15	0.032	*
	1	45	30			
	2	14	22			

Results of a nonparametric trend test for association between F13A1 SNPs and survival status. Genotypes of the SNPs were coded for the number of alternative alleles present and the test was run to see whether there was a trend between the number of alternative alleles and survival status i.e. alive or dead and the direction of the trend, (z-statistic): (-) negative or (+). P-values were considered significant if $p<0.05$. Levels of significance: (*) $p<0.05$, (**) $p<0.01$.

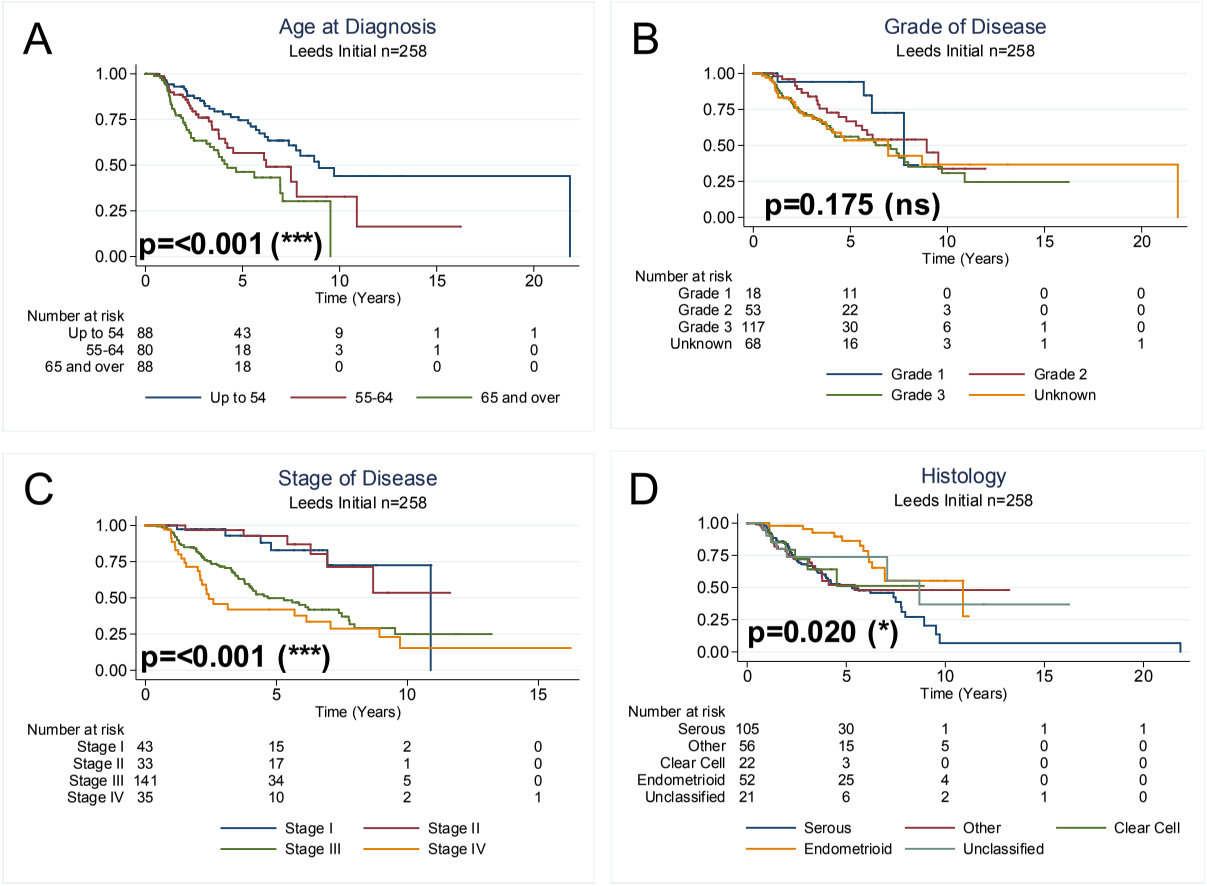

Figure 3-B: Kaplan-Meier Plots for Prognostic Factors in the Leeds Initial Cohort (n=258). Results of a univariate log rank test is given in the bottom left corner of each plot. Risk tables showing the number of patients left at risk every 5 years are below each plot. (A) Age at Diagnosis, (B) Grade of Disease, (C) Stage of Disease and (D) Histology. Results of the log rank test were considered significant if $p<0.05$. The levels of significance: (*) $p<0.05$, (**) $p<0.01$, (***) $p<0.001$ and (ns) not significant.

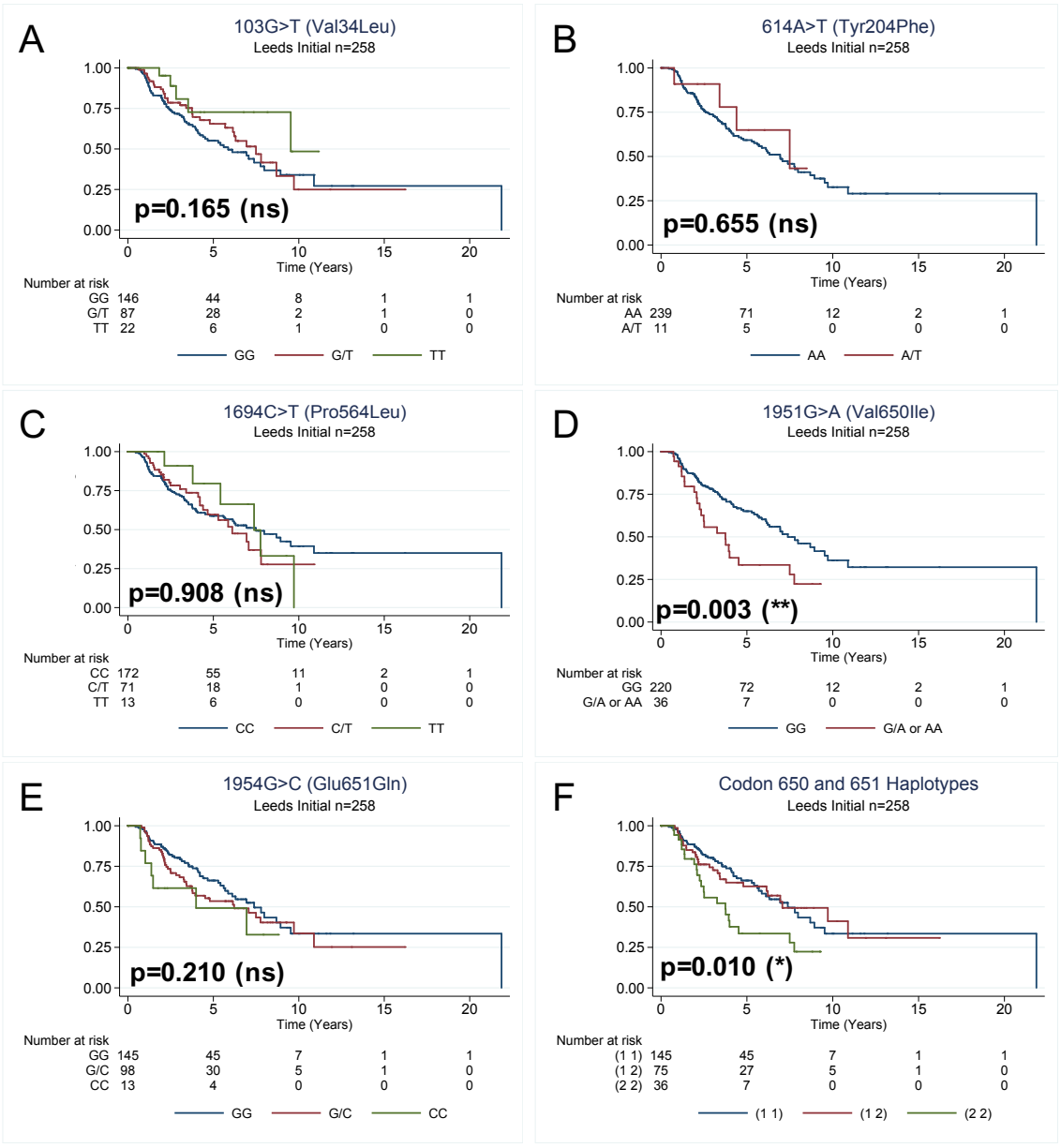

Figure 3-C: Kaplan-Meier Plots for *F13A1* Genotypes in the Leeds Initial Cohort (n=258). Results of a univariate log rank test is given in the bottom left corner of each plot. Risk tables showing the number of patients left at risk every 5 years are below each plot. (A) 103G>T (Val34Leu), (B) 614A>T (Tyr204Phe), (C) 1694C>T (Pro564Leu), (D) 1951G>A (Val650Ile), (E) 1954G>C (Glu651Gln) and (F) Haplotypes for 650 and 651, as these two SNPs are in linkage-disequilibrium with oneanother: (1 = wildtype, and 2 = carrier of at least one copy of the alternative allele). As 1951A is not found without at least copy of 1954C, the haplotype (2 1), does not exist. Results of the log rank test were considered significant if $p<0.05$. The levels of significance: (*) $p<0.05$, (**) $p<0.01$, (***) $p<0.001$ and (ns) not significant.

SNPs are found together in the population. 1954C can be found without 1951A. Carriage of at least one copy of 1954C (Haplotype (1,2)), resulted in a prognosis similar to those of wildtype (Figure 4-D, Plot F) with median survival times of 7.38 for 1954C and 7.07 years for wildtype. However, carriage of 1951A resulted in a poorer prognosis, with a median survival time of 3.78 years. When the two SNPs are assessed separately, it is clear that carriage of 1951A (Figure 4-D, Plot D) is the allele detrimental to survival.

3.6 Multivariate Survival Analysis

Interpretation of univariate analysis alone for associations with survival is inadequate, as complex disease models mean that prognostic factors may be contributing to the disease state in different degrees and therefore multivariate modelling is required. Full details of Cox Proportional Hazards Regression Models (CPHRM) can be found in Chapter 2, Materials and Methods (Section 2.11). In short, an all-in-one methodology rather than a stepwise regression of covariates was used, in order to take all possible covariates into consideration in a disease as complex as cancer. The model included age at diagnosis which was treated as a continuous variable, grade and stage of disease, histology, and the *F13A1* SNPs were all treated as categorical variables (Table 3-7). The linked SNPs 1951G>A and 1954G>C were tested in the model as haplotypes, as this is how they are naturally found in the population.

Age at diagnosis, late stage and endometrioid histology were all significantly associated with overall survival in the CPHRM, when compared to the baseline set covariates (HR=1.00). Age and late stage disease all lead to an increased risk of death with reported hazard ratios >1.00. Patients with endometrioid histology were 50% less likely to die compared to those with serous disease (HR=0.49, p=0.035, 95% Confidence Intervals (CIs) 0.0.25-0.95). The benefit of endometrioid histology was clearly demonstrated in univariate survival analysis, (Figure 3C-Plot D). Patients who were homozygous for the alternative ‘T’ allele for the SNP 103G>T (103T/T) had a significant benefit to their overall survival compared to wildtype individuals (HR=0.34, p=0.024, 95% CIs=0.13-0.86). Although not significant, heterozygous individuals at 103G>T also had a lower hazard ratio, lying in-between the hazard ratio between wildtype and homozygous alternative individuals. For the SNPs 1951G>A and 1954G>C,

those who carry both alternative alleles were over 70% more likely to die compared to wildtype (HR=1.73, p-0.055, 95% CIs=0.99-3.03). Although the result is not strictly significant, it is only just over the set alpha value of 0.05. The clear detriment to survival for double carriage at these SNP sites was previously demonstrated in the univariate analysis (log rank p-value=0.01, trend test p-value 0.032). The other SNPs, 614A>T and 1694C>T were not significant covariates in the built Cox Model.

The larger study (ELO, n=628), identified that double carriage of 1951G>A and 1954G>C was a significant predictor of death (HR=2.10, n=65/612). In this Leeds sub-cohort, for those with double carriage the hazard ratio is 1.71. Unlike the ELO Cohort, carriage of 1954C only, was not a significant predictor of survival, with a reported HR of 1.02. The larger size of the ELO cohort provides a great number of samples for testing, so it may be that for the Leeds Cohort alone, there are not enough individuals to see a significant benefit to survival.

Table 3-7: Hazard Ratios from Cox Proportional Hazards Regression Model for the Leeds Initial Cohort

Covariate/Predictor		HR	Std Error	p-value	Sig.	95% CIs	
						Lower	Upper
Age at Diagnosis		1.04	0.01	<0.001	***	1.02	1.06
Grade	1	1.00					
	2	1.23	0.70	0.722		0.40	3.78
	3	1.40	0.76	0.536		0.48	4.03
	unknown	1.56	0.91	0.446		0.50	4.87
Stage	I	1.00					
	II	1.27	0.77	0.698		0.39	4.15
	III	3.29	1.51	0.009	**	1.34	8.07
	IV	5.22	2.58	0.001	**	1.98	13.74
Histology	Serous	1.00					
	Other	0.80	0.21	0.405		0.47	1.35
	Clear Cell	0.85	0.40	0.723		0.33	2.14
	Endometrioid	0.49	0.17	0.035	*	0.25	0.95
	Unclassified	0.48	0.23	0.130		0.19	1.24
103G>T (Val34Leu)	GG	1.00					
	G/T	0.78	0.19	0.297		0.49	1.25
	TT	0.34	0.16	0.024	*	0.13	0.86
614A>T (Tyr204Phe)	AA	1.00					
	A/T	0.71	0.46	0.594		0.20	2.55
1694C>T (Pro564Leu)	CC	1.00					
	C/T	1.16	0.29	0.554		0.71	1.88
	TT	0.88	0.40	0.787		0.36	2.15
1951G>A (Val650Ile) & 1954G>C (Glu651Gln)	1 1	1.00					
	1 2	1.02	0.26	0.947		0.62	1.67
	2 2	1.73	0.49	0.055		0.99	3.03

Cox Proportional Hazards Regression Modelling used time-event data, with the event reported in this cohort study being death, and time measured in years. The model was built using the co-variates listed in the left-most column. Age at diagnosis was treated as a continuous covariate. Grade, stage, histology and the *F13A1* SNPs were treated as categorical covariates. N=245 for this model, as Cox Proportional Hazards Regression Modelling does not include patients with any missing data for the tested covariates. For 1951G>A and 1954G>C haplotypes: 1=WT and 2= Carriage of the alternative allele. If the Hazard Ratio (HR) is >1.00, then individuals with this covariate are more likely to experience death compared to the baseline covariate (HR=1.00). If the HR <1.00, then those patients with the covariate are less likely to experience death. Covariate hazard ratios were considered significant predictors of death if $p<0.05$. Levels of significance: (*) $p<0.05$, (**) $p<0.01$, with alpha set at 0.05. Abbreviations: Standard Error (Std. Error), Significance (Sig.), and 95% Confidence Intervals (95% CIs). Stage is based on the classification by the International Federation of Gynaecology and Obstetrics.

3.7 The Leeds Mature Data Cohort (n=252)

3.7.1 Comparisons with Leeds Initial Cohort

Mature survival data was collected for the Leeds Cohort in October 2016, 13 years after the original follow-up in 2003. The distribution of prognostic factors and comparison to the initial Leeds Cohort is summarised in Table 3-8. Data was missing for 6 patients, and these data could not be found after thorough investigation. Distribution of *F13A1* SNPs is summarised in Table 3-9. Maximum follow-up time for any patient was 23.4 years (Range: 0.443-23.29 years), with a median survival of 5.86 years . Of the remaining patients, 203 were dead (81%) and 49 were alive (19%) at the time of mature data collection.

3.8 Mature Survival Analysis

3.8.1 Univariate Analysis: Kaplan-Meier and Log Rank Tests

Univariate survival analysis was performed on *F13A1* SNPs. No significant associations were found between SNPs 103G>T, 614A>T or 1694C>T. Significant associations with survival were strengthened in the Mature Leeds Cohort compared to the initial Leeds cohort, (Figure 3-D). The significance of the association between the haplotypes of codons 650 and 651 was stronger compared to the initial round of survival analysis for the Leeds cohort, p=0.007 vs p=0.010, respectively (Figure 3-D, Plot C vs Figure 3-B, Plot F), indicating that the detriment of double carriage of the alternative alleles at these SNP sites is detrimental to long term survival.

3.8.2 Multivariate Analysis

A Cox Proportional Hazards Regression Model was built as before, and included age at diagnosis, stage of disease, grade, histology and the *F13A1* SNPs, (Table 3-10). As identified in the initial round of survival analysis for the Leeds cohort (n=258), late Stage (III and IV) were significant, strong predictors of poor prognosis. Endometrioid histology was again, a significant predictor of improved prognosis with a similar hazard ratio (HR=0.60, p=0.020, 95% CIs=0.39-0.92). The previously seen significance of 103G>T homozygous individuals (103T/T) as a predictor of improved prognosis was no longer present in the mature Leeds cohort (n=252), (HR=0.87, p=0.611, 95% CIs=0.51-1.49). This suggests that 103G>T may be important for shorter-term rather than long-term survival. The significance of double carriage of alternative alleles at 1951G>A and

Table 3-8: Comparison of the Distribution of Prognostic Factors between the Leeds Mature (n=252) and Leeds Initial (n=258) Cohorts

Prognostic Factor	Leeds Mature (n=252)		Leeds Initial (n=258)	
	n	%	n	%
Age at Diagnosis				
Up to 54	88	35.1	88	34.4
55-64	78	31.1	80	31.9
65 and over	85	33.9	88	35.1
Grade				
1	18	7.1	18	7.0
2	53	21.0	53	21.0
3	114	45.2	117	46.4
unknown	67	26.6	70	27.8
Stage				
I	43	17.1	43	16.7
II	32	12.7	33	13.1
III	140	55.6	142	56.3
IV	34	13.5	36	14.3
Unknown	3	1.2	4	1.6
Histology				
Serous	104	41.3	105	40.7
Other	56	22.2	57	22.6
Clear Cell	22	8.7	23	9.1
Endometrioid	50	19.8	52	20.6
Unclassified	20	7.9	21	8.3

Stage is based on the classification by the International Federation of Gynaecology and Obstetrics.

Table 3-9: Comparison and Distribution of *F13A1* SNPs in the Leeds Mature (n=252) and Leeds Initial (n=258) Cohorts

SNP (Amino Acid Change)	Leeds Mature (n=252)		Leeds Initial (n=258)	
	n	%	n	%
103G>T (Val34Leu)				
GG	145	58	146	57
G/T	85	34	89	35
TT	21	8	22	9
614A>T (Tyr204Phe)				
AA	236	96	241	96
A/T	10	4	11	4
TT	0	0	0	0
1694C>T (Pro564Leu)				
CC	170	67	174	67
C/T	69	27	71	28
TT	13	5	13	5
1951G>A (Val650Ile)				
GG	217	86	222	86
G/A	34	13	34	13
AA	1	0	2	1
1954G>C (Glu651Gln)				
GG	143	57	146	57
G/C	97	38	99	38
CC	12	5	13	5

For each SNP, the top line presents the wildtype genotype, followed by the heterozygous genotype and finally the homozygous alternative genotype, for each SNP. The corresponding amino acid change for each SNP site is given in the parentheses. For analyses, 1951G>A (Val650Ile) heterozygotes and homozygous alternative patients were combined in order to prevent the effect of small numbers as n<5. Data for one patient was missing for 103G>T in Leeds Mature (n=251). Data was missing for six patients for 614A>T (n=246).

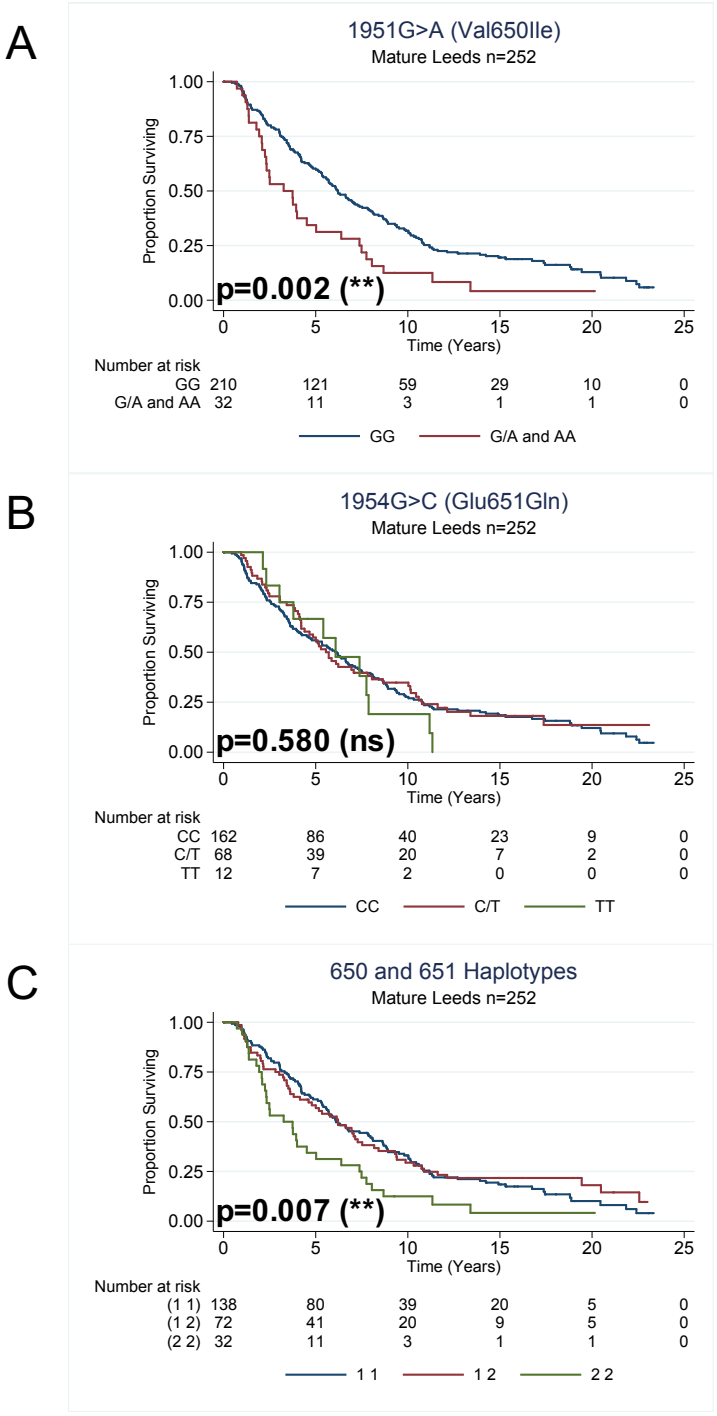

Figure 3-D: Kaplan-Meier Plots for *F13A1* SNPs in the Mature Leeds Cohort (n=252). Results of a univariate log rank test is given in the bottom left corner of each plot. Risk tables showing the number of patients left at risk every 5 years are below each plot. (A) 1951G>A (Val650Ile), (B) 1954G>C (Glu651Gln) and (C) Haplotypes for 650 and 651, as these two SNPs are in linkage-disequilibrium with oneanother: (1 = wildtype, and 2 = carrier of at least one copy of the alternative allele). As 1951A is always found with 1954C, the haplotype (2 1), does not exist. Results of the log rank test were considered significant if $p<0.05$. The levels of significance: (*) $p<0.05$, (**) $p<0.01$, and (ns) not significant.

Table 3-10: Hazard Ratios from Cox Proportional Hazards Regression Model Results for the Leeds Mature Cohort

Covariate/Predictor		HR	Std Error	p-value	Sig.	95% CIs	
						Lower	Upper
Age at Diagnosis		1.02	0.01	<0.001	***	1.01	1.04
Grade	1	1.00					
	2	1.99	0.85	0.106		0.86	4.60
	3	2.60	1.05	0.019	*	1.17	5.75
	unknown	2.40	1.04	0.043	*	1.03	5.62
Stage	I	1.00					
	II	0.96	0.33	0.912		0.49	1.90
	III	1.99	0.56	0.014	*	1.15	3.46
	IV	3.24	1.09	<0.001	***	1.68	6.25
Histology	Serous	1.00					
	Other	0.87	0.17	0.472		0.60	1.27
	Clear Cell	0.77	0.27	0.459		0.38	1.54
	Endometrioid	0.60	0.13	0.020	*	0.39	0.92
	Unclassified	0.60	0.19	0.101		0.32	1.11
103G>T (Val34Leu)	GG	1.00					
	G/T	0.87	0.14	0.402		0.64	1.20
	TT	0.87	0.24	0.611		0.51	1.49
614A>T (Tyr204Phe)	AA	1.00					
	A/T	0.64	0.28	0.299		0.27	1.50
1694C>T (Pro564Leu)	CC	1.00					
	C/T	1.09	0.19	0.609		0.78	1.54
	TT	1.41	0.47	0.297		0.74	2.71
1951G>A (Val650Ile) & 1954G>C (Glu651Gln)	1 1	1.00					
	1 2	0.95	0.16	0.744		0.67	1.33
	2 2	1.86	0.43	0.007	**	1.19	2.92

Cox Proportional Hazards Regression Modelling used time-event data, with the event reported in this cohort study being death, and time measured in years. The model was built using the co-variates listed in the left-most column. Age at diagnosis was treated as a continuous covariate. stage, histology and the *F13A1* SNPs were treated as categorical covariates. N=234 for this model, as Cox Proportional Hazards Regression Modelling does not include patients with any missing data for the tested covariates. If the Hazard Ratio (HR) is >1.00, then individuals with this covariate are more likely to experience death compared to the baseline covariate (HR=1.00). If the HR <1.00, then those patients with the covariate are less likely to experience death. Covariate hazard ratios were considered significant predictors of death if $p<0.05$. Levels of significance: (*) $p<0.05$, (**) $p<0.01$, and (***) $p<0.001$ with alpha set at 0.05. Abbreviations: Standard Error (Std. Error), Significance (Sig.), and 95% Confidence Intervals (95% CIs). Stage is based on the classification by the International Federation of Gynaecology and Obstetrics.

1954G>C as a predictor of death was strengthened in terms of both risk and level of significance. These individuals were nearly twice as likely to die compared to wildtype individuals (HR=1.86, p=0.007, 95% CIs=1.19-2.92). Carriage of 1951A and 1954C appear important for long term survival for ovarian cancer.

3.9 Summary of Results

- The Edinburgh Leeds Oxford (ELO) Cohort identified that two *F13A1* SNPs, 1951G>A (Val650Ile) and 1954G>C (Glu651Gln) were significantly associated with overall survival in ovarian cancer patients. 1951G>A was detrimental to survival and 1954G>C appeared protective (see Chapter 1, Introduction).
- The Leeds sub-cohort was reanalysed as a stand-alone cohort from follow-up data in 2003. The findings of the ELO cohort were mirrored in the Leeds alone sub-cohort (Leeds Initial). Double carriage of alternative alleles at both 1951G>A and 1954G>C was poorer for prognosis, when measured in multivariate analysis: HR=1.73, p=0.056).
- In univariate analysis of SNPs and survival in the Leeds cohort, the SNP 614A>T was significantly associated with grade of disease, however the lack of homozygous alternative patients and the small number of patients carrying the alternative T allele (RAF is only 3%), may be skewing the data and a larger cohort would be required to see whether this SNP is truly associated with grade of disease.
- In addition to 1951G>A and 1954G>C and their associations with overall survival, *F13A1* SNP 103G>T was also associated with overall survival in the Leeds Initial Cohort: 103T/T patients had a significantly better prognosis compared to wildtype 103G/G patients (HR=0.34, p=0.024).
- Mature survival data was collected in October 2016, 13 years after the original follow-up. The associations between 1951G>A and 1954G>C were maintained in long-term follow-up, suggesting these SNPs are important for long-term survival. Double carriage at 1951 and 1954 (HR=1.86, p=0.007)
- In long-term follow-up, 103T/T patients no longer had a significant association with survival in multivariate analysis (p, suggesting this SNP may be important in short term survival.

- The Leeds cohort was biased towards survivors on average of two years and therefore any findings would need to be demonstrated in a cohort of newly diagnosed patients

3.10 Brief Discussion

The Leeds cohort was a unique cohort of patients, due to the recruitment of patients throughout different points in their treatment. There was an inherent bias within the cohort towards women who had survived at least two years. This meant that patients who had succumbed quickly to their disease were likely to be missed. The availability of mature survival data provided an excellent opportunity to further assess how SNPs within the gene for FXIIIA, *F13A1*, affect ovarian cancer prognosis. Long term survival analysis has been undertaken in colorectal (246), breast (244) and prostate cancer (245) with the aim of understanding whether covariates of interest (such as protein expression, genotypes or treatments) vary over time and how they may affect prognosis and disease management. Better understanding of what makes patients survive longer than others is vital as oncology continues its drive towards personalised medicine.

The *F13A1* SNPs 1951G>A and 1954G>C have not previously been associated with diseases, cancer or otherwise, so this work is the first to suggest a role for these SNPs in OC prognosis. The polymorphisms are situated within the second beta barrel of the FXIIIA secondary structure, but are not near the catalytic core or near sites which are associated with conformational changes to the protein during activation (Arg310-Tyr311 and Gln425-Phe426) (156) so the precise effect of these SNPs remains to be explored. The polymorphisms do not appear to alter FXIIIA protein levels or specific activity (166), therefore some other effect may be exerted perhaps through an effect on one of FXIIIA's other roles.

Mature survival data in the Leeds cohort resulted in loss of survival benefit for homozygous alternative patients (103T/T) during long term follow-up. This suggests that the beneficial effect of this SNP on survival may important for shorter term survival. The SNP 103G>T has been associated with thrombotic disease and some cancers (219,220,247,248). Homozygous individuals for 103G>T (103T/T) had a decreased risk of colorectal cancer (219), and carriage of the heterozygous genotype at this SNP site was protective in uterine myoma

(248). However, the effect of 103G>T in cancer is unclear, as 103TT has been associated with a greater risk of oral cancer development (220). Therefore 103G>T appears to exert its affects, which remain to be further elucidated in cancer, in a cancer-type dependent manner. 103T/T results in Leu/Leu at codon 34 in the FXIIIA protein, and this variant results in more rapid and tighter-crosslinking of matrix proteins (191,247). This alteration to crosslinking speed and nature may be changing tumour extracellular matrices or perhaps the variant protein is exerting another effect which remains to be established and requires further investigation. In the mature analysis, 81% of patients carrying 103T/T had died. It is unknown whether these patients died as a result of their cancer or from another co-morbidity or condition. As 103G>T is associated with thrombotic disease, such as ischaemic stroke and myocardial infarction (156,192,196,198,208,247), it may be that patients with this genotype may die from conditions such as these, although examination of 103G>T prevalence in cancer patients with and without thrombosis revealed no differences (195).

Analysis of this ovarian cancer cohort has resulted in some interesting findings which appear to associate *F13A1* SNPs with overall survival. This cohort was biased towards survivors of at least two years, with 75% (n=193/258) of patients surviving over 2 years due to the nature of sample collection. Patients were recruited for the study at all possible clinic appointments, including follow-up appointments and were not limited to appointments for newly diagnosed patients. As a result, the associations found within the cohort would need to be tested in a newly diagnosed cohort of women, in order to assess whether the associations affect survival in a group of women who are followed from the initial diagnosis through to censorship. The next chapter in this thesis sets out to perform survival analysis on a newly diagnosed cohort of women, for this exact purpose.

Chapter 4: *F13A1* SNPs and Survival Intervals in OC in a prospective clinical cohort: ICON7

4.1 Introduction

Analysis of a cohort of ovarian cancer (OC) patients from Leeds identified that SNPs within the *F13A1* gene appeared to be associated with overall survival (Chapter 3). The SNPs 1951G>A and 1954G>C, although in linkage disequilibrium, as 1951G>A is not found without at least one 1954C allele, had opposite effects on prognosis. 1951G>A was detrimental to survival, whereas 1954G>C was found to be beneficial, although presence of the alternative C allele during double carriage was unable to prevent the deleterious effect of the alternative A allele. The cohort of patients from Leeds was biased towards survivors of two years on average, likely due to not being a prospective study, as recruitment included patients who had been newly diagnosed as well as patients who appeared in clinic for follow-up appointments after treatment. Therefore, the potential associations between *F13A1* SNPs and survival in OC required exploration in another cohort of newly diagnosed patients.

A new cohort of OC patients was made available through the ICON7 Clinical Trial Translational Cohort (n=448 for DNA samples), which was the cohort of women who had consented for their samples and data to be used in translational research. The purpose of the ICON7 Clinical trial was to test the benefit of the addition of bevacizumab to the standard chemotherapy regimen of carboplatin and paclitaxel (n=1528). The translational DNA cohort comprising 29% of patients from the whole trial was considered large enough to reflect the full ICON7 cohort in terms of expected associations and survival for OC. This cohort, comprising newly diagnosed patients only, was initially studied for associations between prognostic factors and survival intervals in OC, including progression-free survival (PFS), survival post-progression (SPP) and overall survival (OS). The variables recorded within this cohort also allowed for exploration and testing of association between *F13A1* SNP genotypes and risk of disease progression and response to treatment received.

4.2 ICON7 Cohort

4.2.1 Cohort Characteristics

A comparison of the sample distribution for the translational and full ICON7 cohorts is shown in Table 4-1. The sample distribution for prognostic factors was similar in the two groups, and the translational cohort reflected the trends typically seen in general[1] OC cohorts. Median survival for this translational cohort (n=448) was 4.7 years. At the end of the study period 46.4% of patients were dead and 53.6% were alive. Median age was 57, with ages between 24 and 79 years. The most common histology was serous, and median age at diagnosis was in the menopausal age range. A novel variable available in the ICON7 cohort was 'at high risk of disease progression'. This grouping included patients with Stage IIIC/IV disease, and/or those with 1 cm of disease margin remaining after resective surgery, or where surgery had not been possible. Due to the metastatic potential of late stage OC or tumour bulk which remains in the peritoneum, these women were more likely than others without these factors to experience a worsening in their disease (78). The risk of progression variable was not present in the Leeds cohort, and therefore allowed for a novel exploration of associations between *F13A1* SNPs and risk.

4.2.1 Power Analysis

Power analyses for multivariate Cox Proportional Hazards Regression Modelling was performed to test whether a cohort of this size would be sufficiently powered to detect differences and associations between survival intervals in multivariate testing. For the given sample size of n=448, power was calculated for the detection of hazard ratios from 0.5-2.0 for each of the *F13A1* variants investigated based on the rare allele frequency (RAF) for each of the SNPs, (Figure 4-A). Power analysis for studies involving SNPs have particularly focused on case-control studies, where prevalence in a "control/normal/healthy" population is compared to the "test/disease-state" population. However, in the cohort under investigation in this

---

[1] By "general" these are prospective cohorts which recruit a breadth of ovarian cancer patients which are not excluded based on particular characteristics for example grade, histology or resistance to therapy such as platinum-resistance.

Table 4-1: Comparison of Prognostic Factors Between the Full and Translational ICON7 Clinical Patient Cohorts

Prognostic Factor		Full ICON7		Translational ICON7	
		n=1528	*%*	*n=448*	*%*
Age - Years Median (range)		57 (18-82)		57 (24-79)	
Grade	1	97	*6*	22	*5*
	2	317	*22*	73	*17*
	3	1094	*87*	347	*79*
	unknown	20	*8*	0	*0*
FIGO Stage	I	142	*10*	35	*8*
	II	80	*5*	55	*12*
	III	1045	*71*	306	*68*
	IV	201	*14*	52	*12*
Histology	Serous	1054	*69*	306	*68*
	Mucinous	34	*2*	5	*1*
	Endometriod	117	*8*	32	*7*
	Clear Cell	127	*8*	53	*12*
	Mixed	88	*6*	33	*7*
	Other	108	*7*	19	*4*
High Risk of Progression	No	1063	*70*	298	*67*
	Yes	465	*30*	150	*33*

In the Translational ICON7, some Grade data was missing for 6 patients. These are not classed as Unknown, as the data is missing, rather than grade being undetermined.

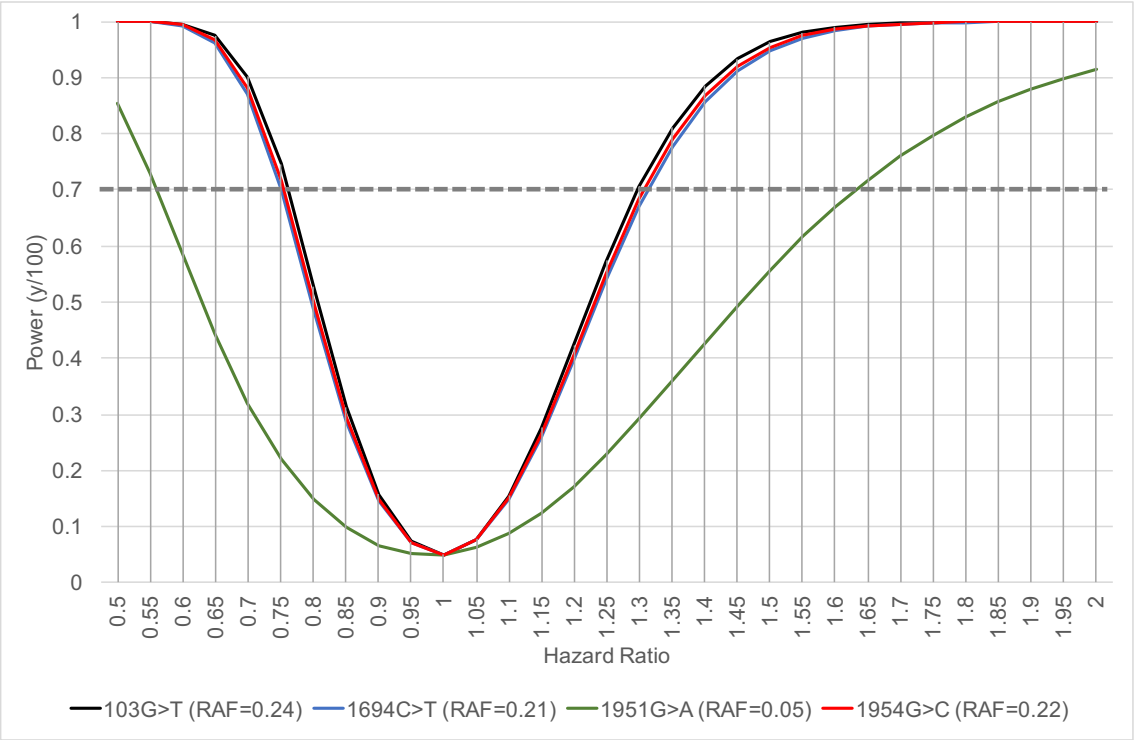

Figure 4-A: Graph to show power to detect hazard ratios for *F13A1* SNPS in a cohort of 448 patients. Power detected using the survSNP package by Owzar *et al*. It is harder to detect smaller changes in hazard ratios without a larger cohort, as demonstrated in the above plot. The grey horizontal dashed line represents 70% power, and any hazards from the point of intersection from this line are sufficiently powered at 70% power. RAF= Rare Allele Frequency, i.e. frequency of the alternative SNP allele.

Chapter, the point of focus is on the effects of SNPs on censored time-to-event data, with the event being progression or death. Although many tools are available to help calculate power for “case-control” studies, they are not appropriate for survival analyses, and therefore other tools are required. One tool that was able to assist in the performance of power analyses for this cohort was the ‘survSNP’ package for the statistical software ‘R” developed by Owzar and colleagues at Duke University (241). Full details are presented in Chapter 2 - Materials and Methods.

For the number of samples available, hazard ratios < 0.75 and >1.35, can be measured at 70% power for SNPS 103G>T, 1694G>T and 1954G>C. For SNP 1951G>A, hazard ratios < 0.55 and >1.63 can be measured at 70% power. As 1951G>A is a much rarer SNP, with a rare allele frequency (RAF) of 0.05, a greater number of samples is required to sufficiently detect hazard ratios at lower, less extreme ranges.

4.3 ICON7 *F13A1* Genotypes

Peripheral blood DNA samples were provided by the MRC Clinical Trials Unit at University College London and each patient sample was sequenced at three exons which contained the *F13A1* SNPs. All sequencing was performed blind to the clinical data to limit any bias towards sample handling. After sequencing, fully anonymised clinical data was made available and a database was generated containing clinical data and genotype at the SNP sites under investigation for use in statistical analysis.

4.3.1 Genotypes and Hardy Weinberg Equilibrium

The ICON7 cohort F13A1 genotyping data is summarised in Table 4-2. All SNPs, except for 1694C>T were in Hardy-Weinburg Equilibrium (HWE Chi-squared p-value=0.004). Interestingly, there were significantly fewer 1694C>T heterozygotes than expected for the observed allele frequency for this SNP, and more homozygotes for the C and T alleles. A similar pattern was observed for the 103G>T SNP, with there being fewer 103G>T heterozygotes than expected, although this difference was not significant (p=0.059).

Table 4-2: Distribution of *F13A1* Single Nucleotide Polymorphisms in the Translational ICON7 Cohort

SNP (Amino Acid Change)	Observed	Observed (%)	Allele Frequenices	Expected	HWE p-value
103G>T (Val34Leu)					
GG	272	61	0.77/0.23	265	0.059
G/T	145	32		159	
TT	31	7		24	
1694C>T (Pro564Leu)					
CC	278	62	0.77/0.23	267	0.004
C/T	136	30		158	
TT	34	8		23	
1951G>A (Val650Ile)					
GG	391	87	0.93/0.07	389	0.133
G/A	52	12		56	
AA	4	1		2	
1954G>C (Glu651Gln)					
GG	258	58	0.76/0.24	256	0.669
G/C	161	36		164	
CC	28	6		26	
650 + 651 Haplotypes					
GG + GG	258	58			
GG + G/C or C/C	133	30			
G/A or A/A + G/C or C/C	56	13			

For 1951G>A and 1954G>C, data could not be acquired for one patient, therefore n=447 for these two SNP sites. Allele frequencies, expected values and test for Hardy-Weinberg Equilibrium (HWE) was performed using the 'genhwi' package in Stata (249). Populations were not in HWE for SNP 1694C>T as $p<0.05$, therefore the null hypothesis that the population is in HWE is rejected. The population was in HWE for all other SNPs.

Table 4-3: Comparison of Allele Frequencies in the ICON7 Translational Cohort to a European population

F13A1 SNP (Amino Acid Change)	Allele Frequency		Significantly Different
	ICON7 (n=448)	gnomAD	
103G>T (Val34Leu)	0.77/0.23	0.76/0.24	No (0.868)
1694C>T (Pro564Leu)	0.77/0.23	0.79/0.21	No (0.733)
1951G>A (Val650Ile)	0.93/0.07	0.95/0.05	No (0.552)
1954G>C (Glu651Gln)	0.76/0.24	0.78/0.22	No (0.737)

Allele frequencies were calculated using the 'genhwi' package in Stata (249). Allele frequencies for a healthy European population were taken from the genome aggregation database (gnomAD). A Chi-squared test was used to test whether the observed values in the two population, ICON7 and gnomAD-European, were significantly different from one another using an online calculator tool (250).

4.3.2 Allele Frequencies Compared to Normal Population

Measurement of allele frequencies i.e. how often one allele appears in one population compared to another, is important for assessing the alternative allele in contributing to a disease state. Allele frequencies of *F13A1* SNPs did not appear to differ greatly from the normal Caucasian population (The ICON7 translational cohort was 98% Caucasian), (Table 4-3).

4.3.3 Linkage Disequilibrium

Estimates of Lewontin's D' linkage disequilibrium found that only 1951G>A and 1954G>C were in linkage disequilibrium with one another (p=<0.001), (Table 4-4A) and significantly associated with one another (Table4-4B). This finding is in line with the literature (192) and within the Leeds Cohort (Chapter 3).

4.4 Associations between Prognostic Factors and *F13A1* SNPs

Tests of association between *F13A1* SNPs and prognostic factors in OC such as grade, stage, and histology of disease were performed. If SNPs were associated with such prognostic factors, then it could further the understanding of how the SNP genotype is contributing to the OC disease state. Associations were tested with Chi-squared tests. 103G>T (Val34Leu) was significantly associated with grade of disease (p=0.047) and 1954G>C was significantly associated with risk of progression (p=0.039), (Table 4-5A). The distribution of genotypes at these SNPS and the prognostic factors found that 34V/L heterozygotes had lower grade than wildtype, but that 34L/L homozygotes had higher grade disease (Table 4-5-B), suggesting heterozygous individuals may have a better prognosis as their disease was more differentiated than others. More heterozygotes 651E/Q individuals were at risk of progression than both homozygous genotypes.

4.5 Univariate Survival Analysis

4.5.1 Overall Survival

Overall survival (OS) is defined as the length of times between the start of the study (Day 0) and either death or censorship (date last seen). Log Rank Tests were used to determine the degree of association, and Kaplan-Meier Plots were generated to demonstrate the relationship of each variable with survival over the study time. Grade and stage were significantly associated with overall survival, as was risk of disease

Table 4-4: Linkage Disequilibrium of *F13A1* SNPs in the ICON7 Translational Cohort Population

A

F13A1 SNP	103G>T (Val34Leu)	1694C>T (Pro564Leu)	1951G>A (Val650Ile)	1954G>C (Glu651Gln)
103G>T (Val34Leu)				
1694C>T (Pro564Leu)	0.09			
1951G>A (Val650Ile)	0.21	0.2		
1954G>C (Glu651Gln)	0.14	0.23	1	

B

F13A1 SNP	103G>T (Val34Leu)	1694C>T (Pro564Leu)	1951G>A (Val650Ile)	1954G>C (Glu651Gln)
103G>T (Val34Leu)				
1694C>T (Pro564Leu)	0.354			
1951G>A (Val650Ile)	0.798	0.422		
1954G>C (Glu651Gln)	0.745	0.719	<0.001	

A: Estimated Lewontin's-D' results for linkage disequilibrium for *F13A1* SNPs, see Chapter 2 Materials and Methods for details of calculations (Chapter 2, Section 2.11.X). **B:** Results of Chi-squared tests for association between *F13A1* SNPs. Results considered significant if p-value was <0.05, with significant results highlighted in yellow. The only significant association between SNP genotypes was for the SNPs 1951G>A and 1954G>C, as these SNPs are in linkage disequilibrium with one another in the normal population, with 1951A is always found with 1954C.

Table 4-5A: Chi-Square Tests of Association between Prognostic Factors and *F13A1* SNPs

Prognostic Factor	103G>T (Val34Leu)		1694C>T (Pro564Leu)		1951G>A (Val650Ile		1954G>C (Glu651Gln)	
	p-value	*Sig.*	*p-value*	*Sig.*	*p-value*	*Sig.*	*p-value*	*Sig.*
Grade	0.047	*	0.644	ns	0.12	ns	0.089	ns
FIGO Stage	0.802	ns	0.793	ns	0.415	ns	0.825	ns
Histology	0.059	ns	0.883	ns	0.353	ns	0.906	ns
At Risk of Progression	0.065	ns	0.413	ns	0.924	ns	0.039	*
Treatment	0.144	ns	0.937	ns	0.82	ns	0.473	ns

Level of significance (Sig.) shown by (*). (*) = $p<0.05$, (ns) = not significant, $p>0.05$. Alpha set at 0.05.

Table4-5B: Distribution of SNP genotypes and Prognostic Factors for Significant Chi-Square Associations

Grade	**VV**		**VL**		**LL**	
	n	*%*	*n*	*%*	*n*	*%*
1	11	4%	11	8%	0	0%
2	41	15%	30	21%	2	6%
3	215	81%	103	72%	29	94%
At High Risk of Progression	**EE**		**EQ**		**QQ**	
	n	*%*	*n*	*%*	*n*	*%*
No	181	70%	95	59%	21	75%
Yes	77	30%	66	41%	7	25%

Val34Leu: VV (Wildtype), VL (Heterozygous), LL (Homozygous Alternative.
Glu651Gln: EE (Wildtype), EQ (Heterozygous), QQ (Homozygous Alternative).

progression, with those at high risk having a poorer prognosis (Figure 4-B). The *F13A1* SNPS were not associated with overall survival in the log rank tests (Figure 4-C).

4.5.2 Progression-Free Survival

Progression-free survival (PFS) is defined as the length of time between the start of the study (Day 0) and the experience of a progression event, which may be defined as a worsening in disease. Both FIGO Stage and risk of disease progression were significantly associated with PFS (for both, $p<0.001$). In the Kaplan-Meier graph, it is clearly demonstrated that increasing stage of disease leads to a shorter progression-free survival (Figure 4-D) Those at high risk of disease progression had demonstrably shorter progression-free survival compared to those not at high risk (at high risk median survival of 12.7 months vs. not high risk median survival of 24.3 months) None of the *F13A1* SNPs were significantly associated with disease progression (Figure 4-E).

4.5.3 Survival Post-Progression

Survival post-progression is defined as the period of time after the experience of progression event to either death or censorship in the study. This survival interval in particular can help increase the understanding of the directionality of an association i.e. can a particular genotype lead to more rapid death after progression or is a certain factor protective after progression and lead to a longer survival time. Just as in the overall survival and progression-free survival intervals, grade of disease, stage and risk of progression were all significantly associated with survival post-progression (Figure 4-F). No *F13A1* SNPs were significantly associated with survival post-progression in univariate analysis (Figure 4-G), however, double carriage of polymorphisms at codon 650 and 651 appeared to have a slightly improved prognosis compared to wildtype and carriage of 651 only.

(1)

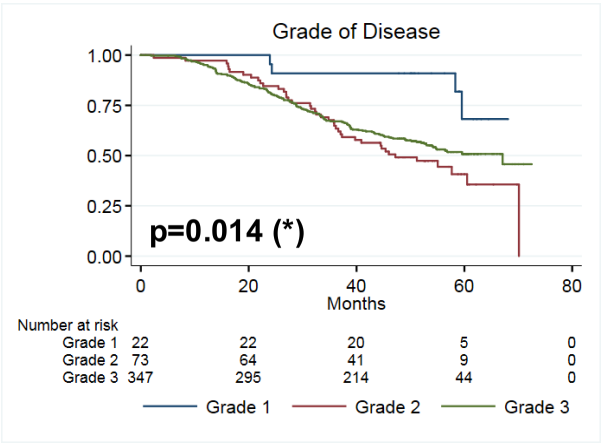

(2)

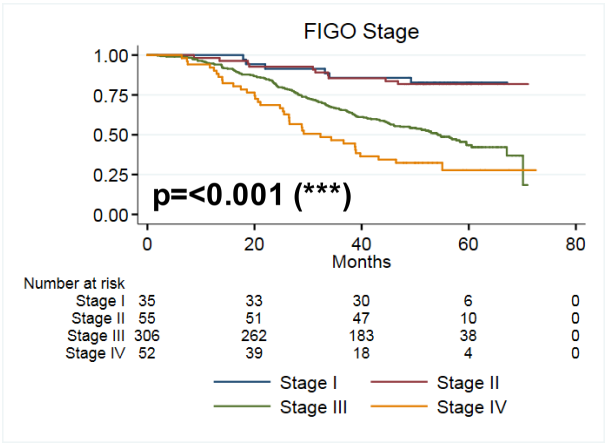

(3)

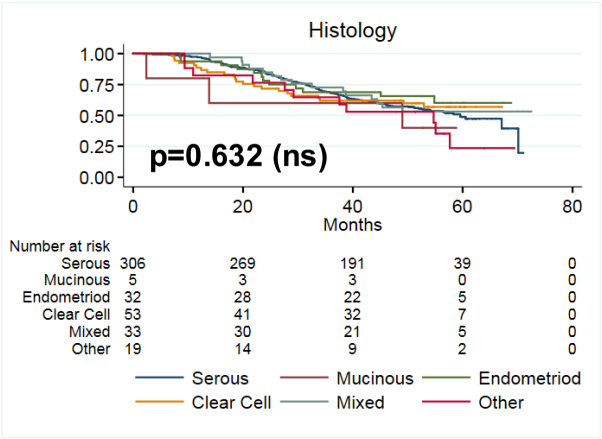

(4)

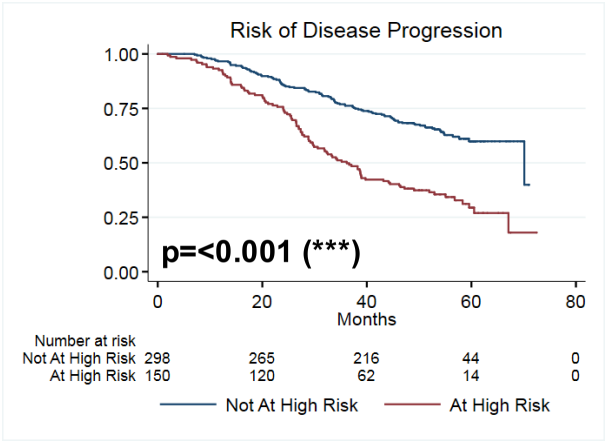

Figure 4-B: Kaplan-Meier Graphs for Overall Survival and prognostic factors. Risk tables of the number of patients at risk at the given number of months on the x-axis (Months) is provided below each graph. The y-axis gives cumulative survival. (1) Grade of Disease, (2) FIGO Stage, (3) Histology and (4) Risk of Disease Progression. Results of a log rank test for association with the survival interval is provided in the bottom left corner of each graph. Significance levels: (*) = p<0.05; (**) = p<0.01; (***) = p<0.001.

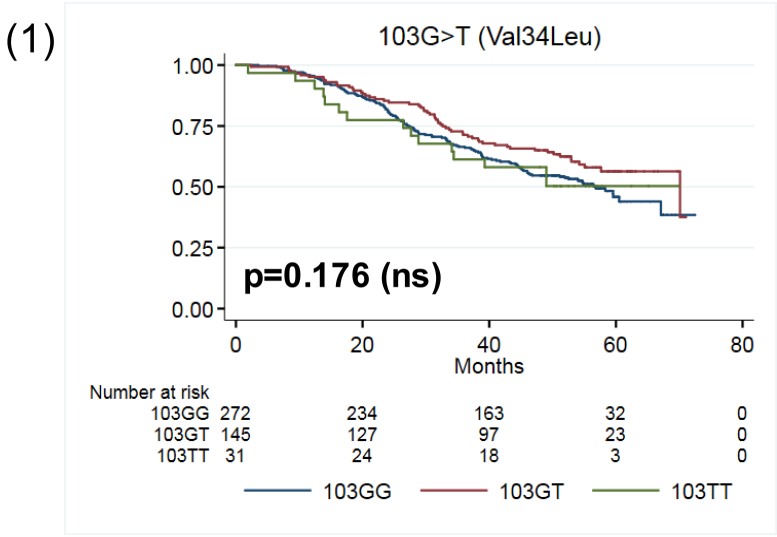

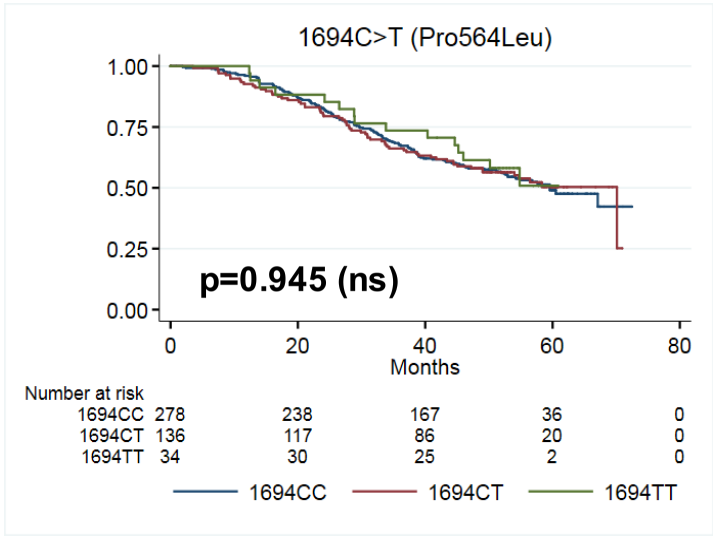

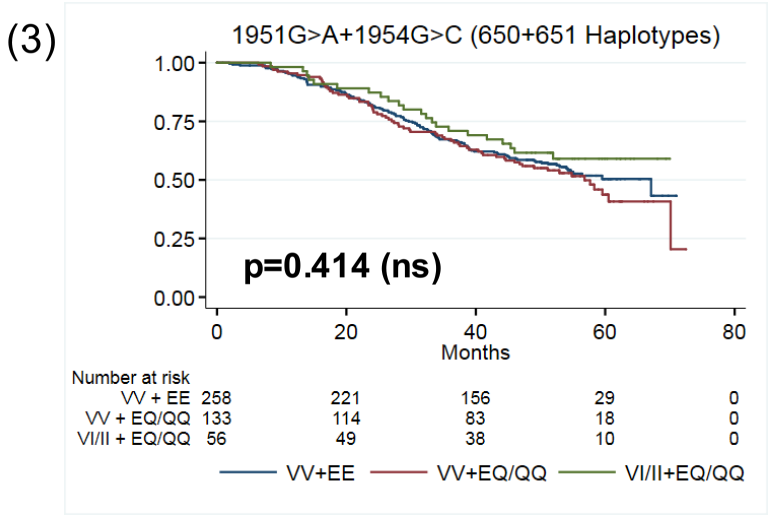

Figure 4-C: Kaplan-Meier Graphs of Overall Survival and *F13A1* SNPs. Risk tables of the number of patients at risk at the given number of months on the x-axis (Months) is provided below each graph. The y-axis gives cumulative survival. (1) 103G>T (Val34Leu), (2) 1694C>T (Pro564Leu), (3) 1951G>A+1954G>C Haplotypes. Results of a log rank test for association with the survival interval is provided in the bottom left corner of each graph. Significance levels: (*) = $p<0.05$; (**) = $p<0.01$; (***) = $p<0.001$, (ns) = not significant.

(1)

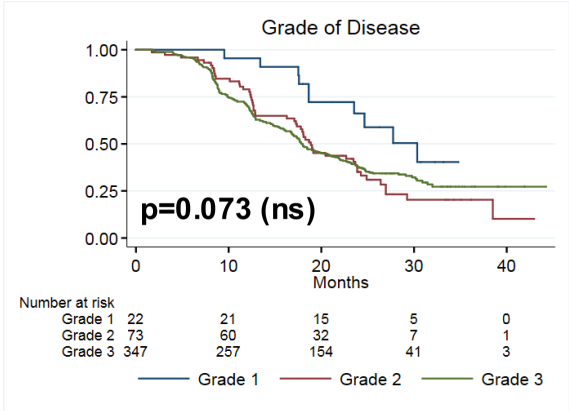

(2)

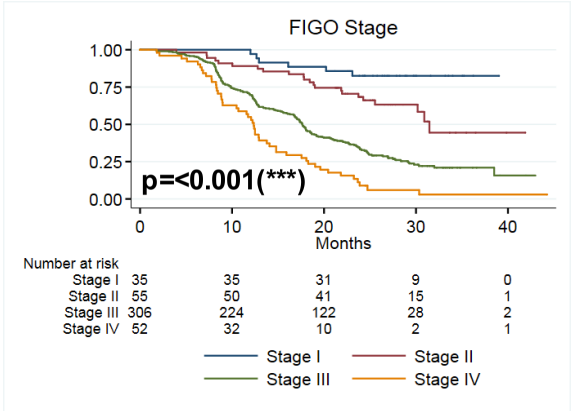

(3)

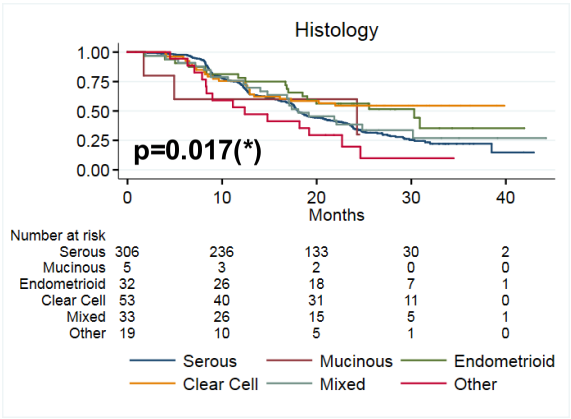

(4)

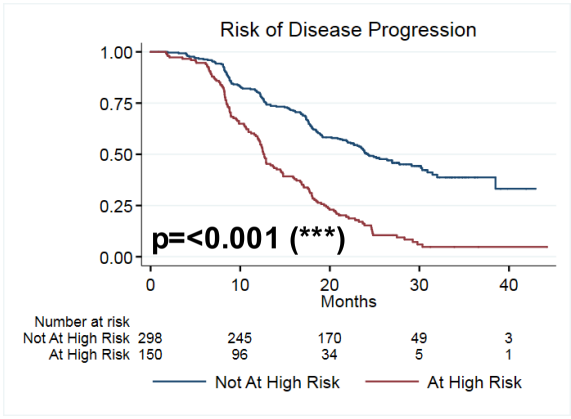

Figure 4-D: Kaplan-Meier Graphs for Progression-Free Survival and prognostic factors. Risk tables of the number of patients at risk at the given number of months on the x-axis (Months) is provided below each graph. The y-axis gives cumulative survival. (1) Grade of Disease, (2) FIGO Stage, (3) Histology and (4) Risk of Disease Progression. Results of a log rank test for association with the survival interval is provided in the bottom left corner of each graph. Significance levels: (*) = p<0.05; (**) = p<0.01; (***) = p<0.001, (ns) = not significant.

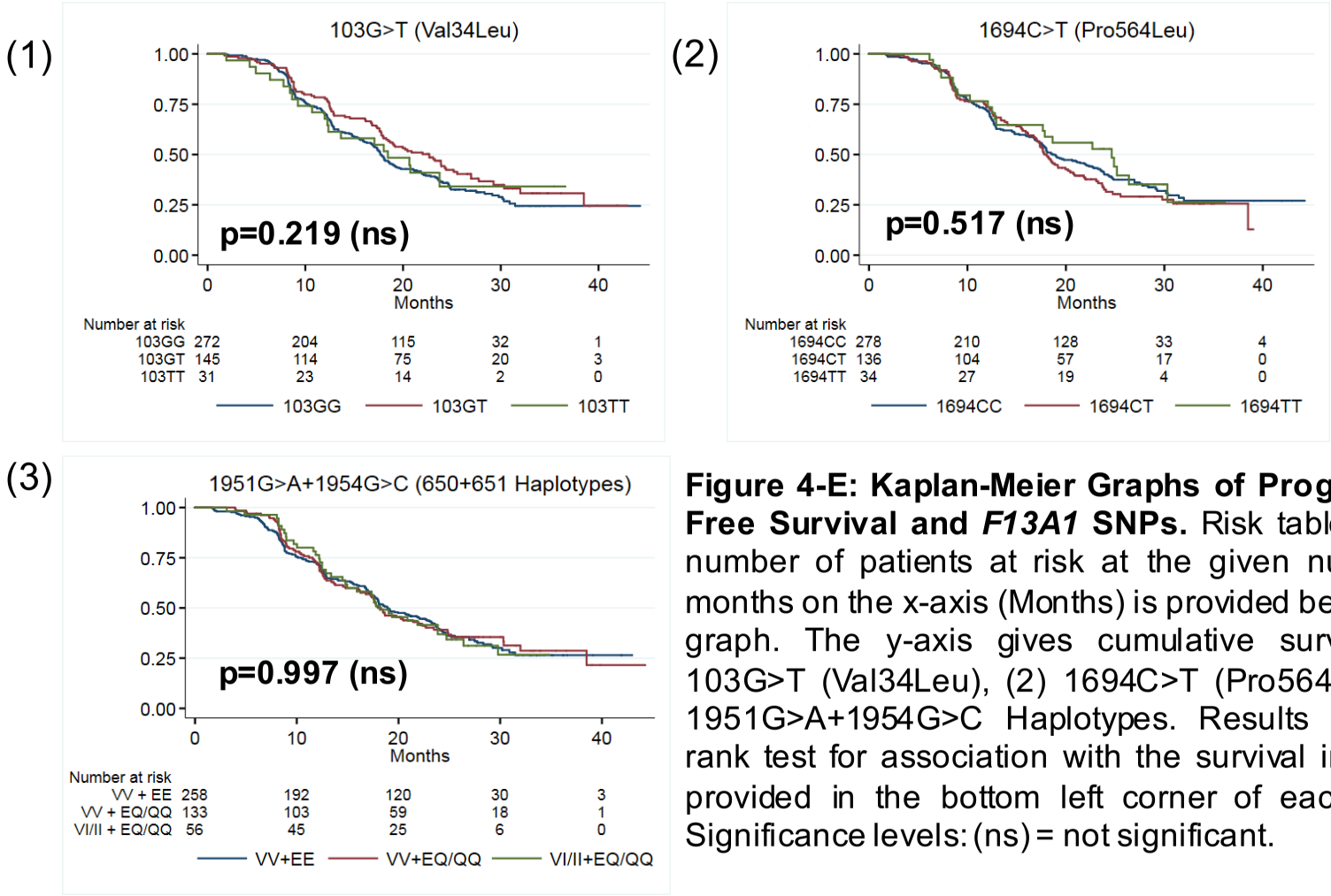

Figure 4-E: Kaplan-Meier Graphs of Progression-Free Survival and *F13A1* SNPs. Risk tables of the number of patients at risk at the given number of months on the x-axis (Months) is provided below each graph. The y-axis gives cumulative survival. (1) 103G>T (Val34Leu), (2) 1694C>T (Pro564Leu), (3) 1951G>A+1954G>C Haplotypes. Results of a log rank test for association with the survival interval is provided in the bottom left corner of each graph. Significance levels: (ns) = not significant.

(1)

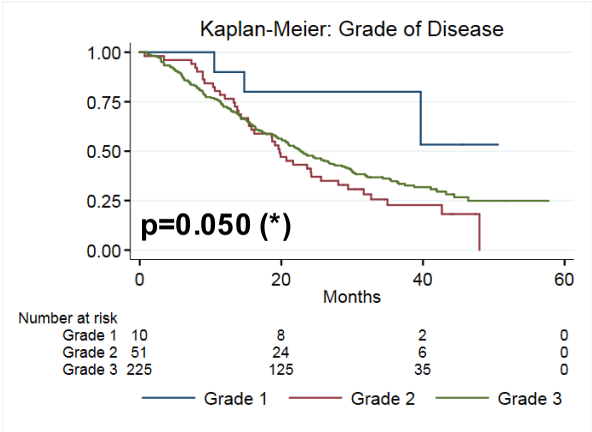

(2)

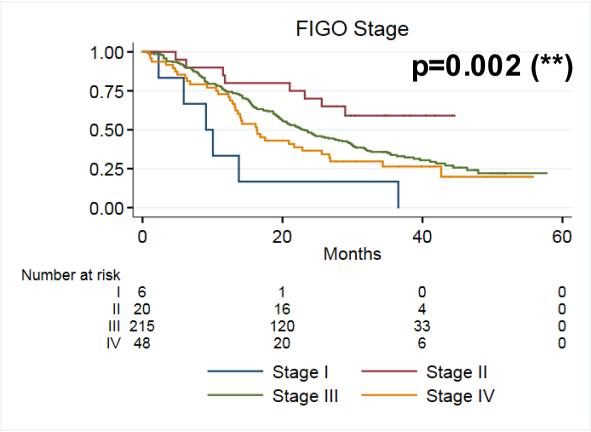

(3)

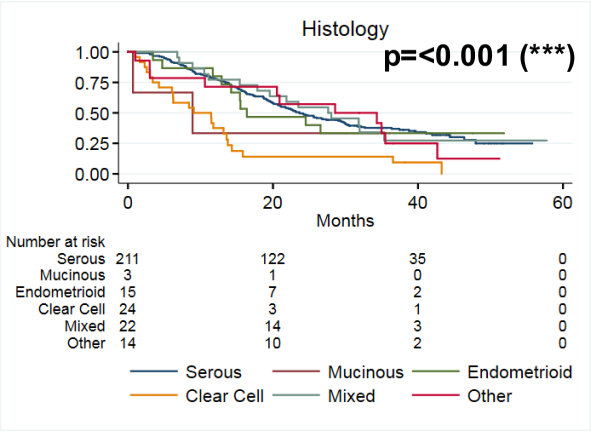

(4)

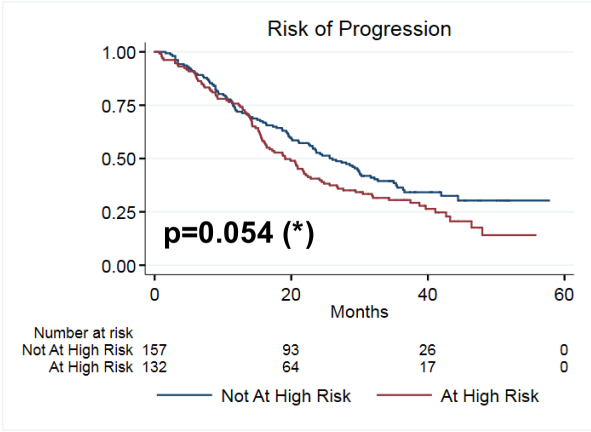

Figure 4-F: Kaplan-Meier Graphs for Survival Post-Progression and prognostic factors. Risk tables of the number of patients at risk at the given number of months on the x-axis (Months) is provided below each graph. The y-axis gives cumulative survival. (1) Grade of Disease, (2) FIGO Stage, (3) Histology and (4) Risk of Disease Progression. Results of a log rank test for association with the survival interval is provided in the bottom left corner of each graph. Significance levels: (*) = p<0.05; (**) = p<0.01; (***) = p<0.001, (ns) = not significant.

(1)

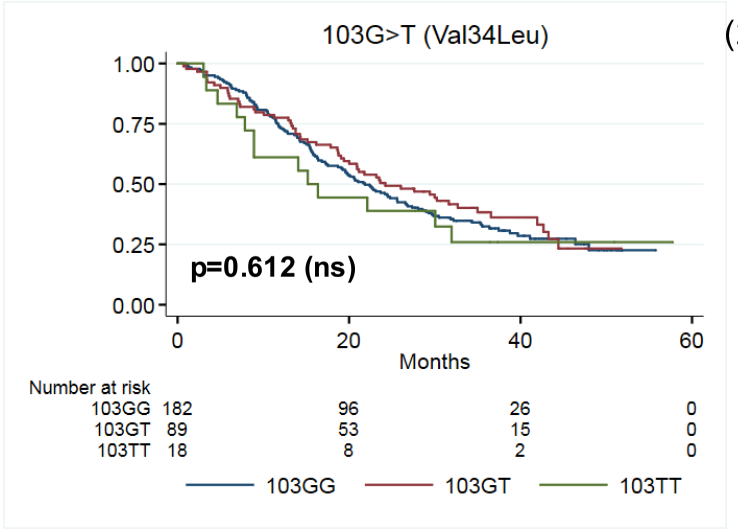

(2)

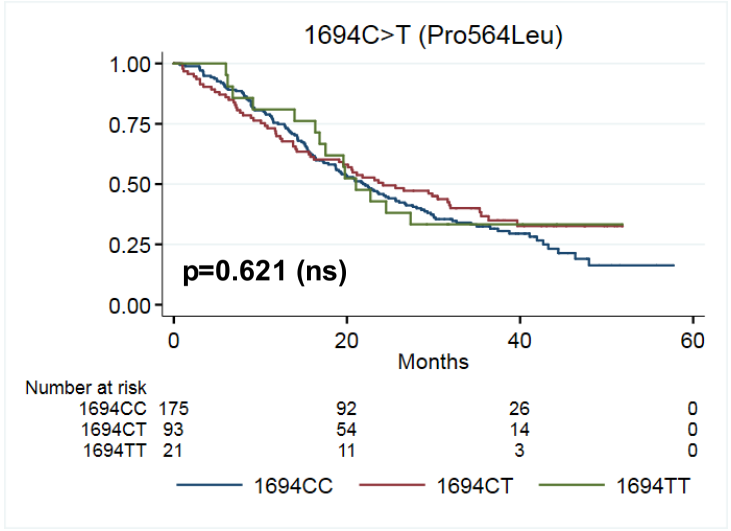

(3)

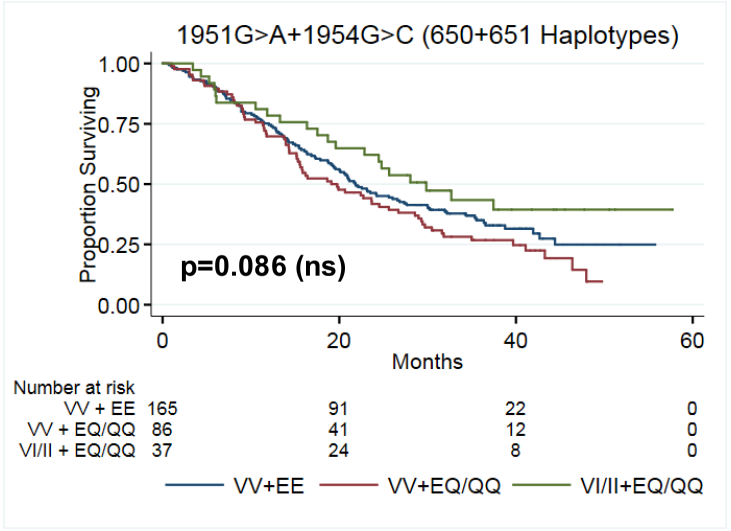

Figure 4-G: Kaplan-Meier Graphs of Survival Post-Progression and *F13A1* SNPs. Risk tables of the number of patients at risk at the given number of months on the x-axis (Months) is provided below each graph. The y-axis gives cumulative survival.(1) 103G>T(Val34Leu), (2) 1694C>T(Pro564Leu), (3) 1951G>A+1954G>C Haplotypes. Results of a log rank test for association with the survival interval is provided in the bottom left corner of each graph. Significance levels (ns) = not significant.

4.6 Multivariate Survival Analysis

Univariate analysis alone did not find a significant association between individual *F13A1* SNPs and survival intervals. It is important to note that univariate analysis is not enough to determine relationships, particularly in such a complex disease state as cancer and multivariate analysis is required. As it is difficult to place more weight on one prognostic factor over another for its contribution to survival, All prognostic factors including all the SNPs of interest were taken forward into multivariate modelling. Due to the heterogeneity of cancer, there are multiple factors in play which may determine prognosis in terms of survival intervals and therapeutic response, therefore, making multivariate analysis paramount in aiming to understand the impact different factors may have in any clinical data cohort.

4.6.1 Overall Survival

In a Cox Proportional Hazards Regression Model, prognostic factors such as late stage, high grade resulted in a greater risk to patient overall survival, (Table 4-6). Clear cell and mucinous histologies had a significantly poorer prognosis compared to serous histology, (HR=3.54 and 4.56, respectively). Unsurprisingly, those at high risk of progression were 61% more likely to die than those not at high risk (HR=1.61).

The only *F13A1* SNP genotype that had a near significant improvement to overall survival was 103G/T (Val34Leu heterozygotes) (HR=0.73, p=0.056). However, homozygous alternative carriers for the 103T allele did not significantly differ from wildtype 103G/G patients (HR=0.97). This was a surprising result, because if there is a benefit to overall survival from one copy of the alternative allele, then it would be expected that two copies would have the same, if not stronger benefit. Although not significant, looking at the direction of the hazard ratios within the 650 and 651 haplotypes, double carriage of the alternative alleles had an improved OS compared to wildtype, (Table 4-6).

Table 4-6: Cox Proportional Hazards Regression Model Results for Overall Survival

Prognostic Factor		n	HR	Std Error	p-value	Significance	95% CI	
		441					Lower	Upper
Age at Diagnosis	(24-79)	441	1.03	0.01	0.002	**	1.01	1.04
Grade	1	22	1.00					
	2	72	3.02	1.61	0.038	*	1.06	8.61
	3	347	2.24	1.16	0.117		0.82	6.17
FIGO Stage	I	35	1.00					
	II	55	1.30	0.69	0.625		0.46	3.68
	III	299	7.07	3.32	<0.001	***	2.82	17.73
	IV	52	8.06	4.14	<0.001	***	2.95	22.03
Histology	Serous	300	1.00					
	Mucinous	5	4.76	3.06	0.015	*	1.35	16.78
	Endoemetrioid	32	1.16	0.36	0.638		0.63	2.13
	Clear Cell	53	3.54	0.99	<0.001	***	2.05	6.11
	Mixed	33	0.89	0.25	0.690		0.52	1.55
	Other	18	1.36	0.46	0.358		0.70	2.65
Treatment Received	CP	213	1.00					
	CP+B	228	1.25	0.18	0.127		0.94	1.65
High Risk of Disease Progression	No	295	1.00					
	Yes	146	1.61	0.28	0.006	**	1.14	2.27
103G>T (Val34Leu)	GG	266	1.00					
	G/T	144	0.73	0.12	0.056		0.53	1.01
	TT	31	0.97	0.28	0.910		0.55	1.71
1694C>T (Pro564Leu)	CC	276	1.00					
	C/T	132	1.05	0.17	0.738		0.77	1.44
	TT	33	1.31	0.37	0.343		0.75	2.28
1951G>A (Val650Ile) + 1954G>C (Glu651Gln) Haplotypes	GG + GG	255	1.00					
	G/G + G/C or C/C	130	0.90	0.14	0.512		0.66	1.23
	G/A +AA or G/C + C/C	56	0.72	0.17	0.163		0.45	1.14

N=441, due to any exclusion of patients where data may be missing for a covariate. Hazard Ratios (HR) >1 indicate a higher risk of experiencing the event measured, in overall survival analysis this is death, compared to the set baseline covariate (HR=1.00). HR<1 indicates that chance of experiencing death is less than baseline covariate. Abbreviations: Carboplatin and Paclitaxel Only (CP); Carboplatin, Paclitaxel and Bevacizumab (CP+B). Alpha was set at 0.05, and p-values considered significant if <0.05; asterisks denote the following levels of significance: (*) p<=0.05; (**) p<=0.01; (***) p<=0.001.

4.6.2 Progression-Free Survival

Later stage and higher grade of disease resulted in a higher risk of disease progression, (Table 4-7). Those at high risk of progression were nearly twice as likely to progress compared to those not at high risk (HR=1.94, p<0.001). None of the *F13A1* SNPs had either a significantly lower or higher risk of progression, although when looking just at the directionality of the hazard ratios, carriage of the T allele at 103G>T and C at 650+651 haplotypes both had an improved prognosis, with HR<1. Carriage of the T allele at 1694C>T resulted in higher HR with increasing number of alleles carried, resulting in progression.

4.6.3 Survival Post-Progression

Clear cell and mucinous histologies were significantly detrimental to survival post progression with hazard ratios >4 and >5, respectively, (Table 4-8). Those with Stage II disease, had a significantly improved prognosis post-progression (HR=0.26, p=0.024). Those in receipt of bevacizumab (CP+B) had a slightly significantly poorer prognosis following disease progression, compared to those who received only the standard chemotherapy regimen (HR=1.37, p=0.043). This finding is also reflected in the full ICON7 cohort analysis that a benefit to survival for bevacizumab treatment was not seen in the general analysis, and that only a defined subset of women benefitted from the addition of bevacizumab.

Just as with overall survival, a significant benefit in overall survival was present for patients heterozygous at 103G>T for survival after progression of disease, (HR=0.69, p=0.030). No other *F13A1* SNPs were significantly associated with survival post-progression. Again, a look into the directionality of the hazard ratios identified an improvement to survival post-progression for double carriage of the alternative alleles at 1951G>A and 1954G>C, which is certainly in contrast to the findings within the Leeds cohort analysis (Chapter 3).

Table 4-7: Cox Proportional Hazards Regression Model Results for Progression-Free Survival

Prognostic Factor		n	HR	Std Error	p-value	Significance	95% CI	
		441					Lower	Upper
Age at Diagnosis	(24-79)	441	1.01	0.01	0.035	*	1.00	1.03
Grade	1	22	1.00					
	2	72	1.67	0.59	0.152		0.83	3.34
	3	347	1.85	0.62	0.064		0.97	3.56
FIGO Stage	I	35	1.00					
	II	55	3.07	1.45	0.018	*	1.22	7.75
	III	299	8.61	3.87	<0.001	***	3.57	20.80
	IV	52	10.73	5.19	<0.001	***	4.16	27.69
Histology	Serous	300	1.00					
	Mucinous	5	2.83	1.75	0.092		0.84	9.51
	Endoemetrioid	32	0.88	0.23	0.618		0.53	1.46
	Clear Cell	53	1.71	0.43	0.032	*	1.05	2.78
	Mixed	33	0.93	0.21	0.740		0.59	1.46
	Other	18	1.59	0.47	0.117		0.89	2.85
Treatment Received	CP	213	1.00					
	CP+B	228	0.85	0.10	0.168		0.67	1.07
High Risk of Disease Progression	No	295	1.00					
	Yes	146	1.94	0.29	<0.001	***	1.45	2.61
103G>T (Val34Leu)	GG	266	1.00					
	G/T	144	0.89	0.12	0.387		0.68	1.16
	TT	31	0.84	0.21	0.485		0.51	1.38
1694C>T (Pro564Leu)	CC	276	1.00					
	C/T	132	1.19	0.16	0.193		0.92	1.54
	TT	33	1.19	0.28	0.457		0.75	1.91
1951G>A (Val650Ile) + 1954G>C (Glu651Gln) Haplotypes	GG + GG	255	1.00					
	G/G + G/C or C/C	130	0.89	0.12	0.37		0.68	1.16
	G/A +AA or G/C + C/C	56	0.81	0.15	0.24		0.56	1.16

N=441, due to any exclusion of patients where data may be missing for a covariate. Hazard Ratios (HR) >1 indicate a higher risk of experiencing the event measured, in progression-free survival analysis this is progression of disease, compared to the set baseline covariate (HR=1.00). HR<1 indicates that chance of experiencing progression is less than baseline covariate (HR=1.00). Abbreviations: Carboplatin and Paclitaxel Only (CP); Carboplatin, Paclitaxel and Bevacizumab (CP+B). Alpha was set at 0.05, and p-values considered significant if <0.05; asterisks denote the following levels of significance: (*) p<=0.05; (**) p<=0.01; (***) p<=0.001.

Table 4-8: Cox Proportional Hazards Regression Model Results for Survival Post-Progression

Prognostic Factor		n	HR	Std Error	p-value	Significance	95% CI	
		285					Lower	Upper
Age at Diagnosis	(24-79)	285	1.03	0.01	0.001	**	1.01	1.05
Grade	1	10	1.00					
	2	50	3.01	1.85	0.073		0.90	10.03
	3	225	1.93	1.15	0.271		0.60	6.23
FIGO Stage	I	6	1.00					
	II	20	0.26	0.15	0.024	*	0.08	0.83
	III	211	0.85	0.43	0.745		0.32	2.27
	IV	48	0.95	0.52	0.930		0.33	2.77
Histology	Serous	208	1.00					
	Mucinous	3	5.52	4.44	0.034	*	1.14	260.68
	Endoemetrioid	15	1.33	0.45	0.402		0.68	2.59
	Clear Cell	24	4.96	1.45	<0.001	***	2.79	8.79
	Mixed	22	0.97	0.27	0.916		0.56	1.69
	Other	13	1.12	0.38	0.735		0.58	2.18
Treatment Received	CP	133	1.00					
	CP+B	152	1.37	0.21	0.043	*	1.01	1.85
High Risk of Disease Progression	No	156	1.00					
	Yes	129	1.06	0.19	0.751		0.75	1.49
103G>T (Val34Leu)	GG	179	1.00					
	G/T	88	0.69	0.12	0.030	*	0.49	0.96
	TT	18	1.13	0.35	0.689		0.61	2.09
1694C>T (Pro564Leu)	CC	174	1.00					
	C/T	90	0.95	0.16	0.752		0.68	1.32
	TT	21	1.12	0.33	0.708		0.62	2.00
1951G>A (Val650Ile) + 1954G>C (Glu651Gln) Haplotypes	GG + GG	164	1.00					
	G/G + G/C or C/C	84	1.05	0.17	0.784		0.75	1.45
	G/A +AA or G/C + C/C	37	0.86	0.21	0.540		0.53	1.39

N=285, only those patients who had progressed in their disease were included in this analysis, and any patient with missing values for any of the covariates was automatically excluded by the model. Hazard Ratios (HR) >1 indicate a higher risk of experiencing the event measured, in survival post-progression survival analysis this is death, compared to the set baseline covariate (HR=1.00). HR<1 indicates that chance of experiencing death is less than baseline level of 1. Abbreviations: Carboplatin and Paclitaxel Only (CP); Carboplatin, Paclitaxel and Bevacizumab (CP+B). Alpha was set at 0.05, and p-values considered significant if <0.05; asterisks denote the following levels of significance: (*) p<=0.05; (**) p<=0.01; (***) p<=0.001.

4.7 Sub-Cohort Analyses

The focus on sub-cohort analysis was on associations with *F13A1* SNPs and survival intervals and although other prognostic factor distributions and associations were checked within the sub-cohorts, to confirm validity (e.g. relationships between grade, stage, histology and influences on survival), they are not reported in the following analyses.

4.7.1 Treatment Received

The ICON7 Trial tested the benefit of the addition of bevacizumab to platinum based chemotherapy. In the translational sample cohort, there was a near 50% split between the two treatment arms and the response to each treatment arm was compared between genotypes and survival intervals. In multivariate analysis of the whole cohort, bevacizumab did not benefit prognosis, reflecting the findings of the whole ICON7 Cohort that bevacizumab did not significantly extend overall survival or prevent progression, expect for those patients at high risk of progression (78,79) (data not shown). An analysis comparing risk groups will be presented in Section 4.6.2.

No work, known to date, has ever been performed to assess whether FXIIIA is involved in response to chemotherapy. FXIIIA does have a role in angiogenesis, as the active transglutaminase promotes pro-angiogenic signalling through crosslinking of the integrin beta-3 and the tyrosine kinase receptor VEGFR2. Bevacizumab is an anti-angiogenic chemotherapy that binds to VEGFA (which normally binds to VEGFR2 to promote signalling). The role of FXIIIA in pro-angiogenic signalling has not assessed whether the presence of *F13A1* SNPs changes the angiogenic signalling promotion. Therefore, could FXIIIA mutants respond differently to anti-angiogenic therapy, or in the absence of anti-angiogenic therapy, do mutants have a differential prognosis, depending on genotype? An exploratory analysis was performed with the ICON7 trial translational samples to investigate whether carriage of the *F13A1* SNPs resulted in a differential response, in terms of survival intervals, for OC patients.

4.7.1.1 Carboplatin & Paclitaxel Only

In the carboplatin and paclitaxel group alone, multivariate analysis identified that none of the *F13A1* SNPs were significantly associated with overall survival or

progression-free survival, however significant associations were identified for survival post-progression, (Table 4-9). Heterozygotes at Val34Leu (103G/T) had a significantly better prognosis than wildtype individuals (HR=0.51, p=0.023, median survival post progression = 32.7 months vs wildtype median survival post-progression = 22.8 months). Carriage of two alternative alleles resulting in homozygous alternative individuals (103T/T), however, although not significantly so, were over twice as likely to die compared to wildtype (103G/G) with median survival post-progression for 103 T/T patients at 8.9 months. Plots of survivor function from the Cox models clearly demonstrate the differences seen between survival intervals and Val34Leu genotypes between the treatments received, (Figure 4-H).

4.7.1.2 Addition of Bevacizumab to Carboplatin & Paclitaxel

Those patients in receipt of bevacizumab alongside the chemotherapy, although not statistically significant, appeared to have a differential response in terms of prognosis depending on the genotype of the patient at Val34Leu (Figure 4-H). The Kaplan-Meier curves show clear differences in prognosis for survival intervals; 103G>T where it appears that those with 103T/T who receive platinum and taxol alone have a better PFS, but once progression occurs, carriage of this genotype is detrimental to survival for them. Patients with 103T/T do worse, whilst heterozygotes 103G/T performed better in terms of PFS and OS when in receipt of bevacizumab. Heterozygotes at 103G>T (103G/T) had a significantly improve OS compared to wildtype (HR=0.65, p=0.054), Table (4-9).

4.7.2 Risk of Disease Progression

Those at high risk of disease progression were those with Grade IIIC/IV who were either unable to have resective surgery or had >1 cm of residual disease margin remaining post-surgery. In the full ICON7 trial, those with high risk disease were the only patients who positively responded to the addition of bevacizumab to their standard chemotherapy regimen (78,79). Analysis of the ICON7 translational cohort in this thesis has identified that the SNP 103G>T in particular heterozygotes at this SNP site, benefited in both OS (although not significantly so for OS) (HR=0.73, p=0.056) and SPP (HR=0.69, p=0.030). Analysis of the

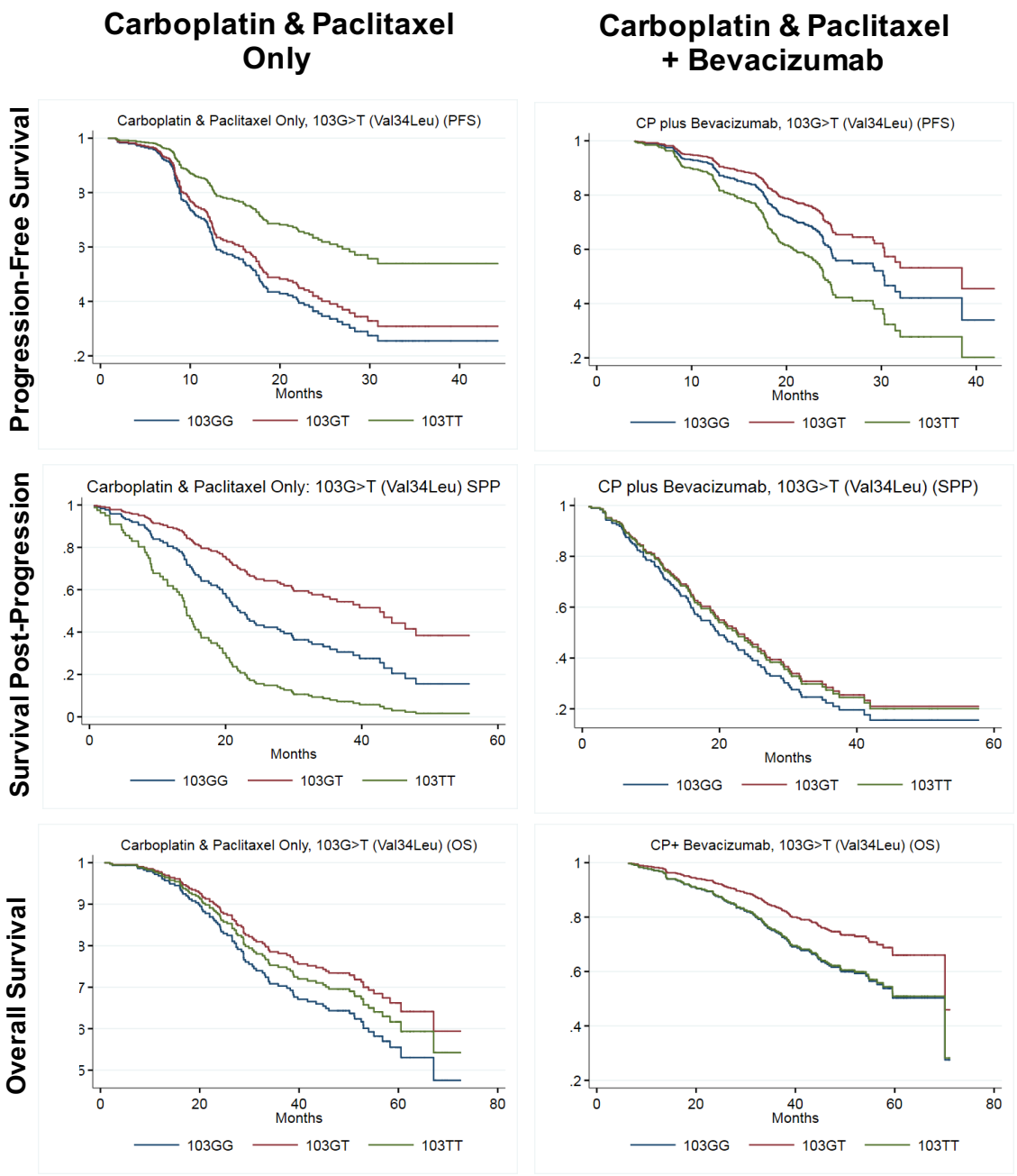

Figure 4-H: Comparison of Plots of Survivor Function from Cox Proportional Hazards Regression Models for Survival Intervals for Treatment Received and 103G>T (Val34Leu) Variants. Left column of plots are for those patients in receipt of the standard platinum-based chemotherapy regimen and right column of plots are for those in receipt of bevacizumab in addition to the standard chemotherapy regimen. Survival interval measured is given on the left of each row. Covariates included in the Cox Model: Age at Diagnosis, Grade, Stage, Histology, Risk of Progression, and the F13A1 genotypes, with 1951G>A and 1954G>C treated as haplotypes, as performed in earlier Cox models.

Table 4-9: Summary of Hazard Ratios for *F13A1* Variants and Treatment Received

n	SNP	SNP Genotype	Survival Interval											
			Progression-Free Survival				Survival Post-Progression				Overall Survival			
			n	HR	p-value	Significance	n (only if progressed)	HR	p-value	Significance	n	HR	p-value	Significance
Carboplatin & Paclitaxel														
213/216	103G>T	103GG	139	1.00			90	1.00			139	1.00		
		103GT	62	0.84	0.442	ns	39	0.51	0.023	*	62	0.69	0.171	ns
		103TT	12	0.45	0.101	ns	4	2.22	0.175	ns	12	0.85	0.747	ns
	1694C>T	1694CC	134	1.00			80	1.00			134	1.00		
		1694CT	62	1.16	0.467	ns	42	0.65	0.130	ns	62	0.81	0.436	ns
		1694TT	17	1.05	0.321	ns	11	1.39	0.458	ns	17	1.82	0.139	ns
	1951G>A +1954G>C Haplotypes	GG + GG	130	1.00			80	1.00			130	1.00		
		GG + G/C or CC	58	0.96	0.860	ns	35	0.94	0.840	ns	58	1.03	0.912	ns
		G/A or AA + G/C or CC	25	0.89	0.672	ns	18	0.99	0.980	ns	25	0.86	0.682	ns
Carboplatin & Paclitaxel + Bevacizumab														
228/232	103G>T	103GG	139	1.00			89	1.00			139	1.00		
		103GT	62	0.78	0.197	ns	49	0.84	0.464	ns	62	0.65	0.054	*
		103TT	12	1.48	0.199	ns	14	0.86	0.701	ns	12	0.97	0.936	ns
	1694C>T	1694CC	134	1.00			94	1.00			134	1.00		
		1694CT	62	1.10	0.605	ns	48	1.23	0.366	ns	62	1.18	0.434	ns
		1694TT	17	0.97	0.930	ns	10	0.88	0.774	ns	17	0.92	0.837	ns
	1951G>A +1954G>C Haplotypes	GG + GG	125	1.00			84	1.00			125	1.00		
		GG + G/C or CC	72	0.93	0.703	ns	49	0.90	0.653	ns	72	0.88	0.557	ns
		G/A or AA + G/C or CC	31	0.79	0.396	ns	19	0.76	0.429	ns	31	0.66	0.219	ns

N given is the number of patients taken into the Cox Proportional Hazards Regression Model, as the Cox Model does not include patients with any missing data points for the given covariates. Hazards Ratios generated from a Cox Model which included the covariates: Age at Diagnosis, Grade, FIGO Stage, Histology, Risk of Progression and the *F13A1* Variants. P-values considered significant if $p<0.05$, with significant findings highlighted in yellow for clarity. HR= Hazard Ratio, Sig.=Significance, (*) = $p<0.05$, (ns) = not significant.

treatment groups in sub-cohort analysis identified a differential response in OS for those patients who received bevacizumab and 103G>T genotype (Table 4-9). So, are heterozygotes at 103G>T associated with high risk of disease, if they are the ones benefiting from bevacizumab? One of the main limitations of this analysis was the inability to perform multivariate Cox modelling due to the small sample size and "lack of convergence" for the survival intervals: progression-free survival and survival post-progression, particularly in the high risk of progression sub-cohort (n=150). Therefore, only analysis for overall survival which was successfully calculated, has been reported for the high risk sub-cohort. All survival intervals are reported for those patients with available data. N=298 for the group not at high risk of progression.

4.7.2.1 Not at High Risk of Progression

Bevacizumab in the Not at High Risk cohort was significantly associated with poorer overall survival (HR=1.64, p=0.017, 95% CI: 1.09-2.45) (table not shown for brevity, see Appendix 3), which fits with the aforementioned full trial findings that only those at high risk of disease progression benefitted from bevacizumab. Similar to analysis of the whole cohort (n=448), heterozygotes at Val34Leu (103G>T, 103GT) had a lower risk of death compared to wildtype individuals, although not significantly so for this 'not at risk of progression' sub-cohort (HR=0.73, p=0.147), (Table 4-10A).

Double carriage of alternative alleles at 1951G>A and 1954G>C also had a near significant benefit to overall survival (HR=0.51, 0.062), (Table 4-9A). This is the first instance where haplotypes for these SNPs, have been seen to have a near significant effect on survival in this cohort, but this does not support the findings observed within the Leeds cohort (Chapters 1 and 3).

4.7.2.2 At High Risk of Disease Progression

SNP 103G>T heterozygotes did again have a benefit to overall survival in the sub-cohort at high risk of disease progression, although not significantly so (HR=0.68, p=0.166 (Table 4-10B, and Appendix 4). Interestingly, in this sub-cohort, homozygous alternative variants at 1694C>T (1694T/T) were over 3 times more likely to die compared to wildtype counterparts (HR=3.65, p=0.004),

Table 4-10A: Summary of Hazard Ratios for *F13A1* Variants and those Not at Risk of Disease Progression.

Not At High Risk of Progression														
	SNP	SNP Genotype	Survival Interval											
			Progression-Free Survival				Survival Post-Progression				Overall Survival			
			n	HR	p-value	Sig.	n (only if progressed)	HR	p-value	Sig.	n	HR	p-value	Sig.
295/298	103G>T	103GG	171	1.00			91	1.00			171	1.00		
		103GT	107	0.88	0.469	ns	55	0.68	0.122	ns	107	0.73	0.146	ns
		103TT	18	1.67	0.151	ns	10	0.89	0.806	ns	18	1.15	0.737	ns
	1694C>T	1694CC	180	1.00			91	1.00			180	1.00		
		1694CT	90	0.35	0.097	ns	52	0.78	0.304	ns	90	0.98	0.919	ns
		1694TT	25	0.94	0.827	ns	13	0.57	0.188	ns	25	0.74	0.428	ns
	1951G>A +1954G>C Haplotypes	GG + GG	180	1.00			97	1.00			180	1.00		
		GG + G/C or CC	78	0.80	0.268	ns	38	1.15	0.572	ns	78	0.95	0.814	ns
		G/A or AA + G/C or CC	37	0.84	0.500	ns	21	0.66	0.280	ns	37	0.51	0.062	ns

N given is the number of patients taken into the Cox Proportional Hazards Regression Model, as the Cox Model does not include patients with any missing data points for the given covariates. Hazards Ratios generated from a Cox Model which included the covariates: Age at Diagnosis, Grade, FIGO Stage, Histology, Treatment Received and the *F13A1* Variants. P-values considered significant if $p<0.05$, with significant findings highlighted in yellow for clarity. HR= Hazard Ratio, Sig.=Significance, (*) = $p<0.05$, (ns) = not significant.

Table 4-10B: Summary of Hazard Ratios for *F13A1* Variants and those at High Risk of Disease Progression

At High Risk of Progression						
	SNP	SNP Genotype	Overall Survival			
			n	HR	p-value	Significance
146/150	103G>T	103GG	96	1.00		
		103GT	37	0.68	0.166	ns
		103TT	13	1.03	0.948	ns
	1694C>T	1694CC	96	1.00		
		1694CT	42	1.15	0.567	ns
		1694TT	8	3.65	0.004	**
	1951G>A +1954G>C Haplotypes	GG + GG	75	1.00		
		GG + G/C or CC	52	1.01	0.974	ns
		G/A or AA + G/C or CC	19	0.99	0.965	ns

N given is the number of patients taken into the Cox Proportional Hazards Regression Model, as the Cox Model does not include patients with any missing data points for the given covariates. Hazards Ratios generated from a Cox Model which included the covariates: Age at Diagnosis, Grade, FIGO Stage, Histology, Treatment Received and the *F13A1* Variants. P-values considered significant if $p<0.05$, with significant findings highlighted in yellow for clarity. HR= Hazard Ratio, Sig.=Significance, (*) = $p<0.05$, (ns) = not significant.

whereas individuals carrying the alternative T allele at this SNP site and not at high risk of progression had a better prognosis with HRs<1, (Table 4-10B). This suggests that carriage of the T allele at 1694 may be detrimental to those at high risk of disease progression.

A small investigation into whether 1694C>T resulted in a differential response to treatment depending on risk group was conducted. Carriers of the T allele at this locus and at high risk of progression had a significantly poorer prognosis if treated with bevacizumab (HR=2.41, p=0.007, n=27/74) whilst those at high risk and in receipt of the standard regimen had a better prognosis, although not significant (HR=0.57, p=0.130, n=26/76), (Table 4-11). Carriers of the T allele at this locus and not at high risk of progression had the reverse relationship, with those treated with bevacizumab benefiting in terms of their prognosis (HR=0.74, p=0.273, n=62/158) and those with the standard regimen only had a poorer prognosis (HR=1.31, p=0.413, n=55/140). Therefore, these findings could suggest that patients carrying the alternative T allele and at high risk of disease progression (i.e. aggressive disease) should not receive bevacizumab, but this would require much more in depth analysis in larger cohorts of patients. The SNP 1694C>T was not significantly associated with any of the prognostic factors in the cohort (Table 4-4) and the exact contribution of 1694C>T to response to bevacizumab would require further exploration.

Table 4-11: Summary of Hazard Ratios for *F13A1* Genotypes for Overall Survival for Risk of Progression and Treatment Received

Risk of Disease Progression	Treatment Received	n	SNP	SNP Genotype	Overall Survival			
					n	HR	p-value	Significance
High Risk	CP Only	76	103G>T	103GG	53	1.00		
				103GT/TT	23	0.63	0.204	ns
			1694C>T	1694CC	50	1.00		
				1694CT/TT	26	0.57	0.130	ns
			1951G>A	1951GG	70	1.00		
				1951GA/AA	6	1.14	0.838	ns
			1954G>C	1954GG	44	1.00		
				1954GC/CC	32	1.16	0.681	ns
	CP plus B	74	103G>T	103GG	46	1.00		
				103GT/TT	28	0.64	0.209	ns
			1694C>T	1694CC	47	1.00		
				1694CT/TT	27	2.41	0.007	**
			1951G>A	1951GG	61	1.00		
				1951GA/AA	13	1.11	0.815	ns
			1954G>C	1954GG	33	1.00		
				1954GC/CC	41	0.73	0.364	ns
Not At High Risk	CP Only	140		103GG	88	1.00		
			103G>T	103GT/TT	52	0.93	0.830	ns
				1694CC	85	1.00		
			1694C>T	1694CT/TT	55	1.31	0.413	ns
				1951GG	121	1.00		
			1951G>A	1951GA/AA	19	0.95	0.929	ns
				1954GG	87	1.00		
			1954G>C	1954GC/CC	53	0.83	0.656	ns
	CP plus B	158		103GG	85	1.00		
			103G>T	103GT/TT	73	0.72	0.205	ns
				1694CC	96	1.00		
			1694C>T	1694CT/TT	62	0.74	0.273	ns
				1951GG	139	1.00		
			1951G>A	1951GA/AA	18	0.38	0.095	ns
				1954GG	94	1.00		
			1954G>C	1954GC/CC	63	0.95	0.843	ns

N given is the number of patients taken into the Cox Proportional Hazards Regression Model, as the Cox Model does not include patients with any missing data points for the given covariates. Hazards Ratios generated from a Cox Model which included the covariates: Age at Diagnosis, Grade, FIGO Stage, Histology, and the *F13A1* Variants. Due to small number of the carriers of the alternative A allele at 1951G>A, heterozygotes (G/A) and homozygous alternative carriers (AA) were combined into one group. P-values considered significant if $p<0.05$, with significant findings highlighted in yellow for clarity. HR= Hazard Ratio, Sig.=Significance, (**) = $p<0.01$, (ns) = not significant.

4.8 Summary of Key Findings

- The ICON7 trial distribution of prognostic factors appeared similar to other clinical trials, with higher grade, later stage and serous histology being the most common factors for patients in the trial.
- Grade of disease, stage of disease and risk of disease progression were all significantly associated with survival intervals: progression-free survival, survival post-progression and overall survival.
- *F13A1* SNP 103G>T was significantly associated with grade of disease (p=0.047, Chi-square), with heterozygotes having lower grade disease than both homozygous variants.
- Although not significant, in univariate survival analysis, 103G/T heterozygotes in general survived longer than both homozygous variants (Kaplan-Meier)
- 103G/T patients had a significant improvement to prognosis for survival post-progression (HR=0.69, p=0.030, 95%CI: 0.49-0.96) and near significantly associated with overall survival (HR=0.71, p-value=0.056, 95% CI: 0.53-1.01).
- Differing 103G>T genotypes had differential response to chemotherapy therapy received when survival intervals were assessed. In univariate survival analysis, 103T/T patients had a longer PFS than other genotypes, but once disease progressed, benefit was lost. In the presence of bevacizumab, this benefit to PFS was not present, and wildtype and heterozygous patients performed better.
- 103G/T patients benefited the most in terms of OS and PFS with bevacizumab, in univariate analysis.
- In multivariate analysis, heterozygous 103G/T patients had near significant benefit to OS when treated with bevacizumab (HR=0.65, p=0.054) compared to wildtype patients
- In multivariate analysis, when treated with platinum and taxol only, 103G/T patients had a significantly better prognosis compared to wildtype patients.
- 103G>T was not significantly associated with risk of disease progression in univariate and multivariate analyses. In general, heterozygotes always had a better prognosis compared to wildtype individuals.

- SNP 1694C>T was significantly associated with poor OS for those with high risk of disease progression (HR=3.65, p=0.004) however, only 8 patients had this genotype and were at high risk of progression, therefore more patients would need to be assessed to see if this were a true result, even though 7/8 (88%) had died.
- The ICON7 clinical trial found that those at high risk of progression benefited from the addition of bevacizumab to their treatment regimen, and when *F13A1* SNPs were explored in higher risk sub-cohort treated with bevacizumab the SNP 1694C>T was associated with detriment to OS when treated with bevacizumab (HR=2.41, p=0.007). However, small numbers of the sub-cohort mean that results must be interpreted with caution and would require further exploration in other clinical cohorts.

4.9 Brief Discussion

The SNP which appeared to benefit overall survival and survival post-progression was 103G>T, but only for heterozygotes at this locus, and no benefit was seen for homozygotes for this alternative allele. This was a strange result, as it would be expected that if carriage of one copy of the T allele was beneficial, then two should have been even more beneficial. This was not the case in this cohort, and throughout further analysis of sub-cohorts, heterozygotes time and time again benefitted over homozygous and wildtype individuals e.g. benefit to overall survival in particular was present regardless of risk of disease progression for 34V/L variants. This suggests that there could be an interesting role for FXIIIA molecules carrying this heterozygous SNP site. 103G>T (Val34Leu) is well established in the literature in a variety of diseases as Factor XIIIA in Leu/Leu individuals is activated more rapidly and results in tighter fibrinogen cross-links following its transglutaminase activity (247). Leu/Leu variants have been associated with thrombotic diseases, such as stroke and myocardial infarction (195,198,208,251). Heterozygotes and wildtype individuals have a reportedly protective effect in uterine myoma (248), and it appears that 34V/L may be having a protective effect in OC, too.

Differential response to treatment received was present in this cohort, depending on 103G>T genotype. Heterozygotes benefited in all survival intervals when treated with bevacizumab. However, 103T/T homozygotes appeared to strongly

benefit for progression-free survival when treated with a standard chemotherapy regimen alone. Once progression occurred, this benefit was lost and survival post-progression was poorer for 103T/T individuals, whilst heterozygous 103G/T individuals survived over twice as long. When in receipt of bevacizumab, 103T/T variants performed the worst in terms of PFS, suggesting that 103T/T variants in particular should potentially not receive bevacizumab.

The SNP 1694C>T (Pro564Leu) may also have a role in response to bevacizumab, although the calculated hazard ratios were from very small population sizes and must be treated with extreme caution. The detriment to OS for carriers of the alternative allele could potentially be linked to alterations in plasma levels of FXIIIA. This polymorphism (Pro564Leu) results in lower plasma FXIII levels (189). However, Leu564 is associated with higher specific activity of FXIIIA (166), and the location of the Pro564Leu polymorphism may result in an effect on substrate binding. No associations were seen with this SNP in analysis of the full cohort with any of the prognostic factors or survival intervals. Therefore, a larger study would be required to determine a role for this SNP in response to therapy.

Previous work on a cohort biased towards survivors >2 years (Chapter 3) found an association with 103G>T for 103T/T patients benefiting (HR=0.34, p=0.024) but this was not maintained in long term survival. Instead, the previous cohort found that SNPs 1951G>A and 1954G>C were associated with overall survival. These results could not be replicated in this study of newly-diagnosed women. This translational cohort from the ICON7 clinical trial, does represent a different group of women, i.e. only newly diagnosed patients were recruited whereas the Leeds Initial Cohort (n=258, Chapter 3) represents a greater cross-section of patients at new diagnosis and subsequent follow-up. So perhaps the SNPs 1951G>A and 1954G>C are more important for long term survival and follow-up? The cohort from Leeds investigated in Chapter 3 were from the Leeds geographical area, so therefore a location bias was also present, which was unlikely to be present in the translational ICON7 cohort investigated in this chapter, due to large number of international centres from which samples were collected. Information was unavailable for the precise geographical location of all the DNA translational cohort samples (n=448).

Many questions are raised as a result of this small investigation. Could the 103G>T SNP be protective up to a point in OC? And if so, what role could heterozygotes be having in particular? How could the heterozygous variant be benefiting survival i.e. is there a difference in activation/activity of heterozygotes? If 103G>T is associated with grade of disease, how could this variant be contributing to the disease differentiation (the actual measure of disease grade)? The next steps would be to try and further determine the role of 103G>T (Val34Leu) in OC. Firstly, an exploration of FXIIIA protein expression in OC could be performed, and are associations between SNP genotypes and expression levels present in OC? It would be interesting to see whether the finding of the association between grade and 103G>T in the clinical data from this cohort, could be replicated in terms of tissue expression. It would also be very interesting to look at whether heterozygotes for 103G>T have either significantly higher or lower protein expression levels, as this may provide a further indication of the role FXIIIA may be having in OC. For heterozygotes, it is unknown what percentage of the FXIIIA molecules exist as a heterodimer versus the homodimers, and how the heterodimer behaves differently with respect to the stability of the molecule and/or its activation, or even association of the heterodimer with the FXIIIB subunit when in circulation.

The prognostic factor data for European Cooperative Oncology Group (ECOG) Performance Status and tumour bulk were missing for this smaller translational cohort from the full ICON7 cohort (78,79). These two prognostic factors are useful in measuring likelihood of disease progression and patient quality of life for tumour bulk and performance status, respectively. The absence prevents the most thorough multivariate analysis as the more covariates representing the disease the better it is for understanding interactions between and contributions of covariates to the disease model. However, the absence of tumour bulk and performance status does not invalidate the multivariate modelling performed in this chapter, as there are enough prognostic factors which describe the OCs of these patients and allowed for sufficient testing of the hypotheses regarding *F13A1* SNPs, OC prognostic factors and survival intervals. This will be addressed more in Chapter 7.

In summary, analysis of a prospective OC cohort, encompassing newly diagnosed patients, has identified that the *F13A1* SNP 103G>T for amino acid change Val34Leu, may have a role in overall survival and survival post-progression in OC patients. Further studies are required to further elucidate the role this SNP may have on OC phenotype and response to therapy.

Chapter 5: Tissue Expression of FXIIIA in Ovarian Cancer

5.1 Introduction

In the previous chapter, associations were found between SNPs within the gene for FXIIIA, *F13A1*, and survival intervals in the ICON7 translational cohort. In particular, the SNP 103G>T stood out in terms of having a potential role as a marker in response to chemotherapy and for survival intervals. Interestingly, heterozygous patients for this SNP (103G/T) were the ones who appeared to have a longer overall survival and survival post-progression rather than their homozygous counterparts. Patients with the genotype 103T/T in receipt of the standard chemotherapy regimen had a longer progression-free survival compared to others, and that once disease progressed those with 103T/T died far sooner. Heterozygous patients also appeared to benefit in all survival intervals when in receipt of bevacizumab. These findings although interesting, required further exploration in *in vitro* analyses due to the limited sample size and power within the cohort, in order to try and understand FXIIIA's role in ovarian cancer progression, response and survival. The next steps were to assess whether a) FXIIIA is expressed in ovarian cancer, and b) are SNPs in *F13A1* and OC prognostic factors such as grade and stage linked to expression levels of FXIIIA in OC tissues? If FXIIIA is expressed, is its function limited to a cross-linker of the matrix, or does it perhaps have another role instead?

Expression of FXIIIA has been explored in studies associated with skin and bone, but little, if anything, has assessed expression of FXIIIA in ovarian cancer. Before using precious tissue samples, an assessment of mRNA levels of *F13A1* was performed through interrogation of publically-available mRNA expression databases. If gene transcription levels were different between normal tissue and ovarian carcinoma, then this could indicate that protein levels may be different and could provide further information on the role of FXIIIA in OC. The overarching question was: is there protein *in situ* in OC patients which may be contributing to prognosis and therapeutic response?

5.2 Databases & Samples Used

5.2.1 CSIOVDB

Several databases on mRNA expression in ovarian cancer exist, including OvMark, KMPlotter and The Ovarian Cancer Database of the Cancer Science Institute Singapore (CSIOVDB) (252). However, the latter is the first to include the molecular subtype information and epithelial-mesenchymal transitioning (EMT) scores. EMT is a phenotypic change which has been associated with cancer progression, as cells move to a more mesenchymal-like phenotype when undergoing metastasis. Correlations may be identified between gene expression and EMT scores in order to assess the potential contribution of the gene to metastatic behaviour. OC is no longer treated as a single disease with transcriptomic analysis having identified five molecular subtypes which vary in their gene expression, prognosis and therapeutic response (45,49,253). The large sample size and detailed collation of all this information into a single database, makes CSIOVDB a powerful tool for the thorough analysis of mRNA expression and impact gene expression may have on OC progression, prognosis and treatment.

(CSIOVDB) is a large microarray gene expression database for analysis of mRNA expression from 3431, representing 3261 unique, patients. Clinico-pathological data in terms of grade, stage, histology, therapeutic response and survival of disease, where available, were collated from numerous other databases including ArrayExpress, the Expression Project for Oncology (ExpO), The Cancer Genome Atlas (TCGA), 40 gene expression omnibus (GEO) accessions and several private/in-house cohorts. Probe intensity was normalised using the robust multi-array average (RMA) algorithm and data were reported as fold change compared to controls. CSIOVDB was interrogated for expression of *F13A1* and findings are presented in this chapter.

5.2.2 Kaplan-Meier Plotter (KM plotter)

KM plotter is a database of mRNA gene chip, mRNA RNA-Seq and miRNA data from several cancers (254). Only mRNA gene chip data is available for ovarian cancer. The data are sourced from genomic spatial events (GSE) and TCGA databases and allows for meta-analysis of the clinical data and gene expression. Databases were collated by KM plotter and probe intensity was normalised with

the Affymetrix MAS5 algorithm and then mean-centred with second scaling normalisation to set average gene expression on each chip to 1000 (254,255). *F13A1* mRNA expression and survival intervals was queried in the OC database (Affymetrix ID: 20335-at). An automatic selection of the best cut-off between low and high expression was set by KM plotter between the lower and upper quartiles.

5.2.3 Ovarian Cancer Tissues into Tissue Microarrays

An exploration of FXIIIA expression had not previously been carried out in OC tissues, presenting a novel opportunity for this project. Expression of FXIIIA was explored in tissues with paraffin-embedded tissue microarrays (TMAs) from the ICON7 translational cohort. It was expected that the highest proportion of expression would be in OC stroma, due to the high mRNA expression results from CSIOVDB, although it was unknown whether FXIIIA would remain present in the tissue after its transglutaminase activity, as its precise role in OC remains to be elucidated. Although FXIIIA is trapped in fibrin clots, near the site of its cross-linking activity, little is known whether this trapping would occur in tumour stroma or if the cross-linking via transglutaminase was FXIIIA's main role in OC. Expression of FXIIIA was expected to be lower in tumour compared to tumour stroma, given the mRNA expression results from CSIOVDB. If the staining was found to be present in immune-like cells within the stroma, then this may suggest a more immunological role for FXIIIA in OC.

Primary OC tumour tissues were collected during resective surgery as part of the ICON7 clinical trial from 360 patients and examined by a histopathologist, prior to setting within the TMAs. TMAs were processed by placing cores from each tissue in paraffin blocks based on whether they consisted of OC tumour, tumour/stroma or stroma. A core was not always available for each category for each patient due to the nature of the sample being taken or may not have an equal distribution of the histopathological categories. It was noted that there were fewer stroma samples in general, perhaps due to sample fragility and difficulty embedding in paraffin for sectioning.

A small investigation was also performed using frozen ovarian cancer samples from the Leeds Tissue Bank to assess the levels of co-localisation between FXIIIA and other key players that may have relevance to this study such as

transglutaminase-2 (TGM2), the product of cross-linking isopeptide bonds, and a substrate expressed in OC tissues, fibrinogen. Establishing co-localisation between any of these proteins *in situ* may help to further elucidate the role FXIIIA in OC.

5.3 Differential mRNA Expression in Ovarian Cancer: An exploration of databases

5.3.2 Results of CSIOVDB Analysis

Expression of *F13A1* mRNA was queried in CSIOVDB, the results of which are summarised in Tables 5-1 to 5-4. *F13A1* mRNA expression was significantly lower between normal stroma, which is more mesenchymal and normal ovary epithelium (p=<0.0005). Ovarian tumours had significantly lower expression compared to normal epithelium. However, the highest expression of *F13A1* mRNA was found in tumour stroma, and was significantly higher than expression in normal stroma (p=<0.0001), normal epithelium (p=0.0207) and ovarian tumours (p=<0.0001). As stroma is more mesenchymal, this suggests *F13A1* mRNA expression is either higher in cells with mesenchymal phenotype compared to epithelial phenotype or there is another population of cells within the stroma that expresses FXIIIA. The higher expression in tumour stroma suggests that FXIIIA may have a role in the tumour matrix, and as FXIIIA can cross-link extracellular matrix proteins through its transglutaminase activity perhaps exert a role in maintenance and/or development of tumour matrices.

Mucinous histology with low metastatic potential, and clear cell histology have the highest mRNA expression (Table 5-2). Multivariate Cox modelling in the ICON7 Cohort (Chapter 4) found that those with clear cell histology had a higher risk of death (HR=3.54, p=<0.001) and progression of disease (HR=1.71, p=0.032). Could this be due to the increased gene expression of *F13A1*, resulting in more FXIIIA protein which may be exerting its roles in tumour matrix formation or angiogenesis, which may be affecting prognosis? High grade serous histology has the lowest expression of *F13A1* mRNA. Low grade serous (or serous histology with low metastatic potential) although had higher expression compared to high grade serous, expression was not significant (p=0.203).

Expression of *F13A1* mRNA decreased with increasing grade and stage of disease, (Tables 5-3). No relationship was seen for *F13A1* mRNA expression and sensitivity to therapy (data not shown). No correlation was identified between age and expression (p=0.461). Interestingly, a positive association was present between increasing *F13A1* expression and EMT score (Spearman Rho 0.289, p=<0.0001). A high EMT score means that there is a higher expression of mesenchymal-associated genes than epithelial-associated genes. As *F13A1* is highly expressed in tumour stroma, which is more mesenchymal in nature (256) the EMT score may only be reflecting that *F13A1* is expressed in more mesenchymal-like cells. Further investigation would therefore be required to establish whether FXIIIA has a role in EMT. The highest mRNA expression in OC molecular subtypes was in the Mesenchymal subtype (MES) and expression was significantly higher compared to all other subtypes measured in CSIOVDB (p<0.001), (Table 5-4).

When expression levels of *F13A1* were split by median expression and analysed for overall and disease-free (progression-free) survival, no significant associations were seen, (Figure 5-A). Median overall survival was 48 months and 46.37 months for low and high mRNA expression, respectively. Median disease-free survival was 22.02 months and 19.00 months for low and high expression, respectively. Only survival analysis based on the whole cohort could be performed with the CSIOVDB and it would have been interesting to see whether there was any benefit to survival intervals if the survival data were stratified based on histological subtype or tissue type.

The high expression of *F13A1* mRNA in tumour stroma compared to normal stroma and ovarian tumours, suggests a role of FXIIIA within the carcinoma stroma. However, higher transcription of mRNA does not necessarily mean an increased level of the expressed protein within the stroma, and further investigation into protein expression within ovarian tissue would be necessary. If higher expression of FXIIIA protein was present in tumour stroma tissue, where was the protein being expressed?

Table 5-1: *F13A1* mRNA Expression in Ovarian Tissue Types in CSIOVDB

A

	Normal Ovary Epithelium	Normal Stroma	Tumour	Tumor Stroma
Mean	8.13	7.38	7.63	8.57
Median	7.965	7.31	7.532	8.554
Range (Q1-Q4)	7.479-8.890	6.878-7.614	6.849-8.322	7.961-8.825

B

Mann-Whitney	Normal Ovary Epithelium	Normal Stroma	Tumour	Tumor Stroma
Normal Ovary Epithelium		0.001	0.000	0.021
Normal Stroma			0.267	0.000
Tumour				0.000
Tumor Stroma				

(A) Fold change in *F13A1* mRNA expression data from ovarian tissues types compared to controls. Expression data were normalised using RMA. (B) P-values from Mann-Whitney U testing for difference between groups, tested between the group give in the far-left column and then the top row. A value of '0.000' indicated that $p<0.001$. Results not significant if $p>0.05$. Abbreviations: Quantile 1 (Q1) – Quantile 4 (Q4).

Table 5-2: *F13A1* mRNA Expression in Ovarian Cancer Histologies in CSIOVDB

A

	Clear Cell	Endometriod	Mucinous	Mucinous-LMP	Serous	Serous-LMP
Mean	8.032	7.778	7.715	7.877	7.612	7.716
Median	7.929	7.619	7.537	8.05	7.503	7.727
Range (Q1-Q4)	7.247-8.613	6.998-8.339	6.965-8.615	7.118-8.380	6.820-8.298	6.892-8.341

B

Mann-Whitney	Clear Cell	Endometriod	Mucinous	Mucinous-LMP	Serous	Serous-LMP
Clear Cell		0.010	0.035	0.734	0.000	0.044
Endometriod			0.858	0.463	0.147	0.855
Mucinous				0.474	0.403	0.747
Mucinous-LMP					0.258	0.591
Serous						0.203
Serous-LMP						

(A) Fold change in *F13A1* mRNA expression data from ovarian cancer histologies compared to controls. Expression data were normalised using RMA. (B) P-values from Mann-Whitney U testing for difference between groups, tested between the group give in the far-left column and then the top row. A value of '0.000' indicated that $p<0.001$. Results not significant if $p>0.05$. Abbreviations: Low Metastatic Potential (LMP), Quantile 1 (Q1) – Quantile 4 (Q4).

Table 5-3: *F13A1* mRNA Expression in Ovarian Cancer Stage and Grade in CSIOVDB

A

Stage	**I**	**II**	**III**	**IV**
Mean	7.904	7.71	7.595	7.641
Median	7.839	5.59	7.521	7.484
Range (Q1-Q4)	7.185-8.483	6.763-8.516	6.877	8.285
Grade	**1**	**2**	**3**	
Mean	8.09	7.705	7.582	
Median	7.948	7.62	7.472	
Range (Q1-Q4)	7.180-8.978	6.896-8.389	6.807-8.233	

B

Mann-Whitney	**I**	**II**	**III**	**IV**
I				
II	0.067			
III	0.000	0.383		
IV	0.006	0.755	0.431	

C

Mann-Whitney	1	2	3
1			
2	0.004		
3	0.000	0.068	

(A) Fold change in *F13A1* mRNA expression data from ovarian cancer stages and grades of disease compared to controls. Expression data were normalised using RMA. (B) P-values from Mann-Whitney U testing for difference between groups for stages of disease, tested between the group give in the far-left column and then the top row. (C) P-values from Mann-Whitney U testing for difference between groups for grades of disease, tested between the group give in the far-left column and then the top row. A value of '0.000' indicated that $p<0.001$. Results not significant if $p>0.05$. Abbreviations: Quantile 1 (Q1) – Quantile 4 (Q4).

Table 5-4: *F13A1* mRNA Expression in Ovarian Cancer Molecular Sub-type in CSIOVDB

A

	Epithelial-A	Epithelial-B	Mesenchymal	Stem-A	Stem-B
Mean	7.596	7.195	8.436	7.221	7.651
Median	7.501	7.147	8.417	7.142	7.567
Range (Q1-Q4)	6.852-8.279	6.564-7.751	7.716-9.138	6.609-7.744	6.885-8.265

B

Mann-Whitney	Epithelial-A	Epithelial-B	Mesenchymal	Stem-A	Stem-B
Epithelial-A					
Epithelial-B	0.000				
Mesenchymal	0.000	0.000			
Stem-A	0.000	0.724	0.000		
Stem-B	0.376	0.866	0.000	0.000	

A) Fold change in *F13A1* mRNA expression data from ovarian cancer molecular sub-types of disease compared to controls. Expression data were normalised using RMA. (B) P-values from Mann-Whitney U testing for difference between groups for stages of disease, tested between the group give in the far-left column and then the top row. A value of '0.000' indicated that $p<0.001$. Results not significant if $p>0.05$. Abbreviations: Quantile 1 (Q1) – Quantile 4 (Q4).

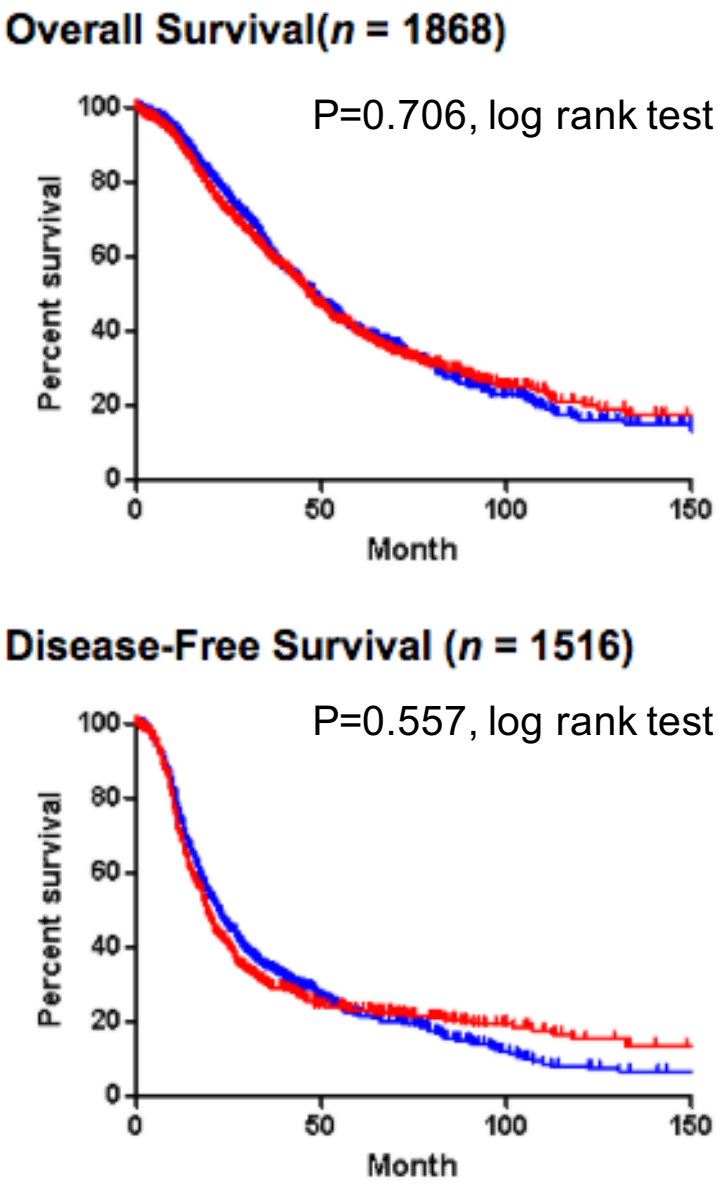

Figure 5-A: Kaplan-Meier plots for *F13A1* mRNA expression and survival intervals from CSIOVDB Analysis. Red = > median expression (high) and blue = < median expression (low). Results of a log rank test between F13A1 expression and survival intervals are given in the top right-hand corner of each plot: overall survival (top) and disease-free (also known as progression-free) survival (bottom).

FXIIIA is expressed in immune-like cells, so is it possible that the increase in tumour stroma expression is due to the presence of tumour-associated macrophages? Or is FXIIIA expressed in the stroma closest to the tumour, suggesting a possible role in communication between matrix and tumour? Could the expression of FXIIIA appear throughout the tumour stroma, and therefore potentially affecting structure and/or angiogenic signalling? In order to address some of these questions regarding expression of FXIIIA in OC, TMAs from OC tumour and stroma from patients in the translational cohort of the ICON7 clinical trial were acquired and stained for FXIIIA.

5.3.2 Expression Result from KM plotter

The results of *F13A1* mRNA expression levels and survival interval analysis from KM plotter analysis are presented in Figure 5B. For progression-free survival (PFS), n=1435 patients were analysed (p=0.14, log rank test), and the cut-off for low vs high *F13A1* expression was 310. Median PFS for low *F13A1* expression was 19 months and for high expression, 20.47 months. For overall survival (OS) n=1656 patients were analysed (p=0.13, log rank test), cut-off was 565 and median survival for low and high expression was 45.97 month and 49.13 months, respectively. For survival post-progression (SPP) n=782 patients were analysed (p=0.021, log rank test), cut-off was 567 and low expression median survival was 42.17 months and 38.7 months for high expression. The only significant association with a survival interval and expression was identified between survival post-progression and high *F13A1* mRNA expression resulting in a better prognosis compared to low mRNA expression. KM plotter comprises a number of databases and the expression was not split based on tissue type, like in the CSIOVDB. Survival post progression was not a survival interval present in the CSIOVDB so it is not possible to compare this result within the two cohorts.

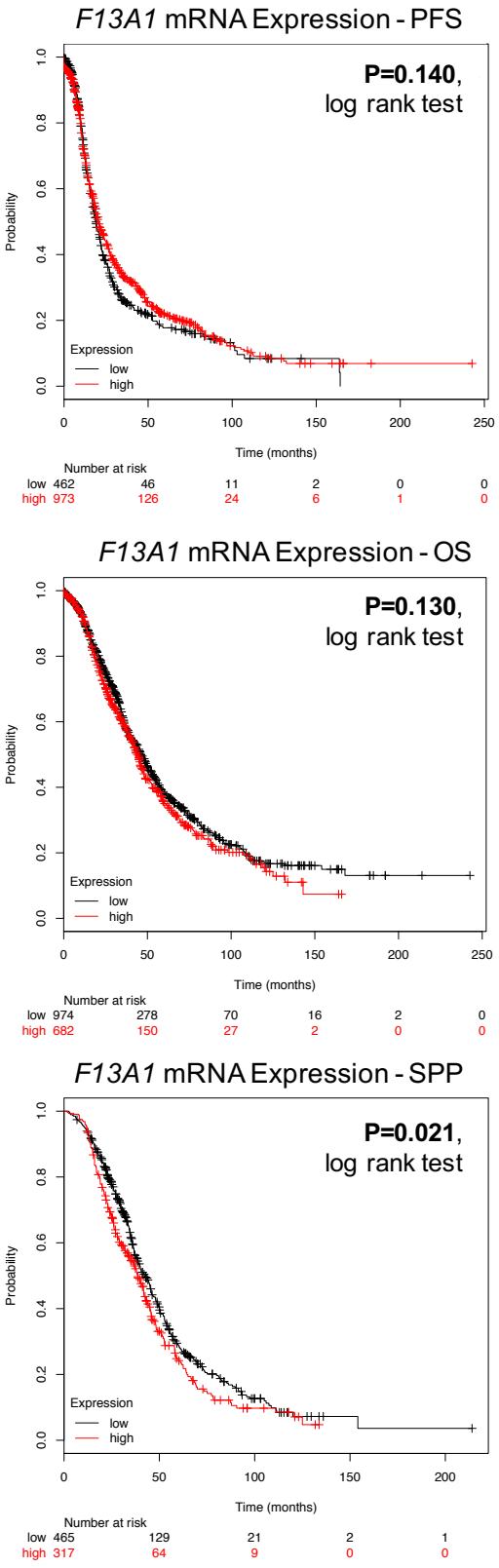

Figure 5-B: Kaplan-Meier Plots for *F13A1* mRNA Expression from KMPlotter Database Analysis. Top: *F13A1* mRNA expression and progression-free survival (n=1435) in KMPlotter Ovarian Cancer Database. Cut off for low/high expression chosen based on automatic selection by KMPlotter = 310 expression intensity out of 1000 (based on microarray normalisation, Győffry B *et al.* 2012.) Middle: *F13A1* mRNA expression and overall survival (n=1656) in KMPlotter Ovarian Cancer Database. Cut off for low/high expression = 565. Bottom: F13A1 mRNA expression and survival post-progression (n=782) in KMPlotter. Cut off for low/high expression = 567. Results of log rank tests are given in the top right hand corner of each plot, with results considered significant if $p<0.05$. Black line represents low expression and red line represents high expression. Risk tables demonstrating the number of patients at risk at each interval of time on the x-axis is given below the plot.

Looking at the Kaplan-Meier plots for both databases, follow-up in KM plotter was for 100 more months than CSIOVDB. The KM plotter results used a calculated cut off based on best threshold detected by the program and was not the median expression. Even if median value was used, the mRNA expression values within the two databases have been normalised differently (MSA5 and mean-centering for KM plotter and RMA for CSIOVDB), so it would be challenging to make direct comparisons. The benefit of high *F13A1* expression to survival post-progression suggested that FXIIIA may be important after disease progression and more studies would need to be undertaken to investigate this finding.

5.4 FXIIIA Expression in Tissues

5.4.1 Tissue Microarray Staining

Tissue microarrays were stained for the levels and locality of expression of FXIIIA. In brief, slides were stained as per the Immunohistochemistry protocol provided in Chapter 2 (Section 2.5). Slides were then scanned at a 20X magnification by the pathology team in the department. Levels of staining, measured as percentage (%) positivity, were quantified using the QuPath software, see Appendix 2 for full script (.groovy). Representative staining in cores can be found in Figure 5-C.

5.4.1.1 Percentage Positivity in Tissue Types

After collation of staining data and the available clinical data, a distribution of the % positivity within the cores across the tissue types was assessed, (Table 5-5). The highest average % positivity was found in OC stroma tissues, and the lowest in OC tumour tissues, (Figure 5-D). Cores that contained both tumour and stroma had an average % positivity in between that of tumour and stroma. A Kruskal-Wallis test identified a significant difference in the distribution of staining levels between the tissue types, (Figure 5-D). In the OC tumour cores, staining did not appear within tumour cells themselves, staining was instead present in cells within the tumour area, perhaps immune-like cells or staining was present in intra-tumour stromal regions, (Figure 5-C). This pattern of staining was seen in ovarian cancer tissue used in work up of the FXIIIA antibody, with staining seen in stromal cells and not in tumour cells, (Figure 5-E).

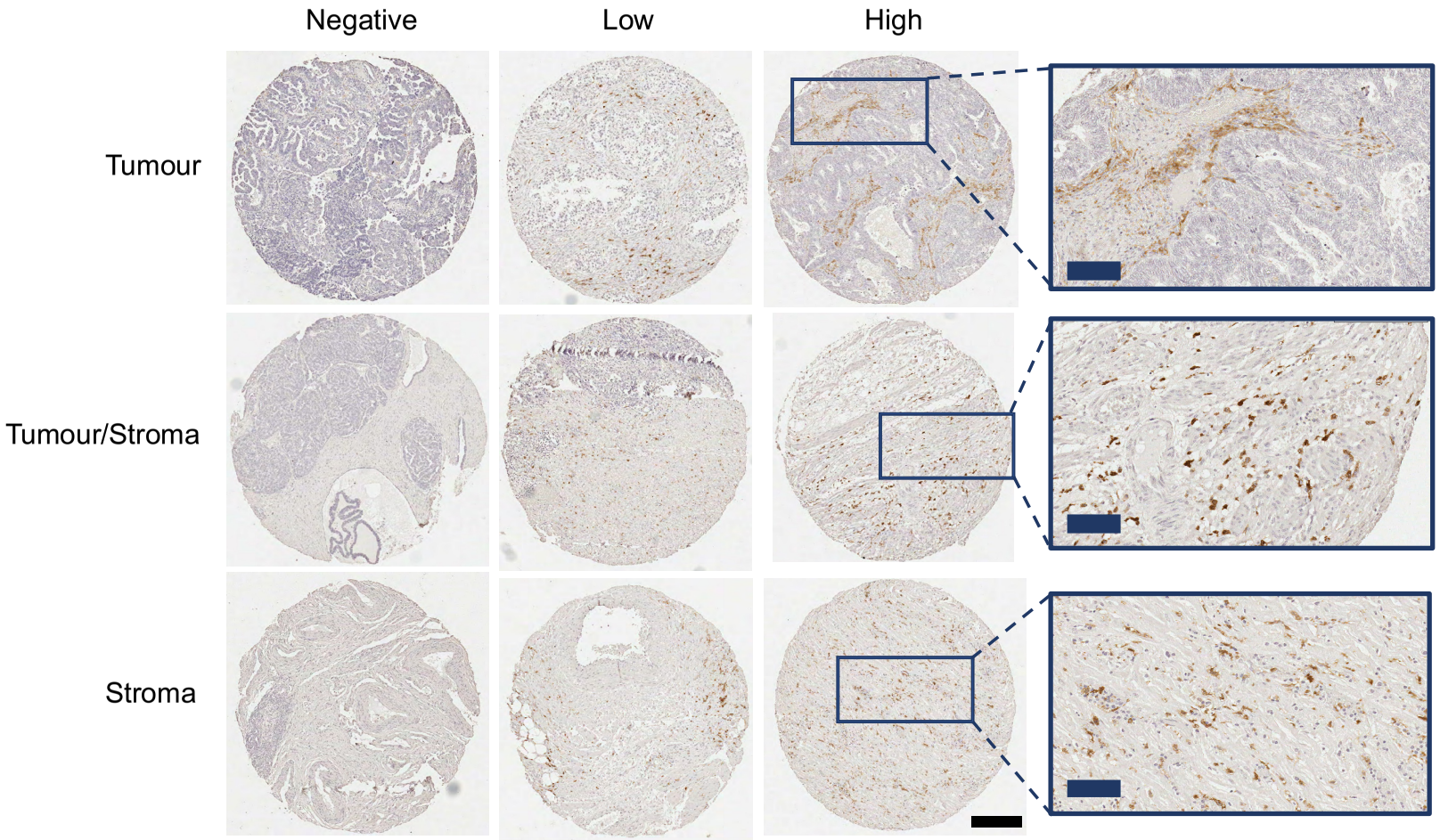

Figure 5-C: Representative Ovarian Cancer Tissue Cores from the ICON7 clinical trial stained for FXIIIA, taken from primary tissue acquired during resective surgery. Formalin-fixed paraffin-embedded tissues were placed into tissue microarrays by a qualified histopathologist based on the tissue-type present in the core. Cores stained for FXIIIA using HPA001804 at 1:200. Negative staining = <1% percentage positivity, Low staining = Quartiles 1 and 2, and High staining = Quartiles 3 and 4. Positivity is demonstrated by brown 3,3'-diaminobenzidine (DAB) staining. Nuclei are counterstained with haematoxylin. Zoomed in sections are highlighted by rec Black bar for whole cores represents 250 µm. Blue bars within the zoomed in sections represent 100 µm.

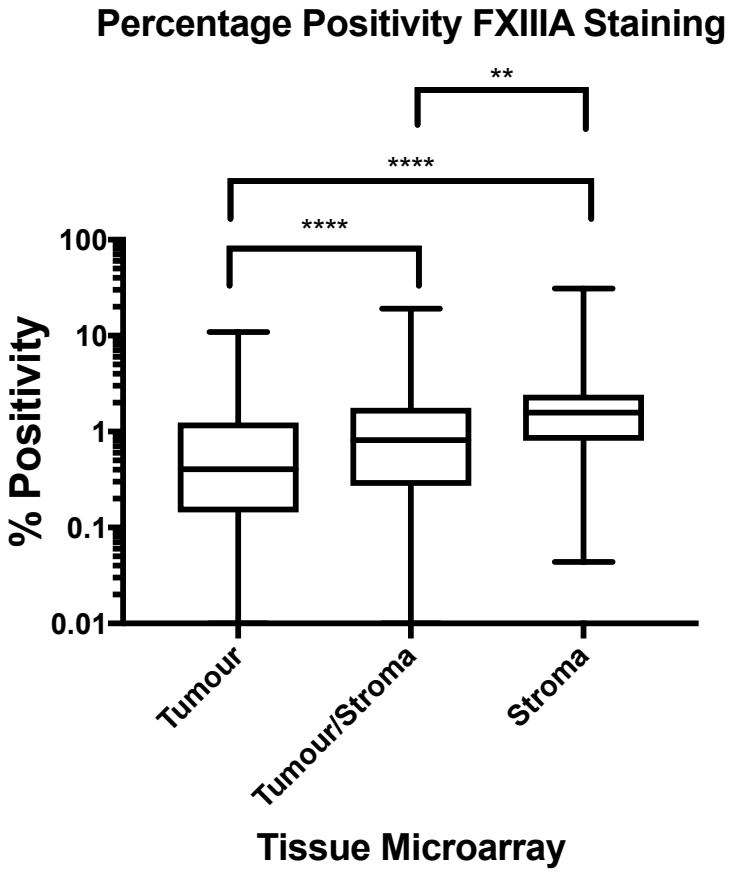

Figure 5-D: Box and Whisker Plot of Percentage Positivity for FXIIIA in ICON7 Tissue Microarrays. The centre line of the box is plotted at the median, the edges of the box extend to the 25th and 75th percentiles for the bottom and top of the box, respectively. The whiskers represent the minimum and maximum values. As the y-axis is logarithmic and the lowest value for % positive staining was 0, the bottom whisker is not shown. The data were not normally distributed (measured with a D'Agostino-Pearson Normality Test) and a Kruskal-Wallis test with Dunn's test for multiple comparisons was used to compare the distribution of values in three groups. A significant difference was seen between tumour and tumour/stroma staining ($p<0.0001$, ****) and between tumour and stroma staining ($p<0.0001$, ****). A significant difference was also seen between tumour/stroma and stroma staining ($p<0.001$, **). P-values were adjusted for multiple comparisons through the Dunn's test.

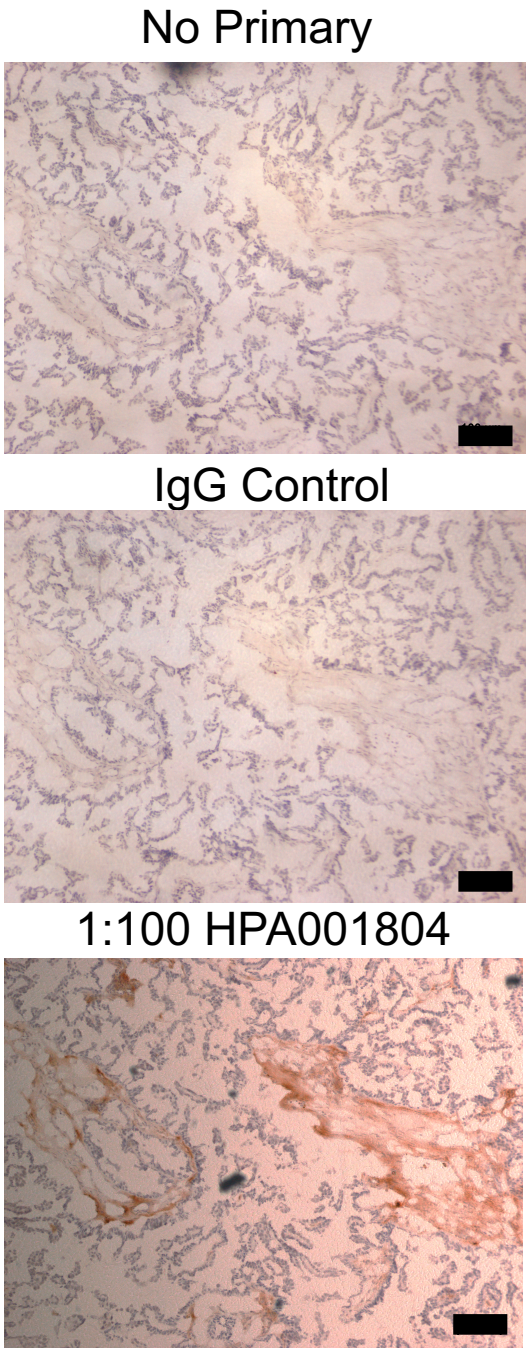

Figure 5-E: Staining of FXIIIA in an ovarian cancer tissue demonstrating staining locality, in non-tumour cells, suggesting a more stromal staining pattern. Tissue was from frozen ovarian cancer sample, used as a control during work up of the FXIIIA antibody. Top: no primary antibody staining control, only antibody diluent added to the tissue section during the primary antibody incubation. Middle: Tissue incubated with rabbit IgG1 isotype control at the same final concentration as the primary HPA001804 antibody to demonstrate that any staining present was due to antigen specificity rather than background caused by the backbone of the antibody: Bottom: Tissue was stained with HPA001804 at 1:100. Black scale bar represents 100 µm. Image brightness was manually increased by 40% for Top and Middle image and by 60% for Bottom, for clarity in print.

As the average staining level in general was so low in the cores, analysis was limited to % positivity. Semi-quantitative scoring methods such as Allred and H-Score were available through the QuPath software, however these scoring methods were originally developed for quantitation of large quantities of staining with clear differences in intensity, such as that for hormone receptors (in the case of H-scoring (257)) or other highly expressed proteins (BMP6 in the case of Allred Scoring (258)). FXIIIA staining had not been explored before in OC before, and therefore presented quantitation challenges which required a simplified approach. Tumour cores from 11 patients were stained with the antibody for FXIIIA, HPA001804 (anti-*F13A1*) as part of the work-up for the Human Protein Atlas (HPA) antibody, to explore whether expression of the protein was detectable in the tumour cells. The results were negative for tumour-cell staining, but analysis of the cores by the HPA team found that where staining was present, it was in the cells surrounding the tumour cells, which appeared to be stromal in nature (259).

Descriptive statistics were generated for FXIIIA expression in each group of cores and are summarised in Table 5-5. The number of cores where positive staining was over 10% was very small, concerns were raised over the suitability of standard scoring methods and how this staining could be statistically analysed when collated with the clinical data, as small numbers within categories set could lead to very limited analysis. Therefore, the first stage was to look at whether there was any association between positive and negative staining. Staining was considered negative if the percentage positivity was less than (<) 1%, and conversely considered positive if positivity was greater than (>) 1%. In OC tumour tissue cores, 76/245 (31%) were positive; in OC tumour/stroma cores, 89/212 (42%) were positive; in OC stroma tissue cores, 90/126 (71%) were positive.

Positive % positivity categories were generated by splitting the percentage data by quartiles, (Figure 5-F). This resulted in even numbers per category, or as close to even as possible. This was the best way to split the data into categories that could be analysed without introducing extreme researcher bias. Quartiles were then compared and combined to form dichotomised categories for ‘lower’ staining (Q1-Q2) and ‘higher’ staining (Q3-Q4).

Table 5-5: Descriptive Statistics for Percentage Positivity for FXIIIA Staining in ICON7 Tissue Microarrays

Descriptive Statistics	Microarray		
	T	TS	S
n	245	212	126
Median (%)	0.40	0.81	1.58
Mean (%)	0.96	1.42	3.61
Std Dev	1.15	2.14	3.61
95% CI Lower	0.78	1.13	1.86
95% CI Upper	1.15	1.71	3.13
Negative Cores (<1%)	169	123	36
Positive Cores (>1%)	76	89	90

Abbreviations: CI = Confidence Interval, T = Tumour Cores, TS = Tumour/Stroma Cores, S = Stroma Cores, n= number of cores, StdDev = Standard Deviation, % = percentage positivity, '<' = less than, '>' greater than.

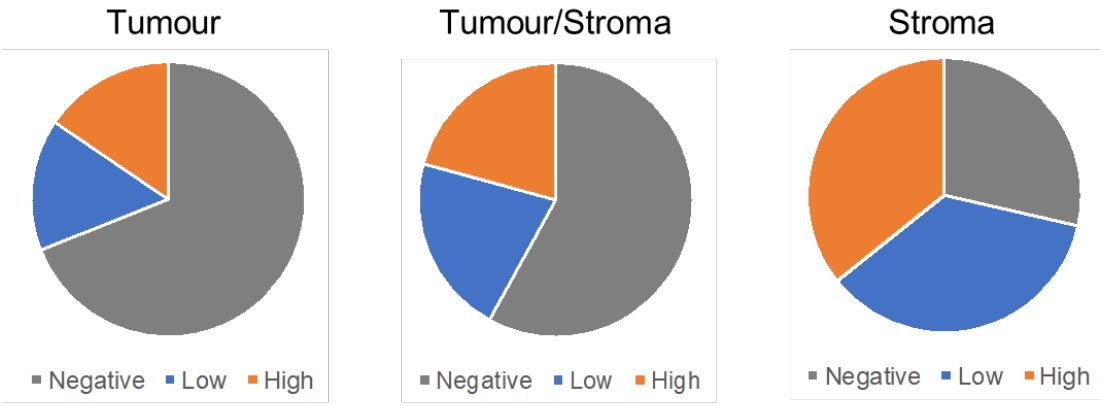

Tissue Microarray	Staining Category		
	Negative	Low (Q1+Q2)	High (Q3+Q4)
Tumour	169 (68%)	38 (16%)	38 (16%)
Tumour/Stroma	123 (58%)	45 (21%)	44 (21%)
Stroma	36 (28%)	45 (36%)	45 (36%)

Figure 5-F: Pie Charts to demonstrate the distribution of staining categories for each OC tissue type in the ICON7 tissue microarray. Table demonstrates the number of cores in each category, with percentages rounded to the nearest whole integer.

5.5 Associations between Prognostic Factors, *F13A1* SNPs and Survival Intervals

The dichotomised categories for % positivity staining were used to test for associations between prognostic factors, SNP genotypes and survival intervals and staining levels (negative, lower (Q1+Q2) or higher (Q3+Q4)), (Figure 5-F). The distribution of prognostic factors in the ICON7 Tissue Microarray cohort is given in Table 5-6. The survival intervals reflect those examined in Chapter 4: overall survival, progression-free survival, and survival post-progression. In short, overall survival (OS) is measured from entry to either death or censorship at the end of the follow-up period; progression-free survival (PFS) is measured from entry to a progression-event such as disease recurrence or worsening; and survival post-progression (SPP) is measured from the progression event to the end of follow-up.

5.5.1 Prognostic Factors

The prognostic factors which were used in Chi-square tests for association were grade, stage of disease, histology, and risk of disease progression. No significant associations were found between prognostic factors and staining levels, suggesting that staining levels are not directly linked to OC phenotype, (Table 5-6).

5.5.2 *F13A1* SNPs

Associations between FXIIIA staining levels and the *F13A1* SNPs (placed into either 'wildtype' or 'carrier of alternative allele' categories) were also tested for by Chi-square tests. Significant associations were identified between V34L and Tumour/Stroma (TS) and Stroma (S) staining categories, p=0.006 and 0.025, respectively, (Table 5-7). For positive OC Stroma staining, of the V34L carriers (V/L and L/L), 43% of cores had lower expression levels and 37% had higher expression; wildtype V34L (VV) patients, 31% had lower expression levels and 35% had higher expression levels, (Table 5-8). There was a higher percentage of negative FXIIIA staining in OC stroma for WT (34%) than in carriers (20%). However, for both V34L genotype categories, the percentage of cores with higher expression levels of FXIIIA was roughly equal (WT: 35%. Carriers: 37%).

Table 5-6: Distribution of Prognostic Factors and *F13A1* SNPs in the ICON7 Tissue Microarray Cohort.

n=273		n	%
Prognostic Factor			
Grade	1	9	3
	2	44	16
	3	219	81
FIGO	I	22	8
	II	35	13
	III	185	68
	IV	31	11
Histology	Serous	185	68
	Mucinous	3	1
	Endometrioid	15	5
	Clear Cell	36	13
	Mixed	24	9
	Other	10	4
At High Risk of Progression	No	180	66
	Yes	93	34
***F13A1* Polymorphisms**			
103G>T (Val34Leu)	VV	170	62
	VL/LL	103	38
1694C>T (Pro564Leu)	PP	171	62
	PL/LL	102	38
650+651 Haplotypes	VV + EE	165	61
	VV + EQ/QQ	77	28
	VI/II + EQ/QQ	30	11

Table 5-7: Results of Chi-Square tests for association between staining levels and prognostic factors.

Chi2 Test for Association	T		TS		S	
Prognostic Factors						
Grade	0.298	ns	0.319	ns	0.361	ns
Stage	0.194	ns	0.183	ns	0.402	ns
Histology	0.324	ns	0.123	ns	0.125	ns
High Risk	0.717	ns	0.399	ns	0.127	ns
***F13A1* SNPs**						
V34L	0.574	ns	0.006	**	0.025	*
P564L	0.209	ns	0.805	ns	0.156	ns
650+651 Haplotypes	0.777	ns	0.627	ns	0.242	ns

Chi-square tests for association were run between the prognostic factors and F13A1 SNPs. Categories are given in Table 5-6. P-values were considered significant if $p<0.05$. Levels of significance are denoted by: (*) $p<0.05$, (**) $p<0.01$, (ns) not significant.

Table 5-8: Distribution of Val34Leu Genotypes and Staining Categories in the ICON7 Tissue Microarrays

Staining	Val34Leu Genotype	% of Val34Leu Genotypes per Staining Category			Total
		Negative	Low (Q1+Q2)	High (Q3+Q4)	
T	WT (V/V)	109 (82%)	22 (17%)	21 (16%)	152
	Carrier (V/L or L/L)	60 (76%)	16 (20%)	17 (22%)	93
				Total	*245*
TS	WT (V/V)	88 (66%)	21 (16%)	24 (18%)	133
	Carrier (V/L or L/L)	35 (44%)	24 (30%)	20 (25%)	79
				Total	*212*
S	WT (V/V)	26 (34%)	24 (31%)	27 (35%)	77
	Carrier (V/L or L/L)	10 (20%)	21 (43%)	18 (37%)	49
				Total	*126*

Raw value on the left and percentage of the respective genotype i.e. wildtype or carrier is given in parentheses Abbreviations: T = Tumour, TS = Tumour/Stroma, S = Stroma, WT = wildtype, V= Valine, L = Leucine, Q= Quartile.

The percentage of positive OC TS staining was higher for wildtype (WT) patients (66%) than Leu-carriers (44%). For Leu-carriers, 25% had higher expression levels whereas for wildtype patients only 18% had higher expression levels. For lower expression levels, 30% were found in Leu-carriers compared to only 16% in wildtype patients.

5.5.3 Survival Intervals: Univariate Analysis

5.5.3.1 General Survival Interval and Staining Level Analysis

A general analysis of the effect of staining intervals on survival intervals was undertaken with Kaplan-Meier plots and log rank tests. No significant associations with the survival intervals were identified, (Figure 5-G). However, for PFS, low TS staining appeared to result in better prognosis compared to negative and high TS staining (p=0.030), (Figure 5-H). Although no significant associations between staining intervals were identified for FXIIIA staining and SPP, the most dramatic effect was seen in the Kaplan-Meier plot for Stroma staining levels and SPP, (Figure 5-I). Presence of positive FXIIIA staining regardless of level (i.e. low or high) appeared to result in a near one year decrease in SPP compared to negative FXIIIA staining. FXIIIA staining in the tumour or in the stroma cores appears to have a negative effect on SPP, although the relationships do not appear as clear in the other survival intervals.

As significant associations between staining levels in TS and S cores and the *F13A1* SNP V34L, were identified during univariate Chi-square tests, an assessment of differences in survival between V34L genotypes and each OC tissue type and for each of the 3 survival intervals under investigation (PFS, SPP and OS) was undertaken. Kaplan-Meier plots provided an important visual tool to assess the difference in survival and log rank tests were performed as a univariate survival analysis of each genotype category and staining levels. Median survival was also measured to compare differences. However, the numbers in each category would be very small and therefore results would need to be interpreted with extreme caution.

No discernible differences or relationships were identified for PFS, and are therefore not presented here. None of the log rank test results were significant, and this was thought to be due to the overall small numbers within each category

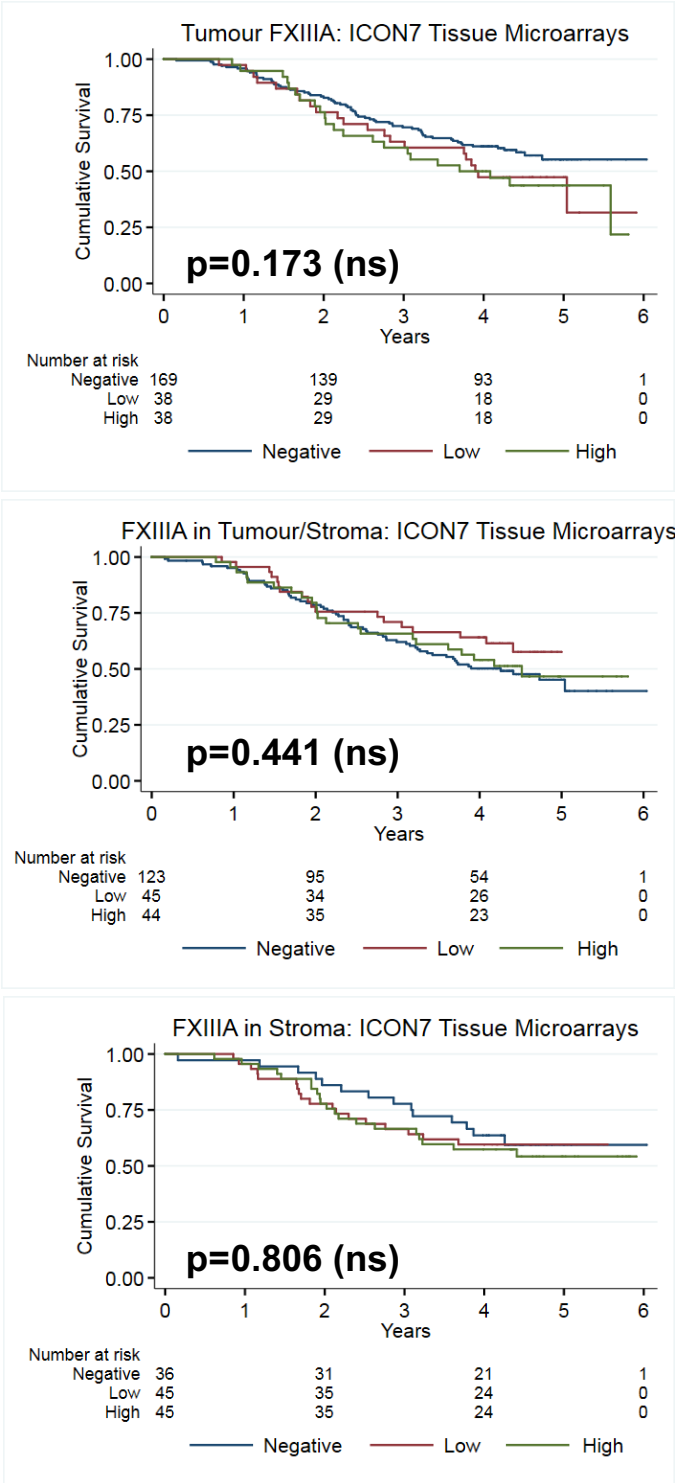

Figure 5-G: Kaplan-Meier Plots for Overall Survival and Staining Levels for the ICON7 Tissue Microarrays. Risk tables are given below each plot. demonstrating the number of patients at risk of death at the given time interval on the x-axis, discounting those who were censored during the interval. Result from log rank tests are given in the bottom left corner of each plot, with results considered significant if $p<0.05$. (ns) = not significant.

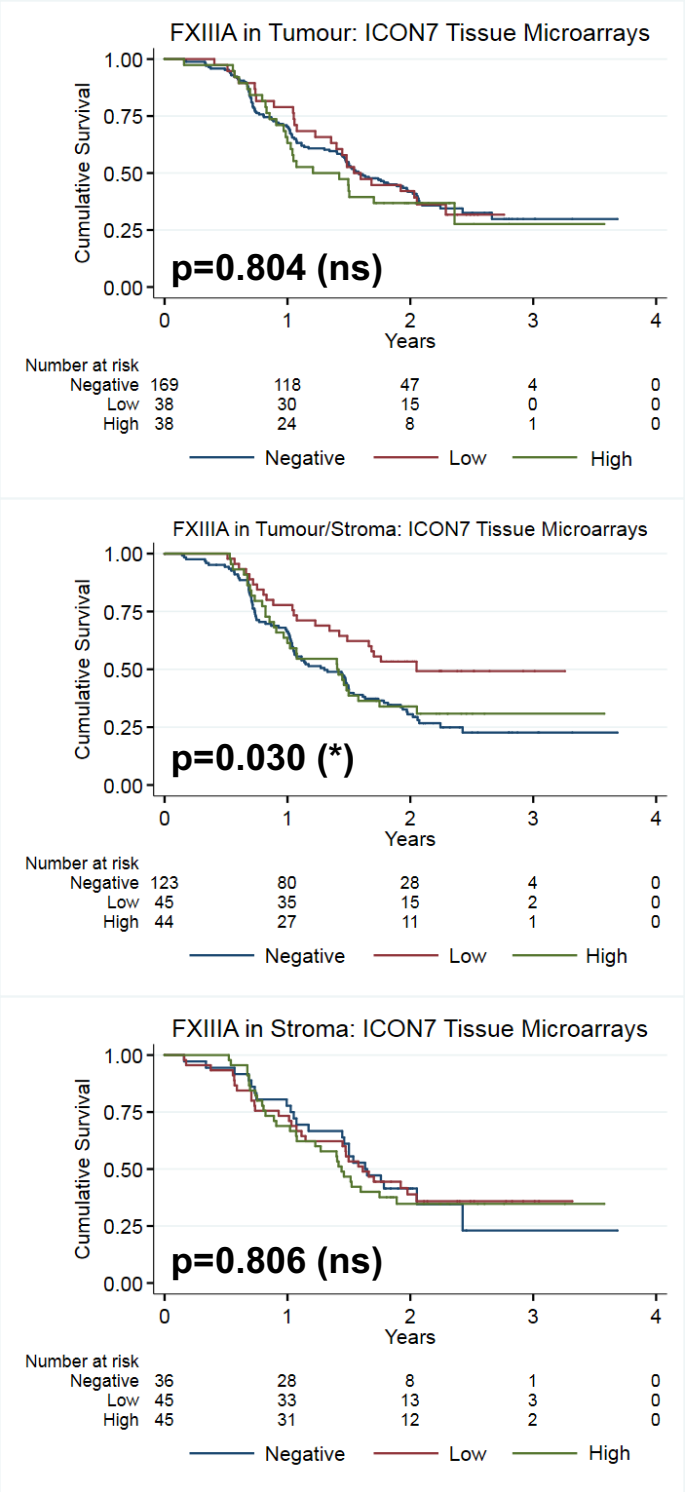

Figure 5-H: Kaplan-Meier Plots for Progression Free Survival and Staining Levels for the ICON7 Tissue Microarrays. Risk tables are given below each plot. demonstrating the number of patients at risk of death at the given time interval on the x-axis, discounting those who were censored during the interval. Result from log rank tests are given in the bottom left corner of each plot, with results considered significant if $p<0.05$. (ns) = not significant, (*) = $p<0.05$.

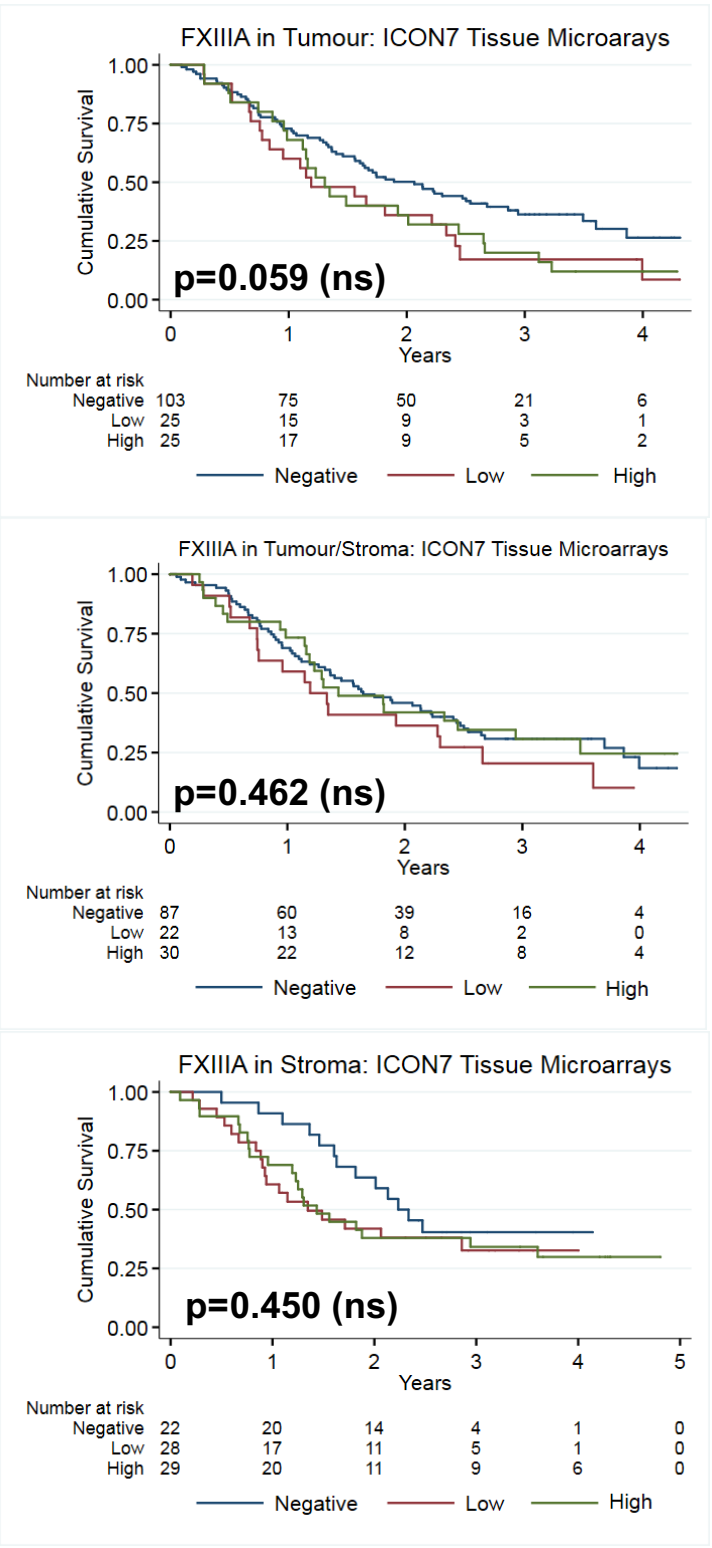

Figure 5-I: Kaplan-Meier Plots for Survival Post-Progression and Staining Levels for the ICON7 Tissue Microarrays. Risk tables are given below each plot. demonstrating the number of patients at risk of death at the given time interval on the x-axis, discounting those who were censored during the interval. Result from log rank tests are given in the bottom left corner of each plot, with results considered significant if $p<0.05$. (ns) = not significant.

Log rank tests are significant when there is clear separation between the plots of the proportion of individuals surviving in a given category. As there were often small numbers in each category, a lot of cross-over between the plots occurred over the time period measured. Visually, however, and through measurement of median survival through interpolation of the KM plots at 50% survival, some interesting differences were identified. These are detailed below.

5.5.3.2 Survival Post-Progression and Val34Leu Genotypes

SPP is the time period measured between a progression event such as disease worsening or recurrence, see Chapter 2 Materials and Methods for full definition as per the ICON7 Clinical Trial Protocol. In Tumour cores (T), Leu-carriers (VL/LL) had a better prognosis after progression if FXIIIA staining was negative (3.6 years VL/LL vs 2.86 years for VV), (Figure 5-J-D, and Table 5-J-G). When FXIIIA staining was positive in T cores, Leu-carriers demonstrated similar median survival times when compared to wildtype individuals.

In TS cores, Leu carriers again demonstrated improved SPP compared to wildtype individuals in the negative staining cores (3.7 years vs 2.41 years, respectively). In contrast higher expression levels, Leu-carriage resulted in a near 50% lower median survival (1.82 years for Leu-carriers vs 3.89 years for wildtype individuals).

In S cores, the story appears reversed from T and T/S cores. WT patients had an improved OS compared to Leu-carriers when FXIIIA staining was negative. For Leu-carriers and FXIIIA expression in OC Stroma, SPP was higher than for wildtype patients (the proportion surviving never reached 50% for Leu-carriers, but was 1.88 years for higher expression in WT patients, the shortest median survival in SPP analysis). It is important to note however, that the numbers for Leu-carriers and Stroma FXIIIA staining are low, especially for negative staining (n=9 at risk at the start of analysis), and therefore a greater sample size would be required for a more definitive comparison between V34L genotypes and FXIIIA expression in the stroma. In general, there were more positive cores in the stroma tissue microarrays, compared to the others and therefore a smaller number of negative cores will always be present in this subset.

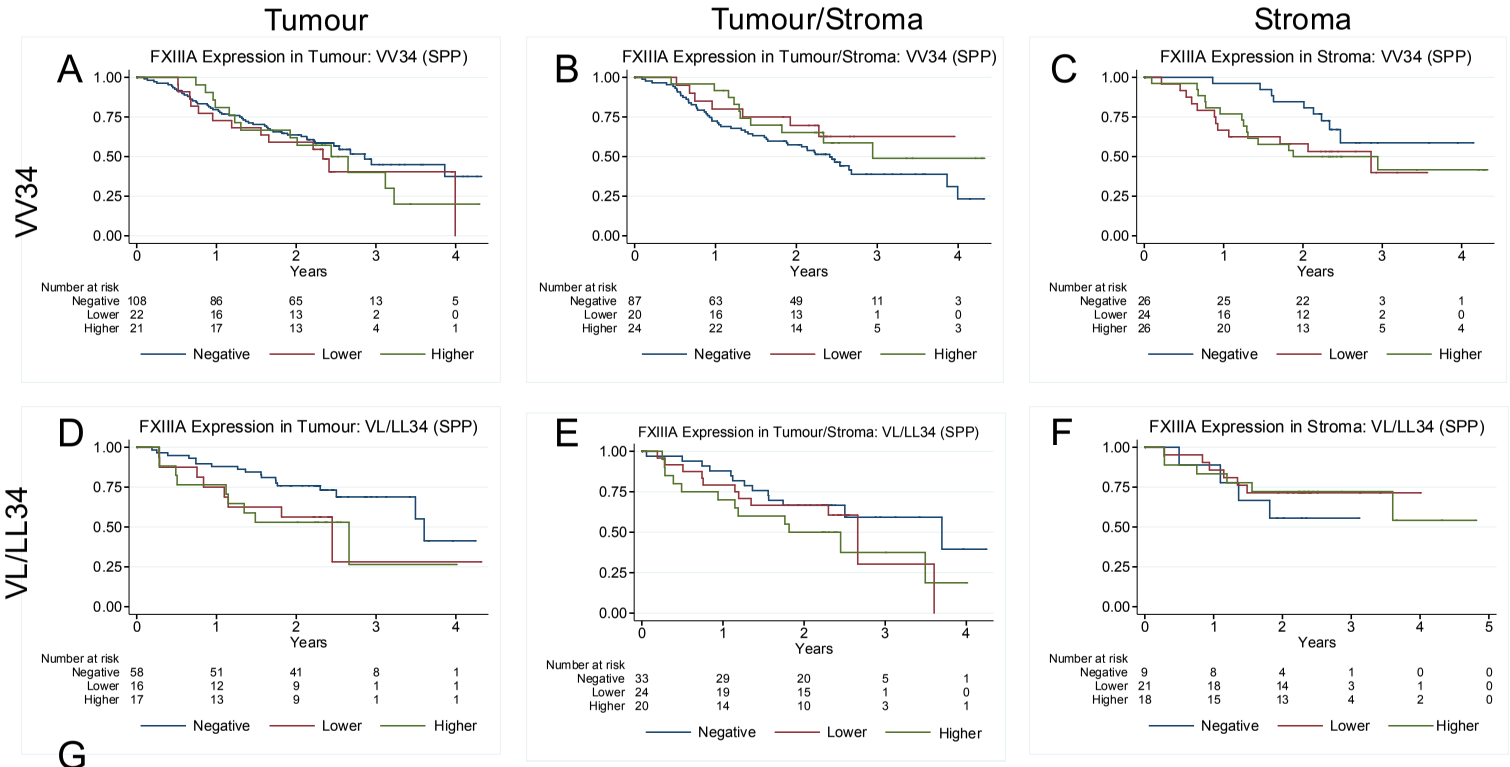

G

	Median Survival - Survival Post-Progression (Years)								
	Tumour			Tumour/Stroma			Stroma		
	Negative	Lower	Higher	Negative	Lower	Higher	Negative	Lower	Higher
VV	2.86	2.34	2.44	2.41	.	3.99	.	2.86	1.88
VL/LL	3.6	2.45	2.66	3.7	2.66	1.82	.	.	.

Figure 5-J: Kaplan Meier Plots of Survival Post-Progression for wildtype V34L (A-C) and carriers of Leu at V34L (D-F). Risk tables of those patients at risk per year on x-axis of time (years) are given below each KM-plot, and exclude those who have been censored within the time interval given. Cumulative survival is on the y-axis. Negative FXIIIA Expression is given by the blue line, lower expression (which combines quartiles 1 (Q1) and 2 (Q2) of percentage positivity) is given by the red line and higher expression (which combines quartiles 3 (Q3) and 4 (Q4) of percentage positivity). Table G gives median progression-free survival in years for each genotype category and core-type. (.) indicates median survival was not reached.

5.5.3.3 Overall Survival and Val34Leu Genotypes

OS is defined as the time measured from entry into the trial i.e. point of diagnosis, through to the end of follow-up where death or censorship are recorded. For T cores, negative expression for both genotype categories resulted in median survivals over 5 years (Figure 5-K, Plot A and D). Leu-carriers with positive FXIIIA in T cores had an average 4 year median survival (average of 3.93+4.03 years) compared to 3.8 years for wildtype carriers (average of 3.85+4.08 years).

In TS cores with negative FXIIIA staining, WT patients had a median OS of 3.71 years and for Leu-carriers this was greater than 5 years (Figure 5-K, Plots B and E, and Table G). For Leu-carriers with positive FXIIIA in TS cores, any degree of positive staining was detrimental to OS. In S cores, the relationships between genotype and FXIIIA expression are entirely reversed between V34L genotypes. Wildtype individuals have a better prognosis than Leu-carriers for negative expression of FXIIIIA, but in the presence of FXIIIA expression in the stroma, Leu-carriers benefit over wildtype (Figure 5-K, Plots C and F).

5.5.3.4 Summary of Univariate Survival Analysis and Val34Leu Genotypes

In OC Stroma, Leu-carriers benefit over WT patients, clearly in terms of OS and less clearly in SPP. Could carriage of the alternative Leu allele at V34L be having an effect within the OC stroma which either makes therapy more effective or metastatic disease less likely? The poorer OS for Leu-carriers in the TS cores, in which both tumour and stroma tissue are present could be indicative of an alternative role for FXIIIA when present close to tumour cells. When TS cores were examined, staining was predominantly in the stromal cells and not common within the tumour cells themselves, as was the case with T cores only where staining appeared to be isolated in what were potentially immune-like cells (although staining was not performed using specific markers to confirm this). Staining was also located in what appeared to be intra-tumour stroma in T cores.

5.6 Multivariate Survival Analysis: FXIIIA Expression

As with all survival analysis, univariate analysis only looks at a small snapshot of the data, and does not factor in the interplay that can occur in a disease as heterogeneous and complex as cancer. Therefore, multivariate modelling, which

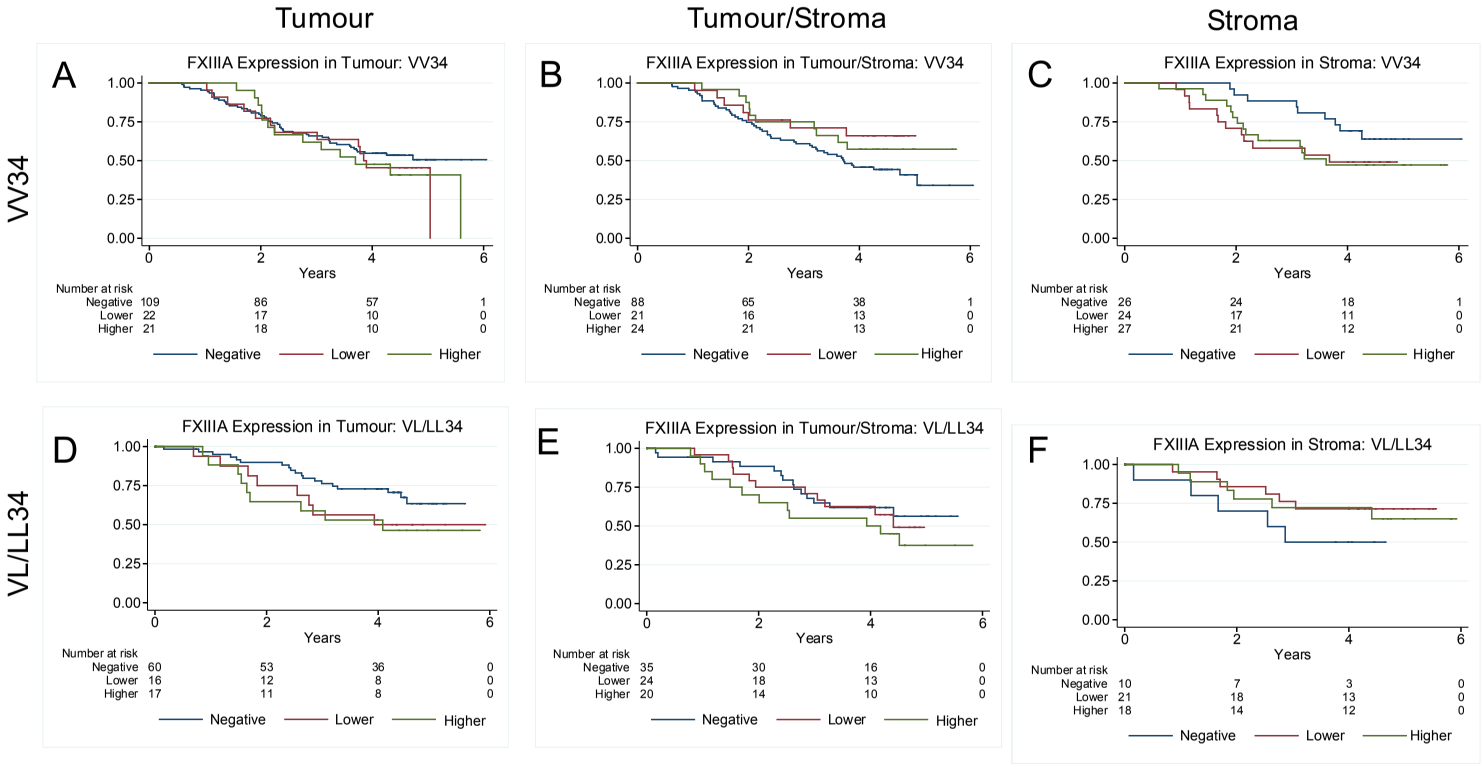

G

	Median Survival - Overall Survival (Years)								
	Tumour			Tumour/Stroma			Stroma		
	Negative	Lower	Higher	Negative	Lower	Higher	Negative	Lower	Higher
VV	.	3.85	3.7	3.71	.	.	.	3.68	3.62
VL/LL	.	3.93	4.08	.	4.41	3.93	2.86	.	.

Figure 5-K: Kaplan Meier Plots of Overall Survival for wildtype V34L (A-C) and carriers of Leu at V34L (D-F). Risk tables of those patients at risk per year on x-axis of time (years) are given below each KM-plot, excluding those who were censored during the time interval given. Cumulative survival is on the y-axis. Negative FXIIIA Expression is given by the blue line, lower expression (which combines quartiles 1 (Q1) and 2 (Q2) of percentage positivity) is given by the red line and higher expression (which combines quartiles 3 (Q3) and 4 (Q4) of percentage positivity). Table G gives median progression-free survival in years for each genotype category and core-type. (.) indicates median survival was not reached.

takes into account numerous variables/covariates and measures their ability to predict survival, is required. Cox Proportional Hazards Regression Modelling was performed to generate hazard ratios as a measure of effect of a covariate on risk to survival, and to also measure whether covariates within the model are significant predictors of survival.

Cox models for OS and SPP, were generated using the following covariates: age at diagnosis, as a continuous variable, grade, stage, histology and risk of progression as factor variables, *F13A1* SNPs: 103G>T (Val34Leu), 1694C>T (Pro564Leu) and haplotypes of codons 650 and 651 as the respective SNPs within these two codons are in complete linkage disequilibrium with one another, and the staining levels for T, TS and S cores (set as categories of negative, lower and higher expression, as performed in the Kaplan-Meier analysis). The number of patients taken into this model was only 91, as only covariates for which there are no missing data points can be used in Cox modelling. Histology was tested as serous histology vs other histologies, as the numbers within each category for histologies other than serous were very small. The baseline in the model was set: grade 1 and 2, FIGO Stage I, Serous histology, those not at high risk of progression, wildtype at SNP sites and negative for each staining category, demonstrated by a hazard ratio (HR) of 1.00.

5.6.1 Progression-Free Survival

In a Cox Proportional Hazards Regression Model (CPHRM) for PFS, age at diagnosis, stage, and risk of progression were all significant predictors of experiencing a progression event, (Table 5-9). Those at high risk of progression were defined as those with either Stage IIIC/IV disease, >1 cm of tumour margin remaining after surgical resection, or where surgery was not possible. With regard to *F13A1* SNPs, carriers of the alternative T-allele at 1694C>T (Pro564Leu), were 2.6 times more likely to have their disease progress (HR=2/59, p=0.006, 95% CIs: 1.27-4.16), (Table 5-9). Double carriage of the SNPs within codons 650 and 651 were significantly protective against progression (HR=0.26, p=0.019, 95% CIs: 0.09-0.80). However, the small number of patients within the double carriage group (n=10) may not result in an accurate reflection of these SNPs' contribution to PFS, as this double carriage analysis for PFS in multivariate modelling in the full translational cohort (n=56/448), although presented a lower hazard ratio, it was not significant.

Table 5-9: Results of a Cox Proportional Hazards Regression Model for Progression-Free Survival

Progression-Free Survival (n=91)								
Covariate/Predictor		n	HR	Std. Error	p-value	Sig	95% CIs	
							Lower	Upper
Age at Diagnosis	57 (24-76)	91	1.06	0.02	0.001	**	1.02	1.09
Grade	1+2	16	1.00					
	3	75	1.01	0.47	0.989	ns	0.40	2.51
FIGO Stage	I+II	19	1.00					
	III+IV	72	10.29	6.27	<0.001	***	3.11	34.00
Histology	Serous	64	1.00					
	Other Histologies	27	1.84	0.63	0.074	ns	0.94	3.59
At High Risk of Progression	No	55	1.00					
	Yes	36	2.59	0.82	0.002	**	1.40	4.81
Val34Leu	VV	55	1.00					
	VL/LL	36	0.60	0.20	0.131	ns	0.31	1.16
Pro564Leu	PP	61	1.00					
	PL/LL	30	2.30	0.70	0.006	**	1.27	4.16
650+651 Haplotypes	VV + EE	64	1.00					
	VV+ EQ/QQ	17	0.70	0.26	0.327	ns	0.34	1.44
	VI/II + EQ/QQ	10	0.26	0.15	0.019	*	0.09	0.80
Tumour FXIIIA Staining	Negative	62	1.00					
	Lower (Q1+Q2)	14	3.70	1.90	0.011	*	1.35	10.12
	Higher (Q3+Q4)	15	1.57	0.79	0.371	ns	0.58	4.23
Tumour/Stroma FXIIIA Staining	Negative	48	1.00					
	Lower (Q1+Q2)	20	0.35	0.16	0.020	*	0.14	0.85
	Higher (Q3+Q4)	23	0.56	0.25	0.198	ns	0.23	1.35
Stroma FXIIIA Staining	Negative	30	1.00					
	Lower (Q1+Q2)	35	1.73	0.68	0.161	ns	0.80	3.74
	Higher (Q3+Q4)	26	2.88	1.18	0.010	*	1.29	6.42

A Cox Proportional Hazards Regression Model was run with the covariates listed in the first column, to test how the covariates influenced risk of experiencing a progression event and whether the covariate was a significant predictor of good or poor progression-free survival (PFS). The total number of patients used in the model was 91, as no data points can be missing from covariates placed into the model. These 91 patients were the patients who had a core taken for each of the tissue types for the tissue microarrays (tumour, tumour/stroma and stroma). The number of patients in each category is given in column 3 (n). A hazard ratio >1 indicates an increased risk of experiencing a progression event, compared to baseline (HR=1.00). A hazard ratio < indicates a decreased risk of experiencing a progression event, compared to baseline. Abbreviations: Hazard Ratio (HR), Standard Error (Std. Error), Level of Significance (Sig.), 95% Confidence Intervals (95% CIs), International Federation of Gynaecology and Obstetrics (FIGO), Valine (V), Leucine (L), Proline (P), Isoleucine(I), Glutamic Acid (E) to Glutamine (Q), Quartiles 1-4 (Q1-Q4).

In terms of FXIIIA Staining, when compared to the baseline of negative staining, lower staining in the OC Tumour, and positive staining in the OC Stroma (regardless of level) resulted in a significantly higher risk of disease progression, (Table 5-9). Hazard ratios increased as levels of FXIIIA staining in the stroma increased (HR=1.00, negative, HR=1.78, lower levels, and HR=2.88, higher levels). Conversely, positive staining in the tumour/stroma cores was significantly protective from progression but only significantly protective at the lower levels of FXIIIA staining.

5.6.2 Survival Post-Progression

In survival post-progression multivariate analysis, only 57 patients were used in the Cox Model as of the 91 patients who had stained data for each tissue type, only 57 progressed. Age at diagnosis and stage of disease were significant predictors of death following a progression event. Histology and grade were not significant predictors, (Table 5-10). None of the *F13A1* polymorphisms were significant predictors of SPP.

Echoing the findings for PFS, lower levels of staining within the tumour cores resulted in a very high and significant risk of death post-progression (HR=15.36, p=<0.001, 4.41-53.54). High levels of OC TS core staining for FXIIIA appeared protective (HR=0.31, p=0.039, 95% CIs: 0.10-0.94). Positive stroma FXIIIA staining resulted in poorer prognosis for SPP, with risk increasing with increasing levels of FXIIIA staining.

5.6.3 Overall Survival

Age at diagnosis, stage of disease and histology were all significant predictors of poorer prognosis in terms of overall survival (OS), (Table 5-11). None of the *F13A1* SNPs were significant predictors of prognosis in this smaller group of ICON7 translational patients, however, as seen in the full translational cohort analysis (n=448, Chapter 4), Leu-carriers at Val34Leu were more likely to survive compared to wildtype patients (HR=0.88, Table 5-11). The benefit of double carriage at codons 650 and 651, like in PFS and SPP, appeared beneficial to OS, but not to a significant extent. Matching the PFS and SPP survival intervals, the directionality of the hazard ratios and the significance of FXIIIA staining levels as predictors of prognosis were the same for OS for T and S cores.

Table 5-10: Results of a Cox Proportional Hazards Regression Model for Survival Post-Progression

Survival Post-Progression (n=57)								
Covariate/Predictor		n	HR	Std. Error	p-value	Sig	95% CIs	
							Lower	Upper
Age at Diagnosis	57 (24-76)	57	1.08	0.03	0.002	**	1.03	1.14
Grade	1+2	7	1.00					
	3	50	0.36	0.22	0.101	ns	0.11	1.22
FIGO Stage	I+II	4	1.00					
	III+IV	53	4.49	3.96	0.088	ns	0.80	25.24
Histology	Serous	35	1.00					
	Other Histologies	22	1.24	0.50	0.599	ns	0.56	2.75
At High Risk of Progression	No	29	1.00					
	Yes	28	0.75	0.31	0.485	ns	0.34	1.67
Val34Leu	VV	36	1.00					
	VL/LL	21	0.88	0.36	0.757	ns	0.40	1.96
Pro564Leu	PP	35	1.00					
	PL/LL	22	0.84	0.34	0.663	ns	0.38	1.86
650+651 Haplotypes	VV + EE	38	1.00					
	VV+ EQ/QQ	14	0.59	0.27	0.257	ns	0.24	1.47
	VI/II + EQ/QQ	5	0.28	0.23	0.124	ns	0.06	1.42
Tumour FXIIIA Staining	Negative	38	1.00					
	Lower (Q1+Q2)	9	15.36	9.78	<0.001	***	4.41	53.54
	Higher (Q3+Q4)	10	1.06	0.80	0.940	ns	0.24	4.69
Tumour/Stroma FXIIIA Staining	Negative	32	1.00					
	Lower (Q1+Q2)	8	1.05	0.71	0.944	ns	0.28	3.95
	Higher (Q3+Q4)	17	0.31	0.18	0.039	*	0.10	0.94
Stroma FXIIIA Staining	Negative	17	1.00					
	Lower (Q1+Q2)	24	3.44	1.72	0.013	*	1.29	9.16
	Higher (Q3+Q4)	16	7.13	4.01	<0.001	***	2.36	21.50

A Cox Proportional Hazards Regression Model was run with the covariates listed in the first column, to test how the covariates influenced risk of death following a progression event and whether the covariate was a significant predictor of good or poor survival post-progression (SPP). The total number of patients used in the model was 57, as no data points can be missing from covariates placed into the model and only those who progressed were included as the survival interval is measuring survival after experience of a progression event. These 57 patients were the patients who had a core taken for each of the tissue types for the tissue microarrays (tumour, tumour/stroma and stroma), and one patient was discounted as they had an SPP of 0 years. The number of patients in each category is given in column 3 (n). A hazard ratio >1 indicates an increased risk of experiencing death following a progression event, compared to baseline (HR=1.00). A hazard ratio < indicates a decreased risk of experiencing death following a progression event, compared to baseline. Abbreviations: Hazard Ratio (HR), Standard Error (Std. Error), Level of Significance (Sig.), 95% Confidence Intervals (95% CIs), International Federation of Gynaecology and Obstetrics (FIGO), Valine (V), Leucine (L), Proline (P), Isoleucine (I), Glutamic Acid (E) to Glutamine (Q), Quartiles 1-4 (Q1-Q4).

Table 5-11: Results of a Cox Proportional Hazards Regression Model for Overall Survival

Overall Survival (n=91)								
Covariate/Predictor		**n**	**HR**	**Std. Error**	**p-value**	**Sig**	**95% CIs**	
Age at Diagnosis	57 (24-76)	91	1.09	0.02	<0.001	***	1.04	1.13
Grade	1+2	16	1.00					
	3	75	0.48	0.27	0.189	ns	0.16	1.44
FIGO Stage	I+II	19	1.00					
	III+IV	72	28.51	25.79	<0.001	***	4.84	167.89
Histology	Serous	64	1.00					
	Other Histologies	27	2.49	0.99	0.021	***	1.15	5.42
At High Risk of Progression	No	55	1.00					
	Yes	36	1.51	0.57	0.267	ns	0.73	3.15
Val34Leu	VV	55	1.00					
	VL/LL	36	0.59	0.23	0.169	ns	0.28	1.25
Pro564Leu	PP	61	1.00					
	PL/LL	30	1.32	0.48	0.455	ns	0.64	2.70
650+651 Haplotypes	VV + EE	64	1.00					
	VV+ EQ/QQ	17	0.73	0.32	0.475	ns	0.31	1.73
	VI/II + EQ/QQ	10	0.34	0.21	0.087	ns	0.10	1.17
Tumour FXIIIA Staining	Negative	62	1.00					
	Lower (Q1+Q2)	14	14.12	8.73	<0.001	***	4.20	47.46
	Higher (Q3+Q4)	15	1.60	1.09	0.486	ns	0.42	6.05
Tumour/Stroma FXIIIA Staining	Negative	48	1.00					
	Lower (Q1+Q2)	20	0.41	0.22	0.102	ns	0.14	1.19
	Higher (Q3+Q4)	23	0.27	0.14	0.015	*	0.09	0.77
Stroma FXIIIA Staining	Negative	30	1.00					
	Lower (Q1+Q2)	35	2.33	1.09	0.070	ns	0.93	5.81
	Higher (Q3+Q4)	26	4.73	2.38	0.002	**	1.76	12.68

A Cox Proportional Hazards Regression Model was run with the covariates listed in the first column, to test how the covariates influenced risk of death and whether the covariate was a significant predictor of good or poor overall survival (OS). The total number of patients used in the model was 90, as no data points can be missing from covariates placed into the model. These 91 patients were the patients who had a core taken for each of the tissue types for the tissue microarrays (tumour, tumour/stroma and stroma. The number of patients in each category is given in column 3 (n). A hazard ratio >1 indicates an increased risk of death, compared to baseline (HR=1.00). A hazard ratio < indicates a decreased risk of death, compared to baseline. Abbreviations: Hazard Ratio (HR), Standard Error (Std. Error), Level of Significance (Sig.), 95% Confidence Intervals (95% CIs), International Federation of Gynaecology and Obstetrics (FIGO), Valine (V), Leucine (L), Proline (P), Isoleucine (I), Glutamic Acid (E) to Glutamine (Q), Quartiles 1-4 (Q1-Q4).

Low levels of FXIIIA staining in T cores are detrimental to OS, as is positive staining within the S cores (all HRs >1). Higher levels of staining within the TS are significantly protective (HR=0.27, p=0.015, 95% CIs: 0.09-0.77).

5.6.4 Summary of Multivariate Survival Analyses

For all three survival intervals investigated, PFS, SPP and OS, low levels of FXIIIA staining within the OC Tumour cores led to a poorer prognosis for patients. Positive staining in the Stroma was also detrimental to survival. CPHRMs were also run with Leu-carriers as the baseline covariate, given the results identified in univariate survival analysis, and the direction and significant of the hazard ratios did not change (data not shown). It appeared therefore, that regardless of Val34Leu genotype, when all other covariates which are associated with OC were taken into account, stroma staining was still an indicator of poor prognosis, and the reasons why this may be remained to be explored.

5.7 Co-localisation of FXIIIA with other Key Proteins

A small cohort of frozen ovarian cancer samples was provided by the Leeds Tissue Bank (n=10) in order to assess the levels of co-localisation between FXIIIA and other key proteins which may be associated with the cross-linking via the transglutaminase activity of FXIIIA. These proteins included: transglutaminase-2 (TGM2), another transglutaminase which is also able to crosslink matrices, fibrinogen which is one of the substrates which is crosslinked by FXIIIA and increased levels of fibrinogen have been found in ovarian cancer (260). FXIIIA crosslinks monomers through the formation of isopeptide bonds, so these were also stained for in the tumour tissues.

The main aim for this portion of the study was to see whether the role of FXIIIA could be further elucidated through its relationships with other proteins *in situ* in OC tissues. It was hypothesised that if FXIIIA is co-localised with one of its main substrates (fibrinogen) and the product of its transglutaminase activity (isopeptide bonds), then this may be indicative of a role for FXIIIA in the extracellular matrix as the major cross-linker which may be influencing cancer behaviour or maintenance. However, if FXIIIA was not found to be co-localised with these proteins, this would suggest that FXIIIA may be exerting an alternative role in OC.

By testing for the presence of an alternative transglutaminase in OC, then the crosslinking of tumour matrices in ovarian cancer may instead be attributed to TGM2 instead. Antibodies against the proteins of interest were worked up in control tissues (Figure 5-L) and run with appropriate controls in every staining run.

5.7.1 Summary of Immunofluorescence Findings

Working with frozen tissues of varying age and quality proved to be challenging, and as a result, immunofluorescence results were limited. FXIIIA and TGM2 were not highly expressed in the OC tissues, but evidence of multiple layers of cells from sectioning and high background proved problematic. From the small number of sections which were in good condition and analysed, there was no evidence of co-localisation between FXIIIA and its substrate fibrinogen or its product, isopeptide bonds, (Figure 5-M). TGM2 was expressed in OC at low levels, but not in the same location as FXIIIA and did not appear to co-localise with fibrinogen. However, many questions are raised regarding whether co-localisation would be expected as it is not known exactly how long either transglutaminase remains at the site of its cross-linking. Some FXIIIA in plasma circulates bound to fibrinogen, but the study in these tissues meant that this co-localisation was not seen.

The staining of the isopeptide antibody also raised concerns regarding its specificity. The antibody was demonstrated to specifically bind to isopeptide bonds generated *in vitro* and this was supported in the literature. However, further exploration of the literature identified that both of the available antibodies for isopeptide bonds were found to bind to acetylated lysine *in vitro*. Acetylated lysine is found within the nuclei, and the strong co-localisation between the nuclear DAPI stain and the ‘isopeptide’ staining led to strong concerns over the suitability of this antibody. Tests for specificity to acetylated lysine was not undertaken for this antibody in the interests of time and the scope of the project, but this work would have been valuable. Due to the concerns raised, this antibody was not used as evidence of isopeptide bonds, and was limited to its ability to co-localise with DAPI and provide good contrast for any positive green immunofluorescences for FXIIIA, TGM2 or fibrinogen.

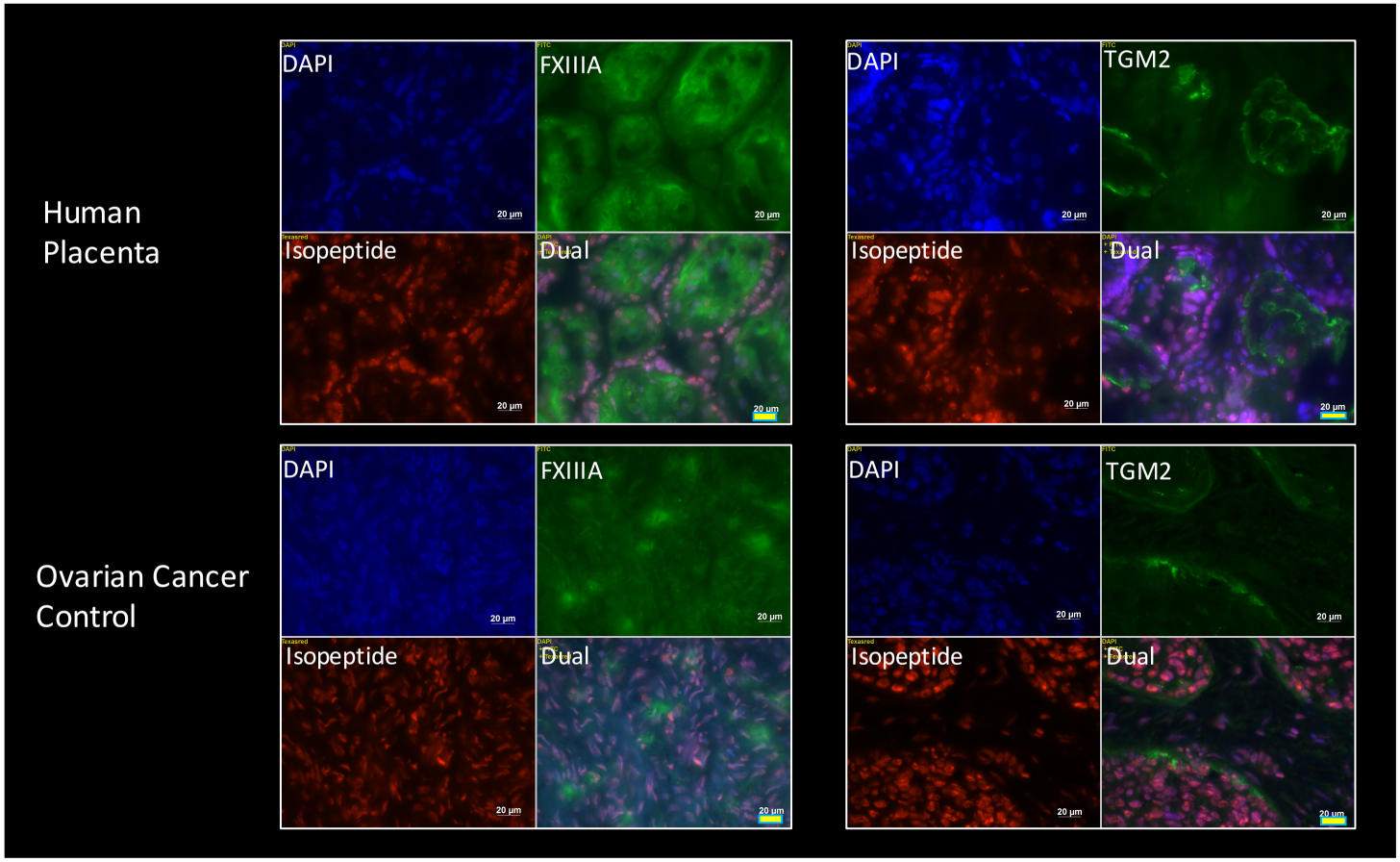

Figure 5-L: Representative Immunofluorescence Staining in Control tissues for work up of antibodies for co-localisation investigation. Staining for FXIIIA was detected with Alexafluor-conjugated goat anti-rabbit AF488 and a FITC emission filter. Staining for isopeptide bonds detected with AlexaFluor-conjugated goat anti-mouse AF594 and a TexasRed emission filter. DAPI stain for nuclei detected with a DAPI emission filter. Top left: human placenta stained for FXIIIA and Isopeptide bonds and nuclei counterstained with DAPI. Top right: human placenta stained for transglutaminase 2 (TGM2) and isopeptide bonds and nuclei counterstained with DAPI. Bottom left: ovarian cancer tissue stained for FXIIIA and isopeptide bonds, with nudei counterstained with DAPI. Bottom right: ovarian cancer tissue stain with for TGM2 and isopeptide bonds. Appropriate no primary controls were run with each staining run. Yellow scale bar = 20 µm. Images acquired with a 63X oil magnification lens.

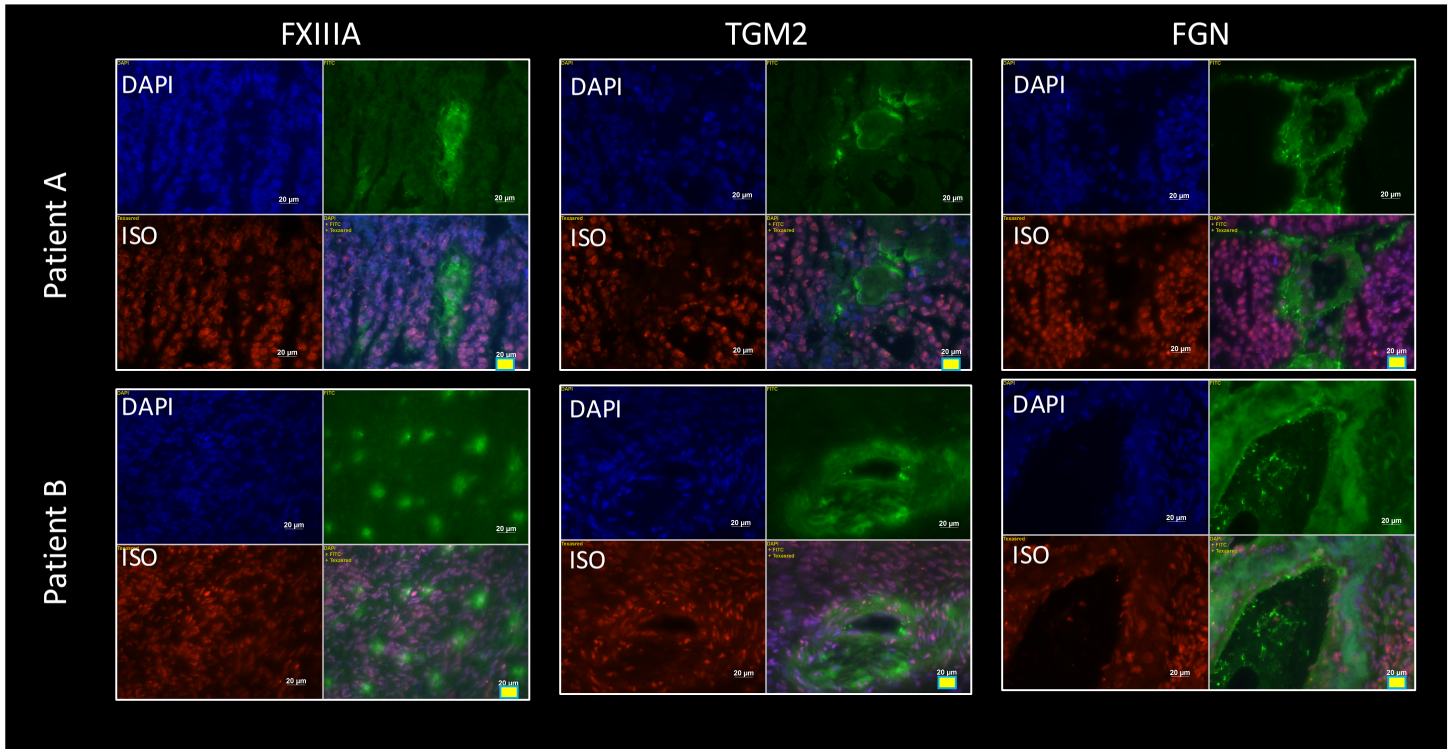

Figure 5-M: Representative Immunofluorescence Staining of OC tissues for two patients. Co-localisation investigation of FXIIIA, transglutaminase-2 and fibrinogen with isopeptide bonds. Staining for FXIIIA, TGM2 and fibrinogen was detected with AlexaFluor-conjugated goat anti-rabbit AF488 and a FITC emission filter. Staining for isopeptide bonds detected with AlexaFluor-conjugated goat anti-mouse AF594 and a TexasRed emission filter. DAPI stain for nuclei detected with a DAPI emission filter. Top set of images are from Patient A and bottom set of images are from Patient B. Yellow scale bar = 20 µm. Images acquired with a 63X oil magnification lens.

5.8 Summary of Results

- In CSIOVDB: highest *F13A1* mRNA expression was found in OC stroma and was significantly higher than expression in normal stroma ($p<0.001$) and OC tumour tissue ($p<0.001$).
- *F13A1* mRNA expression was highest in the Mesenchymal OC subtype ($p<0.0001$) and an increase was also seen in epithelial mesenchymal transitioning (EMT). Stroma is more mesenchymal in nature and these results support the high mRNA expression seen in OC stroma.
- In OC tissue microarrays, the highest average % positivity for staining was seen in OC stroma tissue. There was a significant difference in distribution of staining levels in OC stroma (S), with significantly higher levels compared to tissue containing tumour only (T) or tumour and stroma (TS) ($p<0.0001$ and $p<0.01$, respectively, Kruskal-Wallis Test).
- The *F13A1* SNP 103G>T was significantly associated with TS and S staining categories. Carriers of the alternative allele for Leu had a greater percentage of positive staining for both tissue types.
- In univariate analysis, in Stroma cores, for Leu-carriers, positive FXIIIA staining resulted in a benefit to SPP and OS. For wildtype patients, positive FXIIIA staining was detrimental to SPP and OS.
- In multivariate analysis where all other covariates were taken into account positive stroma staining was always detrimental to survival, whereas tumour/stroma positive staining appeared protective. Leu carriage at Val34Leu (103G>T) was not a significant predictor of survival in the models.
- A small study of co-localisation between FXIIIA protein, and other important proteins such as fibrinogen (a crosslinking substrate), TGM2 (another transglutaminase) and isopeptide bonds (product) did not find evidence of co-localisation of FXIIIA with these other protein, although tissue quality and isopeptide antibody specificity limited this work.

5.9 Brief Discussion

A major gap was waiting to be explored with regard to analysis of FXIIIA expression in ovarian cancer tissues, and this chapter presents work which aimed to fill this gap. Previous work identified differences in plasma levels of FXIIIA between healthy, benign and metastatic disease (221), however the small size of the cohort and age of the work in light of today's current methods meant that this foundation could be built upon. An assessment of *F13A1* gene expression in the CSIOVDB database identified that *F13A1* mRNA was most highly expressed in ovarian cancer stroma, and that mRNA expression was decreased in tumour tissue when compared to normal epithelium. Expression of *F13A1* mRNA in the stroma may be a result from FXIII producing cells within the stroma such as monocytes/macrophages or fibroblasts. A significant decrease in *F13A1* expression was also identified in more metastatic disease (higher stage and grade) compared to early stage, low grade disease. The decrease in gene expression when compared to normal epithelium was also of interest as this mimics the findings of van Wersch and colleagues, in which plasma levels of FXIIIA which were lower in metastatic compared to non-metastatic disease (221).

The highest average percentage positivity of FXIIIA staining was found in stroma cores (S), with the lowest levels in tumour cores (T) and the average percentage positivity for tumour/stroma (TS) cores sitting in between these averages. This result further supports the findings within the mRNA database that the highest mRNA levels are in OC stroma and the lowest in tumour tissue. In general, negative staining resulted in a higher median survival. One of the main differences was found in terms of OS and SPP and stroma staining, with carriers of the alternative Leu allele for polymorphism Val34Leu benefitting over wildtype patients, but this was the opposite in tumour/stroma cores, suggesting an alternative role for FXIIIA in OC depending on its precise staining locality, and this requires further exploration.

In multivariate modelling, low levels of FXIIIA within the tumour and any degree of stroma FXIIIA staining resulted in poorer prognosis. However, tumour/stroma staining appeared protective in terms of prognosis. This finding is confusing and raises more questions than answers in this instance. The staining for FXIIIA did not appear to be in the cancer cells themselves, but rather in stromal cells, and

in intra-tumour stromal regions. The role FXIIIA may be having in the stroma remains unclear, and has not been directly answered in this piece of work. FXIIIA may be acting as a crosslinker of the extracellular matrix, and altering the composition and stiffness of the tumour microenvironment, or perhaps exerting its role in the immune response through expression in macrophage cells present within the tumour microenvironment. As staining for crosslinking and immune cell staining was not performed, this could be an excellent piece of future work. Due to the differential outcomes depending on FXIIIA staining locality particularly in tumour/stroma cores and stroma only cores, the way in which FXIIIA interacts with the stroma would be the next step in understanding the role of FXIIIA in OC.

Chapter 6: The Differential Effect of FXIIIA Val34Leu variants on Angiogenesis

6.1 Introduction

The previous chapter demonstrated that FXIIIA expression in OC tissues is found within the stroma within tumours and surrounding tumours. The source of FXIIIA within these tissues was unlikely to be from blood plasma, as tissue is perfused prior to fixation, so staining seen was mostly likely from cells which express FXIIIA such as fibroblasts and cells of monocytic origin (129,261,262) . Staining within the stroma proved detrimental to survival whilst staining within the tumour/stroma regions was found to be beneficial to survival. Although the role of single nucleotide polymorphisms in the gene for FXIIIA, *F13A1*, has been the main focus of the thesis so far, when SNPs were taken into account with respect to all staining and other prognostic factors in multivariate modelling, SNPs did not significantly influence survival. The SNP, 103G>T (Val34Leu) was associated with tumour/stroma and stroma staining in univariate analysis, and exploration of univariate survival analysis did demonstrate that in terms of both overall survival and survival post-progression, carriers of the alternative Leu-allele, had a better prognosis compared to their wildtype counterparts. However, multivariate analysis, taking into account OC prognostic factors and *F13A1* SNPs indicated that FXIIIA staining in OC stroma was detrimental to survival. Yet, the clear differences in SPP and OS for Leu-variants at V34L sparked questions about the role of FXIIIA in the OC stroma.

The staining results and effects on survival were confusing and presented more questions, and it was clear that FXIIIA may have a differential effect on OC survival depending on where it was located. The association of staining locality with Val34Leu in univariate analysis , also raised some interesting questions due to this mutation being associated with higher transglutaminase activity and tighter fibrin matrices. The transglutaminase activity of FXIIIA results in isopeptide bond crosslinking of matrix-associated proteins, so it may mean that FXIIIA has a role in tumour matrix formation which ultimately leads to either metastatic progression or presents a challenge to therapeutics, due to the poor prognosis identified at high staining levels in multivariate analysis. A benefit to survival within cores in which both OC tumour tissue and OC stroma tissue are present is suggestive of

a role of FXIIIA in tumour crosstalk with its environment that either makes therapy more effective or limits tumour growth. In univariate analysis, Leu-carriers survived for longer when stroma staining was present, so how is this variant influencing the tumour microenvironment to either a) make therapy more effective or b) limit tumour growth and metastasis? One way in which FXIIIA could be interacting with tumours and the microenvironment is through its role in angiogenesis.

Angiogenesis is the recruitment of existing blood vessels to a new site, and with regard to cancer, tumours express pro-angiogenic and pro-growth factors to assist in its growth (263), (Figure 6-A). Without a blood supply, a tumour is unable to undergo expansion as it lacks receipt of oxygen and nutrients. However, once a blood supply is in place, tumours are able to rapidly grow and due to the chaotic nature of the recruited blood supply, the centre of tumours become hypoxic due to a lack of oxygen. The transglutaminase activity is vital for angiogenic signalling as FXIIIA crosslinks the b3 integrin of the alpha5-beta3 integin (αvβ3) to vascular endothelial like growth factor-2 (VEGFR2) (184,187). This crosslinking action promotes angiogenic signalling through upregulation of proteins such as Wilm's Tumour-1 (WT-1) and downregulation of thrombopsonidn-1 (TSP-1), a "brake" on proangiogenic signalling which is removed, allowing for subsequent signalling. FXIIIA has already been established as important for angiogenic signalling in both *in vitro* and *in vivo* environments, although it is not necessary for signalling directly as VEGFA is able to stimulate angiogenesis more rapidly on its own. The presence of FXIIIA as a crosslinker of the b3 integrin to the VEGFR2 receptor was demonstrated to result in sustained angiogenic signalling meaning FXIIIA could be important in the maintenance of pro-angiogenic signalling rather than as a fundamental requirement for angiogenesis (187) (Figure 6-B). The Val34Leu SNP has already been associated with higher transglutaminase activity which forms more densely crosslinked networks, and this SNPs is associated with thrombotic disease. Could this SNP also contribute to changes in the role of FXIIIA in angiogenesis, and could this effect ultimately be the cause of the differential response of patients when FXIIIA is present in ovarian cancer stroma?

There are two possible hypotheses which will be addressed in this chapter: 1) Leu-carriers have a benefit to their OS and SPP because these variants have a

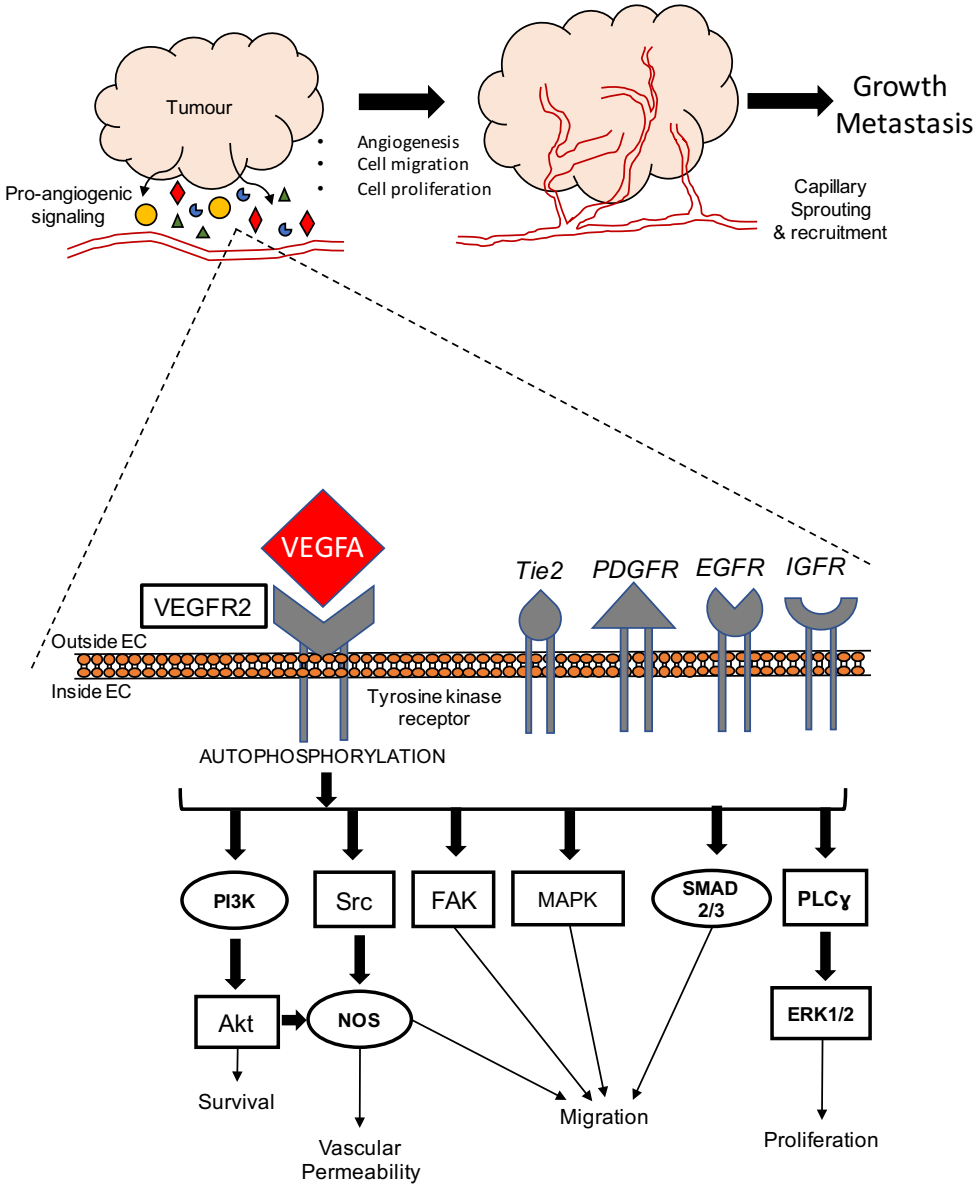

Figure 6-A: Schematic representation of tumour recruitment of a blood supply and a simplified view of key members of the angiogenic signalling cascade. Tumours produce pro-angiogenic factors such as vascular endothelial like growth factor A (VEGFA) in order to recruit a blood supply to the growing tumour mass. A blood supply is vital of the delivery of oxygen and nutrients to support the expanding tumour. VEGFA binds to the tyrosine kinase receptor vascular endothelial like growth factor receptor 2 (VEGFR2), resulting in autophosphorylation of the receptor and promotion of angiogenic signalling which comprises vascular permeability, survival, proliferation and migration. Other tyrosine kinase receptor signalling feeds into the same pathway as VEGFR2. Adapted from Cell Signalling Technologies Angiogenesis Poster (https://www.cellsignal.co.uk/contents/science-cst-pathways-developmental-biology/angiogenesis/pathways-angiogenesis). Abbreviations: Protein Kinase B (Akt), phosphoinositide 3-kinase (PI3K), proto-oncogene tyrosine-protein kinase Src (Src), nitric oxide synthase (NOS), focal adhesion protein (FAK), mitogen-activated protein kinase (MAPK), transforming growth factor-beta superfamily member (SMAD), phosphoinositide phospholipase C-gamma (PLC-Y), extracellular signal-regulated kinases (ERK), angiopoietin-1 receptor (Tie2), platelet-derived growth factor receptor (PDGFR), epidermal growth factor receptor (EGFR), insulin-like growth factor receptor (IGFR).

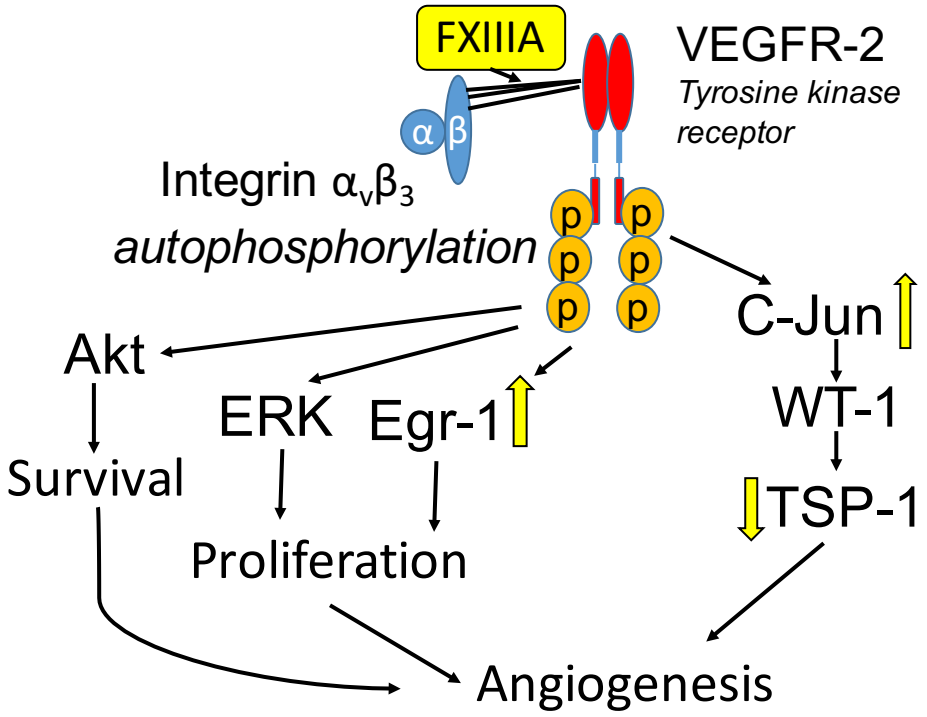

Figure 6-B: The role of Factor XIIIA in angiogenic signalling. The active transglutaminase, Factor XIIIA (FXIIIA) crosslinks the beta-3 portion of the alpha-5-beta-3 integrin (αvβ3), which is necessary for cell proliferation and migration, to the vascular endothelial like growth factor receptor-2 (VEGFR2) which is a tyrosine kinase. Binding of vascular like growth factor-A (VEGFA) to VEGFR2 promotes pro-survival, proliferative and pro-angiogenic signalling. FXIIIA crosslinking is not mandatory for VEGFA binding or for angiogenic signalling to occur, but the presence of FXIIIA appears to maintain the angiogenic signalling for longer than when just VEGFA is present. Crosslinking by FXIIIA appears to upregulate protein expression of early growth response protein-1 (Egr-1) and the proto-oncogene cellular homolog of the viral oncoprotein v-jun (C-Jun). C-Jun is able to signal for angiogenesis through expression of Wilm's tumour protein-1 (WT-1) which results in downregulation of thrombospondin-1 (TSP-1), an inhibitor of angiogenesis. Abbreviations: protein kinase B (Akt) and extra-cellular regulated kinases (ERK). Adapted from Dardik *et al.* 2005 and 2006 (186,187).

negative impact on angiogenesis, meaning the tumour cannot recruit an effective blood supply to sustain tumour development, or 2) Leu variants benefit in terms of survival because the variants improve/increase the angiogenic signalling

resulting in a potentially better delivery of chemotherapeutic agents to the tumour site. Therefore, experiments were set up to test how FXIIIA variants influence angiogenesis, with endothelial tube formation being used as a measure of angiogenesis. Depending on which hypothesis is supported, further hypotheses can then be drawn on the mechanism of action i.e. are FXIIIA V34L variants affecting signalling, and if so, how? Can any differences in signalling be potentially linked to what is demonstrated in the clinical data?

6.2 Developing a Thin Layer Angiogenesis Protocol for HUVEC endothelial tube formation

In order to make the experiments as economical as possible, a protocol was optimised to maximise the use of basement matrix and solutions, whilst ensuring endothelial tube formation could still occur and be measured. A thin layer angiogenesis protocol was developed by Faulkner and colleagues that used as little as 2 µl of basement matrix in wells of a 96 well plate (231). The spreading of such a small volume of basement matrix, and the challenge of maintaining ice-cold conditions within a sterile laminar flow hood meant that the volume was increased to 5 µl per well, with the aim of application to the very centre of the well. Very minimal spreading was used, but when necessary, the matrix was spread using a sterile insert of an Eppendorf Combi-Tip, as described by Faulkner *et al.*, in their thin layer angiogenesis protocol. Sterile inserts from smaller Combi-tips could not be used as this resulted in scratching of the bottom of the wells which interfered with imaging and network development. As the experiments which used basement matrix only took place over a maximum of 24 hours, there were no concerns over evaporation, and the condition of the matrix was examined during the experiments. The total volume of reagents within each well was kept to 200 µl.

Endothelial tube formation assays are sensitive and the number of cells plated must be sufficiently low for tube formation, rather than for a monolayer growth, but too low a cell number results in stressed cells and poorly formed, if any, networks. Cell number was checked as part of the thin-layer angiogenesis protocol and 6000 cells per well was chosen as the ideal plating density, (Figure 6-C). Cell numbers >8000 cells per well demonstrated more varied network formation, with 16000 cells per well, resulting in monolayer growth. Cell densities <4000 cells resulted in small networks. Cells were also checked for their response to an angiogenic stimulus, VEGFA (25 ng/mL), (Figure 6-D). At 8000 cells/well, VEGFA stimulation appeared to result in a smaller average network length compared to normal medium. This may have been a result of potential overcrowding of cells. A cell seeding density of 6000 cells was identified as the happy medium required for measurable networks and successful network development.

Once seeding density was established, the ideal concentration of VEGFA stimulation was determined. Within the literature, there is considerable variation in the concentrations of VEGFA used to stimulate HUVEC with the most common concentrations being 10 or 25 ng/mL. The HUVEC were stimulated with a range of VEGFA concentrations and both of these were found to be suitable for the HUVEC (Figure 6-D-A) and resulted in similar sustained cell viability over time (Figure 6-D-B). The concentration of 25 ng/mL was used as this is commonly used in endothelial tube formation assays performed by others (264,265). Bevacizumab, an antibody against all VEGFA isoforms was tested at a 2.6:1 molar ratio for 25 ng/mL and 50 ng/mL of VEGFA, but appeared to decrease cell viability to too great an extent for further use (Figure 6-D-A). Further optimisation would have been required if bevacizumab was to be used in future experiments.

6.3 Val34Leu variants have a differential effect on endothelial tube formation

Given the results from the immunohistochemical staining within ovarian tissues and the available literature regarding FXIIIA as a pro-angiogenic signaller, it was hypothesised that FXIIIA variants for the Val34Leu SNP, had a differential effect on angiogenesis. There are two hypotheses: 1) Leu-carriers have benefit to their OS and SPP because these variants have a negative impact on angiogenesis,

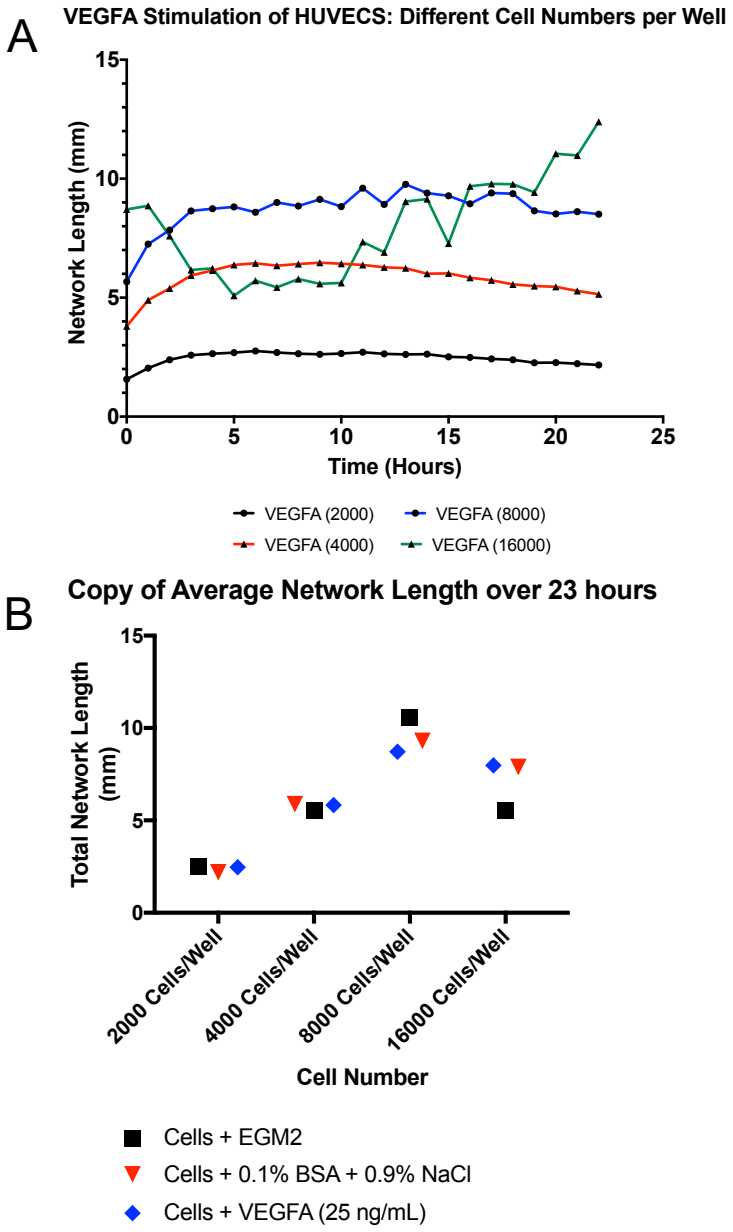

Figure 6-C: Determination of cell seeding density for HUVECs in endothelial tube formation assays on a thin layer of basement matrix. (A) A range of cell seeding densities from 2000-16000 cells per well were seeding onto a thin layer (5 µl) of basement matrix and network formation was measured over 23 hours to determine the ideal concentration of cells which resulted in successful, measurable tube formation and not as a monolayer. (B) The same number of cells densities as in (A) also were tested in the presence of VEGFA at 25 ng/mL as cells should form larger networks in the presence of this stimulation, and average network length over 23 hours was measured. Although the networks did not appear larger on average with VEGFA for the densities measured, the density of 8000 cells resulted in smaller networks with VEGFA stimulation, therefore a lower cell density was required. The density of 16000 cells resulted in more monolayer growth, as shown by the variation in (A) and therefore this density was considered far too high. From these experiments, a seeding density of 6000 cells/well was chosen.

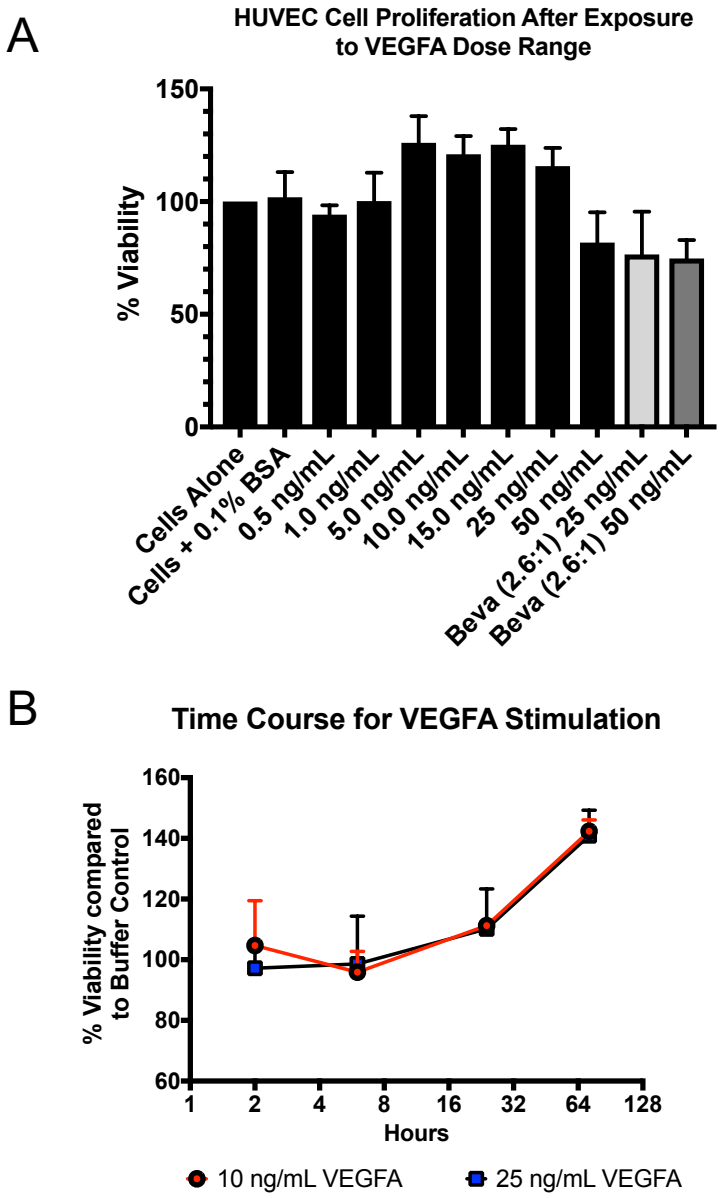

Figure 6-D: Determination of vascular endothelial-like growth factor-A (VEGFA-165) concentration for HUVECs (A) 10000 cells/well were seeded in wells of a 96 well plate and cell proliferation (as a measure of increased cell viability through an MTT assay) was measured after 48 hours, allowing for one cell doubling of HUVEC (which is approximately 32 hours). A range of VEGFA-165 concentrations were tested from 0.5-50 ng/mL. Bevacizumab (Beva) was also tested at a 2.6:1 molar ratio against 25 ng/mL and 50 ng/mL of VEGFA in order to inhibit VEGFA as this drug in a monoclonal antibody against this growth factor. 10-25 ng/mL of VEGFA appeared to give the best response, whilst 50 ng/mL appeared detrimental to survival. Error bars are standard deviation for the mean calculated from triplicate wells (n=1). Bevacizumab also appeared toxic to the cells and therefore it was not used in further experiments. (B) Both 10 and 25 ng/mL of VEGFA were tested in another experiment to measure cell viability, and therefore make inferences on proliferation, over 72 hours. Cell viability was similar for both concentrations of VEGFA and therefore 25 ng/mL was chosen, as this was commonly used in published angiogenesis assays.

meaning the tumour cannot recruit an effective blood supply, or 2) Leu variants benefit in terms of survival because the variants improve/increase the angiogenic signalling resulting in better delivery of chemotherapeutic agents. Therefore, an

experiment was set up to test how FXIIIA variants influence angiogenesis, with endothelial tube formation being used as a measure of angiogenesis.

FXIIIA variants were generated by other Anwar lab members in yeast and recombinant protein was purified and then activated in the presence of thrombin and calcium chloride (see Chapter 2 Materials and Methods for full details). Variants were added to HUVEC in the presence of VEGFA following serum-starvation which to pushed the cells into a more quiescent state. Although not presented with physical data, observation found that without this serum starve, cells did not form endothelial tubes successfully.

In the absence of FXIIIA variants, HUVEC stimulated with VEGFA alone rapidly formed an endothelial tube network which peaked after about 3 hours and then gently declined in size over the following 20 hours, (Figure 6-E-A). In the presence of the wildtype FXIIIA variant (V/V), although the initial rate of formation was slightly slower, the network developed into a larger network which peaked in size around 12 hours. Both Leu-variants (V/L and L/L) responded similarly with average total network lengths being significantly smaller compared to wildtype ($p<0.001$) and VEGFA Alone ($p<0.05$), (Figure 6-E-B).

The initial rates of HUVEC network formation also varied, (Figure 6-E-C). The rate of formation in the presence of both VEGFA and wildtype FXIIIA was similar to that of VEGFA alone, and were not found to be statistically significantly different from one another. The rate of formation in the presence of the heterozygous V34L variant (V/L) was the slowest of the conditions measured, and was significantly less than wildtype and VEGFA alone, but no significant difference was found when compared to the homozygous variant.

The heterozygous and homozygous variants both resulted in significantly smaller networks with lower initial rates of development which is suggestive of the carriage of Leu affecting angiogenesis in both network size, rate of formation and maintenance. Leu-carriers respond better in terms of overall survival when FXIIIA

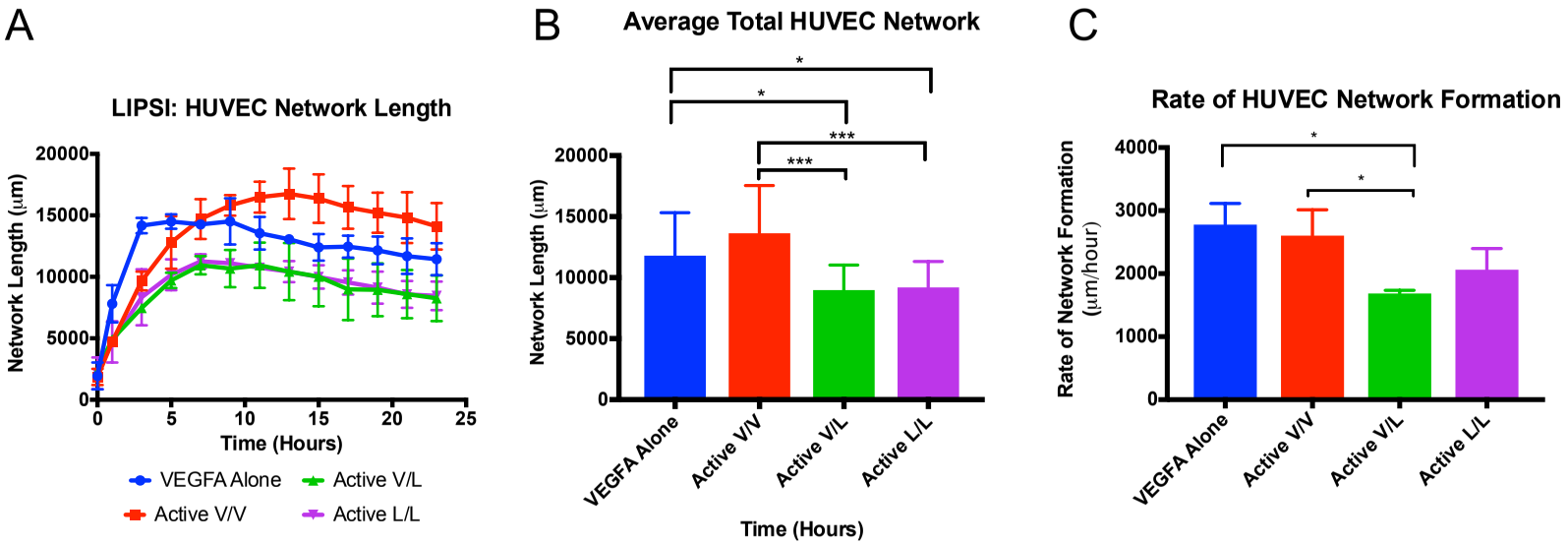

Figure 6-E: Effects of FXIIIA on Endothelial Tube Network Formation using HUVEC. Following serum starvation for 3.5 hours, HUVEC were plated at 6000 cells per well in a 96 well plate on top of 5 µl of basement matrix in the presence of VEGFA-165 (25 ng/mL) or VEGFA plus active FXIIIA from purified recombinant yeast protein. Appropriate buffer controls were run and checked, but data is not presented above. The plate was incubated at 37ºC, 5% CO_2 in a chamber within the Nikon LIPSI live cell imager. (A) Total HUVEC Network Length plotted from hours 0-23 to demonstrate rate of formation, peak network formation and subsequent network decline. Each condition was plated as n=3, and data above are n=2 for VEGFA (due to an imaging issue with the third well) and n=3 for the FXIIIA variants. Error bars represent standard deviation around the mean network length per time point. (B) Average total network length for each condition. Data were non-normally distributed (Shapiro-Wilk test $p<0.01$) and therefore a non-parametric Kruskal-Wallis test was performed. Significant differences in the medians for each condition are reported above the bars, but the bars themselves represent the average network length. There was a strong significant difference in the median network lengths between wildtype (V/V) and Leu-carriers (V/L and L/L) ($p<0.001$. ***). A significant difference was also identified between VEGFA alone in the absence of FXIIIA variants and carriers of Leu, but not for the wildtype FXIIIA variant (V/V), ($p<0.05$, *). (C) Average initial rate of HUVEC endothelial tube network formation in um/hour. Data were normally distributed and therefore a one-way analysis of variance (ANOVA) identified a significantly lower rate of network development for the heterozygous variant (V/L) and VEGFA Alone and the wildtype variant. No significant decrease was identified for the homozygous Leu variant (L/L).

is present in the stroma. Could the presence of Leu mean that tumours are unable to form networks as successfully as wildtype variants?

6.4 Measuring the Active Angiogenic Signalling Axis in HUVECs

The results from the endothelial tube formation assay on the Nikon LIPSI indicated that in the presence of FXIIIA protein and VEGFA, Leu-carriers formed smaller overall networks at a much slower rate compared to wildtype FXIIIA or VEGFA alone. FXIIIA is able to crosslink basement matrices in vitro, due to its transglutaminase activity. Therefore, it was important to test whether the reduction in network formation was due to the nature of the crosslinking of variants, or were the differences seen instead due to a differential effect on the angiogenic signalling cascade.

Due to time constraints, the latter experiment was explored further through a Western Blot for protein expression of angiogenic signalling cascade members from proteins extracted from HUVECs actively undergoing endothelial tube formation. Although FXIIIA has clearly been demonstrated to have a role in angiogenesis, an exploration of the effect of FXIIIA variants on angiogenic signalling is lacking in the literature.

The experiment was scaled up from a 96 well to a 12 well assay in order to increase protein yield for Western Blot analysis. Cells were stimulated as previously described (Chapter 2 Materials and Methods) and checked after 90 minutes to ensure tube formation had begun successfully. Tubes had successfully formed for all conditions, but it appeared that the density of the tubes in the FXIIIA variant wells was lower, but this was purely observational and was not quantified, (Figure 6-F). Proteins were extracted from cells after 5.5 hours of growth, with cells quenched on ice and all tube retrieval occurring on ice for the entire protocol to ensure that proteases and phosphatases would not be active. A western blot run to measure the levels of expression of active angiogenic cascade proteins (phosphorylation of the protein results in activation) in relation to normally growing and serum starved HUVECs. Due to the protein extraction buffer interacting with the protein concentration assay, protein levels could not be measured and therefore maximal protein was loaded per well, (Figure 6-G). Bands were quantified with GAPDH as the loading control and results were

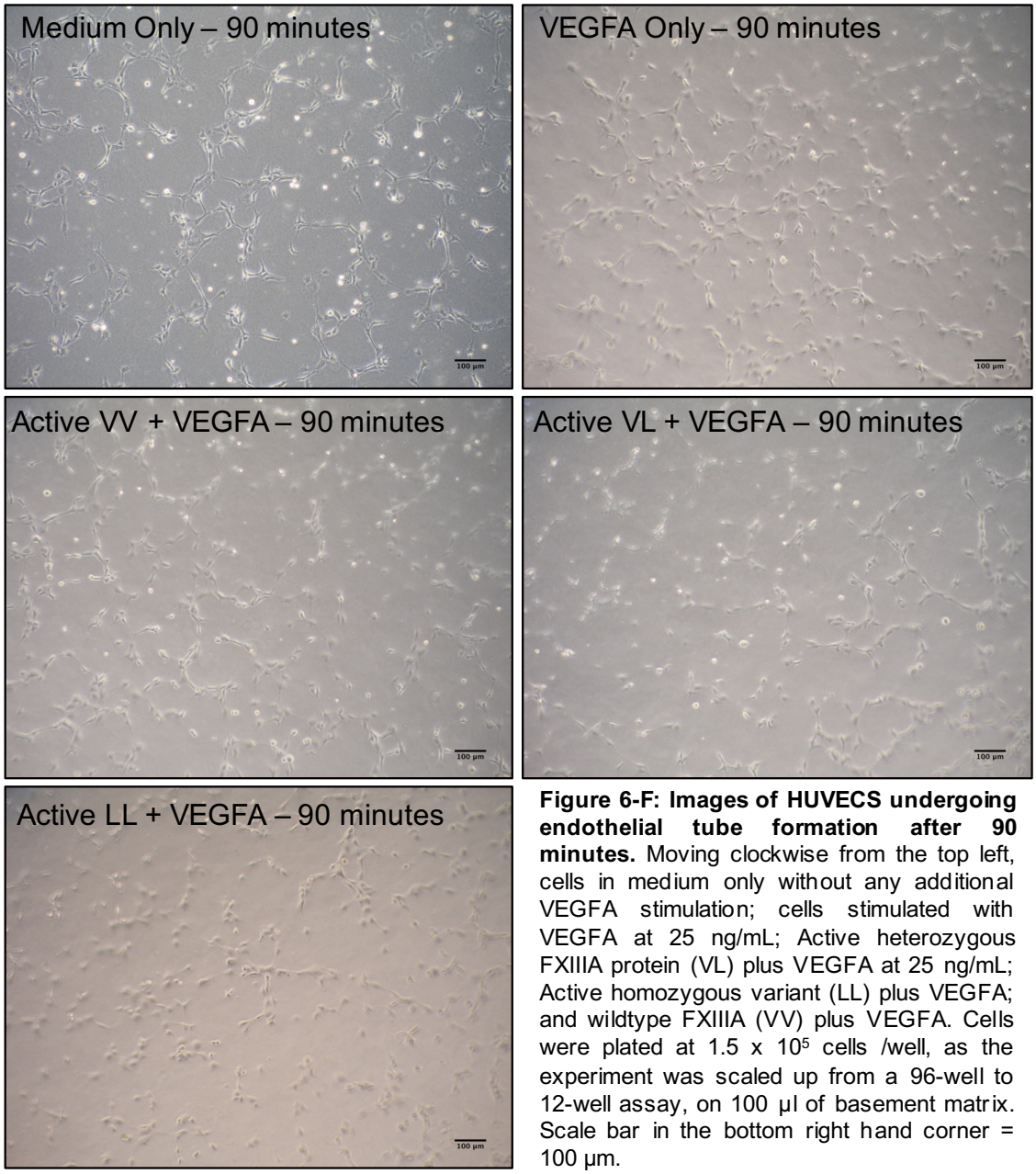

Figure 6-F: Images of HUVECS undergoing endothelial tube formation after 90 minutes. Moving clockwise from the top left, cells in medium only without any additional VEGFA stimulation; cells stimulated with VEGFA at 25 ng/mL; Active heterozygous FXIIIA protein (VL) plus VEGFA at 25 ng/mL; Active homozygous variant (LL) plus VEGFA; and wildtype FXIIIA (VV) plus VEGFA. Cells were plated at 1.5 x 10^5 cells /well, as the experiment was scaled up from a 96-well to 12-well assay, on 100 µl of basement matrix. Scale bar in the bottom right hand corner = 100 µm.

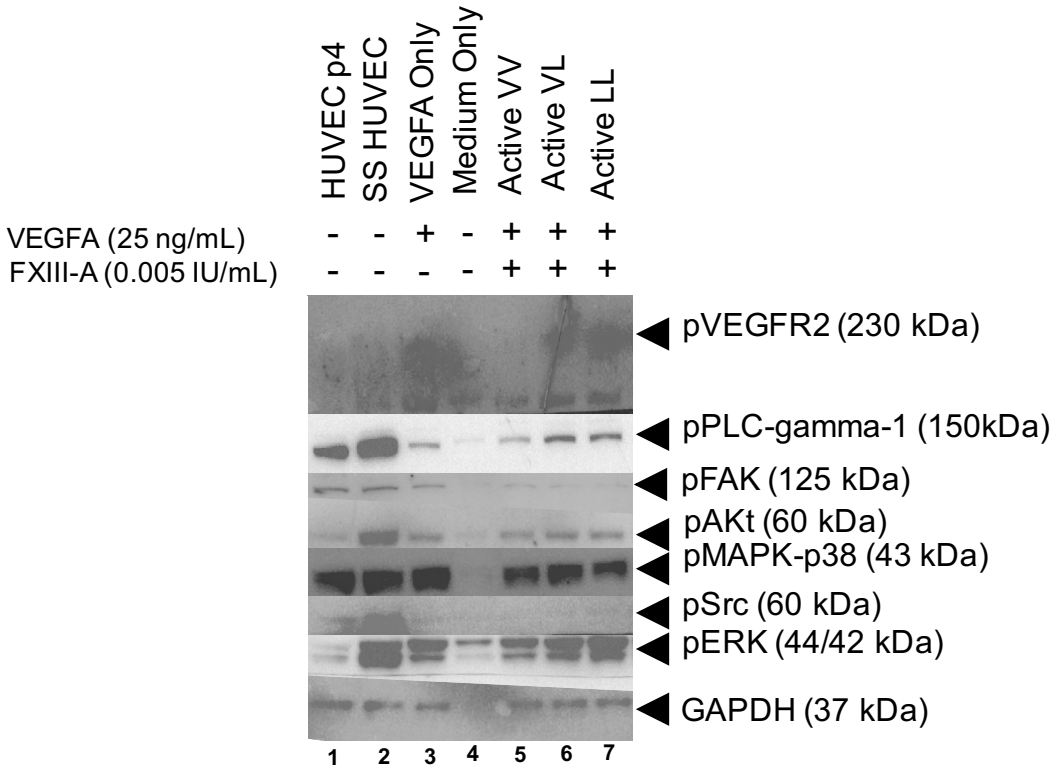

Figure 6-G: Western Blot of Members of the Angiogenesis Axis in HUVECs undergoing active endothelial tube formation (5 hours) in the presence of VEGFA (25 ng/mL). Protein was harvested from HUVEC from triplicate wells for each condition but results are only from one experiment due to the limited resources, the exploratory nature and novelty of the experiment. Lanes left to right: 1) HUVEC p4: cells normally growing in full EGM-2 Medium, harvested at 80% confluence; 2) Serum-starved (SS) cells incubated with serum-free EBM medium for 3.5 hours; 3) Cells stimulated with VEGFA (25 ng/mL) alone; 4) HUVEC serum starved for 3.5 hours and then incubated with full EGM-2 medium alone; Lanes 5-7) Cells serum-starved for 3.5 hours and then incubated with Active Val34Leu purified protein variants (0.005 IU/mL) and VEGFA in full EGM-2 medium, Val34Leu Wildtype (VV), Val34Leu Heterozygous (VL) and Val34Leu Homozygous Alternative (LL), respectively. All primary antibodies were used at a dilution of 1:1000 except for GAPDH which is 1:10000 in 5% skimmed milk in PBS. *Abbreviations*: pVEGFR2 (phosphorylated Vascular Endothelial Growth Factor Receptor 2); pPLC-gamma-1 (phosphorylated phosphoinositide-specific phospholipase C; pFAK (phosphorylated focal adhesion kinase); pAkt (phosphorylated protein kinase B); pSrc (phosphorylated proto-oncogene tyrosine-protein kinase C); pMAPK-38(phosphorylated mitogen-activated protein kinase); pERK (MAPK p44/42); GAPDH (loading control): glyceraldehyde 3-phophae dehydrogenase).

normalised to normally growing HUVECS (Figure 6-H) Serum starvation of HUVECs “resets” cells, pushing them into a more quiescent-like state (flow cytometry of BrdU staining would have confirmed the quiescent state, but this was not performed), which allows the cells to become more responsive to the angiogenic stimulation provided by VEGFA. Protein was also collected from cells in the EGM-2 fully supplemented medium alone, as this medium contained small concentration of numerous growth factors including a small amount of VEGFA (see Chapter 2 Materials and Methods for full details). Unfortunately, protein extraction for cells cultured in medium only following serum starvation did not appear successful, (Figure 6-G, lane 4), and therefore it is difficult to comment on the effect of supplemented medium alone on HUVEC growth following serum starvation.

6.4.1 Western Blot Quantification

The results of the western blot were quantified to examine the differences in protein expression between the different conditions tested (Figure 6-H). As this experiment was only performed once from proteins harvested from cells in triplicate wells, statistical analysis could not be performed. Serum starved HUVECS had an increase, in all proteins measured, but especially in phospho-Akt (pAKT) and phospho-ERK (pERK). These proteins are also members of other signalling cascades and promote survival and proliferation respectively, and as serum starvation induces cellular stress, compensatory signalling was likely to be occurring, (Figure 6-H-A). VEGFA stimulation results in increased pro-survival and proliferative signalling. However, migratory signalling was slightly decreased and the decrease in phospho-PLC-gamma (p-Plc-Y) did not correspond as expected with the increase in pERK.

The addition of FXIIIA variants and VEGFA appeared to have a differential effect on angiogenic signalling, (Figure 6-H-B). There appeared to be a decrease in pVEGFR2 for the wildtype variants on the Western Blot (Figure 6-G), however, the quality of the bands for this protein were poor. Given the degree of signalling for all of the other angiogenic cascade proteins measured, although lower for many when compared to Leu-carriers, it is likely that there was potentially a transfer issue in for the Western Blot, rather than a lack of signal (Figure 6-G, lane 5, and Figure 6-H-B). Another experiment would need to be performed to see if the lack of active tyrosine kinase receptor was a real result. This could be

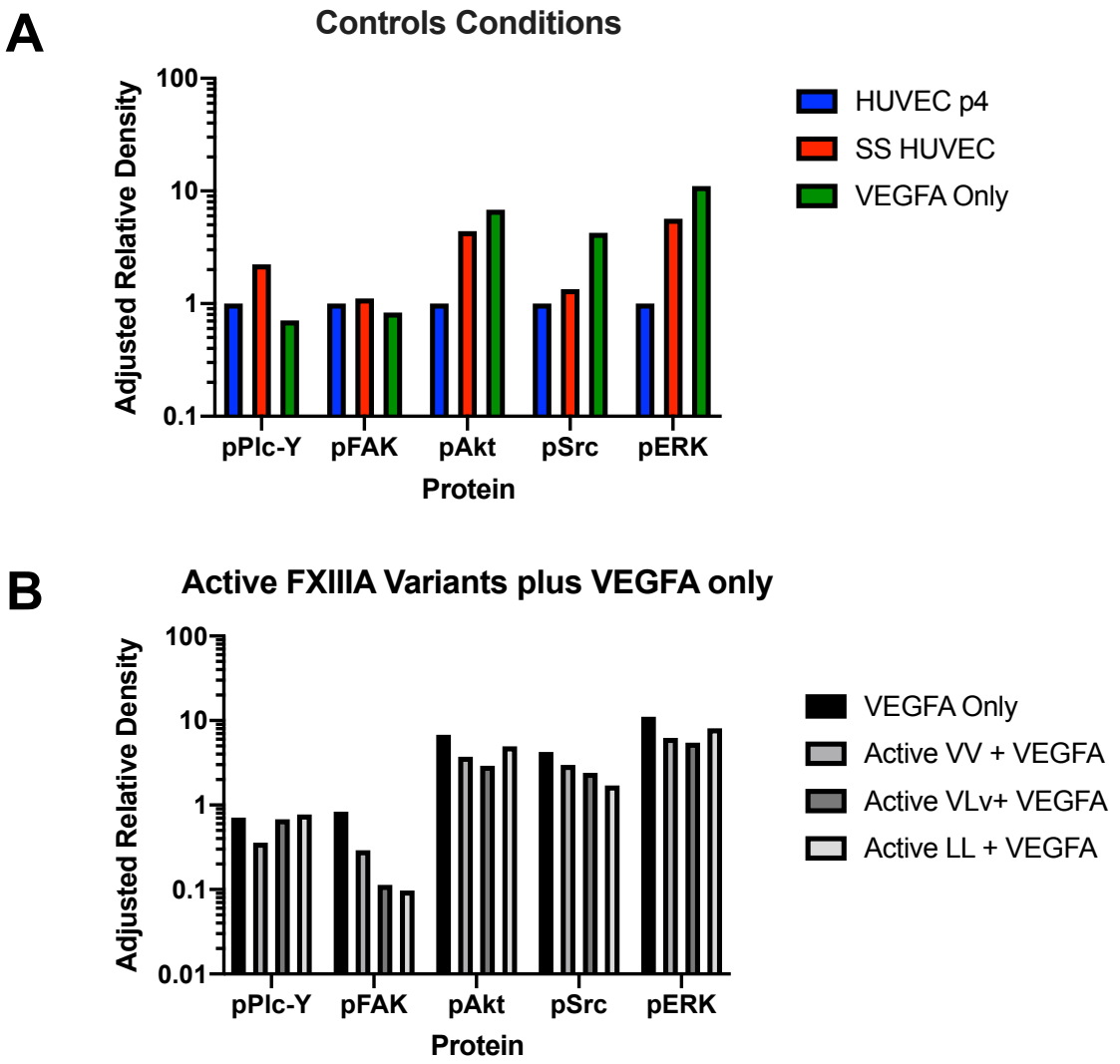

Figure 6-H: Quantification of Western Blot for Active Angiogenic Axis from HUVECs undergoing endothelial tube formation in the presence of FXIIIA variants and VEGFA. Bands from the Western Blot shown in Figure 6-6 were quantified in FIJI (FIJI is Just ImageJ) using the Gel Analysis package. All relative densities on the gel were adjusted for the GAPDH density as a control. (A) Results of relative density were normalised to normally growing HUVEC at passage 4 (p4). Serum-starved (SS) HUVEC were starved for 3.5 hours in basal supplement free medium (EBM). Cells were also grown in the presence of VEGFA stimulation alone (25 ng/mL) following starvation (VEGFA Alone). (B) Quantification of the protein bands for VEGFA alone and for conditions with active FXIIIA Val34Leu variants, wildtype (VV), heterozygous (VL) and homozygous alternative (LL) in addition to VEGFA. Abbreviations for proteins can be found in the figure legend for Figure 6-G.

investigated with RT-PCR to check for down-regulation of gene expression. Therefore, quantification was not undertaken for pVEGFR2, and quantification of the other proteins would be purely qualitative.

The decrease in phospho-FAK (pFAK), for migratory signalling was lower for protein with the Leu at residue 34 (V/L or L/L), which could be a reason for the observed lower rate of network formation in the previous angiogenesis assays performed on the Nikon LIPSI (Figure 6-E). This result also indicated that the decrease in cell migration could be due to a decrease in protein expression, rather than the cells being unable to move across the cross-linked matrix. Although only a small decrease, Leu variant FXIIIA also resulted in less phospho-Src (pSrc) signalling which also contributes to cell migration signalling. A Western blot to measure expression of matrix metalloproteinase 9 (MMP-9) in HUVEC undergoing angiogenic signalling in the presence of FXIIIA variants was undertaken but was not successful (data not shown). This would have provided further evidence for the effects on cell migration. Further work could also have been undertaken in transwell migration assays and scratch-wound assays.

There was increase in pPlc-Y signalling for Leu variants and pERK for the homozygous Leu variants compared to wildtype FXIIIA which indicates a higher level of pro-survival signalling indicating that the presence of FXIIIA for all variants tested did not appear to be detrimental to survival. The active Akt signalling was also indicative of no real change in proliferation. Therefore, the main effect of FXIIIA variants appeared to be in terms of cell migration. As the integrin αvß3 is vital for adhesion and migration, perhaps the crosslinking by the Leu-variants of FXIIIA mean that cells are unable to migrate or adhere as effectively compared to crosslinking in the presence of the wildtype variant.

6.5 Summary of Findings

- A thin layer endothelial tube formation assay was optimised for basement matrix volume, HUVEC seeding density and VEGFA concentration to assess the effects of FXIIIA Val34Leu variants on angiogenesis.
- Presence of wildtype V/V variant appeared to sustain angiogenic signalling for longer than VEGFA alone.

- The 34Leu variant resulted in significantly smaller endothelial tube networks ($p<0.001$, Kruskal-Wallis)
- Presence of the V/L variant resulted in a significantly smaller rate of network formation compared to VEGFA alone and presence of the wildtype variant ($p<0.05$, one way ANOVA)
- Lower levels of phospho-FAK and phospho-Src, proteins important in cell migration, were seen in cells actively undergoing endothelial tube formation in the presence of V/L and L/L variants.

6.6 Brief Discussion

FXIIIA has a well-established role in the promotion of angiogenic signalling. However, no work to date has been published on the effect of FXIIIA variants on this angiogenic role. Patients who carried a variant Leu allele for the SNP 103G>T, resulting in the amino acid change Val34Leu, responded differently compared to their wildtype counterparts when FXIIIA staining was present in the stroma of ovarian cancer tissues. Potentially different roles for FXIIIA in OC were indicated depending on its staining locality, but the resulting difference for variants was an interesting avenue to explore. Whilst FXIIIA has multiple roles, including in wound-healing, immune response and angiogenesis, not all could be explored, although it was hypothesised that the immune response role and angiogenesis role were those most in play in OC due to the nature of the staining present in the tumour, through what looked to be tumour associated immune-like cells and then stromal cells which were potentially fibroblasts/endothelial cells. Angiogenesis was taken forward as the role to be explored for FXIIIA variants because of the data previously seen in Chapter 4, where Val34Leu variant patients appeared to respond differently to the addition of bevacizumab, an anti-angiogenic therapy, which supplemented a standard platinum chemotherapy regimen.

Endothelial tube formation assays measured tube networks in the presence of active FXIIIA Val34Leu variant proteins. The initial rate of network formation was similar for wildtype FXIIIA and VEGFA alone, but as noted by a previous group, the presence of FXIIIA alone appeared to maintain angiogenic signalling for longer compared to VEGFA Alone (187). In these experiments, both VEGFA and FXIIIA were present for a more accurate reflection of a tumour microenvironment,

where VEGFA signalling would be present for tumour recruitment of a blood supply, and from tissue expression work (Chapter 5) FXIIIA is also present in the tumour microenvironment. The experiments did not test the effects of FXIIIA on its own, and in future experiments this would be of value, to determine whether the decrease in cell signalling was due to toxicity of FXIIIA or due to an effect on molecular signalling. Cell viability assays would be useful to run alongside tube formation assays, for this purpose.

The presence of FXIIIA Leu variants resulted in smaller networks which peaked in maximum network formation sooner and had slower initial rates of network formation compared to wildtype FXIIIA. To determine whether this was a result of any differences in the molecular signalling or because FXIIIA Leu variants affected the crosslinking of the basement matrix in such a way that inhibited network growth, a Western Blot was performed using protein extracted from cells actively undergoing endothelial tube formation.

The decrease in pFAK and pSrc in cells incubated with Leu variants suggest an effect on migratory signalling and may provide a reason for the smaller networks seen within the LIPSI experiment. Survival and proliferative signalling did not appear to differ between the variants. This suggests that the Leu-variant FXIIIA may either be crosslinking the beta-3 integrin of αvβ3 to VEGFR2 in a different or in a less stable way which affects cell adhesion and migration and ultimately leads to smaller angiogenic networks. Smaller network formation may explain why patients who are Leu-carriers experience better overall and progression-free survival when FXIIIA is present in the stroma. It may also explain why in a clinical data cohort, heterozygous Val34Leu patients had an improved overall survival and survival post-progression. When bevacizumab was given to heterozygous patients (Chapter 4, Section 4.6.1), these patients responded better in terms of OS and SPP. However, Leu/Leu homozygotes had a similar OS to wildtype FXIIIA, so therefore still much remains to be understood about how Val34Leu variants of FXIIIA are affecting ovarian cancer.

This chapter has presented data from novel experiments which are believed to the be first to explore how variants of FXIIIA are affecting its role in angiogenesis, which may explain why Leu-carriers respond differentially in terms of survival

intervals in OC. The complexity, and exploratory nature of the experiments meant that repeats would need to be performed in order to replicate the findings shown, but the results so far indicated that this work could help to further the understanding of the role that Val34Leu in the FXIIIA protein is contributing to the ovarian cancer disease state. Many more questions have been raised as a result of this work and will be discussed in Chapter 7.

Chapter 7: Discussion and Future Work

7.1 Brief Summary of Thesis Findings

This thesis presents the first in depth exploration of *F13A1* SNPs in epithelial ovarian cancer outcome, using ovarian cancer clinical data cohorts and tissue samples. FXIIIA protein expression was explored for the first time in OC, demonstrating high staining levels in OC stroma, with findings supported through exploration of collated mRNA databases. Expression of FXIIIA in OC stroma was detrimental to patient survival in multivariate analysis, and *F13A1* genotype influences survival intervals. The SNP 103G>T (Val34Leu) emerged as a potentially important player in tumour microenvironment interactions in OC, given the conflicting results between the univariate and multivariate analysis between FXIIIA staining levels in OC tissue and survival.

The foundation of this PhD project on FXIIIA in ovarian cancer started with analysis of a multi-centre, national study of a cross-section of patients from Edinburgh, Leeds and Oxford (ELO, n=612). These women were newly diagnosed or attending follow-up appointments for cancer monitoring, and genotyping of SNPs was completed by the Anwar Laboratory here at the University of Leeds in which two exonic SNPs 1951G>A and 1954G>A within exon 14 of the gene for FXIIIA, *F13A1*, were found to be associated with overall survival (unpublished data, Chapter 1, Project Development). 1951G>A and 1954G>C are in complete linkage disequilibrium with one another, with 1951A always found with 1954C. Patients with double carriage of these SNPs, resulting in a double-carrier haplotype, were over twice as likely to experience death when compared to wildtype patients (HR =2.10, p=0.002). Neither SNP had been associated with disease previously, and appear to have a minimal effect on normal FXIIIA activity levels (166). Therefore, this was the first instance where these SNPs appear to have an association with cancer or any disease state.

The Leeds sub-cohort (n=258), taken from the ELO Cohort, was assessed on its own with the mature, long-term survival data which was available. The associations between the 1951A+1954C haplotype, found that this double carriage of the alternative alleles, like in the full ELO cohort, resulted in a poorer prognosis compared to wildtype patients, (Hazard Ratio (HR) =1.72, p=0.059).

Although this result was only just over the threshold chosen for the level of significance, and the significant risk of death identified in the full ELO cohort, but not in the smaller Leeds sub-cohort is likely because of the larger sample size (n=258 vs 612). Homozygous patients for the alternative T allele at 103G>T were found to benefit in terms of OS, and this result was not seen in the full ELO cohort. Analysis of the mature survival data found that the risk of death for those patients with double carriage of the 1951 and 1954 SNPs was significantly higher than that for the initial cohort (HR=1.96, p=0.003). However, the benefit of 103T/T was lost in long-term follow-up, suggesting that this SNP may be important earlier in OC survival. The maintenance and strengthening of the association between the 1951A+1954C haplotype suggest that it may be able to be used as an indicator of long-term prognosis in OC. However, as with most studies further validation in multiple and varied patient cohorts would be required before this SNP could be classed as a true prognostic factor.

In the second clinical cohort, a sub-cohort from the ICON7 clinical trial and consisting of newly diagnosed patients, the association between the aforementioned 650/651 haplotype and OS was not present for this group of patients. This raised questions regarding whether the 650/651 haplotype was important in a specific group of patients, as the Leeds cohort consisted of a greater cross-section of patients in their disease with newly diagnosed patients, patients undergoing multiple lines of therapy and those in disease follow-up. However, in the ICON7 translational cohort, SNP 103G>T (Val34Leu) appeared to benefit survival for heterozygous patients at this locus for both OS and SPP and demonstrated significant benefit in terms of OS for those patients in receipt of the anti-angiogenic agent, bevacizumab. Val34Leu has been implicated in several other cancers, such as oral, colorectal and uterine myoma with the exact benefit/detriment to survival for carriers of the Leu-allele unclear, due to conflicting findings.

High expression of FXIIIA protein in OC stroma of patients from the ICON7 translational sub-cohort, and was associated with poorer prognosis. However, Val34Leu (V34L) variants, appeared to have a differential survival outcomes compared to wildtype patients. Leu-carriers demonstrated an advantage to their survival over wildtype patients in the presence of the disadvantageous stroma

staining. When the role of FXIIIA in angiogenesis was explored, the presence of V34L variants resulted in significantly smaller angiogenic networks resulting from a potential decrease in proteins related to migratory signalling. Patients with the V34L variants may therefore have a better prognosis because tumours are not able to recruit a large enough blood supply, resulting in smaller tumours which are potentially more treatable, resulting in the increase in survival for these patients.

7.2 Why was it of interest to study Factor XIIIA in ovarian cancer?

FXIIIA is a transglutaminase with its “fingers in lots of pies” with regard to its numerous roles in normal processes (164). Its main role is as a cross-linker of fibrin monomers in wound-healing, exerted though its transglutaminase activity by generation of isopeptide bonds between fibrin monomers in the coagulation cascade, forming stable clot structures. Other roles of FXIIIA in addition to wound-healing include inflammation, the immune response and angiogenesis (164,177,186). Turning to the classic hallmarks of cancer, Hanahan and Weinburg identify that these processes are also important in cancer maintenance and development (266). Therefore, it is not an ill-conceived step to suggest that this multi-role protein may somehow be influencing cancer.

Groups have linked Factor XIIIA to cancers other than ovarian. High levels of FXIII-A expression in bone lymphoblasts, measured by flow cytometry, were found to be significantly associated with long-term survival in childhood acute lymphoblastic leukaemia (216). Patients with advanced non-small cell lung cancer (NSCLC) diagnosed at later stages had higher plasma FXIII activity than earlier stage patients (214). Lower FXIII plasma concentrations were identified in malignant gastric, breast and melanoma (212,267). In oral cancer, carriers of the alternative Leu allele at V34L had an increased risk of developing this cancer (220) but for colorectal cancer, heterozygotes at this locus, had a decreased risk of development (219). There is not a clear consensus on how this coagulation factor affects cancer, and the contradictory findings suggest different roles for FXIIIA, depending on cancer type being assessed and depending on what measure of FXIIIA is made i.e. plasma levels, activity or tissue expression.

With specific regard to OC and Factor XIIIA, the work performed to date by other groups has been very limited. A small study of 58 patients, 32 of which were diagnosed with an ovarian malignancy, found that median plasma activity levels were higher in the presence of a tumour (both benign and malignant) when compared to age-matched healthy controls. Levels were lower in those with metastatic malignant disease compared to benign and non-metastatic disease (221). Lower levels in metastatic disease were hypothesised to be due to a result of consumption of FXIIIA during the formation of the matrices surrounding a tumour through its cross-linking activity. Other work had found that consumption of FXIIIA during activation of the clotting system assisted tumour maintenance (268). However, following this work, very little was performed on OC and Factor XIII specifically since the early 1990s. A review highlighted the importance of the coagulation system in ovarian cancer (269), although much of the primary literature has instead focused on transglutaminase 2 (TGM2) and OC (270). The roles of FXIIIA and the limited work presented a foundation upon which to explore how this transglutaminase may be exerting its effects in OC.

7.3 *F13A1* gene expression is present in OC and differentially distributed across OC tissues

Gene expression of *F13A1* is not considered a classical prognostic factor. Analysis of The Cancer Genome Atlas (TCGA) performed by the team behind the Human Protein Atlas (HPA) (271,272), does report a poorer prognosis in renal cancer patients when *F13A1* gene expression is high (259). Analysis of the ovarian cancer sub-cohort of the TCGA (n=373) although did demonstrate a worse prognosis for higher expression of *F13A1* through a log rank test for a Kaplan-Meier plot ($p=0.0068$). As the p-value was not <0.001, the result was not considered significant by the HPA (273). However, interrogation of the CSIODBV (252), a database of 3261 patients, collated from international ovarian cancer gene expression studies including the TCGA, yielded some interesting results on expression of *F13A1* and how it may influence OC.

Expression of *F13A1* interrogated in the CSIODBV was significantly lower in more aggressive disease, late stage and higher grade (252). This supports the findings of van Wersch who identified that plasma levels of FXIIIA were lower in metastatic compared to non-metastatic disease (221), perhaps due to the

increased consumption of FXIIIA for crosslinking in more aggressive disease. Gene expression was measured in tumour cells, and therefore the lower levels of gene expression seen in disease with a higher metastatic potential is likely from cellular, rather than plasma FXIIIA. Cellular sources of FXIIIA are from cells of bone marrow origin and fibroblasts. It is promising to see that levels of both gene expression and blood plasma are lower in disease as this still fits with the consumption hypothesis, and the source of FXIIIA may be of ill-consequence to its effect. Higher levels of expression in lower metastatic potential disease further supports the hypothesis that aggressive disease consumes more of the FXIIIA locally in support of tumour matrix formation, or conceivably, as explored later in the thesis, that FXIIIA is being used in other cancer-associated processes such as angiogenesis. Levels of FXIIIA in circulation were not measured in this work, and would be valuable to assess whether patients with lower levels of FXIIIA in general, or whether metastatic patients specifically, have lower FXIIIA levels and are therefore more prone to aggressive disease.

The Mesenchymal molecular subtype (MES) of serous OC was significantly associated with an increase in *F13A*1 gene expression (252,253). The MES has a large stroma component (256) supplementing the significantly higher gene expression identified in malignant stroma. Collagen expression and active transforming growth factor-beta (TGF-ß) signalling are associated with metastatic disease in the MES (256). As FXIIIA is able to crosslink collagen and tissue transglutaminases activate TGF-ß signalling (274), although the precise role of FXIIIA in this is yet to be fully understood (184), FXIIIA may have a role in metastatic progression through its presence in OC stroma.

7.4 *F13A1* SNPs are associated with Survival intervals in Ovarian Cancer

7.4.1 SNP 103G>T is associated with improved prognosis

A SNP that appeared to be associated with survival benefit, in the Leeds cohort was 103G>T (V34L). Homozygous alternative patients (TT, resulting in Leu/Leu (L/L)) had a significant decrease in risk of death compared to wildtype patients (HR=0.34, p=0.024). As mentioned previously, V34L has been associated with other cancers and thrombotic disease, as carriers of the Leu-allele had a decreased risk of developing colorectal cancer (219) and the wildtype and

heterozygous genotype appeared protective in uterine myoma (248). Val34Leu is associated with thrombotic disease such as myocardial infarction (197,198) and ischaemic stroke (193,208). This benefit to survival was lost however, when examined in the mature survival data, suggesting that the benefit is only present in the shorter term for patients carrying this mutation.

The SNP 103G>T again appeared to influence survival in ovarian cancer when a newly diagnosed cohort of OC patients from the ICON7 clinical trial was analysed in Chapter 4. Not only was the ICON7 translational cohort a group consisting of only newly diagnosed patients, there were also several survival intervals measured including overall survival (OS) and progression-free survival (PFS). The survival interval, survival post-progression (SPP) was calculated by subtracted the PFS from the OS and using death as the indictor. Heterozygous individuals (V/L) demonstrated an improved overall and survival post-progression compared to wildtype patients (V/V) (HR=0.72, p=0.045; HR=0.67, p=0.021, respectively). However, there was no significant benefit seen for homozygous alternative individuals for either survival interval (L/L).

The benefit only for heterozygous patients was odd, as it would be expected that if the presence of one copy of the alternative allele served to benefit, then two copies should at least have an additive effect to said benefit. This result may be an example of heterozygote advantage. Heterozygote advantage, more colloquially called “hybrid vigour” is where heterozygotic individuals for SNPs seem to have a better “fitness” over both homozygotic genotypes, and therefore heterozygotes persist in the natural population (275). Evidence of this phenomenon has been identified in other cancer types for other SNPs in breast (276) and bladder (277) cancer, NSCLC (278) and non-Hodgkin lymphoma (279). No evidence of full heterozygote advantage has been seen for *F13A1* SNPs, and this is believed to be the first piece of work which demonstrates a significant advantage for just heterozygotes at 103G>T in *F13A1*.

7.4.2 1951G>A and 1954G>C Haplotype Associations could not be repeated

The associations between 1951G>A and 1954G>C and survival could not be replicated in the ICON7 translational cohort analysis. A significant finding for these SNPs was limited to a univariate association between risk of disease

progression and 1954G>C (p=0.039), but this result did not hold in multivariate modelling and the Chi^2 result could not give any indication of directionality of this association. The ICON7 group did represent a group of women who were only newly diagnosed patients and did not represent the same cross-section of women from whom data were collected in the Leeds cohort. There is also the potential for geographical bias; the Leeds cohort is limited to women attending clinic in West Yorkshire, whereas the ICON7 trial recruited women from many international centres. Although full location data were not available for the ICON7 samples, and Leeds was one of the collection centres, it is highly unlikely they are all from Leeds-based patients. However, the frequency of the SNPs is similar in each of the cohort so geographic bias is unlikely, and is likely due to over-representation of a specific group of women which remain to be fully identified.

7.5 103G>T may influence response to anti-angiogenic therapy

The treatment sub-cohorts were extracted and analysed from the ICON7 translational cohort, to test whether *F13A1* SNPs influenced response to the chemotherapy given. SNP 103G>T appeared to influence response to bevacizumab and to the standard regimen of carboplatin and paclitaxel, alone. In the standard regimen treated group, L/L individuals demonstrated a distinct advantage for progression-free survival (PFS) (Figure 4-H and Cox Model Results: L/L: HR=0.45, p=0.100, V/L: HR=0.84, p=0.442, V/V=: HR=1.00), although clearly not significant. However, in receipt of bevacizumab, V/V and V/L individuals outperformed L/L patients with to PFS benefit of over six months (V/L: HR=0.78, p=0.197, L/L:1.48, p=0.199, V/V: HR=1.00).

Once a progression-event in disease had been experienced, patients in receipt of platinum therapy only L/L patients had a lower SPP, approximately 18 months, compared to V/V patients (approximately 22 months) and V/L patients (at 33 months), (Figure 4-H). When in receipt of bevacizumab, all variants performed similarly with a median SPP of approximately 24 months. For OS, patients in receipt of bevacizumab and carrying V/L survived for longer compared to both homozygous variants, supporting an argument for heterozygote advantage for this SNP when treated with the anti-angiogenic agent. The full ICON7 trial findings did only find a benefit to bevacizumab specifically in those women with high risk of disease progression (78).

When the ‘risk-of-progression’ sub-cohorts were analysed, again V/L patients demonstrated an improvement to all survival intervals from which measurements could be acquired. Due to a lack of convergence of the data, it was not possible to assess PFS and SPP in the “at risk” population (n=150), and this was likely due to the small sample size. With a larger group of patients, it would be possible to explore all survival intervals. With the definition of “at risk of progression” made so clear in the ICON7 protocol, this definition could be applied to other clinical cohorts for which disease stage and surgical data are available.

The benefit of V/L and L/L variants to survival intervals and therapeutic response suggests that this variant is having an effect on the cancer which results in smaller tumours, poorer maintenance of the tumour, or an influence on the success of the chemotherapeutic agent. It is known that Leu-variants can alter the rate of and formation of matrices, but is it possible that this is affecting response to therapy against the cancer or is it more likely that the variant is influencing one of FXIII’s other roles. A resulting unfavourable tumour environment may be produced in these variants, which is why these patients survive for so much longer, compared to heterozygotes and those carrying wildtype FXIIIA. The V34L variant has not been found to contribute to the mechanism of action of either carboplatin or paclitaxel, which are DNA-targeting or cytoskeletal-targeting agents, respectively. A decrease in FXIIIA expression was identified in paclitaxel-associated lymphedema and scleroderma in patients treated for breast cancer (280), and FXIIIA expression has also been used as diagnostic tools in skin disease diagnoses (281). Although not completely understood, scleroderma is thought to be caused by changes in interstitial tissue pressure as a result of taxane therapy (282) and treatment results in an increase in fibrosis (283), and a decrease in FXIIIA expression occurs in dermal fibroblasts.

7.6 Tissue expression of FXIIIA protein affects OC survival intervals

7.6.1 High levels of FXIIIA staining in OC stroma and tumour resulted in poorer outcome, but staining in tumour/stroma cores appeared protective

Immunohistochemical expression of FXIIIA protein has been explored in bone and skin tissues and disorders such as leprosy (215,284–287), with expression

in dendritic cells of the dermis, in microglia and immune cells in brain tissue (288), macrophage staining in uterine tissue (165), and positive staining in adipocytes (289). Breast and colorectal carcinoma stroma has been stained for FXIIIA and the transglutaminase was found in macrophages in the invasive margin (290). Positive FXIIIA staining has also been found in neoplasm connective tissues, at a higher level than normal tissues (291). Only plasma levels of FXIIIA, rather than any form of protein expression, have been measured in ovarian cancer, specifically (221).

Interrogation of the CSIOVDB gene expression database, which comprised multiple international studies of ovarian cancer gene expression, resulted in the highest expression of *F13A1* in malignant stroma compared to tumour, and healthy epithelium and stroma. Therefore, it would be expected that FXIIIA would be expressed in OC tissues, particularly in OC stroma, however, the exact location or cell type of the staining is unknown. In the tissue microarrays, staining was predicted to be from fibroblasts within the stroma or macrophages, as it was unlikely that the source of FXIIIA would from be the blood plasma due to the nature of tissue preparation in the generation of the tissue microarrays. However, in order to ascertain where the staining was coming from, co-localisation experiments with immune or connective tissue markers or for FXIIIB, the carrier protein with the FXIIIA dimer in the plasma, would be necessary.

Staining for FXIIIA protein in formalin-fixed, paraffin-embedded tissue microarrays demonstrated the highest average percentage positivity within stroma cores (Chapter 5), fitting with the findings from the gene expression database interrogation. The lowest average percentage positivity was in tumour cores, and cores containing both tumour and stroma resulted in percentage positivity between the two tissues types. The precise location of the staining could only roughly be determined, as only slides for one round of staining were provided. It was felt that determining the actual presence of FXIIIA within OC tissues was the first important step, and that further hypotheses on precise location/contribution of FXIIIA could be developed, thereafter. Tumour cells themselves did not appear to stain for FXIIIA. Instead, cells within the tumour, likely to be immune-like cells given their location and size, stained positively but markers such as CD34 and interleukins would provide valuable insight if more

tissue microarray slides were available. Tumour-associated stroma, intra-tumour stroma and general OC stromal cells stained positively for FXIIIA, when present, and could be identified by the distinct cell morphology.

In multivariate analysis, FXIIIA staining within the OC tumour cores and the stroma tissue cores had a negative influence on survival intervals, with hazard ratios >1 and were classed as significant predictors of risk, when compared to negative FXIIIA staining. However, in the cores where both tumour and stroma were present, high levels of FXIIIA staining appeared protective, when compared to negative staining. These results were unexpected and suggested that FXIIIA influenced survival in different manners depending on location. The lack of tumour cell staining, and the staining of stromal margins next to tumour tissues, appears similar to that of the breast and colorectal margins in which FXIIIA was present (290), although was not confirmed to be in immune cells in this work. This suggests that FXIIIA is involved in tumour to microenvironment cross-talk. The protective effect means that patients are surviving for longer when tumour/stroma staining is present, and therefore FXIIIA's possible interaction with tumour cells and the stromal margin next to the cancer is disadvantageous to tumour growth and/or maintenance.

The great risk to survival when FXIIIA stroma staining is present, suggests that stromal staining itself may lead to conditions which are advantageous to the tumour, and thus poorer for the patient. It is hypothesised that tumour matrix cross-linking by FXIIIA may be promoting a more aggressive environment. FXIII has been shown to be important in early micrometastases (292) Changes to matrix composition or the degree of crosslinking may also affect the surrounding matrix stiffness. Increased matrix stiffness has been associated with epithelial-mesenchymal transitioning of tumour cells (113,293) resulting in promotion of more aggressive metastatic phenotypes as cells change to escape the matrix (114,294,295). Although FXIIIA is used *in vitro* to generate the matrices in tumour stiffness studies, FXIIIA itself has not specifically been linked to alterations in tumour matrix stiffness. It has however been found to stiffen fibrin (296) and clots in 34Leu individuals lyse more slowly than those made in WT individuals (297), so an affect on tumour matrices is likely. However, composition of matrix is what

appears to increase stiffness, so it may also have been interesting to stain for matrix associated proteins in the ICON7 ovarian tissue microarrays.

Stroma is more mesenchymal in nature, and high levels of FXIIIA expression are found in the MES (252,253,256). Molecular subtype analysis was not performed on each of the tissue cores stained for FXIIIA, and this data was not available for analysis. Molecular subtyping of the ICON7 tissue samples from Germany (which were not available for the tissues in the microarray used in thesis (personal communication, T. Perren) were, however, performed by Kommoss *et al.* (298). Patients with the proliferative and mesenchymal subtypes demonstrated the greatest benefit to PFS from bevacizumab over the other molecular subtypes. Given the results from the ICON7 translational cohort analysis of peripheral blood DNA, and the differences in PFS for LL variant, it could be hypothesised that the other molecular subtypes are associated with this FXIIIA variant, as LL variants respond better without bevacizumab. Being able to generate or access molecular subtype data for the ICON7 tissues analysed in this cohort would have been very informative and exciting to investigate. A link could have been made between the levels of FXIIIA protein expression and molecular subtype, in addition to genotype associations. If these associations were identified, then SNP genotyping for 103G>T in *F13A1* could be a useful diagnostic tool to determine whether a patient should receive bevacizumab. As the tissue type cores were taken from primary tumours during resective surgery, and therefore taken before any chemotherapy was given, an investigation into whether FXIIIA staining levels changed with treatment was not possible, but could also be an interesting piece of future work.

7.6.2 Val34Leu variants altered the prognosis of high stroma staining

Val34Leu in univariate analysis was associated with OC stroma (S) and OC tumour/stroma (tumour and stroma, T/S) staining levels (Chapter 5). When assessed via Kaplan-Meier plots, carriers of Leu had an improved OS and SPP when FXIIIA staining was present in the OC tumour or OC stroma, regardless of whether staining was low or high. However, Leu-carriers performed poorer when OC Tumour/Stroma levels of FXIIIA were positive while wildtype patients performed better. Stroma staining in general resulted in a poorer prognosis for OC patients, and Leu-carriers benefited over wildtype patients when FXIIIA was present in stroma. Therefore, the carriage of Leu when expressed, may be

promoting patient survival, but through what method? And for the opposite observation for Leu-carriers for when T/S staining is present, how is the Leu-variant resulting in poorer patient survival? No evidence of heterozygote advantage was tested in this cohort as the number of patients taken into the Cox proportional hazards regression modelling was very small (n=91), as this form of multivariate modelling requires that no data points are missing for patients within the model, and not every patient had each tissue type core extracted from their primary cancer. Therefore, VL and LL patients were pooled to form the Leu-carrier categories in order to keep category numbers high enough for meaningful statistical analysis.

7.7 Val34Leu variants of FXIIIA influence angiogenic network development and signalling

The results of the staining raised a number of questions, but due to time limitations, the next steps in the investigation into the role of FXIIIA in ovarian cancer had to be focused. A number of paths of investigation lay ahead, and but were limited to *in vitro* studies as *in vivo* work or acquisition of further patient samples was not possible within the time frame. The stroma and potential interactions therein were chosen as the point for focus for experimental planning. This was due to the supporting gene expression evidence and the differential prognosis for stroma staining for V34L variants. The multiple roles of FXIIIA have already been touched upon, but the role in angiogenesis took precedence for hypothesis generation. The tissue samples on which staining was performed were taken from patients within a clinical trial testing the benefit of an anti-angiogenic to the standard OC chemotherapy regimen. Although tissues were harvested prior to treatment, it may be that FXIIIA in the stroma contributed to differential therapeutic response. It was hypothesised that the V34L variant was exerting its positive effect on survival by somehow influencing the angiogenic pathway.

In an endothelial tube formation assay, recombinant FXIIIA Val34Leu protein variants were activated in the presence of thrombin and calcium, and then added to human umbilical vein endothelial cells (HUVEC) in the presence of VEGFA, the main signalling molecule for pro-angiogenic signalling. HUVEC treated with V/L or L/L variants formed smaller endothelial tube networks which were slower

to develop and peaked in their total development sooner than wildtype FXIIIA or VEGFA alone (Chapter 6). These results appeared to support the hypothesis, that Leu-variants have negative impact on angiogenesis.

The role of FXIIIA in angiogenesis has been explored in both *in vitro* and *in vivo* models (185–187,299). FXIIIA from pooled human plasma (Fibrogammin) was used in these studies, meaning a mixture of FXIIIA variants may have been present. To current knowledge, FXIIIA variants and the role they contribute to angiogenic signalling has yet to be explored. Therefore, the experiments in Chapter 6, were the first to do so. The Leu variant for Val34Leu has been associated with higher specific activity and tighter matrices generated from crosslinking fibrin. Could the small networks be due to a difference in how the beta-3 integrin is crosslinked to the VEGFR2 receptor? Are these variant proteins less stable overall, and therefore less enzyme is available to crosslink compared to the wildtype protein? Protein stability experiments and co-immunoprecipitation experiments, similar to those performed by Dardik *et al.*, would be valuable future work to help further understanding of the difference between Val34Leu variants with respect to angiogenesis.

Working with the observations seen in the tube formation assays, the decrease in total network length and slower rate of reaction was hypothesised to be due to either a) an alteration in angiogenic signalling because of the FXIIIA variants present or b) the variants altered the matrix surrounding the cells and slowed their ability to migrate. FXIIIA is able to crosslink the basement matrix upon which the HUVEC are seeded and subsequently form their endothelial tube networks, and the presence of the variants did result in observable changes to the matrix. Therefore, it was important to determine whether the inhibition of network formation was due to the crosslinks in the matrix or due to an inhibition of angiogenic signalling. Cell migration is a part of angiogenesis, as endothelial cells are stimulated and recruited from already developed capillaries, and it is highly likely that an influence on angiogenic signalling may be affecting the migratory signalling, too.

A Western blot of protein expression in cells actively undergoing endothelial tube formation was performed. Active protein signalling, demonstrated by detection of

phosphorylated proteins, was measured for proteins within the four main arms of angiogenic signalling: cell survival (pPlc-gamma, pAkt), migration (pSrc, pFAK) and proliferation (pERK1/2) and vascular permeability (pSrc). The novelty of this experiment was rather exciting as this was the first to assess the effect of FXIIIA variants on the angiogenic signalling cascade. Cells were harvested on ice, and the experiment was challenging due to the small number of cells upon the matrix and the delicacy of the technique to ensure collection of cell networks from the basement matrix. Equal loading of protein could not be determined until the end of the Western blot protocol due to issues with the protein concentration assay. Maximal protein was therefore loaded in each lane, and subsequent quantification in ImageJ allowed for loading control correction for each lane.

The exploratory nature of the experiment and the degree of hands-on time required, meant that only one experiment of triplicate wells per condition was performed. It was therefore not possible to run meaningful statistical analysis but quantification of protein expression from the protein bands on the Western blot proved interesting. As expected a decrease in migratory signalling proteins was seen, when cells were stimulated to form endothelial tubes in the presence of V34L variants. Both pSrc and pFak were expressed at lower levels compared to cells incubated in the presence of wildtype FXIIIA. Integrin binding also promotes the activation of FAK which binds to Src for cytoskeletal changes through F-actin (294). As FXIIIA exerts its pro-angiogenic effect through its crosslinking of the beta-3 integrin to VEGFR2, V34L variants may be resulting in altered cross-linking and therefore a reduction in pro-angiogenic signalling. A decrease in this migratory signalling would explain why smaller networks were formed.

There did not appear to be a consistent decrease in other members of the angiogenic axis. In fact, for pPlc-gamma-1, an increase in this active signalling protein was seen for Leu-variants. Plc-gamma-1 is one of the first proteins involved in signal transduction following growth-factor mediated activation through the tyrosine kinase receptor (300). As the other TKR were not measured, it is difficult to say whether the increase in pPLc-gamma-1 is coming from VEGFR2 signalling alone or as a result of other TKR signalling, as other growth factors such as EGF, IGF and PDGF were all present in the HUVEC medium.

It is not possible to compare the amount of pVEGFR2 in wildtype stimulated HUVEC, because it is not possible to confirm if the lack of active receptor was a genuine result or as rather suspected, the result of an issue in transfer of the proteins to the membrane used for protein detection. Quantification of this protein was not possible. The lack of pVEGFR2 seen in the Western Blot for the wildtype variant does not follow the findings in the literature, that FXIIIA crosslinking is pro-angiogenic (187), and the presence of downstream angiogenic signalling suggests that pVEGFR2 levels in the wildtype protein stimulated cells would at least be similar to the Leu-variants. The pro-survival signalling (pPLC-gamma and pAkt) also suggests that the presence of the FXIIIA variants is not inherently toxic to the cells.

The reduction in cell migration, but promotion of other angiogenic signalling, does not rule out the possibility that the crosslinked matrix may be having an effect. It is known that V34L variants alter the nature of fibrin matrices, and this may be affecting the cells' interaction with the extracellular matrix. Migration and adhesion are necessary for successful angiogenesis, with adhesion taking place through integrin binding and FXIIIA has a role in endothelial cell adhesion through the avb3 integrin (301). An attempt to measure the level of integrin beta-3 in cells actively undergoing endothelial tube formation was made, but this Western blot proved unsuccessful and there was not enough protein to run a further blot. This result could have been helpful in determining whether the loss of migratory signalling could have been caused by a decrease in presence of the integrin, potentially caused by indirect effects of the Leu-variants, and therefore, there was decrease in migration. Adhesion assays could also have been good to perform, in order to establish whether endothelial cell adhesion was prevented by the crosslinked matrices.

The presence of FXIIIA in the GelTrex™ basement matrix was not tested directly in these experiments. The basement matrix is derived from murine Engelbreth-Holm-Swarm sarcoma, it contains collagen and laminin as major components. There is no evidence of fibrinogen in the matrix, as other literature has added fibrinogen as a supplement to GelTrex (302). In this thesis, it was noted that during tube formation experiments for conditions in which FXIIIA was absent from the medium, no crosslinking of the matrix was seen, however, as thrombin was

not added to control wells (as the absence of thrombin was itself a control for FXIIIA activation), it is not known whether FXIIIA was in the basement matrix. This could be tested through a Western Blot, using antibody HPA001804 to detect FXIIIA in diluted matrix or potentially *in situ* within wells using a red fluorescently conjugated FXIIIA antibody. The red spectrum would avoid the auto-fluorescence of collagen in the green spectrum.

The results of the tube formation assay suggest that the V34L variants somehow alter migration, and based on what is known about the molecular basis of FXIIIA in angiogenesis, it is likely that there is an effect on the beta-3 integrin and either the crosslinking of this integrin to VEGFR2 or as a result of downregulation of the integrin, or even an upregulation in an inhibitor of the integrin which means cells struggle to adhere to the matrix and therefore migrate. In terms of what this means for the therapeutic response seen for V34L variants, the results of the *in vitro* angiogenesis assay and the Western blot support the idea that Leu-variants are unable to form as successful vessel networks as wildtype variants. However, it is not an effect on angiogenic signalling itself, but rather an effect on migration of the endothelial cells which may be the challenge faced by tumours for successful recruitment of a blood supply. Less successful recruitment would result in smaller tumours which would be easier to treat and less likely to metastasise.

7.8: Limitations and Further Work

7.8.1 Clinical Data Cohorts

Although future work has been briefly touched upon in the preceding discussion, a detailed overview of the potential future experiments and hypotheses generated will be discussed in the following section. This work is the first to demonstrate associations between the *F13A1* SNPs 1951G>A and 1954G>C and 103G>T and survival in OC. The inability to replicate the finding for 1951 and 1954 haplotypes and survival from the Leeds cohort of patients, within the newly diagnosed ICON7 patients suggests that these SNPs may play a role at different stages of disease. The Leeds cohort although did contain a mixture of newly-diagnosed and follow-up patients, the follow up time for the cohort as a whole was far longer than ICON7 trial, and perhaps mature survival data for those

patients within the ICON7 trial would reveal an association between these SNPs and long-term survival. The benefit to survival for carriers of the SNP 103G>T was present in initial analysis of the Leeds cohort, but lost during long term mature survival analysis, suggesting this SNP could be important earlier in OC. This may explain why this SNP was so significant within the ICON7 group of patients, as these patients were all entered into the trial at the point of their diagnosis. It is clear that analysis of other groups of patients is required to further understand whether these SNPs influence survival intervals in OC. Study of another Leeds local cohort, and an international cohort would both be of importance to assess whether there is a true geographical bias of *F13A1* genotypes within the West Yorkshire area.

The OC prognostic factors analysed within this thesis were limited. Two main prognostic factors which were absent for ICON7 and Leeds cohorts were tumour bulk, or the residual disease remaining after cytoreductive surgery, and ECOG Performance Status. Performance status describes how OC limits the daily living abilities of patients (303). The status score ranges from Grade 0-5, where 0 is a patient who is fully active and can perform daily tasks without any restrictions, whereas 4 is a patient who is completely disabled, often confined to their bed and is not able to self-care. These measures are routinely used in clinical trials, and have been analysed for the full ICON7 trial (n=1528) (78,79). An further exploratory analysis of the ICON7 trial, focusing particularly on stage and extent of residual disease was performed in 2019 (304). This exploratory analysis concluded that benefit to PFS following the addition of bevacizumab to chemotherapy was present regardless of stage or residual disease remaining. Benefit to OS however, was only identified for late stage disease and >1cm residual disease remaining. Although stage data was present For the translational sub-cohort of ICON7 trial analysed in this thesis, remaining tumour bulk data and performance status were unavailable following the database request from the MRC. Had these data for these prognostic factors been provided, then the survival analysis performed would be more complete and would assist in defining the association between *F13A1* SNP genotype and OC. Having these other prognostic factors may have influenced the multivariate analysis findings, which often were very close to the set alpha value of 0.05.

Treatment data, tumour bulk and performance data were absent for the Leeds cohort. When requests were made for treatment data for the Leeds patients, access would require labour-intensive delineation of raw patient medical records. Raw clinical files with patient identifiable data which could not be accessed by K Hutchinson. It was decided that for the purposes of this thesis the prognostic factors provided, albeit limited, were sufficient to test the hypotheses which had been developed.

Both clinical cohort studies were also limited to a racial majority of Caucasian individuals. *F13A1* SNP allele frequencies and FXIIIA activity does differ between races, particularly between individual of Asian and African descent, in comparison to Caucasians (305,306). An exploration of *F13A1* SNP genotypes and measurable outcomes in ovarian cancer, like prognostic factors and survival intervals in clinical trials with recruitment at other international centres would present an exciting opportunity and may even lead to results which could have international benefit.

The availability of the ICON7 translational cohort presented a novel opportunity to explore *F13A1* genotypes in a newly diagnosed cohort of women, but also the stratification of patients into two treatment arms, and the unique “at risk of progression variable” allowed for further hypothesis generation. It would be interesting to explore other clinical trials (not limited to just OC) in which different treatments were used, and in different regimens to assess whether *F13A1* SNPs, such as 103G>T, were able to result in a differential response to therapy as demonstrated within the ICON7 trial. Chemotherapies such as paclitaxel appear to influence the development of fibrosis in patients (280,283,291), and given FXIIIA’s role in fibrosis, investigation into the role of FXIIIA in treatment-associated symptoms could also prove beneficial to clinical knowledge.

The desire to understand the role of FXIIIA in the most current definition of cancer is also very strong. The Leeds and ICON7 clinical cohorts were performed when FIGO staging was still commonplace to define OC. Nowadays, ovarian cancer is treated as a heterogeneous collection of diseases, separated not only by molecular subtype, but also defined in how responsive they are to treatment.

Serous epithelial ovarian cancer is now commonly defined as high grade serous OC (HGSOC) and low grade serous OC (LGSOC), both of which differ in mutational status and therapeutic response. Exploring the role FXIIIA may have within these more modern classifications would certainly be of clinical relevance, and the age of the cohorts and definitions within them are one of the main limitations of this investigation.

7.8.2 Statistical Testing

Sample size is always an important factor when studying clinical cohorts and assessment of SNPs must always be interpreted with caution. Rarely does a single SNP influence total clinical outcome, and is the subsequent alteration to interactions and signalling which are the real game-changers within a disease. The SNP is often a signpost to a more complex process or set of processes which are in play. The sample sizes of cohort used in this thesis were tested for suitable power for multivariate modelling and limitations to the power of the detection of hazard ratios was present. Large cohort sizes are almost certainly required to provide further evidence for FXIIIA as a player in OC. Analysis of sub-cohorts did take place as a form of exploratory analysis, but the extraction of sub-cohorts does come with the consequence of a loss of power for the results obtained, due to a reduction in sample size. This could be combatted through large sample sizes.

Statistically there is also the controversial topic of use of the Bonferroni adjustment (307,308). In a detailed review by R Armstrong, arguments for the necessity of the adjustment from both sides were clearly presented in the case of ophthalmology research (309), but the conclusions are applicable to many scientific disciplines including that of this thesis. Although some feel that this form of statistical adjustment should be mandatory (310,311), others are inclined to believe that the Bonferroni adjustment is unnecessary and may lead to “missed” results for the sake of reducing Type I error (312,313). Although there were many statistical tests performed, the p-values presented in this thesis did not have the Bonferroni adjustment applied. The arguments supported are that Bonferroni is not always necessary and at times, can put good research at risk of dismissal. Type I error is the error of generating false positive results, whereas Type II error is the error of false negatives, or “missing” potential results. Bonferroni adjustments attempt to decrease Type I error but therefore can increase Type II.

Although the analysis in this thesis was considered exploratory for sub-cohorts, the hypotheses were clearly defined before proceeding into testing and the results from exploratory analysis which lead to hypotheses for further investigation do not require adjustment (309,313). And although multiple tests were used, each test used a different statistical model, and all p-values that resulted in a significant result were treated with appropriate interpretation and caution, and this was felt to be of far more importance than application of Bonferroni.

7.8.3 Patient Tissue Samples

The study of FXIIIA expression in tissues yielded some interesting results, which were demonstrated for the first time in OC. One of the main limitations was the quantity of tissue microarray slides available for testing, which led to only staining of FXIIIA being possible, and the results of which were presented in Chapter 5. There was no further possibility to explore the source of FXIIIA within the OC stroma or tumour tissues, and this information would have been invaluable in dictating the next steps. Staining for immune cells, fibroblasts and for the carrier protein FXIIIB would have allowed for assessment of cellular or plasma contribution of FXIIIA within the OC tissues.

Co-localisation for TGM2, fibrinogen and isopeptide bonds with FXIIIA in frozen tissues proved problematic due to the necessity to section tissues at 7 μm, thus often including 1.5 layers of cells, and the age and storage of the tissues also resulted in challenging immunofluorescent staining. With fresh samples, it may have been easier to section and increase section quality, and thereby improve staining. The suspected issues with the isopeptide antibody were discussed in Chapter 5, with both available clones from which antibodies were generated showed cross-reactivity with acetylated lysines and other similar structure (314,315). Acetylated lysines are often found in histones within the nucleus, which may explain the strong co-localisation between isopeptide and DAPI, the nuclear stain, in the acquired immunofluorescence images. A new antibody would need to be generate that was demonstrated to not have cross-reactivity, and currently this is not available on the market, but would be very beneficial to the study of isopeptide bonds in clinical samples, as a measure of FXIIIA crosslinking activity *in situ*.

The number of patients for which each tissue-type sample was acquired (tumour, tumour-stroma and stroma) was limited to 91 patients. The fragility of stroma cores was visible, and number of cores were dismissed from analysis due to artefacts, folded cores or too little tissue available at the site of core due to breakage. A large sample size of tissues with clinical data, and peripheral blood DNA available for genotyping of *F13A1* SNPs would strengthen the results of this thesis and provide further support for the role of FXIIIA in OC stroma. A larger sample size would also shed light on the benefit of positive FXIIIA staining in the tumour/stroma, which remains one of the most ambiguous set of results within this thesis, and generates many more questions than it does answers.

In order to further assess the expression of FXIIIA in OC tissues, RNA could have been extracted from tissues and RT-PCR performed to measure gene expression and this could have been correlated with visible protein expression. However, fresh tissues would have been required to acquire to highest quality of RNA for experiments. The extraction of RNA would also have allowed for molecular subtyping of OC through RNA-Seq to occur which would provide valued insight into FXIIIA in molecular subtypes of OC and could support the mRNA database findings of increased expression in certain subtypes over others. As the OC molecular subtypes respond in different ways to chemotherapy, further experiments could be performed to test whether FXIIIA SNPs predict therapeutic response.

7.8.4 Angiogenic Assays

The endothelial tube formation assays and Western blot of the active angiogenic cascade demonstrated novelty and were challenging yet incredibly interesting to perform. The main limitation is the number of experiments that were performed due to a limit in time and imaging resources available. Protein was harvested from cells in triplicate wells for each condition, but could do with being repeated to assess whether the results could be replicated. What is promising, is that although the results are from a single experiment, they do appear to make some biological sense. A decrease in endothelial tube network could be due to a decrease in migratory signalling. As for beta-3 integrin, a Western blot was probed for matrix metalloproteinase 9 (MMP-9) as a measure of cell migration, as MMP-9 is expressed by HUVECs as part of matrix remodelling (316). Unfortunately, this Western blot was not successful and it was not possible to

repeat at the time due to a lack of protein. However, repetition of the experiment that would be scaled for more wells per condition in a 12 well assay, or scaled up further to a 6 well or 10 centimetre dishes would increase protein yield for multiple Western blot experiments.

In the lysing of cells, the lysis buffer did contain protease inhibitors, which prevent protein degradation as the cells are ruptured, but the lysis buffer did not contain phosphatase inhibitors, as mentioned in Chapter 2 Section 2.10.1, which prevent degradation of phosphorylated proteins. The cell and tube harvesting and all lysis steps were however performed on ice. Prior to cell lysis the cells were on ice for at least 4 hours and the likelihood of active cell processes occurring was highly unlikely, due to the low temperature slowing, or virtually inhibiting any enzymatic reactions. The successful detection of these proteins via Western Blot also meant that degradation did not appear evident, except perhaps for pVEGFR2, but it was uncertain whether the poor-quality blotting was due to protein degradation or poor transfer of proteins during the Western Blot protocol, as previously mentioned. Phosphatase inhibitors could easily be incorporated into the cell lysis buffer in subsequent experiments.

The number of active angiogenic proteins measured in the angiogenic axis was limited to those provided within the CST Angiogenesis Antibody Sampler Kit (#8696T) that was purchased to provide the best initial view of the angiogenic signalling cascade, with the added benefit that all the antibodies in the kit had been optimised for Western blot detection. Other proteins in the angiogenic cascade which could have been measured are numerous but may include NOS (317,318), SMAD2/3 (256,319–321), neuropillin-1 (322–327), Notch signalling (328), ephrins (329–331), Sprouty proteins (332–334) and angiopoietins (335–340) . The other tyrosine kinases, such as PDGFR (341,342), IGFR (343–346) and EGFR (347) which feeds into the same signalling pathways as VEGFR2, and have a demonstrable role in ovarian cancer could also have been assessed to see whether FXIIIA influenced signalling through these receptors.

Factor XIIIA was not tested on its own as a control in the angiogenic tube formation assays. This was omitted as it was thought to be more biologically relevant to have both VEGFA and FXIIIA present during the test conditions, as

both in theory would be present near OC tumours given the results of the positive FXIIIA in OC stroma cores, presented in Chapter 5. VEGFA alone was used as a control, to measure the angiogenic response in the absence of FXIIIA, as the effects of the variants was the primary objective of these experiments. In future assays, FXIIIA could be tested on its own, in the absence of VEGFA, to determine the effects on endothelial tube formation, and to determine whether the slowing of tube network development was due to active changes due to the presence of FXIIIA or due to toxicity of FXIIIA, which was not measured in the assays. Toxicity however, is unlikely, given the extent of tube formation demonstrated within the assays, but for the sake of thoroughness and future publication, would be a good set of experiments to perform.

In vitro experiments testing the effects of bevacizumab in the context of the angiogenesis assays would have presented an exciting and clinically relevant series of tests, especially given the source of patient data and samples from one of the principal bevacizumab clinical trials (ICON7). Remnants of bevacizumab were acquired for translational research and tested on HUVEC, but bevacizumab appeared toxic to cells and results in preliminary tests on the ability of the drug to inhibit angiogenic-stimulated proliferation were not consistent and considered unreliable. An alternative option for future work would either be to acquire fresh bevacizumab or to try one of the “biosimilars” which are currently being developed as the pharmaceutical structure of bevacizumab is now out of patent. One of these bevacizumab biosimilars, Mvasi (bevacizumab-awwb), was approved by the Food and Drug Administration in the United States, for use in non-small cell lung cancer, and metastatic cervical, renal and colorectal cancers (348,349). If approved for use in the United Kingdom, it could be used in experiments not only limited to those described here.

7.9 Concluding Remarks

This thesis aimed to build upon the limited work which had explored levels of FXIIIA in ovarian cancer (OC). Associations between SNPs within the *F13A1* gene could be used as predictors of survival outcome, in particular the linked SNPs 1951G>A and 1954G>C, and perhaps to a greater extent, the SNP

103G>T. The SNP 103G>T demonstrated heterozygote advantage in overall survival and survival post-progression intervals. This SNP also appeared to potentially influence response to platinum-based chemotherapy and the addition of the anti-angiogenic agent, bevacizumab. The resulting amino acid change from this SNP, V34L, had been linked to other disease types including cancer and thrombotic events, due to increased specific activity and crosslink density for Leu-variants. An exploration of patient tissues identified expression of FXIIIA mainly in the stromal tissue of OC and *in vitro* work established that the migratory signalling arm of the angiogenic signalling cascade is likely affected by the presence of Leu-variants. This may be why patients with this variant have a better prognosis over wildtype patients, as angiogenic recruitment is less successful, resulting in smaller tumours which would decrease metastatic potential and may be easier to treat.

As with all investigations, the questions and hypotheses which follow this work are numerous and this thesis has only scratched the surface of the role V34L could be contributing to ovarian cancer prognosis. V34L is worthy of further exploration in OC and other cancer types, and may have a bright future as a predictor of prognosis. The effects of this SNP, in particular regard to cell migration, could further the understanding of the interaction within the extracellular matrix and how these interactions lead to OC development, maintenance and spread.

Appendices

Appendix I: Ethical Approvals for Translational Research Projects

NHS
London MREC
The Old Refectory
Central Middlesex Hospital
Acton Lane
London
NW10 7NS

Telephone: 0208 453 2336
Facsimile: 0208 453 2466

14 September 2006

Dr Timothy Perren
Academic NHS Consultant and Honorary Senior Clinical Lecturer
CRUK Clinical Centre in Leeds
St James's University Hospital,
Leeds LS9 7TF

Dear Dr Perren

Full title of study: **ICON7 - A randomised, two-arm, multi-centre, Gynaecologic Cancer InterGroup (GCIG) trial of adding bevacizumab to standard chemotherapy (carboplatin and paclitaxel) in patients with epithelial ovarian cancer**
REC reference number: **06/MRE02/52**
Protocol number: **2**
EudraCT number: **2005 - 003929 - 22**

Thank you for your letter of 22 August 2006, responding to the Committee's request for further information on the above research and submitting revised documentation.

The further information has been considered on behalf of the Committee by the Vice Chairman, in consultation with two members.

Confirmation of ethical opinion

On behalf of the Committee, I am pleased to confirm a favourable ethical opinion for the above research on the basis described in the application form, protocol and supporting documentation as revised.

However, it was agreed that the measurement of blood to be taken for the study should be described as teaspoons or tablespoons in addition to ml in the patient information sheet. A revised patient information sheet should be sent to the London MREC for information only.

Ethical review of research sites

The favourable opinion applies to the research sites listed on the attached form. Confirmation of approval for other sites listed in the application will be issued as soon as local assessors have confirmed they have no objection.

Conditions of approval

The favourable opinion is given provided that you comply with the conditions set out in the attached document. You are advised to study the conditions carefully.

Approved documents

The final list of documents reviewed and approved by the Committee is as follows:

Document	*Version*	*Date*
Application	1	26 June 2006
Investigator CV	CV for Dr Timothy Perren	26 June 2006
Protocol	2	21 August 2006

Covering Letter	Letter to Ms Braley from Dr Perren	26 June 2006
Letter from Sponsor	Letter from Dr Ian Viney	06 February 2006
Peer Review	Fax to Dr Perren from Dr Kaur & Reference 3, 5, 6 & 7	27 September 2005
Statistician Comments	Letter from Professor Mahesh Parmar	22 June 2006
Questionnaire: EQ-5D- Health Questionnaire	dated 1987	
Questionnaire: EORTC QLQ-C30	3	
GP/Consultant Information Sheets	Trial Summary for GPs Version 1	21 August 2006
GP/Consultant Information Sheets	GP Letter Version 1	21 August 2006
Participant Information Sheet	1	21 August 2006
Participant Consent Form: Supplementary Patient Consent Form - Biological Samples	1	21 August 2006
Participant Consent Form	1	21 August 2006
Investigator's Brochure	for Bevacizumab 13th Version dated October 2005	
Response to Request for Further Information	Letter to Dr Steiner from Dr Perren	22 August 2006
Investigator's Brochure Addendum No. 1	dated March 2006	
Translational / Laboratory Research - An Explanation	2	21 August 2006
Quality of Life Questionnaires - An Explanation	2	21 August 2006
Part B Section 3 - Justification of Radiation Exposure		26 July 2006
Request for Authorisation from MHRA Form		26 June 2006
Letter to Dr Perren from Dr Kaur		15 May 2006
Letter from Mr Norman Thompson		20 June 2006

Research governance approval

The study should not commence at any NHS site until the local Principal Investigator has obtained final research governance approval from the R&D Department for the relevant NHS care organisation.

Statement of compliance

This Committee is recognised by the United Kingdom Ethics Committee Authority under the Medicines for Human Use (Clinical Trials) Regulations 2004, and is authorised to carry out the ethical review of clinical trials of investigational medicinal products.

The Committee is fully compliant with the Regulations as they relate to ethics committees and the conditions and principles of good clinical practice.

The Committee is constituted in accordance with the Governance Arrangements for Research Ethics Committees (July 2001) and complies fully with the Standard Operating Procedures for Research Ethics Committees in the UK.

06/MRE02/52 Please quote this number on all correspondence

With the Committee's best wishes for the success of this project

Yours sincerely

P. Jeanne Braley

Dr John W Keen
Vice Chairman

SF1 list of approved sites

London MREC
The Old Refectory
Central Middlesex Hospital
Acton Lane
London
NW10 7NS

Telephone: 0208 453 2336
Facsimile: 0208 453 2466

5th October 2006

Dr Timothy Perren
Academic NHS Consultant and Honorary Senior Clinical Lecturer
CRUK Clinical Centre in Leeds
St James's University Hospital,
Leeds LS9 7TF

Dear Dr Perren

Full title of study:	**ICON7 - A randomised, two-arm, multi-centre, Gynaecologic Cancer InterGroup (GCIG) trial of adding bevacizumab to standard chemotherapy (carboplatin and paclitaxel) in patients with epithelial ovarian cancer**
REC reference number:	**06/MRE02/52**
Protocol number:	**2**
EudraCT number:	**2005 - 003929 - 22**

Thank you for your letter dated 26th September 2006 regarding the above study.

The documents enclosed were as follows:

Letter to Ms Braley from Dr Perren	Dated 26 September 2006
Patient Information Sheet & Consent Form Version 1	Dated 21 September 2006
Supplementary Patient Consent Form – Biological Samples Version 1	Dated 21 September 2006
Translational / Laboratory Research – An explanation Version 2	Dated 21 September 2006

These documents were noted by the Chairman of the London MREC on 5th October 2006.

Best wishes

Yours sincerely

Louise Braley

Louise Braley
Manager
The London Multicentre Research Ethics Committee

Chairman Bill Kilgallen OBE
Chief Executive David Johnson

THE LEEDS TEACHING HOSPITALS

Local Research Ethics Committee

Room 5.2, Clinical Sciences Building
St James's University Hospital
Beckett Street, Leeds LS9 7TF
e-mail: comdhfo@stjames.leeds.ac.uk

19 October 2000

Enquiries to: Ann Prothero (Ethics Secretary)
Direct Line/Extension: 0113 (20) 65652

Dr R Anwar
Principal Research Fellow
Molecular Medicine Unit
Level 6
Clinical Sciences Building
St James's University Hospital

Dear Dr Anwar

Project No 00/189: Investigating the role of factor XIIIA gene polymorphisms in epithelial ovarian cancer

Thank you for your letter of 5 October enclosing a revised patient information sheet and confirming that the use of anonymised DNA samples for research purposes has been removed from the protocol. I am pleased to confirm that your study has now been approved by the Ethics Committee.

We would be very interested to receive a copy of your findings at some future date.

Yours sincerely

Ann Prothero

cc **Dr P R F Dear**
Chairman
Leeds Health Authority / St James's and Seacroft University Hospitals
Clinical Research (Ethics) Committee

Appendix II: Script for QuPath

(1) setImageType('BRIGHTFIELD_H_DAB');

(2) if (!isTMADearrayed()) {

(3)
runPlugin('qupath.imagej.detect.dearray.TMADearrayerPluginIJ', '{"coreDiameterMM": 1.25, "labelsHorizontal": "1-16", "labelsVertical": "A-J", "labelOrder": "Row first", "densityThreshold": 5, "boundsScale": 105}');

(4) return;

(5) }

(6) setColorDeconvolutionStains('{"Name" : "H-DAB KH070819", "Stain 1" : "Hematoxylin", "Values 1" : "0.53808 0.70498 0.46203 ", "Stain 2" : "DAB", "Values 2" : "0.34208 0.48571 0.80441 ", "Background" : " 239 242 239 "}');

(7) runPlugin('qupath.imagej.detect.tissue.SimpleTissueDetection2', '{"threshold": 230, "requestedPixelSizeMicrons": 4.0, "minAreaMicrons": 2000.0, "maxHoleAreaMicrons": 1000.0, "darkBackground": false, "smoothImage": true, "medianCleanup": true, "dilateBoundaries": false, "smoothCoordinates": true, "excludeOnBoundary": false, "singleAnnotation": true}');

(8) runPlugin('qupath.imagej.detect.nuclei.PositiveCellDetection', '{"detectionImageBrightfield": "Hematoxylin OD", "requestedPixelSizeMicrons": 0.01, "backgroundRadiusMicrons": 8.0, "medianRadiusMicrons": 0.0, "sigmaMicrons": 1.5, "minAreaMicrons": 10.0, "maxAreaMicrons": 400.0, "threshold": 0.01, "maxBackground": 2.0, "watershedPostProcess": true, "excludeDAB": false, "cellExpansionMicrons": 5.0, "includeNuclei": true, "smoothBoundaries": true, "makeMeasurements": true, "thresholdCompartment": "Nucleus: DAB OD mean", "thresholdPositive1": 0.2, "thresholdPositive2": 0.4, "thresholdPositive3": 0.6, "singleThreshold": false}');

(9) selectTMACores();

Appendix III: Full Cox Model for Patients in Not at High Risk of Progression Sub-cohort ICON7

Covariate	HR	Std Error	p-value	Sig	95% CI	
					Lower	Upper
Age at Diagnosis	1.03	0.01	0.010	*	1.01	1.06
Grade						
1	1.00					
2	5.14	3.87	0.030	*	1.18	22.46
3	3.26	2.37	0.104		0.78	13.58
FIGO Stage						
I	1.00					
II	1.34	0.72	0.586		0.47	3.87
III	6.55	3.26	<0.001	***	2.47	17.38
Histology						
Serous	1.00					
Mucinous	2.44	1.19	0.260		0.52	11.54
Endometrioid	1.14	0.46	0.750		0.51	2.53
Clear Cell	3.16	1.14	0.002	**	1.55	6.42
Mixed	1.04	0.43	0.917		0.46	2.35
Other	1.54	0.74	0.372		0.60	3.97
Treatment						
CP	1.00					
CP+B	1.64	0.34	0.017	*	1.09	2.45
103G>T						
GG	1.00					
G/T	0.73	1.16	0.146		0.48	1.12
TT	1.15	0.49	0.737		0.50	2.66
1694C>T						
CC	1.00					
C/T	0.98	0.22	0.919		0.63	1.51
TT	0.74	0.28	0.428		0.35	1.57
1951G>A + 1951G>C Haplotypes						
GG +GG	1.00					
GG + G/C or C/C	0.95	0.22	0.814		0.61	1.48
G/A or A/A + G/C or C/C	0.51	0.18	0.062		0.25	1.03
n=295						

CP = Carboplatin and Paclitaxel Only, CP+B = CP plus Bevacizumab.

Appendix IV: Full Cox Model for Patients At High Risk of Progression Sub-cohort ICON7

Covariate	HR	Std Error	p-value	Sig	95% CI	
					Lower	Upper
Age at Diagnosis	1.02	0.01	0.076		1.00	1.05
Grade						
1	1.00					
2	2.07	1.71	0.376		0.41	10.42
3	1.67	1.33	0.519		0.35	7.97
FIGO Stage						
I	1.00					
IV	1.09	0.25	0.707		0.69	1.71
Histology						
Serous	1.00					
Mucinous	233.30	343.29	<0.001	***	13.04	4172.88
Endometrioid	1.27	0.66	0.650		0.45	3.54
Clear Cell	4.50	2.04	0.001	**	1.85	10.93
Mixed	0.86	0.33	0.693		0.40	1.83
Other	1.39	0.69	0.505		0.53	3.66
Treatment						
CP	1.00					
CP+B	0.98	0.22	0.941		0.64	1.51
103G>T						
GG	1.00					
G/T	0.67	0.19	0.166		0.38	1.18
TT	1.03	0.41	0.948		0.47	2.24
1694C>T						
CC	1.00					
C/T	1.15	0.28	0.567		0.71	1.85
TT	3.65	1.65	0.004	***	1.51	8.84
1951G>A + 1951G>C Haplotypes						
GG +GG	1.00					
GG + G/C or C/C	1.01	0.28	0.974		0.64	1.59
G/A or A/A + G/C or C/C	0.99	1.65	0.965		0.50	1.93
n=146						

CP = Carboplatin and Paclitaxel Only, CP+B = CP plus Bevacizumab.

References

1. Siegel R, Miller K, Jemal A. Cancer statistics , 2015 . CA Cancer J Clin. 2015;65(1):21254.
2. Globocan. World 2018 [Internet]. Internatioanl Agency for Research on Cancer: The Global Cancer Observatory. 2019 [cited 2019 Sep 9]. Available from: http://gco.iarc.fr/today/data/factsheets/populations/900-world-fact-sheets.pdf
3. NCIN. A Profile of Ovarian Cancer in England [Internet]. National Cancer Intelligence Network Data Briefings. 2012 [cited 2019 Jul 29]. Available from: http://www.ncin.org.uk/publications/data_briefings/a_profile_of_ovarian_cancer_in_england
4. Cancer Research UK. One-, five- and ten-year survival for ovarian cancer. Ovarian Cancer Survival Statistics. 2014.
5. Foulkes WD, Gore M, McCluggage WG. Rare non-epithelial ovarian neoplasms: pathology, genetics and treatment. Gynecol Oncol. Elsevier; 2016;142(1):190–8.
6. Keder L, Olsen M. Gynecologic Care. Cambridge: Cambridge University Press; 2018. 474 p.
7. Shih I-M, Kurman R. Ovarian Tumorigenesis A Proposed Model Based on Morphological and Molecular Genetic Analysis. Am J Pathol. 2004;164(5):1511–8.
8. Bell DA, Scully RE. Early de novo ovarian carcinoma. A study of fourteen cases. Cancer. United States; 1994 Apr;73(7):1859–64.
9. Kurman RJ, Shih I-M. The origin and pathogenesis of epithelial ovarian cancer: a proposed unifying theory. Am J Surg Pathol [Internet]. 2010 Mar;34(3):433–43. Available from: https://www.ncbi.nlm.nih.gov/pubmed/20154587
10. Fathalla MF. Incessant Ovulation - A Factor in Ovarian Neoplasia. Lancet. 1971;July:163.
11. Huusom LD, Frederiksen K, Hogdall EVS, Glud E, Christensen L, Hogdall CK, et al. Association of reproductive factors, oral contraceptive use and selected lifestyle factors with the risk of ovarian borderline tumors: a Danish case-control study. Cancer Causes Control. Netherlands; 2006 Aug;17(6):821–9.
12. Tsilidis KK, Allen NE, Key TJ, Dossus L, Lukanova A, Bakken K, et al. Oral contraceptive use and reproductive factors and risk of ovarian cancer in the European Prospective Investigation into Cancer and Nutrition. Br J Cancer. England; 2011 Oct;105(9):1436–42.
13. Sharief LAT, Kadir RA. Congenital factor XIII deficiency in women: a systematic review of literature. Haemophilia [Internet]. 2013 Nov 1;19(6):e349–57. Available from: http://dx.doi.org/10.1111/hae.12259
14. Schildkraut J. Epithelial Ovarian Cancer Risk Among Women With Polycystic Ovary Syndrome. Obstet Gynecol [Internet]. 1996 Oct [cited 2015 Oct 29];88(4):554–9. Available from: http://www.sciencedirect.com/science/article/pii/0029784496002268
15. Gottschau M, Kjaer SK, Jensen A, Munk C, Mellemkjaer L. Risk of cancer among women with polycystic ovary syndrome: a Danish cohort study. Gynecol Oncol [Internet]. 2015 Jan [cited 2015 Oct 27];136(1):99–103. Available from:

http://www.sciencedirect.com/science/article/pii/S0090825814014759
16. Momenimovahed Z, Tiznobaik A, Taheri S, Salehiniya H. Ovarian cancer in the world: epidemiology and risk factors. Int J Womens Health [Internet]. Dove; 2019 Apr 30;11:287–99. Available from: https://www.ncbi.nlm.nih.gov/pubmed/31118829
17. Erickson BK, Conner MG, Landen Jr. CN. The role of the fallopian tube in the origin of ovarian cancer. Am J Obstet Gynecol. 2013;209(5):409–14.
18. Leeper K, Garcia R, Swisher E, Goff B, Greer B, Paley P. Pathologic findings in prophylactic oophorectomy specimens in high-risk women. Gynecol Oncol. United States; 2002 Oct;87(1):52–6.
19. Piek JMJ, Verheijen RHM, Kenemans P, Massuger LF, Bulten H, van Diest PJ. BRCA1/2-related ovarian cancers are of tubal origin: a hypothesis. Gynecol Oncol [Internet]. Elsevier; 2003 Aug 1;90(2):491. Available from: https://doi.org/10.1016/S0090-8258(03)00365-2
20. Marquez RT, Baggerly KA, Patterson AP, Liu J, Broaddus R, Frumovitz M, et al. Patterns of gene expression in different histotypes of epithelial ovarian cancer correlate with those in normal fallopian tube, endometrium, and colon. Clin cancer Res. AACR; 2005;11(17):6116–26.
21. Cass I, Holschneider C, Datta N, Barbuto D, Walts AE, Karlan BY. BRCA-mutation-associated fallopian tube carcinoma: a distinct clinical phenotype? Obstet Gynecol. United States; 2005 Dec;106(6):1327–34.
22. Callahan MJ, Crum CP, Medeiros F, Kindelberger DW, Elvin JA, Garber JE, et al. Primary fallopian tube malignancies in BRCA-positive women undergoing surgery for ovarian cancer risk reduction. J Clin Oncol. United States; 2007 Sep;25(25):3985–90.
23. Zhang Y, Cao L, Nguyen D, Lu H. TP53 mutations in epithelial ovarian cancer. Transl Cancer Res [Internet]. 2016 Dec;5(6):650–63. Available from: https://www.ncbi.nlm.nih.gov/pubmed/30613473
24. Soussi T, Ishioka C, Claustres M, Beroud C. Locus-specific mutation databases: pitfalls and good practice based on the p53 experience. Nature reviews. Cancer. England; 2006. p. 83–90.
25. Lee Y, Medeiros F, Kindelberger D, Callahan MJ, Muto MG, Crum CP. Advances in the recognition of tubal intraepithelial carcinoma: applications to cancer screening and the pathogenesis of ovarian cancer. Adv Anat Pathol. United States; 2006 Jan;13(1):1–7.
26. Przybycin CG, Kurman RJ, Ronnett BM, Shih I-M, Vang R. Are all pelvic (nonuterine) serous carcinomas of tubal origin? Am J Surg Pathol. United States; 2010 Oct;34(10):1407–16.
27. Kuhn E, Kurman RJ, Vang R, Sehdev AS, Han G, Soslow R, et al. TP53 mutations in serous tubal intraepithelial carcinoma and concurrent pelvic high-grade serous carcinoma--evidence supporting the clonal relationship of the two lesions. J Pathol. England; 2012 Feb;226(3):421–6.
28. Peyssonnaux C, Eychène A. The Raf/MEK/ERK pathway: new concepts of activation. Biol Cell. Wiley Online Library; 2001;93(1-2):53–62.
29. Singer G, Oldt III R, Cohen Y, Wang BG, Sidransky D, Kurman RJ, et al. Mutations in BRAF and KRAS characterize the development of low-grade ovarian serous carcinoma. J Natl Cancer Inst. Oxford University Press; 2003;95(6):484–6.
30. Vang R, Shih I-M, Kurman RJ. Ovarian low-grade and high-grade serous carcinoma: pathogenesis, clinicopathologic and molecular biologic features, and diagnostic problems. Adv Anat Pathol. NIH Public Access; 2009;16(5):267.

31. Kohler MF, Marks JR, Wiseman RW, Jacobs IJ, Davidoff AM, Clarke-Pearson DL, et al. Spectrum of mutation and frequency of allelic deletion of the p53 gene in ovarian cancer. JNCI J Natl Cancer Inst. Oxford University Press; 1993;85(18):1513–9.
32. Kupryjańczyk J, Thor AD, Beauchamp R, Merritt V, Edgerton SM, Bell DA, et al. p53 gene mutations and protein accumulation in human ovarian cancer. Proc Natl Acad Sci. National Acad Sciences; 1993;90(11):4961–5.
33. Chan W-Y, Cheung K-K, Schorge JO, Huang L-W, Welch WR, Bell DA, et al. Bcl-2 and p53 protein expression, apoptosis, and p53 mutation in human epithelial ovarian cancers. Am J Pathol. Elsevier; 2000;156(2):409–17.
34. Ross JS, Yang F, Kallakury B V, Sheehan CE, Ambros RA, Muraca PJ. HER-2/neu oncogene amplification by fluorescence in situ hybridization in epithelial tumors of the ovary. Am J Clin Pathol. England; 1999 Mar;111(3):311–6.
35. Bonazzoli E, Cocco E, Lopez S, Bellone S, Zammataro L, Bianchi A, et al. PI3K oncogenic mutations mediate resistance to afatinib in HER2/neu overexpressing gynecological cancers. Gynecol Oncol. United States; 2019 Apr;153(1):158–64.
36. Bellacosa A, De Feo D, Godwin AK, Bell DW, Cheng JQ, Altomare DA, et al. Molecular alterations of the AKT2 oncogene in ovarian and breast carcinomas. Int J cancer. Wiley Online Library; 1995;64(4):280–5.
37. Cheng JQ, Ruggeri B, Klein WM, Sonoda G, Altomare DA, Watson DK, et al. Amplification of AKT2 in human pancreatic cells and inhibition of AKT2 expression and tumorigenicity by antisense RNA. Proc Natl Acad Sci. National Acad Sciences; 1996;93(8):3636–41.
38. Nakayama K, Nakayama N, Kurman RJ, Cope L, Pohl G, Samuels Y, et al. Sequence mutations and amplification of PIK3CA and AKT2 genes in purified ovarian serous neoplasms. Cancer Biol Ther. Taylor & Francis; 2006;5(7):779–85.
39. Xing H, Weng D, Chen G, Tao W, Zhu T, Yang X, et al. Activation of fibronectin/PI-3K/Akt2 leads to chemoresistance to docetaxel by regulating survivin protein expression in ovarian and breast cancer cells. Cancer Lett. Elsevier; 2008;261(1):108–19.
40. Garzetti GG, Ciavattini A, Goteri G, De Nictolis M, Stramazzotti D, Lucarini G, et al. Ki67 antigen immunostaining (MIB 1 monoclonal antibody) in serous ovarian tumors: index of proliferative activity with prognostic significance. Gynecol Oncol. United States; 1995 Feb;56(2):169–74.
41. Sallum LF, Andrade L, Bastos Eloy da Costa L, Ramalho S, Ferracini AC, Natal R de A, et al. BRCA1, Ki67, and β-Catenin Immunoexpression Is Not Related to Differentiation, Platinum Response, or Prognosis in Women With Low- and High-Grade Serous Ovarian Carcinoma. Int J Gynecol Cancer [Internet]. 2018 Mar 1;28(3):437 LP-447. Available from: http://ijgc.bmj.com/content/28/3/437.abstract
42. Urosevic M, Willers J, Mueller B, Kempf W, Burg G, Dummer R. HLA-G protein up-regulation in primary cutaneous lymphomas is associated with interleukin-10 expression in large cell T-cell lymphomas and indolent B-cell lymphomas. Blood. United States; 2002 Jan;99(2):609–17.
43. Singer G, Rebmann V, Chen Y-C, Liu H-T, Ali SZ, Reinsberg J, et al. HLA-G is a potential tumor marker in malignant ascites. Clin Cancer Res.

United States; 2003 Oct;9(12):4460–4.
44. Lisio M-A, Fu L, Goyeneche A, Gao Z-H, Telleria C. High-Grade Serous Ovarian Cancer: Basic Sciences, Clinical and Therapeutic Standpoints. Int J Mol Sci [Internet]. MDPI; 2019 Feb 22;20(4):952. Available from: https://www.ncbi.nlm.nih.gov/pubmed/30813239
45. Tothill RW, Tinker A V, George J, Brown R, Fox SB, Lade S, et al. Novel Molecular Subtypes of Serous and Endometrioid Ovarian Cancer Linked to Clinical Outcome. Clin Cancer Res [Internet]. 2008 Aug 15;14(16):5198–208. Available from: http://clincancerres.aacrjournals.org/content/14/16/5198.abstract
46. Network CGAR. Integrated genomic analyses of ovarian carcinoma. Nature. Nature Publishing Group; 2011;474(7353):609.
47. Verhaak RGW, Tamayo P, Yang J-Y, Hubbard D, Zhang H, Creighton CJ, et al. Prognostically relevant gene signatures of high-grade serous ovarian carcinoma. J Clin Invest. United States; 2013 Jan;123(1):517–25.
48. Konecny GE, Wang C, Hamidi H, Winterhoff B, Kalli KR, Dering J, et al. Prognostic and Therapeutic Relevance of Molecular Subtypes in High-Grade Serous Ovarian Cancer. JNCI J Natl Cancer Inst [Internet]. 2014 Sep 30;106(10). Available from: https://doi.org/10.1093/jnci/dju249
49. Wang C, Armasu SM, Kalli KR, Maurer MJ, Heinzen EP, Keeney GL, et al. Pooled Clustering of High-Grade Serous Ovarian Cancer Gene Expression Leads to Novel Consensus Subtypes Associated with Survival and Surgical Outcomes. Clin Cancer Res [Internet]. 2017 Aug 1;23(15):4077 LP-4085. Available from: http://clincancerres.aacrjournals.org/content/23/15/4077.abstract
50. Prat J, Oncology FC on G. Staging classification for cancer of the ovary, fallopian tube, and peritoneum. Int J Gynecol Obstet. Wiley Online Library; 2014;124(1):1–5.
51. Javadi S, Ganeshan DM, Qayyum A, Iyer RB, Bhosale P. Ovarian Cancer, the revised FIGO Staging System, and the Role of Imaging. Am J Roentgenol. 2016;206(6):1351–60.
52. Jacobs I, Oram D, Fairbanks J, Turner J, Frost C, Grudzinskas JG. A risk of malignancy index incorporating CA 125, ultrasound and menopausal status for the accurate preoperative diagnosis of ovarian cancer. BJOG An Int J Obstet Gynaecol. Wiley Online Library; 1990;97(10):922–9.
53. Qayyum A, Coakley F V, Westphalen AC, Hricak H, Okuno WT, Powell B. Role of CT and MR imaging in predicting optimal cytoreduction of newly diagnosed primary epithelial ovarian cancer. Gynecol Oncol [Internet]. 2005;96(2):301–6. Available from: http://www.sciencedirect.com/science/article/pii/S0090825804008248
54. National Institute for Care and Health Excellence. Ovarian Cancer: Recognition and Initial Management [Internet]. Clinical Guidelines CG122. 2011 [cited 2019 Sep 11]. Available from: https://www.nice.org.uk/guidance/cg122
55. Elattar A, Bryant A, Winter-Roach BA, Hatem M, Naik R. Optimal primary surgical treatment for advanced epithelial ovarian cancer. Cochrane database Syst Rev [Internet]. John Wiley & Sons, Ltd; 2011 Aug 10;2011(8):CD007565-CD007565. Available from: https://www.ncbi.nlm.nih.gov/pubmed/21833960
56. Fields EC, McGuire WP, Lin L, Temkin SM. Radiation Treatment in Women with Ovarian Cancer: Past, Present, and Future. Front Oncol [Internet]. Frontiers Media S.A.; 2017 Aug 21;7:177. Available from:

https://www.ncbi.nlm.nih.gov/pubmed/28871275
57. Hall EJ, Giaccia AJ. Radiobiology for the Radiologist. Lippincott Williams & Wilkins; 2006.
58. Reed E. Platinum-DNA adduct, nucleotide excision repair and platinum based anti-cancer chemotherapy. Cancer Treat Rev. Elsevier; 1998;24(5):331–44.
59. Bowden NA. Nucleotide excision repair: Why is it not used to predict response to platinum-based chemotherapy? Cancer Lett [Internet]. 2014;346(2):163–71. Available from: http://www.sciencedirect.com/science/article/pii/S0304383514000317
60. Luvero D, Milani A, Ledermann JA. Treatment options in recurrent ovarian cancer: latest evidence and clinical potential. Ther Adv Med Oncol [Internet]. SAGE Publications; 2014 Sep;6(5):229–39. Available from: https://www.ncbi.nlm.nih.gov/pubmed/25342990
61. Stuart GCE, Kitchener H, Bacon M, duBois A, Friedlander M, Ledermann J, et al. 2010 Gynecologic Cancer InterGroup (GCIG) consensus statement on clinical trials in ovarian cancer: report from the Fourth Ovarian Cancer Consensus Conference. Int J Gynecol Cancer. England; 2011 May;21(4):750–5.
62. Friedlander M, Trimble E, Tinker A, Alberts D, Avall-Lundqvist E, Brady M, et al. Clinical trials in recurrent ovarian cancer. Int J Gynecol Cancer. England; 2011 May;21(4):771–5.
63. Horwitz SB. Taxol (paclitaxel): mechanisms of action. Ann Oncol Off J Eur Soc Med Oncol. 1994;5:S3-6.
64. NICE. Guidance on the use of paclitaxel in the treatment of ovarian cancer: NICE technology appraisal guidance [TA55]. London; 2003.
65. Morgan RD, Clamp AR, Zhou C, Saunders G, Mescallado N, Welch R, et al. Dose-dense cisplatin with gemcitabine for relapsed platinum-resistant ovarian cancer. Int J Gynecol Cancer. England; 2019 Jan;
66. Mutch DG, Orlando M, Goss T, Teneriello MG, Gordon AN, McMeekin SD, et al. Randomized phase III trial of gemcitabine compared with pegylated liposomal doxorubicin in patients with platinum-resistant ovarian cancer. J Clin Oncol. American Society of Clinical Oncology; 2007;25(19):2811–8.
67. Pujade-Lauraine E, Wagner U, Aavall-Lundqvist E, Gebski V, Heywood M, Vasey PA, et al. Pegylated liposomal Doxorubicin and Carboplatin compared with Paclitaxel and Carboplatin for patients with platinum-sensitive ovarian cancer in late relapse. J Clin Oncol. United States; 2010 Jul;28(20):3323–9.
68. Huang Y-F, Kuo MT, Liu Y-S, Cheng Y-M, Wu P-Y, Chou C-Y. A Dose Escalation Study of Trientine Plus Carboplatin and Pegylated Liposomal Doxorubicin in Women With a First Relapse of Epithelial Ovarian, Tubal, and Peritoneal Cancer Within 12 Months After Platinum-Based Chemotherapy. Frontiers in oncology. Switzerland; 2019. p. 437.
69. Fujiwara H, Ushijima K, Nagao S, Takei Y, Shimada M, Takano M, et al. A phase II randomized controlled study of pegylated liposomal doxorubicin and carboplatin vs. gemcitabine and carboplatin for platinum-sensitive recurrent ovarian cancer (GOTIC003/intergroup study). Int J Clin Oncol. Japan; 2019 Oct;24(10):1284–91.
70. Hanahan D, Weinberg RA. Hallmarks of cancer: the next generation. Cell [Internet]. Elsevier; 2011;144(5):646–74. Available from: http://www.cell.com/article/S0092867411001279/fulltext

71. Masoumi Moghaddam S, Amini A, Morris D, Pourgholami M. Significance of vascular endothelial growth factor in growth and peritoneal dissemination of ovarian cancer. Cancer metastasis reviews. 2011. 143-162 p.
72. Anagnostopoulos A, Taylor S, Kirwan J. Ovarian cancer: current management and future directions. Obstet Gynaecol Reprod Med. 2014;25(2):37–42.
73. Ferrara N, Hillan KJ, Novotny W. Bevacizumab (Avastin), a humanized anti-VEGF monoclonal antibody for cancer therapy. Biochem Biophys Res Commun [Internet]. 2005;333(2):328–35. Available from: http://www.sciencedirect.com/science/article/pii/S0006291X05011344
74. Burger RA, Brady MF, Bookman MA, Fleming GF, Monk BJ, Huang H, et al. Incorporation of bevacizumab in the primary treatment of ovarian cancer. N Engl J Med. Mass Medical Soc; 2011;365(26):2473–83.
75. NICE. Ovarian Cancer: Recognition and Initial Management (CG122). London; 2011.
76. Dyer M, Richardson J, Robertson J, Adam J. NICE guidance on bevacizumab in combination with paclitaxel and carboplatin for the first-line treatment of advanced ovarian cancer. Lancet Oncol [Internet]. 2013 Jul [cited 2016 Jan 6];14(8):689–90. Available from: http://www.sciencedirect.com/science/article/pii/S1470204513702481
77. Colombo N, Conte PF, Pignata S, Raspagliesi F, Scambia G. Bevacizumab in ovarian cancer: Focus on clinical data and future perspectives. Crit Rev Oncol Hematol [Internet]. 2016 Jan [cited 2016 Jan 6];97:335–48. Available from: http://www.sciencedirect.com/science/article/pii/S1040842815300329
78. Perren TJ, Swart AM, Pfisterer J, Ledermann JA, Pujade-Lauraine E, Kristensen G, et al. A Phase 3 Trial of Bevacizumab in Ovarian Cancer. N Engl J Med [Internet]. Massachusetts Medical Society; 2011 Dec 28;365(26):2484–96. Available from: http://dx.doi.org/10.1056/NEJMoa1103799
79. Oza AM, Cook AD, Pfisterer J, Embleton A, Ledermann JA, Pujade-Lauraine E, et al. Standard chemotherapy with or without bevacizumab for women with newly diagnosed ovarian cancer (ICON7): overall survival results of a phase 3 randomised trial. Lancet Oncol [Internet]. 2015 Aug [cited 2015 Dec 30];16(8):928–36. Available from: http://www.sciencedirect.com/science/article/pii/S1470204515000868
80. Aghajanian C, Blank S V, Goff BA, Judson PL, Teneriello MG, Husain A, et al. OCEANS: a randomized, double-blind, placebo-controlled phase III trial of chemotherapy with or without bevacizumab in patients with platinum-sensitive recurrent epithelial ovarian, primary peritoneal, or fallopian tube cancer. J Clin Oncol. American Society of Clinical Oncology; 2012;30(17):2039.
81. Pujade-Lauraine E, Hilpert F, Weber B, Reuss A, Poveda A, Kristensen G, et al. Bevacizumab combined with chemotherapy for platinum-resistant recurrent ovarian cancer: the AURELIA open-label randomized phase III trial. Obstet Gynecol Surv. LWW; 2014;69(7):402–4.
82. Coleman RL, Brady MF, Herzog TJ, Sabbatini P, Armstrong DK, Walker JL, et al. A phase III randomized controlled clinical trial of carboplatin and paclitaxel alone or in combination with bevacizumab followed by bevacizumab and secondary cytoreductive surgery in platinum-sensitive, recurrent ovarian, peritoneal primary and fallopian . Gynecol Oncol.

Elsevier; 2015;137:3–4.
83. Spratlin JL, Cohen RB, Eadens M, Gore L, Camidge DR, Diab S, et al. Phase I pharmacologic and biologic study of ramucirumab (IMC-1121B), a fully human immunoglobulin G1 monoclonal antibody targeting the vascular endothelial growth factor receptor-2. J Clin Oncol. American Society of Clinical Oncology; 2010;28(5):780–7.
84. Matei D, Sill MW, Lankes HA, DeGeest K, Bristow RE, Mutch D, et al. Activity of sorafenib in recurrent ovarian cancer and primary peritoneal carcinomatosis: a gynecologic oncology group trial. J Clin Oncol. American Society of Clinical Oncology; 2011;29(1):69–75.
85. Biagi JJ, Oza AM, Chalchal HI, Grimshaw R, Ellard SL, Lee U, et al. A phase II study of sunitinib in patients with recurrent epithelial ovarian and primary peritoneal carcinoma: an NCIC Clinical Trials Group Study. Ann Oncol. Eur Soc Med Oncology; 2011;22(2):335–40.
86. Davidson BA, Secord AA. Profile of pazopanib and its potential in the treatment of epithelial ovarian cancer. Int J Womens Health. New Zealand; 2014;6:289–300.
87. Havrilesky LJ, Abernethy AP. Quality of life in ICON7: need for patients' perspectives. Lancet Oncol [Internet]. 2013 Mar [cited 2016 Jan 6];14(3):183–5. Available from: http://www.sciencedirect.com/science/article/pii/S1470204512705909
88. Rossi L, Verrico M, Zaccarelli E, Papa A, Colonna M, Strudel M, et al. Bevacizumab in ovarian cancer: A critical review of phase III studies. Oncotarget. Impact Journals, LLC; 2017;8(7):12389.
89. Stark D, Nankivell M, Pujade-Lauraine E, Kristensen G, Elit L, Stockler M, et al. Standard chemotherapy with or without bevacizumab in advanced ovarian cancer: quality-of-life outcomes from the International Collaboration on Ovarian Neoplasms (ICON7) phase 3 randomised trial. Lancet Oncol [Internet]. 2013 Mar [cited 2015 Dec 3];14(3):236–43. Available from: http://www.sciencedirect.com/science/article/pii/S1470204512705673
90. Ramus SJ, Gayther SA. The contribution of BRCA1 and BRCA2 to ovarian cancer. Mol Oncol. United States; 2009 Apr;3(2):138–50.
91. Merajver SD, Pham TM, Caduff RF, Chen M, Poy EL, Cooney KA, et al. Somatic mutations in the BRCA1 gene in sporadic ovarian tumours. Nat Genet. United States; 1995 Apr;9(4):439–43.
92. Ashworth A. A synthetic lethal therapeutic approach: poly(ADP) ribose polymerase inhibitors for the treatment of cancers deficient in DNA double-strand break repair. J Clin Oncol. United States; 2008 Aug;26(22):3785–90.
93. Fong PC, Yap TA, Boss DS, Carden CP, Mergui-Roelvink M, Gourley C, et al. Poly(ADP)-ribose polymerase inhibition: frequent durable responses in BRCA carrier ovarian cancer correlating with platinum-free interval. J Clin Oncol. United States; 2010 May;28(15):2512–9.
94. Ledermann JA, Pujade-Lauraine E. Olaparib as maintenance treatment for patients with platinum-sensitive relapsed ovarian cancer. Ther Adv Med Oncol. England; 2019;11:1758835919849753.
95. Vetter MH, Hays JL. Use of Targeted Therapeutics in Epithelial Ovarian Cancer: A Review of Current Literature and Future Directions. Clin Ther [Internet]. 2018;40(3):361–71. Available from: http://www.sciencedirect.com/science/article/pii/S0149291818300456
96. Bedard PL, Tabernero J, Janku F, Wainberg ZA, Paz-Ares L,

Vansteenkiste J, et al. A phase Ib dose-escalation study of the oral pan-PI3K inhibitor buparlisib (BKM120) in combination with the oral MEK1/2 inhibitor trametinib (GSK1120212) in patients with selected advanced solid tumors. Clin Cancer Res. AACR; 2015;21(4):730–8.

97. Thorpe LM, Yuzugullu H, Zhao JJ. PI3K in cancer: divergent roles of isoforms, modes of activation and therapeutic targeting. Nat Rev Cancer [Internet]. Nature Publishing Group, a division of Macmillan Publishers Limited. All Rights Reserved.; 2014 Dec 23;15:7. Available from: https://doi.org/10.1038/nrc3860
98. Goltsov A, Faratian D, Langdon SP, Bown J, Goryanin I, Harrison DJ. Compensatory effects in the PI3K/PTEN/AKT signaling network following receptor tyrosine kinase inhibition. Cell Signal [Internet]. 2011;23(2):407–16. Available from: http://www.sciencedirect.com/science/article/pii/S0898656810002986
99. Lutz RJ. Targeting the folate receptor for the treatment of ovarian cancer. Transl Cancer Res Vol 4, No 1 (February 2015) Transl Cancer Res (Epithelial ovarian cancer Treat Integr Mol targeting) [Internet]. 2015; Available from: http://tcr.amegroups.com/article/view/3838
100. Ledermann JA, Canevari S, Thigpen T. Targeting the folate receptor: diagnostic and therapeutic approaches to personalize cancer treatments. Ann Oncol. Oxford University Press; 2015;26(10):2034–43.
101. Cortez AJ, Tudrej P, Kujawa KA, Lisowska KM. Advances in ovarian cancer therapy. Cancer Chemother Pharmacol [Internet]. 2018;81(1):17–38. Available from: https://doi.org/10.1007/s00280-017-3501-8
102. Hafter R, Klaubert W, Gollwitzer R, von Hugo R, Graeff H. Crosslinked fibrin derivatives and fibronectin in ascitic fluid from patients with ovarian cancer compared to ascitic fluid in liver cirrhosis. Thromb Res [Internet]. 1984;35(1):53–64. Available from: http://www.sciencedirect.com/science/article/pii/0049384884903128
103. Wilhelm O, Hafter R, Coppenrath E, Pflanz MA, Schmitt M, Babic R, et al. Fibrin-fibronectin compounds in human ovarian tumor ascites and their possible relation to the tumor stroma. Cancer Res. United States; 1988 Jun;48(12):3507–14.
104. Rieppi M, Vergani V, Gatto C, Zanetta G, Allavena P, Taraboletti G, et al. Mesothelial cells induce the motility of human ovarian carcinoma cells. Int J cancer. Wiley Online Library; 1999;80(2):303–7.
105. Kenny HA, Kaur S, Coussens LM, Lengyel E. The initial steps of ovarian cancer cell metastasis are mediated by MMP-2 cleavage of vitronectin and fibronectin. J Clin Invest. Am Soc Clin Investig; 2008;118(4):1367–79.
106. Kenny HA, Chiang C-Y, White EA, Schryver EM, Habis M, Romero IL, et al. Mesothelial cells promote early ovarian cancer metastasis through fibronectin secretion. J Clin Invest. Am Soc Clin Investig; 2014;124(10):4614–28.
107. Wang JP, Hielscher A. Fibronectin: How Its Aberrant Expression in Tumors May Improve Therapeutic Targeting. J Cancer [Internet]. Ivyspring International Publisher; 2017 Feb 25;8(4):674–82. Available from: https://www.ncbi.nlm.nih.gov/pubmed/28367247
108. Tomasini-Johansson BR, Kaufman NR, Ensenberger MG, Ozeri V, Hanski E, Mosher DF. A 49-residue peptide from adhesin F1 of Streptococcus pyogenes inhibits fibronectin matrix assembly. J Biol Chem. United States; 2001 Jun;276(26):23430–9.
109. Chiang H-Y, Korshunov VA, Serour A, Shi F, Sottile J. Fibronectin is an

important regulator of flow-induced vascular remodeling. Arterioscler Thromb Vasc Biol. United States; 2009 Jul;29(7):1074–9.
110. Hielscher A, Ellis K, Qiu C, Porterfield J, Gerecht S. Fibronectin Deposition Participates in Extracellular Matrix Assembly and Vascular Morphogenesis. PLoS One. United States; 2016;11(1):e0147600.
111. Cho A, Howell VM, Colvin EK. The Extracellular Matrix in Epithelial Ovarian Cancer – A Piece of a Puzzle. Front Oncol [Internet]. Frontiers Media S.A.; 2015 Nov 2;5:245. Available from: http://www.ncbi.nlm.nih.gov/pmc/articles/PMC4629462/
112. Shen Y, Shen R, Ge L, Zhu Q, Li F. Fibrillar type I collagen matrices enhance metastasis/invasion of ovarian epithelial cancer via β1 integrin and PTEN signals. Int J Gynecol Cancer. BMJ Specialist Journals; 2012;22(8):1316–24.
113. Rice AJ, Cortes E, Lachowski D, Cheung BCH, Karim SA, Morton JP, et al. Matrix stiffness induces epithelial–mesenchymal transition and promotes chemoresistance in pancreatic cancer cells. Oncogenesis. Nature Publishing Group; 2017;6(7):e352.
114. McKenzie AJ, Hicks SR, Svec K V, Naughton H, Edmunds ZL, Howe AK. The mechanical microenvironment regulates ovarian cancer cell morphology, migration, and spheroid disaggregation. Sci Rep [Internet]. 2018;8(1):7228. Available from: https://doi.org/10.1038/s41598-018-25589-0
115. Oudin MJ, Weaver VM. Physical and Chemical Gradients in the Tumor Microenvironment Regulate Tumor Cell Invasion, Migration, and Metastasis. Cold Spring Harb Symp Quant Biol [Internet]. 2016 Jan 1;81:189–205. Available from: http://symposium.cshlp.org/content/81/189.abstract
116. Smoter M, Bodnar L, Grala B, Stec R, Zieniuk K, Kozlowski W, et al. Tau protein as a potential predictive marker in epithelial ovarian cancer patients treated with paclitaxel/platinum first-line chemotherapy. J Exp Clin Cancer Res. BioMed Central; 2013;32(1):25.
117. Gurler H, Yu Y, Choi J, Kajdacsy-Balla A, Barbolina M. Three-dimensional collagen type I matrix up-regulates nuclear isoforms of the microtubule associated protein tau implicated in resistance to paclitaxel therapy in ovarian carcinoma. Int J Mol Sci. Multidisciplinary Digital Publishing Institute; 2015;16(2):3419–33.
118. Kessenbrock K, Plaks V, Werb Z. Matrix Metalloproteinases: Regulators of the Tumor Microenvironment. Cell. 2010;141.
119. Wang L, Jin X, Lin D, Liu Z, Zhang X, Lu Y, et al. Clinicopathologic significance of claudin-6, occludin, and matrix metalloproteinases− 2 expression in ovarian carcinoma. Diagn Pathol. BioMed Central; 2013;8(1):190.
120. Che Y-L, Luo S-J, Li G, Cheng M, Gao Y-M, Li X-M, et al. The C3G/Rap1 pathway promotes secretion of MMP-2 and MMP-9 and is involved in serous ovarian cancer metastasis. Cancer Lett. Elsevier; 2015;359(2):241–9.
121. Sillanpää S, Anttila M, Voutilainen K, Ropponen K, Turpeenniemi-Hujanen T, Puistola U, et al. Prognostic significance of matrix metalloproteinase-9 (MMP-9) in epithelial ovarian cancer. Gynecol Oncol. Elsevier; 2007;104(2):296–303.
122. Bergers G, Brekken R, McMahon G, Vu TH, Itoh T, Tamaki K, et al. Matrix metalloproteinase-9 triggers the angiogenic switch during

carcinogenesis. Nat Cell Biol. England; 2000 Oct;2(10):737–44.
123. Facchiano A, Facchiano F. Transglutaminases and their substrates in biology and human diseases: 50 years of growing. Amino Acids. Springer; 2009;36(4):599–614.
124. Muszbek L, Haramura G, Polgar J. Transformation of cellular factor XIII into an active zymogen transglutaminase in thrombin-stimulated platelets. Thromb Haemost. GERMANY; 1995 Apr;73(4):702–5.
125. Bohn H. Comparative studies on the fibrin-stabilizing factors from human plasma, platelets and placenta. Ann N Y Acad Sci. 1972;202:256–72.
126. The Human Protein Atlas. F13A1. Tissue Atlas.
127. Yorifuji H, Anderson K, Lynch GW, Van de Water L, McDonagh J. B protein of factor XIII: differentiation between free B and complexed B. Blood. 1988;72(5):1645–50.
128. Schwartz ML, Pizzo S V, Hill RL, McKee PA. Human factor XIII from plasma and platelets molecular weights, subunit structures, proteolytic activation, and cross-linking of fibrinogen and fibrin. J Biol Chem. ASBMB; 1973;248(4):1395–407.
129. Ádány R, Bárdos H. Factor XIII subunit A as an intracellular transglutaminase. Cell Mol Life Sci C [Internet]. 2003;60(6):1049–60. Available from: http://dx.doi.org/10.1007/s00018-003-2178-9
130. KOMÁROMI I, BAGOLY Z, MUSZBEK L. Factor XIII: novel structural and functional aspects. J Thromb Haemost [Internet]. Wiley Online Library; 2011;9(1):9–20. Available from: http:https://doi.org/10.1111/j.1538-7836.2010.04070.x
131. Yee VC, Pederson LC, Le Trong I, Bishop PD, Stenkamp RE, Teller DC. Three-dimensional structure of a transglutaminase: Human blood coagulation factor XIII. Proc Natl Acad Sci USA. 1994;91:7296–300.
132. Fox B, Yee V, Pederson L, Le Trong I, Bishop PD, Stenkamp RE, et al. Identification of the Calcium Binding Site and a Novel Ytterbium Site in Blood Coagulation Factor XIII by X-ray Crystallography. J Biol Chem. 1999;274(8):4917–23.
133. Stieler M, Weber J, Hils M, Kolb P, Heine A, Büchold C, et al. Structure of active coagulation factor XIII triggered by calcium binding: basis for the design of next-generation anticoagulants. Angew Commun Int Ed. 2013;52:11930–4.
134. Singh S, Akhter SM, Dodt J, Volkers P, Reuter A, Reinhart C, et al. Identification of Potential Novel Interacting Partners for Coagulation Factor XIII B (FXIII-B) Subunit, a Protein Associated with a Rare Bleeding Disorder. International Journal of Molecular Sciences. 2019.
135. Garzon RJ, Pratt KP, Bishop PD, Le Trong I, Stenkamp RE, Teller DC. Tryptophan 279 is Essential for the Transglutaminase Activity of Coagulation Factor XIII: Functional and Structural Characterization [Internet]. Royal Society for Structural Biology Protein Data Bank; Available from: https://www.rcsb.org/structure/1EX0
136. Weiss MS, Metzner HJ, Hilgenfeld R. Two non-proline cis peptide bonds may be important for factor XIII function. FEBS Lett. Wiley Online Library; 1998;423(3):291–6.
137. Ichinose A, Davie EW. Characterization of the gene for the a subunit of human factor XIII (plasma transglutaminase), a blood coagulation factor. Proc Natl Acad Sci U S A [Internet]. 1988;85(16):5829–33. Available from: http://www.ncbi.nlm.nih.gov/pubmed/2901091
138. Ichinose A, McMullen BA, Fujikawa K, Davie EW. Amino acid sequence

of the b subunit of human factor XIII, a protein composed of ten repetitive segments. Biochemistry. United States; 1986 Aug;25(16):4633–8.
139. Carrell NA, Erickson HP, McDonagh J. Electron microscopy and hydrodynamic properties of factor XIII subunits. J Biol Chem. United States; 1989 Jan;264(1):551–6.
140. Gupta S, Biswas A, Akhter MS, Krettler C, Reinhart C, Dodt J, et al. Revisiting the mechanism of coagulation factor XIII activation and regulation from a structure/functional perspective. Sci Rep [Internet]. Nature Publishing Group; 2016 Jul 25;6:30105. Available from: https://www.ncbi.nlm.nih.gov/pubmed/27453290
141. Souri M, Osaki T, Ichinose A. The Non-catalytic B Subunit of Coagulation Factor XIII Accelerates Fibrin Cross-linking. J Biol Chem. United States; 2015 May;290(19):12027–39.
142. Singh S, Akhter MS, Dodt J, Sharma A, Kaniyappan S, Yadegari H, et al. Disruption of Structural Disulfides of Coagulation FXIII-B Subunit; Functional Implications for a Rare Bleeding Disorder. Int J Mol Sci. Switzerland; 2019 Apr;20(8).
143. Katona É, Pénzes K, Csapó A, Fazakas F, Udvardy ML, Bagoly Z, et al. Interaction of factor XIII subunits. Blood. Am Soc Hematology; 2014;123(11):1757–63.
144. Janus TJ, Lewis SD, Lorand L, Shafer JA. Promotion of thrombin-catalyzed activation of factor XIII by fibrinogen. Biochemistry. UNITED STATES; 1983 Dec;22(26):6269–72.
145. Ivaskevicius V, Biswas A, Bevans C, Schroeder V, Kohler HP, Rott H, et al. Identification of eight novel coagulation factor XIII subunit A mutations: implied consequences for structure and function. Haematologica [Internet]. 2010;95(6):956–62. Available from: http://www.pubmedcentral.nih.gov/articlerender.fcgi?artid=2878794&tool=pmcentrez&rendertype=abstract
146. Pedersen LC, Yee VC, Bishop PD, Le Trong I, Teller DC, Stenkamp RE. Transglutaminase factor XIII uses proteinase-like catalytic triad to crosslink macromolecules. Protein Sci. United States; 1994 Jul;3(7):1131–5.
147. Kristiansen GK, Andersen MD. Reversible Activation of Cellular Factor XIII by Calcium. J Biol Chem [Internet]. 9650 Rockville Pike, Bethesda, MD 20814, U.S.A.: American Society for Biochemistry and Molecular Biology; 2011 Mar 18;286(11):9833–9. Available from: http://www.ncbi.nlm.nih.gov/pmc/articles/PMC3059041/
148. Muszbek L, Polgár J, Boda Z. Platelet factor XIII becomes active without the release of activation peptide during platelet activation. Thromb Haemost. Schattauer GmbH; 1993;70(3):282–5.
149. Polgár J, Hidasi V, Muszbek L. Non-proteolytic activation of cellular protransglutaminase (placenta macrophage factor XIII). Biochem J. Portland Press Limited; 1990;267(2):557–60.
150. Mitchell JL, Lionikiene AS, Fraser SR, Whyte CS, Booth NA, Mutch NJ. Functional factor XIII-A is exposed on the stimulated platelet surface. Blood [Internet]. 2014 Oct 20;124(26):3982–90. Available from: http://www.bloodjournal.org/content/124/26/3982.abstract
151. Al-Jallad HF, Myneni VD, Piercy-Kotb SA, Chabot N, Mulani A, Keillor JW, et al. Plasma membrane factor XIIIA transglutaminase activity regulates osteoblast matrix secretion and deposition by affecting microtubule dynamics. PLoS One. Public Library of Science;

2011;6(1):e15893.
152. Piercy-Kotb SA, Mousa A, Al-Jallad HF, Myneni VD, Chicatun F, Nazhat SN, et al. Factor XIIIA transglutaminase expression and secretion by osteoblasts is regulated by extracellular matrix collagen and the MAP kinase signaling pathway. J Cell Physiol. Wiley Online Library; 2012;227(7):2936–46.
153. Ádány R, Bárdos H, Antal M, Módis L, Sárváry A, Szücs S, et al. Factor XIII of blood coagulation as a nuclear crosslinking enzyme. Thromb Haemost. Schattauer GmbH; 2001;85(5):845–51.
154. Cordell PA, Kile BT, Standeven KF, Josefson EC, Pease RJ, Grant PJ. Association of coagulation factor XIII-A with Golgi proteins within monocyte-macrophages: implications for subcellular trafficking and secretion. Blood. 2010;115:2674–81.
155. Nikolajsen CL, Dyrlund TF, Poulsen ET, Enghild JJ, Scavenius C. Coagulation factor XIIIa substrates in human plasma: identification and incorporation into the clot. J Biol Chem. United States; 2014 Mar;289(10):6526–34.
156. Ariens RAS, Lai T-S, Weisel JW, Greenberg CS, Grant PJ. Role of factor XIII in fibrin clot formation and effects of genetic polymorphisms. Blood. United States; 2002 Aug;100(3):743–54.
157. Richardson VR, Cordell P, Standeven KF, Carter AM. Substrates of Factor XIII-A: roles in thrombosis and wound healing. Clin Sci [Internet]. 2013 Feb 1;124(3):123–37. Available from: http://www.clinsci.org/content/124/3/123.abstract
158. Folk JE. Mechanism and basis for specificity of transglutaminasecatalyzed-(-glutamyl) lysine bond formation. Adv Enzym Relat Areas Mol Biol. 1983;54:1–56.
159. Lorand L, Ong HH, Lipinski B, Rule NG, Downey J, Jacobsen A. Lysine as amine donor in fibrin crosslinking. Biochem Biophys Res Commun [Internet]. 1966;25(6):629–37. Available from: http://www.sciencedirect.com/science/article/pii/0006291X66905018
160. Matacic S, Loewy AG. The identification of isopeptide crosslinks in insoluble fibrin. Biochem Biophys Res Commun. United States; 1968 Feb;30(4):356–62.
161. Shi D-Y, Wang S-J. Advances of Coagulation Factor XIII. Chin Med J (Engl) [Internet]. Medknow Publications & Media Pvt Ltd; 2017 Jan 20;130(2):219–23. Available from: https://www.ncbi.nlm.nih.gov/pubmed/28091415
162. Fraser SR, Booth NA, Mutch NJ. The antifibrinolytic function of factor XIII is exclusively expressed through alpha(2)-antiplasmin cross-linking. Blood. United States; 2011 Jun;117(23):6371–4.
163. TRANDAB. FXIIIa Substrates [Internet]. 2007 [cited 2019 Sep 12]. Available from: http://genomics.dote.hu/wiki/index.php/Category:FXIIIa
164. Muszbek L, Bereczky Z, Bagoly Z, Komáromi I, Katona É. Factor XIII: A Coagulation Factor With Multiple Plasmatic and Cellular Functions. Physiol Rev [Internet]. 2011 Jul 8;91(3):931–72. Available from: http://physrev.physiology.org/content/91/3/931.abstract
165. Adány R, Muszbek L. Immunohistochemical detection of factor XIII subunit a in histiocytes of human uterus. Histochemistry [Internet]. 1989;91(2):169–74. Available from: https://doi.org/10.1007/BF00492391
166. Anwar R, Gallivan L, Edmonds SD, Markham AF. Genotype/phenotype correlations for coagulation factor XIII: specific normal polymorphisms are

associated with high or low factor XIII specific activity. Blood. Am Soc Hematology; 1999;93(3):897–905.
167. López Ramírez Y, Vivenes M, Miller A, Pulido A, López Mora J, Arocha-Piñango CL, et al. Prevalence of the coagulation factor XIII polymorphism Val34Leu in women with recurrent miscarriage. Clin Chim Acta [Internet]. 2006 Dec [cited 2016 Mar 4];374(1–2):69–74. Available from: http://www.sciencedirect.com/science/article/pii/S0009898106003366
168. Jeddi-Tehrani M, Torabi R, Mohammadzadeh A, Arefi S, Keramatipour M, Zeraati H, et al. Investigating Association of Three Polymorphisms of Coagulation Factor XIII and Recurrent Pregnancy Loss. Am J Reprod Immunol [Internet]. Blackwell Publishing Ltd; 2010 Sep 1;64(3):212–7. Available from: http://dx.doi.org/10.1111/j.1600-0897.2010.00838.x
169. Al-Khabori M, Pathare A, Menegatti M, Peyvandi F. Recombinant factor XIII A-subunit in a patient with factor XIII deficiency and recurrent pregnancy loss. J Thromb Haemost. England; 2018 Jun;16(6):1052–4.
170. Jung JH, Kim J-H, Song GG, Choi SJ. Association of the F13A1 Val34Leu polymorphism and recurrent pregnancy loss: A meta-analysis. Eur J Obstet Gynecol Reprod Biol. Ireland; 2017 Aug;215:234–40.
171. Bigdeli R, Younesi MR, Panahnejad E, Asgary V, Heidarzadeh S, Mazaheri H, et al. Association between thrombophilia gene polymorphisms and recurrent pregnancy loss risk in the Iranian population. Syst Biol Reprod Med. England; 2018 Aug;64(4):274–82.
172. Diaz-Nunez M, Rabanal A, Exposito A, Ferrando M, Quintana F, Soria JM, et al. Recurrent Miscarriage and Implantation Failure of Unknown Cause Studied by a Panel of Thrombophilia Conditions: Increased Frequency of FXIII Val34Leu Polymorphism. J Reprod Infertil. Iran; 2019;20(2):76–82.
173. Porrello A, Leslie PL, Harrison EB, Gorentla BK, Kattula S, Ghosh SK, et al. Factor XIIIA—expressing inflammatory monocytes promote lung squamous cancer through fibrin cross-linking. Nat Commun [Internet]. 2018;9(1):1988. Available from: https://doi.org/10.1038/s41467-018-04355-w
174. Seitz R, Leugner F, Katschinski M, Immel A, Kraus M, Egbring R, et al. Ulcerative colitis and Crohn's disease: factor XIII, inflammation and haemostasis. Digestion. Karger Publishers; 1994;55(6):361–7.
175. Torocsik D, Bardos H, Nagy L, Adany R. Identification of factor XIII-A as a marker of alternative macrophage activation. Cell Mol Life Sci. Switzerland; 2005 Sep;62(18):2132–9.
176. Raghu H, Cruz C, Rewerts CL, Frederick MD, Thornton S, Mullins ES, et al. Transglutaminase factor XIII promotes arthritis through mechanisms linked to inflammation and bone erosion. Blood. United States; 2015 Jan;125(3):427–37.
177. Esnault S, Kelly EA, Sorkness RL, Evans MD, Busse WW, Jarjour NN. Airway factor XIII associates with type 2 inflammation and airway obstruction in asthmatic patients. J Allergy Clin Immunol. United States; 2016 Mar;137(3):767–73.e6.
178. Tao G-Z, Liu B, Zhang R, Liu G, Abdullah F, Harris MC, et al. Impaired Activity of Blood Coagulant Factor XIII in Patients with Necrotizing Enterocolitis. Sci Rep. England; 2015 Aug;5:13119.
179. Moretti FA, Chauhan AK, Iaconcig A, Porro F, Baralle FE, Muro AF. A major fraction of fibronectin present in the extracellular matrix of tissues is plasma-derived. J Biol Chem. ASBMB; 2007;282(38):28057–62.

180. Bentmann A, Kawelke N, Moss D, Zentgraf H, Bala Y, Berger I, et al. Circulating fibronectin affects bone matrix, whereas osteoblast fibronectin modulates osteoblast function. J Bone Miner Res. Wiley Online Library; 2010;25(4):706–15.
181. Mousa A, Cui C, Song A, Myneni VD, Sun H, Li JJ, et al. Transglutaminases factor XIII-A and TG2 regulate resorption, adipogenesis and plasma fibronectin homeostasis in bone and bone marrow. Cell Death Differ [Internet]. 2017/04/07. Nature Publishing Group; 2017 May;24(5):844–54. Available from: https://www.ncbi.nlm.nih.gov/pubmed/28387755
182. Cordell PA, Newell LM, Standeven KF, Adamson PJ, Simpson KR, Smith KA, et al. Normal bone deposition occurs in mice deficient in factor XIII-A and transglutaminase 2. Matrix Biol. Elsevier; 2015;43:85–96.
183. Semenza GL. Vasculogenesis, angiogenesis, and arteriogenesis: mechanisms of blood vessel formation and remodeling. J Cell Biochem. Wiley Online Library; 2007;102(4):840–7.
184. Dardik R, Loscalzo J, Inbal a. Factor XIII (FXIII) and angiogenesis. J Thromb Haemost [Internet]. 2006;4(1):19–25. Available from: http://www.ncbi.nlm.nih.gov/pubmed/16855365
185. Dardik R, Solomon A, Loscalzo J, Eskaraev R, Bialik A, Goldberg I, et al. Novel proangiogenic effect of factor XIII associated with suppression of thrombospondin 1 expression. Arterioscler Thromb Vasc Biol. 2003;23(8):1472–7.
186. Dardik R, Loscalzo J, Inbal A. Factor XIII (FXIII) and angiogenesis. Journal of Thrombosis and Haemostasis. 2006. p. 19–25.
187. Dardik R, Loscalzo J, Eskaraev R, Inbal A. Molecular Mechanisms Underlying the Proangiogenic Effect of Factor XIII. Arterioscler Thromb Vasc Biol [Internet]. 2005 Mar 1;25(3):526–32. Available from: http://atvb.ahajournals.org/content/25/3/526.abstract
188. Gemmati D, Vigliano M, Burini G, Mari R, Hossam Abd El Mohsein H, Parmeggiani F, et al. Coagulation Factor XIIIA (F13A1): Novel Perspectives in Treatment and Pharmacogenetics. Curr Pharm Des. 2016;22:1449–59.
189. Gallivan L, Markham AF, Anwar R. The Leu564 factor XIIIA variant results in significantly lower plasma factor XIII levels than the Pro564 variant. Thromb Haemost. 1999;82(4):1368–70.
190. Kohler HP, Ariens RA, Whitaker P, Grant PJ. A common coding polymorphism in the FXIII A-subunit gene (FXIIIVal34Leu) affects cross-linking activity. Thrombosis and haemostasis. Germany; 1998. p. 704.
191. Ariens RA, Philippou H, Nagaswami C, Weisel JW, Lane DA, Grant PJ. The factor XIII V34L polymorphism accelerates thrombin activation of factor XIII and affects cross-linked fibrin structure. Blood. United States; 2000 Aug;96(3):988–95.
192. de Lange M, Andrew T, Snieder H, Ge D, Futers TS, Standeven K, et al. Joint Linkage and Association of Six Single-Nucleotide Polymorphisms in the Factor XIII-A Subunit Gene Point to V34L As the Main Functional Locus. Arterioscler Thromb Vasc Biol [Internet]. 2006 Aug 1;26(8):1914–9. Available from: http://atvb.ahajournals.org/content/26/8/1914.abstract
193. Li B, Zhang L, Yin Y, Pi Y, Yang Q, Gao C, et al. Lack of evidence for association between factor XIII-A Val34Leu polymorphism and ischemic stroke: a meta-analysis of 8,800 subjects. Thromb Res [Internet]. 2012 Oct [cited 2015 Oct 16];130(4):654–60. Available from:

http://www.sciencedirect.com/science/article/pii/S0049384811006268
194. Kobbervig C, Williams E. FXIII polymorphisms, fibrin clot structure and thrombotic risk. Biophys Chem. 2004;112(2):223–8.
195. Ramacciotti E, Wolosker N, Puech-Leao P, Zeratti EA, Gusson PR, del Giglio A, et al. Prevalence of factor V Leiden, FII G20210A, FXIII Val34Leu and MTHFR C677T polymorphisms in cancer patients with and without venous thrombosis. Thromb Res [Internet]. 2003 Feb [cited 2016 Jan 20];109(4):171–4. Available from: http://www.sciencedirect.com/science/article/pii/S0049384803001798
196. Van Hylckama Vlieg A, Komanasin N, Ariens RAS, Poort SR, Grant PJ, Bertina RM, et al. Factor XIII Val34Leu polymorphism, factor XIII antigen levels and activity and the risk of deep venous thrombosis. Br J Haematol. England; 2002 Oct;119(1):169–75.
197. Ansani L, Marchesini J, Pestelli G, Luisi G, Scillitani G, Longo G, et al. F13A1 Gene Variant (V34L) and Residual Circulating FXIIIA Levels Predict Short- and Long-Term Mortality in Acute Myocardial Infarction after Coronary Angioplasty. Int J Mol Sci. 2018;19(9).
198. Balogh L, Katona E, Mezei ZA, Kallai J, Gindele R, Edes I, et al. Effect of factor XIII levels and polymorphisms on the risk of myocardial infarction in young patients. Mol Cell Biochem. Netherlands; 2018 Nov;448(1–2):199–209.
199. Glover CJ, McIntire L V, Brown CH, Natelson EA. Rheological properties of fibrin clots. Effects of fibrinogen concentration, Factor XIII deficiency, and Factor XIII inhibition. J Lab Clin Med. Elsevier; 1975;86(4):644–56.
200. Jensen PH, Lorand L, Ebbesen P, Gliemann J. Type-2 plasminogen-activator inhibitor is a substrate for trophoblast transglutaminase and Factor XIIIa: Transglutaminase-catalyzed cross-linking to cellular and extracellular structures. Eur J Biochem. Wiley Online Library; 1993;214(1):141–6.
201. Rao KMK, Newcomb TF. Clot retraction in a factor XIII free system. Scand J Haematol. Wiley Online Library; 1980;24(2):142–8.
202. Jelenska M, Kopeć M, Breddin K. On the retraction of collagen and fibrin induced by normal, defective and modified platelets. Pathophysiol Haemost Thromb. Karger Publishers; 1985;15(3):169–75.
203. Kasahara K, Souri M, Kaneda M, Miki T, Yamamoto N, Ichinose A. Impaired clot retraction in factor XIII A subunit–deficient mice. Blood. Am Soc Hematology; 2010;115(6):1277–9.
204. Aleman MM, Holle LA, Stember KG, Devette CI, Monroe DM, Wolberg AS. Cystamine preparations exhibit anticoagulant activity. PLoS One. Public Library of Science; 2015;10(4):e0124448.
205. Aleman MM, Byrnes JR, Wang J-G, Tran R, Lam WA, Di Paola J, et al. Factor XIII activity mediates red blood cell retention in venous thrombi. J Clin Invest. Am Soc Clin Investig; 2014;124(8):3590–600.
206. Cines DB, Lebedeva T, Nagaswami C, Hayes V, Massefski W, Litvinov RI, et al. Clot contraction: compression of erythrocytes into tightly packed polyhedra and redistribution of platelets and fibrin. Blood. Am Soc Hematology; 2014;123(10):1596–603.
207. Wolberg A. Factor XIII and Red Blood Cells in Venous Thrombosis. Blood. 2015;126(23):SC1-14.
208. Reiner a P, Schwartz SM, Frank MB, Longstreth WT, Hindorff L a, Teramura G, et al. Polymorphisms of coagulation factor XIII subunit A and risk of nonfatal hemorrhagic stroke in young white women. Stroke.

2001;32:2580–6.
209. Bereczky Z, Muszbek L. Factor XIII and venous thromboembolism. In: Seminars in thrombosis and hemostasis. © Thieme Medical Publishers; 2011. p. 305–14.
210. Kucher N, Schroeder V, Kohler HP. Role of blood coagulation factor XIII in patients with acute pulmonary embolism. Correlation of factor XIII antigen levels with pulmonary occlusion rate, fibrinogen, D-dimer, and clot firmness. Thromb Haemost. Germany; 2003 Sep;90(3):434–8.
211. Tinholt M, Sandset PM, Iversen N. Polymorphisms of the coagulation system and risk of cancer. Thromb Res. 2016;140:S49–54.
212. Wojtukiewicz MZ, Kloczko J, Bielawiec M, Galar M. Heterogeneity of factor XIII plasmatic substrate concentrations in different tumour types. In: Factor XIII Second International Conference, Marbury, July 9-10, 1991. Stuttgart-New York: Schattauer Verlag; 1993.
213. Morrissey C, True LD, Roudier MP, Coleman IM, Hawley S, Nelson PS, et al. Differential expression of angiogenesis associated genes in prostate cancer bone, liver and lymph node metastases. Clin Exp Metastasis [Internet]. 2008;25(4):377–88. Available from: https://doi.org/10.1007/s10585-007-9116-4
214. Lee SH, Suh IB, Lee EJ, Hur GY, Lee SY, Lee SY, et al. Relationships of Coagulation Factor XIII Activity with Cell-Type and Stage of Non-Small Cell Lung Cancer. Yonsei Med J [Internet]. Yonsei University College of Medicine; 2013 Nov;54(6):1394–9. Available from: http://synapse.koreamed.org/DOIx.php?id=10.3349%2Fymj.2013.54.6.1394
215. Kiss F, Hevessy Z, Veszpremi A, Katona E, Kiss C, Vereb G, et al. Leukemic lymphoblasts, a novel expression site of coagulation factor XIII subunit A. Thromb Haemost [Internet]. 2006;96(2):176–82. Available from: http://www.ncbi.nlm.nih.gov/pubmed/16894461
216. Karai B, Hevessy Z, Szantho E, Csathy L, Ujfalusi A, Gyurina K, et al. Expression of Coagulation Factor XIII Subunit A Correlates with Outcome in Childhood Acute Lymphoblastic Leukemia. Pathol Oncol Res. Netherlands; 2018 Apr;24(2):345–52.
217. Kappelmayer J, Simon A, Katona E, Szanto A, Nagy L, Kiss A, et al. Coagulation factor XIII-A a flow cytometric intracellular marker in the classification of acute myeloid leukemias. Thromb Haemost. 2005;94(2):454–9.
218. Kiss F, Simon A, Csathy L, Hevessy Z, Katona E, Kiss C, et al. A Coagulation Factor Becomes Useful in the Study of Acute Leukemias: Studies with Blood Coagulation Factor XIII. Int Soc Anal Cytol Cytom Part A. 2008;73A:194–201.
219. Vossen CY, Hoffmeister M, Chang-Claude JC, Rosendaal FR, Brenner H. Clotting factor gene polymorphisms and colorectal cancer risk. J Clin Oncol. United States; 2011 May;29(13):1722–7.
220. Vairaktaris E, Vassiliou S, Yapijakis C, Spyridonidou S, Vylliotis A, Derka S, et al. Increased risk for oral cancer is associated with coagulation factor XIII but not with factor XII. Oncol Rep. Greece; 2007 Dec;18(6):1537–43.
221. Wersch JWJ van, Peters C, Ubachs JMH. Coagulation factor XIII in plasma of patients with benign and malignant gynaecological tumours. Clin Chem Lab Med. 1994;32(9):681–4.
222. Nagy JA, Masse EM, Herzberg KT, Meyers MS, Yeo K-T, Yeo T-K, et al.

Pathogenesis of Ascites Tumor Growth: Vascular Permeability Factor, Vascular Hyperpermeability, and Ascites Fluid Accumulation. Cancer Res [Internet]. 1995 Jan 15;55(2):360–8. Available from: http://cancerres.aacrjournals.org/content/55/2/360.abstract

223. van Hinsbergh VWM, Collen A, Koolwijk P. Role of Fibrin Matrix in Angiogenesis. Ann N Y Acad Sci [Internet]. John Wiley & Sons, Ltd (10.1111); 2001 Jun 1;936(1):426–37. Available from: https://doi.org/10.1111/j.1749-6632.2001.tb03526.x
224. Feng X, Tonneson MG, Mousa SA, Clark RAF. Fibrin and Collagen Differentially but Synergistically Regulate Sprout Angiogenesis of Human Dermal Microvascular Endothelial Cells in 3-Dimensional Matrix. Int J Cell Biol. 2013;2013(ID:231279).
225. Hadjipanayi E, Kuhn P-H, Moog P, Bauer A-T, Kuekrek H, Mirzoyan L, et al. The Fibrin Matrix Regulates Angiogenic Responses within the Hemostatic Microenvironment through Biochemical Control. PLoS One [Internet]. Public Library of Science; 2015 Aug 28;10(8):e0135618. Available from: https://doi.org/10.1371/journal.pone.0135618
226. Calvert AH, Newell DR, Gumbrell LA, O'Reilly S, Burnell M, Boxall FE, et al. Carboplatin dosage: prospective evaluation of a simple formula based on renal function. J Clin Oncol. United States; 1989 Nov;7(11):1748–56.
227. National Comprehensive Cancer Network. Appendix B: Carboplatin Dosing [Internet]. NCCN Chemotherapy Order Templates (NCCN Templates (R)). 2018 [cited 2019 Sep 14]. Available from: https://www.nccn.org/professionals/OrderTemplates/PDF/appendix_B.pdf
228. Lonza. Clonetics Endothelial Cell System Technical Information & Instructions [Internet]. 2018 [cited 2019 Sep 25]. p. 1–15. Available from: https://bioscience.lonza.com/lonza_bs/US/en/download/product/asset/29423
229. Mosmann T. Rapid colorimetric assay for cellular growth and survival: application to proliferation and cytotoxicity assays. J Immunol Methods. Elsevier; 1983;65(1–2):55–63.
230. Riss TL, Moravec RA, Niles AL, Duellman S, Benink HA, Worzella TJ, et al. Cell Viability Assays. In: Sittampalam GS, A G, Brimacombe K, Al. E, editors. Assay Guidance Manual [Internet]. Bethesda, MA: Eli Lilly & Company and the National Center for Advancing Translational Sciences; 2013.
231. Faulkner A, Purcell R, Hibbert A, Latham S, Thomson S, Hall WL, et al. A thin layer angiogenesis assay: a modified basement matrix assay for assessment of endothelial cell differentiation. BMC Cell Biol [Internet]. BioMed Central; 2014 Dec 5;15:41. Available from: https://www.ncbi.nlm.nih.gov/pubmed/25476021
232. Merck. Angiogenesis Tube Formation Protocol [Internet]. ECM Gel Matrix: Protocols Using EHS Basement Membrane Extracts. 2019 [cited 2019 Sep 18]. Available from: https://www.sigmaaldrich.com/technical-documents/articles/biofiles/ecm-gel-product-protocols.html
233. Nolan-Stevaux O, Zhong W, Culp S, Shaffer K, Hoover J, Wickramasinghe D, et al. Endoglin Requirement for BMP9 Signaling in Endothelial Cells Reveals New Mechanism of Action for Selective Anti-Endoglin Antibodies. PLoS One [Internet]. Public Library of Science; 2012 Dec 27;7(12):e50920. Available from: https://doi.org/10.1371/journal.pone.0050920
234. Anwar R, Stewart a D, Miloszewski KJ, Losowsky MS, Markham a F.

Molecular basis of inherited factor XIII deficiency: identification of multiple mutations provides insights into protein function. Br J Haematol [Internet]. 1995;91(3):728–35. Available from: http://www.ncbi.nlm.nih.gov/pubmed/8555083

235. Schroeder V, Vuissoz J-M, Caflisch A, Kohler HP. Factor XIII activation peptide is released into plasma upon cleavage by thrombin and shows a different structure compared to its bound form. Thromb Haemost. Germany; 2007 Jun;97(6):890–8.
236. Carpentier G, Martinelli M, Courty J, Cascone I. Angiogenesis Analyzer for ImageJ. In: 4th ImageJ User and Developer Conference Proceedings. Mondorf-les-Bains, Luxembourg; 2012. p. 198–201.
237. Schneider CA, Rasband WS, Eliceiri KW. NIH Image to ImageJ: 25 years of image analysis. Nat Methods. 2012;9(7):671–5.
238. Xie D, Ju D, Speyer C, Gorski D, Kosir MA. Strategic Endothelial Cell Tube Formation Assay: Comparing Extracellular Matrix and Growth Factor Reduced Extracellular Matrix. J Vis Exp [Internet]. MyJove Corporation; 2016 Aug 14;(114):54074. Available from: https://www.ncbi.nlm.nih.gov/pubmed/27585062
239. Schindelin J, Arganda-Carreras I, Frise E, Kaynig V, Longair M, Pietzsch T, et al. Fiji: an open-source platform for biological-image analysis. Nat Methods [Internet]. 2012;9(7):676–82. Available from: https://doi.org/10.1038/nmeth.2019
240. R Core Team. R: A language and enviornment for statistical computing [Internet]. R Foundation for Statistical Computing. 2013 [cited 2019 Jul 18]. Available from: http://www.r-project.org
241. Owzar K, Li Z, Cox N, Jung S-H. Power and sample size calculations for SNP association studies with censored time-to-event outcomes. Genet Epidemiol [Internet]. 2012/06/08. 2012 Sep;36(6):538–48. Available from: https://www.ncbi.nlm.nih.gov/pubmed/22685040
242. Owzar K, Li Z, Cox N, Jung S-H, Chanyee Y. Package “survSNP” [Internet]. Power Calculations for SNP Studies with Censored Outcomes. 2016 [cited 2019 Jul 18]. Available from: https://bitbucket.org/kowzar/survsnp
243. MRC/NCRI Gynecologic Cancer Intergroup. ICON7 Protocol Version 4.0 [Internet]. ICON7 Bevacizumab in Ovarian Cancer. 2009 [cited 2016 Jan 21]. Available from: https://www.ctu.mrc.ac.uk/media/1316/icon7-protocol-v-40-15-october-09.pdf
244. Natarajan L, Pu M, Parker BA, Thomson CA, Caan B, Flatt SW, et al. Time-Varying Effects of Prognostic Factors Associated with Disease-Free Survival in Breast Cancer. Am J Epidemiol. 2009;169(12):1463–70.
245. Gravis G, Boher J-M, Joly F, Soulie M, Albiges L, Priou F, et al. Androgen Deprivation Therapy (ADT) Plus Docetaxel Verus ADT Alone in Metastatic Noncastrate Prostate Cancer: Impact of Metastatic Burden and Long-term Survival Analysis of the Randomized Phase 3 GETUG-AFU15 Trial. Eur Urol. 2016;70(2):256–62.
246. Yu Y, Carey M, Pollett W, Green J, Dicks E, Parfey P, et al. The long-term survival characteristics of a cohort of colorectal cancer patients and baseline varialbes associated with survival outcomes with or without time-varying effects. BMC Med. 2019;17(Article 150).
247. Kobbervig C, Williams E. FXIII polymorphisms, fibrin clot structure and thrombotic risk. Biophys Chem. 2004;112(2–3 SPEC. ISS.):223–8.
248. Ahmadi M, Nasiri M, Ebrahimi A. Thrombosis-Related Factors FV and

F13A1 Mutations in Uterine Myomas. Zahedan J Res Med Sci. 2016;(e4836).
249. Cleves M. Hardy-Weinberg equilibrium test and allele frequency estimation. Stata Tech Bull. 1999 Feb 1;8.
250. Stangroom J. Chi Square Calculator for 2x2 [Internet]. Social Science Statistics. 2019 [cited 2019 Sep 17]. Available from: https://www.socscistatistics.com/tests/chisquare/default.aspx
251. Bagoly Z, Koncz Z, Hársfalvi J, Muszbek L. Factor XIII, clot structure, thrombosis. Thromb Res. 2012;129(3):382–7.
252. Tan T, Yang H, Ye J, Low J, Choolani M, Tan D, et al. CSIODVB: a microarray gene expression database of epithelial ovarian cancer subtype. Oncotarget. 2015;6(41):43843–52.
253. Tan TZ, Miow QH, Huang RY-J, Wong MK, Ye J, Lau JA, et al. Functional genomics identifies five distinct molecular subtypes with clinical relevance and pathways for growth control in epithelial ovarian cancer. EMBO Mol Med. England; 2013 Jul;5(7):1051–66.
254. Gyorffy B, Lanczky A, Szallasi Z. Implementing an online tool for genome-wide validation of survival-associated biomarkers in ovarian-cancer using microarray data from 1287 patients. Endocr Relat Cancer. England; 2012 Apr;19(2):197–208.
255. Gyorffy B, Molnar B, Lage H, Szallasi Z, Eklund AC. Evaluation of Microarray Preprocessing Algorithms Based on Concordance with RT-PCR in Clinical Samples. PLoS One [Internet]. Public Library of Science; 2009 May 21;4(5):e5645. Available from: https://doi.org/10.1371/journal.pone.0005645
256. Zhang Q, Wang C, Cliby WA. Cancer-associated stroma significantly contributes to the mesenchymal subtype signature of serous ovarian cancer. Gynecol Oncol [Internet]. 2019;152(2):368–74. Available from: http://www.sciencedirect.com/science/article/pii/S009082581831415X
257. Hirsch FR, Varella-Garcia M, Bunn Jr PA, Di Maria M V, Veve R, Bremnes RM, et al. Epidermal growth factor receptor in non–small-cell lung carcinomas: correlation between gene copy number and protein expression and impact on prognosis. J Clin Oncol. American Society of Clinical Oncology; 2003;21(20):3798–807.
258. Kejner AE, Burch MB, Sweeny L, Rosenthal EL. Bone morphogenetic protein 6 expression in oral cavity squamous cell cancer is associated with bone invasion. Laryngoscope. United States; 2013 Dec;123(12):3061–5.
259. The Human Protein Atlas. F13A1 [Internet]. Pathology Atlas: Ovarian Cancer. 2019 [cited 2019 Aug 21]. Available from: https://www.proteinatlas.org/ENSG00000124491-F13A1/pathology/tissue/ovarian+cancer
260. Polterauer S, Grimm C, Seebacher V, Concin N, Marth C, Tomovski C, et al. Plasma Fibrinogen Levels and Prognosis in Patients with Ovarian Cancer: A Multicenter Study. Oncol [Internet]. 2009 Oct 1;14(10):979–85. Available from: http://theoncologist.alphamedpress.org/content/14/10/979.abstract
261. Nemes Z, Thomazy V. Identification of Histiocytic Reticulum Cells by the Immunohistochemical Demonstration of Factor XIII (F-XIIIa) in Human Lymph Nodes. J Pathol. 1986;149:121–32.
262. Nemeth AJ, Penneys NS. Factor XIIIa is expressed by fibroblasts in fibrovascular tumors. J Cutan Pathol. 1989;16:266–71.

263. Yoneda J, Kuniyasu H, Price JE, Bucana CD, Fidler IJ, Crispens MA. Expression of Angiogenesis-Related Genes and Progression of Human Ovarian Carcinomas in Nude Mice. J Natl Cancer Inst [Internet]. 1998 Mar 18;90(6):447–54. Available from: http://jnci.oxfordjournals.org/content/90/6/447.abstract
264. Herzog B, Pellet-Many C, Britton G, Hartzoulakis B, Zachary IC, Heldin C-H. VEGF binding to NRP1 is essential for VEGF stimulation of endothelial cell migration, complex formation between NRP1 and VEGFR2, and signaling via FAK Tyr407 phosphorylation. Mol Biol Cell [Internet]. American Society for Cell Biology (mboc); 2011 Jun 8;22(15):2766–76. Available from: https://doi.org/10.1091/mbc.e09-12-1061
265. Oh H, Takagi H, Otani A, Koyama S, Kemmochi S, Uemura A, et al. Selective induction of neuropilin-1 by vascular endothelial growth factor (VEGF): A mechanism contributing to VEGF-induced angiogenesis. Proc Natl Acad Sci [Internet]. 2002 Jan 8;99(1):383 LP-388. Available from: http://www.pnas.org/content/99/1/383.abstract
266. Hanahan D, Weinberg RA. Hallmarks of cancer: The next generation. Cell. 2011. p. 646–74.
267. Wojtukiewicz MZ, Zacharski LR, Memoli VA, Kisiel W, Kudryk BJ, Rousseau SM, et al. Malignant melanoma. Interaction with coagulation and fibrinolysis pathways in situ. Am J Clin Pathol. England; 1990 Apr;93(4):516–21.
268. Dvorak HF, Harvey VS, Estrella P, Brown LF, McDonagh J, Dvorak AM. Fibrin containing gels induce angiogenesis. Implications for tumor stroma generation and wound healing. Lab Invest. United States; 1987 Dec;57(6):673–86.
269. Wang X, Wang E, Kavanagh JJ, Freedman RS. Ovarian cancer, the coagulation pathway, and inflammation. J Transl Med [Internet]. London: BioMed Central; 2005 Jun 21;3:25. Available from: http://www.ncbi.nlm.nih.gov/pmc/articles/PMC1182397/
270. Hwang JY, Mangala LS, Fok JY, Lin YG, Merritt WM, Spannuth WA, et al. Clinical and Biological Significance of Tissue Transglutaminase in Ovarian Carcinoma. Cancer Res [Internet]. 2008 Jul 15;68(14):5849–58. Available from: http://cancerres.aacrjournals.org/content/68/14/5849.abstract
271. Uhlen M, Zhang C, Lee S, Sjostedt E, Fagerberg L, Bidkhori G, et al. A pathology atlas of the human cancer transcriptome. Science. United States; 2017 Aug;357(6352).
272. The Human Protein Atlas. The Human Protein Atlas [Internet]. [cited 2019 Sep 3]. Available from: http://www.proteinatlas.org
273. The Human Protein Atlas. TCGA RNA-seq data [Internet]. Technical Data: Assays & Annotation. [cited 2019 Sep 3]. Available from: https://www.proteinatlas.org/about/assays+annotation
274. Haroon Z, Hettasch J, Lai T-S, Dewhirst M, Greenberg C. Tissue transglutaminase is expressed, active, and directly involved in rat dermal wound healing and angiogenesis. Fed Am Soc Exp Biol. 1999;13(13).
275. Cagliani R, Riva S, Marino C, Fumagalli M, D'Angelo MG, Riva V, et al. Variants in SNAP25 are targets of natural selection and influence verbal performances in women. Cell Mol Life Sci [Internet]. 2012;69(10):1705–15. Available from: https://doi.org/10.1007/s00018-011-0896-y
276. Gochhait S, Bukhari SIA, Bairwa N, Vadhera S, Darvishi K, Raish M, et al. Implication of BRCA2-26G>A 5' untranslated region polymorphism in

susceptibility to sporadic breast cacner and its modulation by p53 codon 72 Arg>Pro polymorphism. Breast Cancer Res. 2007;9(R71).
277. Verhaegh GW, Verkleij L, Vermeulen SHHM, den Heijer M, Witjes JA, Kiemeney LA. Polymorphisms in the H19 Gene and the Risk of Bladder Cancer. Eur Urol [Internet]. 2008;54(5):1118–26. Available from: http://www.sciencedirect.com/science/article/pii/S0302283808001115
278. Li X, Shao M, Wang S, Zhao X, Chen H, Qian J, et al. Heterozygote advantage of methylenetetrahydrofolate reductase polymorphisms on clinical outcomes in advanced non-small cell lung cancer (NSCLC) patients treated with platinum-based chemotherapy. Tumor Biol [Internet]. 2014;35(11):11159–70. Available from: https://doi.org/10.1007/s13277-014-2427-6
279. Wang S, Abdou A, Morton L, Thomas R, Cerhan J, Gao X, et al. Human leukocyte antigen class I and II alleles in non-Hodgkin lymphoma etiology. Blood. 2010;115(23):4820–3.
280. Colson F, Sigha B, Arrese J, Quatresooz P, Rorvive A, Collignon J, et al. Paclitaxel-Related Lymphedema and Scleroderma-Like Skin Changes. J Clin Case Reports. 2013;3(11).
281. Paragh L, Törõcsik D. Factor XIII Subunit A in the Skin: Applications in Diagnosis and Treatment. Biomed Res Int. 2017;2017(ID 3571861).
282. Bronstad A, Berg A, Reed RK. Effects of the taxanes paclitaxel and docetaxel on edema formation and interstitial fluid pressure. Am J Physiol Heart Circ Physiol. United States; 2004 Aug;287(2):H963-8.
283. Liu X, Zhu S, Wang T, Hummers L, Wigley FM, Goldschmidt-Clermont PJ, et al. Paclitaxel modulates TGFbeta signaling in scleroderma skin grafts in immunodeficient mice. PLoS Med. United States; 2005 Dec;2(12):e354.
284. Hsi ED, Nickoloff BJ. Dermatofibroma and dermatofibrosarcoma protuberans: an immunohistochemical study reveals distinctive antigenic profiles. J Dermatol Sci [Internet]. 1996;11(1):1–9. Available from: http://www.sciencedirect.com/science/article/pii/0923181195004092
285. Hirai KE, Aarão TL de S, Silva LM, de Sousa JR, de Souza J, Dias LB, et al. Langerhans cells (CD1a and CD207), dermal dendrocytes (FXIIIa) and plasmacytoid dendritic cells (CD123) in skin lesions of leprosy patients. Microb Pathog [Internet]. 2016;91:18–25. Available from: http://www.sciencedirect.com/science/article/pii/S0882401015301364
286. Song Y, Sakamoto F, Ito M. Characterization of factor XIIIa+ dendritic cells in dermatofibroma: Immunohistochemical, electron and immunoelectron microscopical observations. J Dermatol Sci [Internet]. 2005;39(2):89–96. Available from: http://www.sciencedirect.com/science/article/pii/S0923181105000551
287. Raval JS, Berg AN, Djokic M, Roth CG, Rollins-Raval MA. Factor XIII Subunit A Immunohistochemical Expression is Associated With Inferior Outcomes in Acute Promyelocytic Leukemia. Appl Immunohistochem Mol Morphol AIMM. United States; 2018 Mar;26(3):202–5.
288. Akiyama H, Kondo H, Ikeda K, Arai T, Kato M, McGleer PL. Immunohistochemical detection of coagulation factor XIIIa in postmortem human brain tissue. Neurosci Lett [Internet]. 1995;202(1):29–32. Available from: http://www.sciencedirect.com/science/article/pii/0304394095121889
289. Myneni VD, Hitomi K, Kaartinen MT. Factor XIII-A transglutaminase acts as a switch between preadipocyte proliferation and differentiation. Blood.

United States; 2014 Aug;124(8):1344–53.
290. Turnock K, Bulmer JN, Gray C. Phenotypic characterization of macrophage subpopulations and localization of factor XIII in the stromal cells of carcinomas. Histochem J [Internet]. 1990;22(12):661–6. Available from: https://doi.org/10.1007/BF01047450
291. Toida M, Watanabe F, Tsai C-S, Okutomi T, Tatematsu N, Oka N. Factor XIIIa-containing cells and fibrosis in oral and maxillofacial lesions: An immunohistochemical study. Oral Surgery, Oral Med Oral Pathol [Internet]. 1989;68(3):293–9. Available from: http://www.sciencedirect.com/science/article/pii/0030422089902144
292. Palumbo JS, Barney KA, Blevins EA, Shaw MA, Mishra A, Flick MJ, et al. Factor XIII transglutaminase supports hematogenous tumor cell metastasis through a mechanism dependent on natural killer cell function. J Thromb Haemost [Internet]. Blackwell Publishing Ltd; 2008 May 1;6(5):812–9. Available from: http://dx.doi.org/10.1111/j.1538-7836.2008.02938.x
293. O'Connor JW, Gomez EW. Biomechanics of TGFβ-induced epithelial-mesenchymal transition: implications for fibrosis and cancer. Clin Transl Med. SpringerOpen; 2014;3(1):23.
294. Gkretsi V, Stylianopoulos T. Cell Adhesion and Matrix Stiffness: Coordinating Cancer Cell Invasion and Metastasis [Internet]. Frontiers in Oncology . 2018. p. 145. Available from: https://www.frontiersin.org/article/10.3389/fonc.2018.00145
295. Seewaldt V. ECM stiffness paves the way for tumor cells. Nat Med [Internet]. Nature Publishing Group, a division of Macmillan Publishers Limited. All Rights Reserved.; 2014 Apr 7;20:332. Available from: https://doi.org/10.1038/nm.3523
296. Kurniawan NA, Grimberge J, Koopman J, Koenderink GH. Factor XIII stiffens fibrin cltos by causing fiber compaction. J Thromb Haemost. 2014;12:1687–96.
297. Silvain J, Pena A, Hulot JS, Cayla G, Bellemain-Appaix A, Vignalou JB, et al. Altered fibrin clot structure/function and FXIII Leu34 genetic variant in patients with premature coronary artery disease. Thromb Haemost. 2011;106(3):511–20.
298. Kommoss S, Winterhoff B, Oberg AL, Konecny GE, Wang C, Riska SM, et al. Bevacizumab May Differentially Improve Ovarian Cancer Outcome in Patients with Proliferative and Mesenchymal Molecular Subtypes. Clin Cancer Res. United States; 2017 Jul;23(14):3794–801.
299. Dardik R, Leor J, Skutelsky E, Castel D, Holbova R, Schiby G, et al. Evaluation of the pro-angiogenic effect of factor XIII in heterotopic mouse heart allografts and FXIII-deficient mice. Thromb Haemost. 2006;95(3):546–50.
300. Takahashi T, Shibuya M. The 230 kDa mature form of KDR/Flk-1 (VEGF receptor-2) activates the PLC-γ pathway and partially induces mitotic signals in NIH3T3 fibroblasts. Oncogene. Nature Publishing Group; 1997;14(17):2079.
301. Dallabrida SM, Falls LA, Farrell DH. Factor XIIIa supports microvascular endothelial cell adhesion and inhibits capillary tube formation in fibrin. Blood [Internet]. 2000 Apr 15;95(8):2586 LP-2592. Available from: http://www.bloodjournal.org/content/95/8/2586.abstract
302. Bakooshli MA, Lippmann ES, Mulcahy B, Iyer N, Nguyen CT, Tung K, et al. A 3D culture model of innervated human skeletal muscle enables

studies of the adult neuromuscular junction. Elife. eLife Sciences Publications Limited; 2019;8:e44530.
303. Oken MM, Creech RH, Tormey DC, Horton J, Davis TE, McFadden ET, et al. Toxicity and response criteria of the Eastern Cooperative Oncology Group. Am J Clin Oncol. United States; 1982 Dec;5(6):649–55.
304. Gonzalez Martin A, Oza AM, Embleton AC, Pfisterer J, Ledermann JA, Pujade-Lauraine E, et al. Exploratory outcome analyses according to stage and/or residual disease in the ICON7 trial of carboplatin and paclitaxel with or without bevacizumab for newly diagnosed ovarian cancer. Gynecol Oncol. United States; 2019 Jan;152(1):53–60.
305. Attié-Castro FA, Zago MA, Lavinha J, Elion J, Rodriguez-Delfin L, Guerreiro JF, et al. Ethnic heterogeneity of the factor XIII Val34Leu polymorphism. Thromb Haemost. Schattauer GmbH; 2000;84(10):601–3.
306. Saha N, Aston CE, Low PS, Kamboh MI. Racial and genetic determinants of plasma factor XIII activity. Genet Epidemiol Off Publ Int Genet Epidemiol Soc. Wiley Online Library; 2000;19(4):440–55.
307. Neyman J, Pearson ES. On the use and interpretation of certain test criteria for purposes of statistical inference, part I. Biometrika A. 1967;20:1–2.
308. Dunn OJ. Multiple comparisons among means. J Am Stat Assoc. Taylor & Francis Group; 1961;56(293):52–64.
309. Armstrong RA. When to use the Bonferroni correction. Ophthalmic Physiol Opt. England; 2014 Sep;34(5):502–8.
310. Ottenbacher KJ. Quantitative evaluation of multiplicity in epidemiology and public health research. Am J Epidemiol. Oxford University Press; 1998;147(7):615–9.
311. Moyé LA. P-value interpretation and alpha allocation in clinical trials. Ann Epidemiol. Elsevier; 1998;8(6):351–7.
312. Rothman KJ. No adjustments are needed for multiple comparisons. Epidemiology. JSTOR; 1990;43–6.
313. Perneger T V. What's wrong with Bonferroni adjustments. Bmj. British Medical Journal Publishing Group; 1998;316(7139):1236–8.
314. Roch AM, Noel P, el Alaoui S, Charlot C, Quash G. Differential expression of isopeptide bonds N epsilon (gamma-glutamyl) lysine in benign and malignant human breast lesions: an immunohistochemical study. Int J cancer. United States; 1991 May;48(2):215–20.
315. Thomas V, Fournet G, Simonet F, Roch A-M, Ceylan I, El Alaouia S, et al. Definition of the fine specificity of the monoclonal antibody 81D4: its reactivity with lysine and polyamine isopeptide cross-links. J Immunol Methods [Internet]. 2004;292(1):83–95. Available from: http://www.sciencedirect.com/science/article/pii/S0022175904002303
316. Mauro A, Buscemi M, Gerbino A. Immunohistochemical and transcriptional expression of matrix metalloproteinases in full-term human umbilical cord and human umbilical vein endothelial cells. J Mol Histol. Netherlands; 2010 Dec;41(6):367–77.
317. Cooke JP. NO and angiogenesis. Atheroscler Suppl. Netherlands; 2003 Dec;4(4):53–60.
318. Roberts DD, Isenberg JS, Ridnour LA, Wink DA. Nitric Oxide and Its Gatekeeper Thrombospondin-1 in Tumor Angiogenesis. Clin Cancer Res [Internet]. 2007 Feb 1;13(3):795 LP-798. Available from: http://clincancerres.aacrjournals.org/content/13/3/795.abstract
319. Petersen M, Pardali E, Van Der Horst G, Cheung H, Van Den Hoogen C,

Van Der Pluijm G, et al. Smad2 and Smad3 have opposing roles in breast cancer bone metastasis by differentially affecting tumor angiogenesis. Oncogene. Nature Publishing Group; 2010;29(9):1351.
320. Itoh F, Itoh S, Adachi T, Ichikawa K, Matsumura Y, Takagi T, et al. Smad2/Smad3 in endothelium is indispensable for vascular stability via S1PR1 and N-cadherin expressions. Blood. United States; 2012 May;119(22):5320–8.
321. Lin S, Xie J, Gong T, Shi S, Zhang T, Fu N, et al. Smad signal pathway regulates angiogenesis via endothelial cell in an adipose-derived stromal cell/endothelial cell co-culture, 3D gel model. Mol Cell Biochem. Netherlands; 2016 Jan;412(1–2):281–8.
322. Miao H-Q, LEE P, LIN H, SOKER S, KLAGSBRUN M. Neuropilin-1 expression by tumor cells promotes tumor angiogenesis and progression. FASEB J. Federation of American Societies for Experimental Biology; 2000;14(15):2532–9.
323. Yamada Y, Takakura N, Yasue H, Ogawa H, Fujisawa H, Suda T. Exogenous clustered neuropilin 1 enhances vasculogenesis and angiogenesis. Blood. Am Soc Hematology; 2001;97(6):1671–8.
324. Baba T, Kariya M, Higuchi T, Mandai M, Matsumura N, Kondoh E, et al. Neuropilin-1 promotes unlimited growth of ovarian cancer by evading contact inhibition. Gynecol Oncol. United States; 2007 Jun;105(3):703–11.
325. Robinson SD, Reynolds LE, Kostourou V, Reynolds AR, da Silva RG, Tavora B, et al. αvβ3 Integrin Limits the Contribution of Neuropilin-1 to Vascular Endothelial Growth Factor-induced Angiogenesis. J Biol Chem [Internet]. 2009 Dec 4;284(49):33966–81. Available from: http://www.jbc.org/content/284/49/33966.abstract
326. Geretti E, Shimizu A, Klagsbrun M. Neuropilin structure governs VEGF and semaphorin binding and regulates angiogenesis. Angiogenesis [Internet]. 2008;11(1):31–9. Available from: https://doi.org/10.1007/s10456-008-9097-1
327. Alice P, Alessandro F, Christiana R. Neuropilin Regulation of Angiogenesis, Arteriogenesis, and Vascular Permeability. Microcirculation [Internet]. Wiley/Blackwell (10.1111); 2014 Feb 12;21(4):315–23. Available from: https://doi.org/10.1111/micc.12124
328. Shawber CJ, Das I, Francisco E, Kitajewski JAN. Notch signaling in primary endothelial cells. Ann N Y Acad Sci. Wiley Online Library; 2003;995(1):162–70.
329. Adams RH, Wilkinson GA, Weiss C, Diella F, Gale NW, Deutsch U, et al. Roles of ephrinB ligands and EphB receptors in cardiovascular development: demarcation of arterial/venous domains, vascular morphogenesis, and sprouting angiogenesis. Genes Dev. Cold Spring Harbor Lab; 1999;13(3):295–306.
330. Cheng N, Brantley DM, Chen J. The ephrins and Eph receptors in angiogenesis. Cytokine Growth Factor Rev. Elsevier; 2002;13(1):75–85.
331. Cheng N, Brantley DM, Liu H, Lin Q, Enriquez M, Gale N, et al. Blockade of EphA Receptor Tyrosine Kinase Activation Inhibits Vascular Endothelial Cell Growth Factor-Induced Angiogenesis11 NIH Grants HD36400 and DK47078; JDF grant I-2001-519; DOD grant BC010265; American Heart Association Grant 97300889N; ACS Institut. Mol Cancer Res. AACR; 2002;1(1):2–11.
332. Lee SH, Schloss DJ, Jarvis L, Krasnow MA, Swain JL. Inhibition of

angiogenesis by a mouse sprouty protein. J Biol Chem. ASBMB; 2001;276(6):4128–33.
333. Lee S, Nguyen TMB, Kovalenko D, Adhikari N, Grindle S, Polster SP, et al. Sprouty1 inhibits angiogenesis in association with up-regulation of p21 and p27. Mol Cell Biochem. Springer; 2010;338(1–2):255–61.
334. Wietecha MS, Chen L, Ranzer MJ, Anderson K, Ying C, Patel TB, et al. Sprouty2 downregulates angiogenesis during mouse skin wound healing. Am J Physiol Circ Physiol. American Physiological Society Bethesda, MD; 2010;300(2):H459–67.
335. Suri C, Jones PF, Patan S, Bartunkova S, Maisonpierre PC, Davis S, et al. Requisite role of angiopoietin-1, a ligand for the TIE2 receptor, during embryonic angiogenesis. Cell. Elsevier; 1996;87(7):1171–80.
336. Koblizek TI, Weiss C, Yancopoulos GD, Deutsch U, Risau W. Angiopoietin-1 induces sprouting angiogenesis in vitro. Curr Biol. Elsevier; 1998;8(9):529–32.
337. Gale NW, Thurston G, Hackett SF, Renard R, Wang Q, McClain J, et al. Angiopoietin-2 is required for postnatal angiogenesis and lymphatic patterning, and only the latter role is rescued by Angiopoietin-1. Dev Cell. Elsevier; 2002;3(3):411–23.
338. Tse V, Xu L, Yung YC, Santarelli JG, Juan D, Fabel K, et al. The temporal–spatial expression of VEGF, angiopoietins-1 and 2, and Tie-2 during tumor angiogenesis and their functional correlation with tumor neovascular architecture. Neurol Res [Internet]. Taylor & Francis; 2003 Oct 1;25(7):729–38. Available from: http://www.tandfonline.com/doi/abs/10.1179/016164103101202084
339. Bamias A, Pignata S, Pujade-Lauraine E. Angiogenesis: a promising therapeutic target for ovarian cancer. Crit Rev Oncol Hematol [Internet]. 2012 Dec [cited 2015 Oct 21];84(3):314–26. Available from: http://www.sciencedirect.com/science/article/pii/S1040842812000996
340. Secord AA, Nixon AB, Hurwitz HI. The search for biomarkers to direct antiangiogenic treatment in epithelial ovarian cancer. Gynecol Oncol [Internet]. 2014;135(2):349–58. Available from: http://www.sciencedirect.com/science/article/pii/S0090825814012864
341. Avril S, Dincer Y, Malinowsky K, Wolff C, Gundisch S, Hapfelmeier A, et al. Increased PDGFR-beta and VEGFR-2 protein levels are associated with resistance to platinum-based chemotherapy and adverse outcome of ovarian cancer patients. Oncotarget. United States; 2017 Nov;8(58):97851–61.
342. Szubert S, Moszynski R, Szpurek D, Romaniuk B, Sajdak S, Nowicki M, et al. The expression of Platelet-derived Growth factor receptors (PDGFRs) and their correlation with overall survival of patients with ovarian cancer. Ginekol Pol. Poland; 2019;90(5):242–9.
343. Gershtein E, Kushlinskii N. Clinical prospects of IGF-signaling system components study in ovarian cancer patients. Drug Metab Pers Ther. Germany; 2015 Jun;30(2):75–85.
344. Singh RK, Dhadve A, Sakpal A, De A, Ray P. An active IGF-1R-AKT signaling imparts functional heterogeneity in ovarian CSC population. Sci Rep. England; 2016 Nov;6:36612.
345. Du J, Shi H-R, Ren F, Wang J-L, Wu Q-H, Li X, et al. Inhibition of the IGF signaling pathway reverses cisplatin resistance in ovarian cancer cells. BMC Cancer. England; 2017 Dec;17(1):851.
346. Wang X, Zhu Q, Lin Y, Wu L, Wu X, Wang K, et al. Crosstalk between

TEMs and endothelial cells modulates angiogenesis and metastasis via IGF1-IGF1R signalling in epithelial ovarian cancer. Br J Cancer. England; 2017 Oct;117(9):1371–82.

347. Lemmon MA, Schlessinger J, Ferguson KM. The EGFR family: not so prototypical receptor tyrosine kinases. Cold Spring Harb Perspect Biol. United States; 2014 Apr;6(4):a020768.
348. Amgen. FDA appoves bevacizumab biosimilar Mvasi [Internet]. Generics and Biosimilar Initiative: News. 2017 [cited 2019 Sep 3]. Available from: http://www.gabionline.net/Biosimilars/News/FDA-approves-bevacizumab-biosimilar-Mvasi
349. Epstein M. Food and Drug Administration guidances on biosimilars: an update for the gastroenterologist. Therap Adv Gastroenterol [Internet]. SAGE Publications; 2018 Oct 3;11:1756284818799600–1756284818799600. Available from: https://www.ncbi.nlm.nih.gov/pubmed/30302126